УДК : 616.24-036-092-073.7-079.4

BUKOVINIAN STATE MEDICAL UNIVERSITY
DEPARTMENT OF PHTHISIOLOGY AND PULMONOLOGY

**TODORIKO L.D., PIDVERBETSKA O.V.,
SEMIANIV I.O., YEREMENCHUK I.V., SLYVKA V.I.,
PIDVERBETSKYI O.YA., TODERIKA YA.I.**

CLINICAL AND RADIOLOGICAL FEATURES AND DIFFERENTIAL DIAGNOSIS OF LUNG DISEASES

teaching manual for senior students
of institutions of higher medical education
(materials for independent preparation for practical classes)

Chernivtsi, 2025

Recommended by the Academic Council of Bukovinian State Medical University: teaching manual *"Clinical and radiological features and differential diagnosis of lung diseases"* for senior students of institutions of higher medical education (materials for independent preparation for practical classes) (protocol № 6 dated December 23, 2025).
Teaching manual *"Clinical and radiological features and differential diagnosis of lung diseases"* for senior students of institutions of higher medical education (materials for independent preparation for practical classes).
Authors: Todoriko L.D., Pidverbetska O.V., Semianiv I.O., Yeremenchuk I.V., Slyvka V.I., Pidverbetskyi O.Ya., Toderika Ya.I.
Bukovinian State Medical University; 2025. 263 p.

Reviewers:
Yu.M. Valetskyi – Head of the Department of Nursing and Emergency Medicine, Municipal Institution of Higher Education "Volyn Medical Institute", Doctor of Medical Sciences, Professor.

L.A. Hryshchuk – Professor of the Department of Propedeutics of Internal Medicine and Phthisiology, I. Horbachevsky Ternopil National Medical University; Doctor of Medical Sciences, Professor.

This study guide provides senior medical students with a structured overview of the clinical and radiological features essential for diagnosing lung diseases, with a particular emphasis on tuberculosis. It integrates fundamental imaging principles with detailed analyses of differential diagnostic approaches across a wide spectrum of pulmonary pathologies. Designed for independent preparation, the manual supports the development of practical diagnostic skills needed for clinical training and professional practice.

The teaching manual *"Clinical and radiological features and differential diagnosis of lung diseases"* for senior students of institutions of higher medical education (materials for independent preparation for practical classes) was approved at the meeting of the Academic Council of Bukovinian State Medical University, protocol № 6 dated December 23, 2025.

ISBN 978-617-519-224-5

C O N T E N T S

List of abbreviations

Amx/Clv - Amoxillin/Clavulanatre
ATT - Anti-tuberculosis therapy
ART - Antiretroviral therapy
DOTS - Directly observed treatment - short course (WHO strategy)
DST - Drug susceptibility testing
CP – Contuniatin phase of anti-TB treatment
Cfz- CLOFAZIMIN
CPT - Co-trimoxazole preventive therapy
Clr - Clarithromycin
Cs - Cycloserine
E - Ethambutol
Eto - Ethionamide
H - Isoniazid
Km - Kanamycin
Lfx – Levofloxacin
Lzd **–** Linezolid
Mfx - Moxifloxacin
Gfx - Gatifloxacin
Ofx – Ofloxacin
PAS - paraaminosalicylic acid
Trd - Terizidone
FLD - first line drugs (in the context of anti-TB drugs or medicines)
R – Rifampicin
Rfb - Rifabutin
S - Streptomycin
SAT - Self-administered treatment
SLD - Second line drugs (in the context of anti-TB drugs or medicines)
STR - Standard treatment regimen
Z – Pyrazinamide.

Introduction

Today, we are witnessing significant changes in our understanding of the systemic principles and approaches to combating tuberculosis (TB), as Ukraine's educational system is implementing a training concept for healthcare professionals developed in accordance with the requirements of the World Federation for Medical Education and the key provisions of the Bologna Process. Modern challenges—namely the steady increase in the number of patients with drug-resistant and, in particular, multidrug-resistant tuberculosis, as well as TB/HIV and TB/HIV/hepatitis comorbidity—necessitate the inclusion of new sections of phthisiology in the curricula of medical students and physicians, alongside expanding the volume of material devoted to the diagnosis and differential diagnosis of pulmonary diseases.

In today's context of rapid scientific and technological progress, the issue of educational quality is especially relevant. Innovative technologies that offer opportunities to enhance educational processes are therefore of great interest. The educational sector, including medical education, is undergoing profound reforms and integration into the European Higher Education Area, requiring all its components to conform to widely accepted international standards. According to the new Unified Protocol "Tuberculosis," the detection of TB cases must be performed by primary healthcare physicians, which demands strong knowledge and skills in interpreting imaging studies—an essential foundation of high-quality diagnosis of pulmonary diseases.

Addressing tuberculosis, as a socially significant and dangerous disease, remains one of the priorities of national public health policy. It requires a program-targeted approach and the implementation of comprehensive strategies to counteract the epidemic. It should be noted that individuals aged 20 to 49—representing the main segment of the working population and the economic backbone of the country—are the most vulnerable to Mycobacterium tuberculosis infection. Ukraine has developed the necessary regulatory framework, the implementation of which enables significant influence on the epidemic process and can substantially reduce its intensity.

The modern development of medicine requires continuous improvement of diagnostic, therapeutic, and preventive measures for respiratory diseases in line with evidence-based practice. The system of standardizing medical care is aimed at developing medical-technological documents that help physicians act effectively in specific clinical situations while avoiding unnecessary or erroneous interventions. To improve knowledge related to the diagnosis of pulmonary diseases—particularly through the use of modern imaging methods—this educational manual has been created. It is intended to support the training of general practitioners and family medicine physicians.

Chapter 1

FUNDAMENTALS OF RADIOLOGICAL DIAGNOSTICS

Radiological Methods

The most widely used diagnostic method is **chest fluoroscopy**, which allows the clinician to assess the transparency of the lung fields, identify areas of consolidation (infiltrates, pneumosclerosis, neoplasms) and cavities within the lung parenchyma, detect foreign bodies in the trachea and bronchi, and determine the presence of fluid or air in the pleural cavity, as well as coarse pleural adhesions and fibrous bands.

Fluorography is a type of chest radiological examination in which an image is captured on small-format film. It is used for large-scale population screening.

Chest radiography is performed to diagnose and document pathological changes in the respiratory organs identified during fluoroscopy. Some abnormalities are better visualised on a radiograph than during fluoroscopy.

Tomography enables layer-by-layer radiological examination of the lungs. It is used for more precise diagnosis of tumors, small infiltrates, cavities, and caverns.

1.1. Computed Tomography

During **computed tomography (CT)**, only thin slices of tissue are exposed to X-rays. There is no superimposition or blurring of structures located outside the selected slice. As a result, the image has a contrast resolution that significantly exceeds that of projection radiography. Technical solutions in CT systems differ across manufacturers, and several generations of CT scanners currently exist. The scanner's "generation" (first, second, third, fourth, etc.) corresponds to the configuration of the "tube–detector" system.

The X-ray tube emits a thin, collimated, fan-shaped beam perpendicular to the long axis of the body. This beam may be wide enough to cover the entire body diameter. By adjusting collimation, the beam thickness can be changed (e.g., from 1 to 10 mm), and therefore the slice thickness also varies. The X-ray beam passing through the patient is

detected not by film but by a system of dedicated detectors. These detectors may contain crystals of various chemical compounds (e.g., sodium iodide) or pressurized xenon chambers. X-ray photons generate electrical signals within the detectors. The higher the intensity of the primary beam that reaches the detector, the stronger the resulting electrical signal. By measuring the attenuated radiation, the system calculates the degree of primary beam attenuation.
CT detectors are approximately **100 times more sensitive** than radiographic film in detecting differences in X-ray intensity, and therefore equally more sensitive in detecting attenuation differences.

Acquisition of a CT Image
The process of obtaining a CT slice at a selected level involves the following steps:
Formation of the required X-ray beam width (collimation).
Scanning of the object by rotational and translational movement of the “emitter–detector” assembly around the stationary patient.
Measurement of the attenuated radiation and conversion of the signals into digital form.
Computer synthesis of the tomogram from the total set of measurements corresponding to the selected slice.
Display of the reconstructed image on a video monitor.
The strictly collimated beam passes only through the plane of interest, while registration of scattered radiation is minimized. This significantly improves the visualisation of tissues—especially those with low contrast. Reduction of scattered radiation is achieved by primary collimators at the tube output and secondary collimators positioned before the detectors.
At identical X-ray energies, materials with a higher relative molecular mass attenuate X-rays more strongly than materials with a lower molecular mass. Such attenuation can be easily measured. However, the human body is highly heterogeneous, so detectors frequently record beams of identical intensity that have passed through completely different structures. This occurs, for example, when passing through a homogeneous object of significant thickness compared to a heterogeneous object with the same total density.

During rotation of the X-ray tube around the patient, detectors register **1.5 to 6 million signals** from different points (projections). Importantly, each point of the object is projected multiple times onto various detector positions.
The detected signals are transformed into digital form and processed by the computer, which reconstructs the image as a matrix of values representing the attenuation coefficient of each voxel.

Image Reconstruction and Matrix Parameters
CT scanners typically use primary matrices of:
256 × 256,
320 × 320,
512 × 512,
1024 × 1024 pixels.
Image quality increases with:
a larger number of detectors,
a greater number of projections per rotation,
a larger reconstruction matrix.
Each CT slice is generated as a 10 mm section reconstructed on a 160 × 160 matrix. The attenuation coefficients are expressed in **Hounsfield Units (HU)**:
–1000 HU = air
0 HU = water
+1000 HU = dense bone
Typical attenuation values:
fat: –100 to 0 HU
cerebrospinal fluid: 2–16 HU
blood: 28–62 HU
The system’s sensitivity in detecting density differences in standard mode is ~5 HU (0.5%). On the monitor, high-density structures (e.g., bone) appear bright, low-density structures appear dark. The display’s gradation capacity is 15–16 half-tone levels, approximately 130 HU per level.
Diagnostic accuracy depends largely on matrix size and contrast resolution. For example:
At 80 × 80 matrix, diagnostic error rate = 27%

At 160 × 160 matrix → reduced to 11%
CT systems have two types of resolution:
spatial resolution (determined by matrix pixel size, usually ~1.5 × 1.5 mm)
contrast resolution (~5 HU, or 0.5%)
By comparison, conventional radiography detects density differences of 10–20%.
However, significant differences in density between adjacent structures may create artifacts, especially near dense bone (e.g., temporal bones, skull vault), leading to the loss of small low-density lesions.
A key requirement for CT imaging is **the patient's immobility**, as even minor movement produces artifacts:
dark streaks from low-density structures (air)
bright streaks from high-density structures (bone, metal clips)
These artifacts reduce diagnostic clarity.

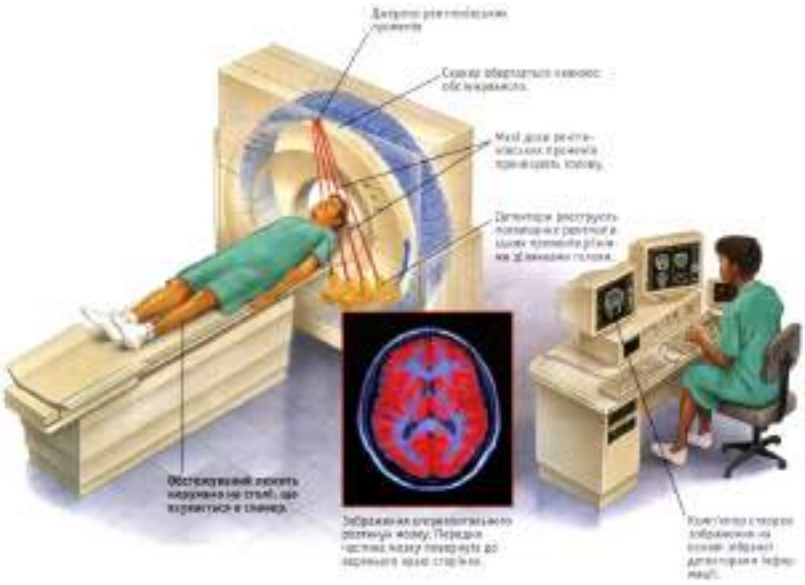

Spiral Computed Tomography – English Translation
A new scanning concept—**spiral (helical) CT**—has recently emerged, significantly improving the efficiency and speed of imaging the selected anatomical region.
Spiral Computed Tomography
The idea of spiral scanning was first patented by the Japanese company **Toshiba** in 1986, and T. Katakura with colleagues performed the first clinical study on a spiral CT scanner in 1989. The introduction of spiral

CT into clinical practice in 1989 became the most significant advancement in the 20-year history of computed tomography and opened fundamentally new possibilities for diagnosing a wide range of pathological conditions.

As is known, in conventional CT a single scan produces an image of one slice, and the scan cycle is repeated after the table is moved to obtain the required number of sequential layers. In spiral CT, the X-ray tube rotates continuously around the region of interest while the patient table moves steadily in the longitudinal direction. The trajectory of the X-ray beam relative to the long axis of the body thus assumes a **spiral form**, which gave the method its name.

Unlike conventional CT, in spiral scanning the final position of a slice does not coincide with the actual acquisition point because the patient moves during scanning. Rapid tube rotation in spiral systems and the absence of pauses between scanning cycles (previously required to reposition the table) greatly reduce examination time. This increases the throughput of the CT unit and simplifies scanning in patients who cannot hold their breath for long periods, remain still, or tolerate lengthy procedures (trauma patients, young children, severely ill individuals).

The high scanning speed provides **sharper images with fewer motion artifacts**, improving visualization of moving organs in the chest and abdomen. Reduced exposure time also makes the method safer for the patient.

Among the key advantages of spiral CT is the ability to **reconstruct images in any chosen plane**. Because spiral CT collects data from the entire scanned volume, it is possible to obtain an image of any section within that volume. By allowing the entire region of interest to be scanned during a single breath-hold, spiral CT prevents “missing” small lesions that might otherwise slip between sequential slices—thereby improving detection of small focal lesions in parenchymal organs.

Spiral CT also provides new possibilities for **multiplanar and three-dimensional reconstructions**, which are becoming increasingly important in diagnostics, preoperative planning for maxillofacial deformities and trauma, and in evaluating spinal and major joint injuries. Spiral CT enables imaging of long anatomical segments (up to 1 meter), opening new prospects for **CT angiography**, allowing entire vascular

segments to be visualized in a short scan time. Dedicated processing software makes it possible to isolate vessels, atherosclerotic plaques, and thrombi. Unlike MRI, CT angiography does not produce flow or metallic stent artifacts.

Another promising application of 3D reconstructions based on spiral CT data is **virtual endoscopy**. Such a system, developed by Picker for their high-speed spiral scanners (Q-series) and named *Voyager*, preserves high spatial resolution (21.5 lp/cm) during scanning. The use of the LAPP system (a high-performance parallel processor architecture) enables true three-dimensional visualization, selective highlighting of specific tissues (“fourth dimension”), and simultaneous visualization of bone, soft tissue, and vessels.

The Voyager system simultaneously displays the surfaces of hollow organs and extramural structures (lymph nodes, tumors, vessels). The resulting images form a natural sequence of virtual endoscopic views. Navigation software automatically determines the trajectory of the “virtual endoscope,” although manual adjustments are possible. Surface relief and artificial shadowing can also be produced. Image sequences can be easily converted into standard VHS video for use in tele-radiology.

The system is primarily intended for detecting obstructive lesions of the upper airways, tumors of the esophagus, stomach, and colon, atherosclerotic lesions of large vessels, diseases of the paranasal sinuses, urinary bladder, and spinal canal. Virtual endoscopy data help determine the optimal biopsy site and plan surgical intervention. The method can be used independently or serve as a bridge between tomographic and conventional endoscopic techniques.

Spiral CT provides **greater diagnostic information** compared to conventional CT. The new technology effectively overcomes such limitations as fixed slice thickness, data averaging, missed areas due to inconsistent breath-holding, and misalignment of scanning planes with the course of bronchi or vessels—all of which complicate the evaluation of hollow organ lumens.

At the same time, spiral CT increases wear on X-ray tubes. Extensive use of multiplanar and 3D reconstructions requires higher radiologist expertise. Although scanning time and data acquisition have decreased,

image reconstruction still requires time and computational resources. The large volume of data also increases the workload for radiologists. Thus, shortened patient scanning time does not necessarily shorten the time needed to obtain the final diagnostic result. Efficient use of spiral CT often requires a dedicated workstation for post-processing.

Despite economic challenges, spiral CT will undoubtedly take a prominent place in radiology as a **high-speed, highly sensitive, and specific diagnostic method**.

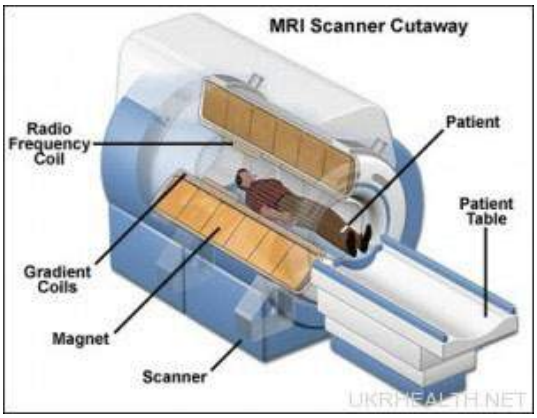

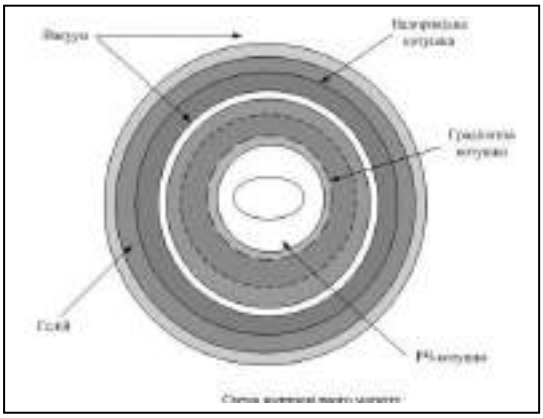

Sometimes contrast enhancement is used with the help of paramagnetic contrast agents (for example, Magnevist, Gadovist, Omniscan, Tomovist), which are administered intravenously in a volume of 5 to 20 ml. Contrast agents used in MRI may cause allergic or adverse reactions (nausea, vomiting, allergic-like reactions of the skin and mucous membranes). Delayed reactions are also possible, such as weakness, sweating, pallor, seizures. These reactions are usually mild or moderate and respond well to medical treatment. Anaphylactoid reactions are extremely rare (0.01–0.1%), but they may be severe or even fatal, therefore it is essential to take a careful allergic history regarding any previous adverse or allergic reactions to contrast media, drugs, or any other substances.

1.2. Magnetic Resonance Imaging

The MRI method is used as a navigation system during robotic and radiosurgical procedures.

Two types of magnetic resonance scanners exist: closed and open systems.

A closed-type MRI scanner is a magnetic field chamber into which the patient is placed for examination.

Open-type MRI scanners have numerous advantages. They provide modern capabilities for image formation, a wide range of clinical applications, and remain open to the surrounding environment during scanning. Open MRI systems are designed for examining patients of any age and body weight, as well as those suffering from claustrophobia (fear of enclosed spaces). The C-shaped open magnet design ensures convenient access to the patient during the diagnostic procedure, allowing a family member or physician to remain in close proximity to a small child, a severely ill patient, or an elderly person. The wide angle of view increases patient comfort and minimizes claustrophobia and anxiety during the examination.

Advantages of MRI include high-quality visualization of lung tissue, clear differentiation of vascular and soft-tissue structures and fluid, the ability to clarify tumour characteristics during contrast enhancement and their invasion into adjacent organs, visualization of pathological changes in lymphoid tissue, and the absence of ionizing radiation exposure to the patient. However, the method also has limitations – in particular, the inability to visualize bronchoalveolar structures. Absolute indications for MRI include suspected vascular origin of pulmonary abnormalities, mediastinal pathology, presence of fluid, focal lesions, cysts of various origins, pleural tumours, and pleuritis of unclear etiology.

1.3. Radiological signs in diseases of the respiratory system

Radiological syndromes of respiratory diseases

Radiological manifestations of pathological processes in the lungs are quite diverse, but they are based on only four phenomena:

- shadowing (opacity) or enlightenment (increased translucency) of the lung fields,
- changes in the lung pattern,
- changes in the lung roots.

Shadowing of the lungs is most often due to accumulation of inflammatory exudate or fluid in the alveoli, reduced aeration of the lungs as a result of bronchial obstruction or compression of the lung, or replacement of pulmonary parenchyma by pathological tissue. It should

be remembered that this phenomenon may also be caused by extrapulmonary processes: tumours of the chest wall, diaphragm, or mediastinum projecting into the lung fields, or fluid accumulation in the pleural cavity.

Enlightenment (increased translucency) is caused by a decrease in the amount of tissue per unit lung volume. This occurs with increased aeration of the entire lung or part of it, or with formation of air-containing cavities in the lung parenchyma. In addition, increased translucency of a lung field may be due to gas accumulation in the pleural cavity.

Changes in the lung pattern arise either from an interstitial component or from disturbed blood and lymph flow in the lungs.

Changes in the radiological appearance of the lung roots may be due to involvement of any of their structural elements: vessels, bronchi, fat tissue, lymph nodes.

In general, nine radiological syndromes are distinguished, covering the entire spectrum of respiratory pathology:

1. **Total (subtotal) opacity of a lung field** – may be seen in:
   - consolidation (loss of aeration) of lung tissue of any origin (inflammatory infiltration, cirrhosis, atelectasis). In inflammatory infiltration the opacity is usually heterogeneous with relatively rapid dynamics. In atelectasis the opacity is homogeneous, lung volume is reduced, the mediastinum shifts toward the lesion, the hemithorax appears narrowed, and the ipsilateral hemidiaphragm is elevated. In pulmonary cirrhosis the opacity is often heterogeneous, the lung root may be deformed and pulled to one side, and the hemithorax is narrowed;
   - pleural thickening – parietal and interlobar fibrous plaques, adhesions (strands) occurring in chronic subpleural inflammatory processes, often with thickening of interlobar pleura;
   - presence of pathological content in the pleural cavity – fluid or intra-abdominal organs in diaphragmatic hernia. In such cases the mediastinum may be shifted to the opposite side;
   - large tumour – the mediastinal shadow may likewise be displaced to the opposite side;

- absence of a lung – seen in congenital anomalies or after pneumonectomy, accompanied by mediastinal shift toward the affected side and narrowing of the hemithorax.

2. **Localized opacities** – may be caused by intrapulmonary or extrapulmonary processes, which can be differentiated by multi-projection imaging of the chest.

- *Intrapulmonary localized opacities* (pneumonia, pulmonary tuberculosis, abscess, tumour, cyst, peripheral tumour, etc.) are usually located directly in lung tissue (seen in all projections) and move with the lung during respiration.
- *Extrapulmonary opacities*:
  - fluid in the pleural cavity – in the upright position the shadow occupies the lower part of the hemithorax, merging with the diaphragm; the upper border of the exudate has a curved contour (Ellis–Damoiseau line), whereas in transudate the upper border is horizontal. In the lateral decubitus position the shadow (fluid) lies dependently, spreading along the pleural cavity;
  - loculated parietal and interlobar pleuritis – a convex opacity with a sharp inner contour that merges with the parietal pleura, or a lenticular shadow with clear contours in the interlobar fissure, which does not change its shape with changes in patient position;
  - lesions arising from the chest wall: soft-tissue tumours, rib anomalies and tumours (they move with the ribs during breathing);
  - lesions arising from the diaphragm – tumours, cysts, diaphragmatic relaxation;
  - mediastinal masses – often cause unilateral or bilateral widening of the mediastinal shadow (enlarged lymph nodes or clusters of nodes, thymic tumours, vascular anomalies, retrosternal goitre, etc.).

3. **Round opacity**. Round shadows of varying density, structure, and size in lung tissue occur in peripheral carcinoma, tuberculosis, cysts, solitary metastases, etc.

- *Peripheral carcinoma* typically appears as a spherical or ovoid homogeneous opacity with sharp but irregular, lobulated outer contours. Sometimes the tumour may undergo cavitation.

- *Tuberculous infiltrate* is a low-density opacity of small size (1.5–2 cm) with ill-defined outer margins and surrounding small-focal seeding. In a cavitating infiltrate, a cavity appears within the lesion.
- *Tuberculoma* is a dense (organized) infiltrate with small calcified foci and peripheral small-focal seeding.
- *Cyst* (echinococcal, retention, bronchial) – a homogeneous, fluid-filled oval shadow with sharp contours. Due to the elasticity of the lesion its shape may change with respiration.
- *Metastasis*. A solitary metastasis appears as a small, round, homogeneous opacity with indistinct, irregular contours that must be differentiated from peripheral carcinoma, tuberculous infiltrate, etc. Multiple round opacities usually indicate metastatic disease.
- *Vascular anomalies* – e.g. arteriovenous aneurysms – are characterized by intrinsic pulsation.

4. **Focal shadows and limited disseminations** – shadows up to 1 cm in diameter are conventionally termed foci. Their size is subdivided into: miliary (up to 2 mm), small (3–4 mm), medium (5–7 mm), and large (8–10 mm) foci. Focal shadows may differ in density and sharpness of contours (depending on the phase of activity). A few foci (usually a small group of 3–4) are termed solitary foci; limited dissemination refers to multiple foci within no more than two segments. This syndrome is most often seen in focal tuberculosis, metastases, aspiration pneumonia, etc.

5. **Extensive focal disseminations**. In this syndrome, the extent of pulmonary involvement usually exceeds two segments and is regarded as widespread dissemination; bilateral disease is termed diffuse dissemination. This pattern is seen in disseminated tuberculosis, sarcoidosis, pneumoconioses, carcinomatosis, etc.

- *Acute hematogenous disseminated tuberculosis* presents as diffuse, evenly distributed, symmetrical, monomorphic miliary or small-focal dissemination.
- *Chronic disseminated tuberculosis* is characterized by polymorphism of foci and the presence of fibrotic changes.
- *Sarcoidosis* (stage II) shows varying-size focal shadows and symmetrical involvement, with interstitial changes in perihilar regions and enlarged lymph nodes.

- *Pneumoconiosis* – medium-sized focal shadows in both lungs, marked interstitial changes, calcification of intrapulmonary foci and conglomerates, as well as mediastinal lymph nodes; occupational exposure is present in the history.
- *Carcinomatosis* – widespread hematogenous dissemination with medium and large foci on both sides, often with indistinct contours.

6. **Air-containing cavity** – most frequently seen in congenital cystic disease, emphysematous bullae, abscesses, destructive forms of tuberculosis, cavitary peripheral carcinoma, evacuated echinococcal cysts, etc. Among extrapulmonary processes, it occurs in pneumothorax, diaphragmatic hernia, etc.
7. **Extensive hyperlucency** – increased transparency of lung tissue on one or more lung fields. This is observed in regional or total (diffuse) emphysema. Diffuse emphysema may be unilateral or bilateral. Unilateral total hyperlucency is most often due to valve obstruction of a main bronchus. The hyperlucent lung syndrome is also seen in total unilateral pneumothorax, with complete absence of lung markings on the radiograph and a collapsed lung near the hilum.
8. **Changes in lung pattern**. These arise from impaired pulmonary circulation or lymphatic drainage, or interstitial fibrosis, and may manifest as either increased or decreased lung markings.
   - *Increased lung markings* – enlargement and increased number of vascular/bronchial elements per unit area, seen in: arterial hyperemia in heart defects; interstitial edema; interstitial fibrosis in chronic bronchitis; pneumoconioses, sarcoidosis, collagenoses, alveolitis, etc.
   - *Decreased lung markings* – reduction in the number of elements per unit volume, seen in hypovolemia of the pulmonary circulation in heart defects, emphysema, etc. The extent of reduction may be limited, total, unilateral, or bilateral.
9. **Changes in lung roots** may be unilateral or bilateral. They present as changes in size, shape, structure, density, and contour.
   - Enlargement and deformation of lung roots may occur due to enlarged lymph nodes, vascular dilatation, or tumours.
   - Blurring of root structure arises in edema and fibrosis;

- Increased density is seen with calcified lymph nodes in tuberculosis or silicotuberculosis.
- A polycyclic root contour is observed with grouped enlarged lymph nodes (unilateral – tuberculous lymphadenitis; bilateral – sarcoidosis, Hodgkin's disease, lymphosarcoma, metastases, etc.); a lobulated (nodular) contour is typical of central exobronchial tumours.

These skiagraphic phenomena can be further detailed depending on their length, shape, structure, and configuration.

Thus, nine radiological syndromes are distinguished, reflecting practically the entire spectrum of respiratory pathology.

In summary, a syndromic approach to radiological diagnosis of respiratory diseases proves highly effective. It accelerates and facilitates recognition of numerous pathological processes in the lungs and pleura, and forms the basis for rational planning of further imaging studies. At the same time, one must keep in mind the possibility of combinations of different syndromes, which may either simplify or, conversely, complicate the final nosological diagnosis.

1.3. Radiological Symptoms in Respiratory Diseases

Various pathological processes in the lungs may be accompanied by the development of the following radiological symptoms: alteration of the pulmonary pattern, areas of increased attenuation (opacification), areas of decreased attenuation (lucency), and changes in the lung roots (hilar structures).

1. Alteration of the Pulmonary Pattern

The intensity of the pulmonary pattern on chest radiographs depends primarily on:

1. **The degree of vascular engorgement** — increased vascular filling leads to the enhancement of pulmonary markings. This makes it possible to differentiate arterial, venous, or mixed types of pulmonary congestion.
2. **Thickening of the peribronchial and perivascular interstitial tissue** due to pathological processes (most commonly inflammatory, e.g., in chronic bronchitis).

2. Pulmonary Opacification (Increased Attenuation)

Pulmonary opacification occurs when normally aerated, radiolucent lung tissue becomes denser due to inflammatory, tumorous, degenerative-dystrophic processes, or due to lung segment/lobe collapse (atelectasis).

It is observed in the following conditions:

- Accumulation of fluid in the pleural cavity, segmental loss of aeration due to bronchial obstruction (**obstructive atelectasis**), or compression of lung regions by fluid or air in the pleural space (**compressive atelectasis**);
- Accumulation of serous fluid within alveoli (**pulmonary edema**) or inflammatory exudate (**pneumonia**);
- Replacement of normal alveolar tissue by dense material (**pulmonary fibrosis**, **tuberculoma**, **tumor**).

3. Pulmonary Lucency (Decreased Attenuation)

Lucent zones on radiographs indicate reduced soft-tissue volume and, consequently, increased air content in the whole lung or part of it. Lucencies may be diffuse (emphysema, complete pneumothorax) or localized.

They occur in:

- Cavitary lung destruction (cavities in tuberculous infiltration, abscesses, disintegrating tumors, emptied cysts);
- Air accumulation in the pleural space (**pneumothorax**);
- Increased lung aeration (**pulmonary emphysema**).

Internal (intrapulmonary) and external (extrapulmonary) causes of opacification/lucency must be distinguished during radiological evaluation.

Intrapulmonary Opacities

Classified by number:

- **Solitary** — one to three dense foci (small or large);
- **Multiple** — numerous small foci;
- **Unilateral** — limited to one lung;
- **Bilateral** — present in both lungs.

Classified by size:

- **Focal shadows** — up to 1 cm (conventional term in phthisiology);
- **Infiltration-like shadows** — larger than 1 cm;
- **Large opacities** — involving part of a segment or an entire lobe (e.g., lobar pneumonia, cirrhosis, atelectasis).

Classified by shape:

- **Focal (round/oval, ≤1 cm)** — typical for pulmonary tuberculosis.
- **Round or spherical (>1 cm)** — found in peripheral lung cancer, tuberculous infiltrates, tuberculomas, solitary metastases, cystic lesions, round pneumonia, etc.
- **Triangular/pyramidal** — typical for segmental involvement (segmental pneumonia or atelectasis).
- **Irregular-shaped** — extensive inflammatory processes involving several segments or a whole lobe.
- **Lens-shaped** — in localized (encysted) interlobar or parietal pleuritis.
- **Linear** — due to thickened peribronchial/perivascular interstitium, chronic bronchitis, pneumosclerosis, or pleural adhesions.

By intensity (density):

- **Low-intensity** — faint opacities, often reflecting active inflammation (e.g., focal pneumonia, early infiltrative tuberculosis).
- **Moderate-intensity** — less dense than ribs; indicate partial organization of inflammatory tissue.
- **High-intensity** — similar to bone density; indicate advanced fibrosis or calcification.

By contour clarity:

- **Sharp contours** — well-demarcated margins; may reflect encapsulation or expansile tumor growth.
- **Blurred contours** — surrounding inflammatory or tumorous infiltration.

By structure:

- **Homogeneous** — uniform density.
- **Heterogeneous** — containing cavities, calcifications, septations, or mixed elements.

Intrapulmonary Lucencies

Observed in:

- **Pulmonary emphysema** (local, regional, diffuse)
- **Lung tissue destruction** (cavities in abscesses, infiltrative tuberculosis, tuberculomas, cavitary cancer, solitary metastasis)
- **Air-filled cysts**

Extrapulmonary Opacities

May be caused by:

Pleural origin:

- Exudate, transudate, hemothorax, empyema;
- Paracostal and interlobar loculated pleuritis.

Pleural/Chest wall structures:

- Pleural thickening/plaques;
- Rib pathology (fractures, cysts, osteochondromas, chest wall deformities).

Spinal origin:

- Neurinomas, paravertebral abscesses, deformities in tuberculous spondylitis.

Mediastinal origin:

- Enlarged mediastinal lymph nodes (tuberculous lymphadenitis, lymphoma, sarcoma, metastases).

Esophageal origin:

- Esophageal dilatation (achalasia, cardiospasm, cicatricial strictures).

Extrapulmonary Lucencies

Occur in:

- **Pneumothorax** — air in pleural cavity (spontaneous, diagnostic, therapeutic)
- **Hydropneumothorax** — air + fluid
- **Hemopneumothorax** — air + blood
- **Pyopneumothorax** — air + pus

Functional Radiological Signs

Observed during fluoroscopy:

- **Diaphragmatic movement** — downward on inspiration, upward on expiration.
- **Paradoxical diaphragmatic movement** — upward on inspiration, downward on expiration (due to phrenic nerve injury).
- **Mediastinal shift during forced inspiration** — towards partially obstructed bronchi (**Holzknecht–Jacobson sign**).
- **Fixed mediastinal shift** — toward the side of segmental/lobar atelectasis.
- **Persistent elevation of the diaphragm** — due to volume loss of affected lung segments.
- **Change in shape of a lesion during respiration** — indicates elastic properties (useful in differentiating tumors from cysts).

4. Changes in the Lung Roots (Hila)

- **Unstructured hilum** — occurs due to vascular congestion, inflammatory infiltration, edema, or enlarged lymph nodes; may also be obscured by overlying pathological shadows.
- **Hilum shift toward pathology** — seen in chronic inflammatory changes with fibrosis or in atelectasis.
- **Hilum enlargement** — due to vascular dilatation, edema, fibrosis, or enlarged lymph nodes.
- **Hilum reduction** — due to decreased pulmonary blood flow (Tetralogy of Fallot, pulmonary artery stenosis).

Chapter 2

CLINICAL AND RADIOLOGICAL FEATURES OF DIAGNOSTICS AND DIFFERENTIAL DIAGNOSIS OF LUNG DISEASES AND TUBERCULOSIS

2.1. Primary Tuberculosis Complex

The **primary tuberculosis complex (PTC)** is characterized by the development of inflammatory changes in the lungs, involvement of the intrathoracic lymph nodes, and lymphangitis. It is most frequently observed in children.

The nosological diagnosis *"primary tuberculosis complex"* was introduced by Ranke and refers to the presence of:

- a **primary focus in the lung** (pulmonary component),
- a **cluster of affected intrathoracic lymph nodes** (nodal/glandular component), and
- a **specific lymphangitis** along the lymphatic vessels extending from the pulmonary focus toward the involved lymph nodes.

This form of tuberculosis is more common among children who have not received timely BCG vaccination.

In its clinical course, the primary tuberculosis complex progresses through **four stages**:

- **Initial – pneumonic stage** (Fig. 2.1.1)

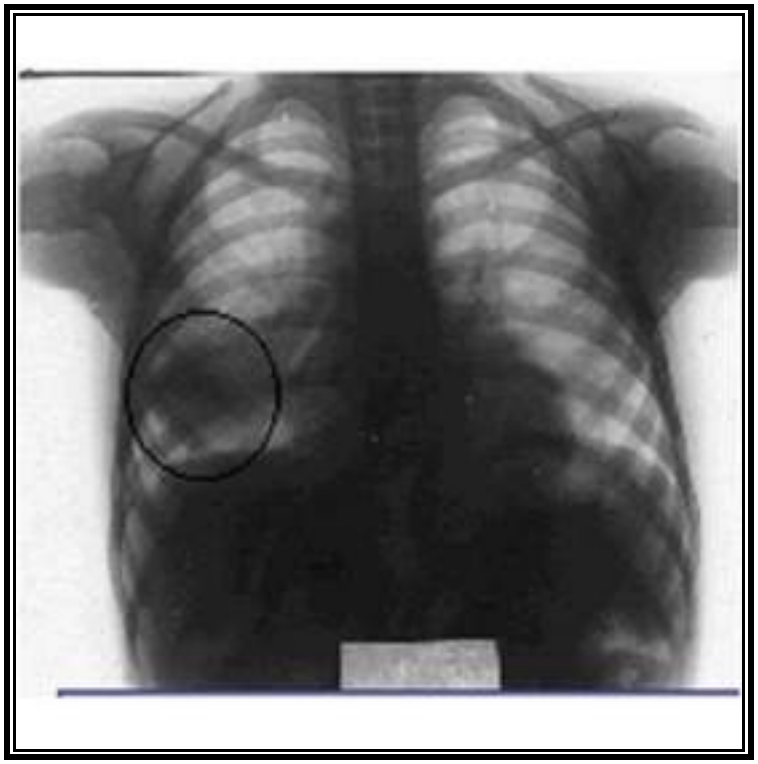

- **Organizational stage**, characterized by the onset of resorption of the infiltrative zone and the appearance of **bipolarity (the Redeker sign)** (Fig. 2.1.2).

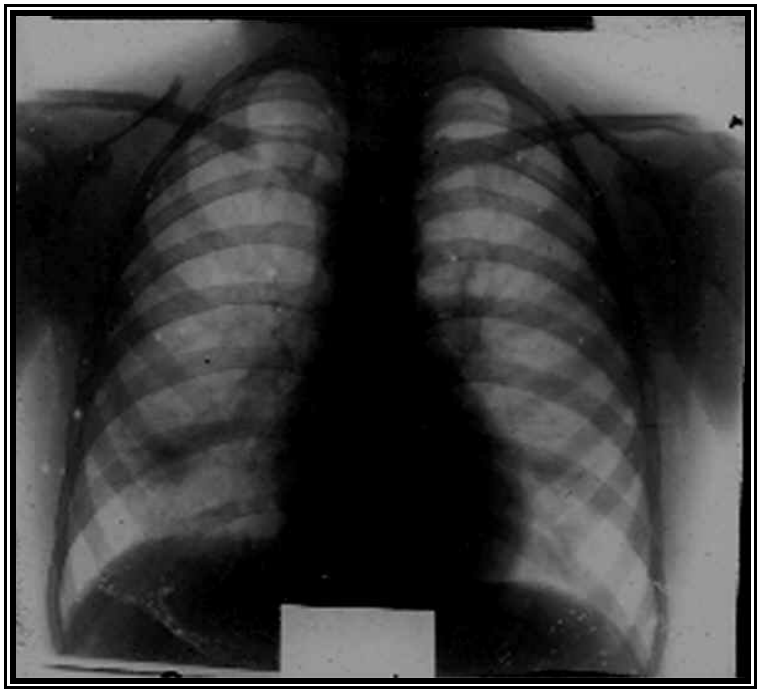

➢ **Consolidation stage** (Fig. 2.1.3)

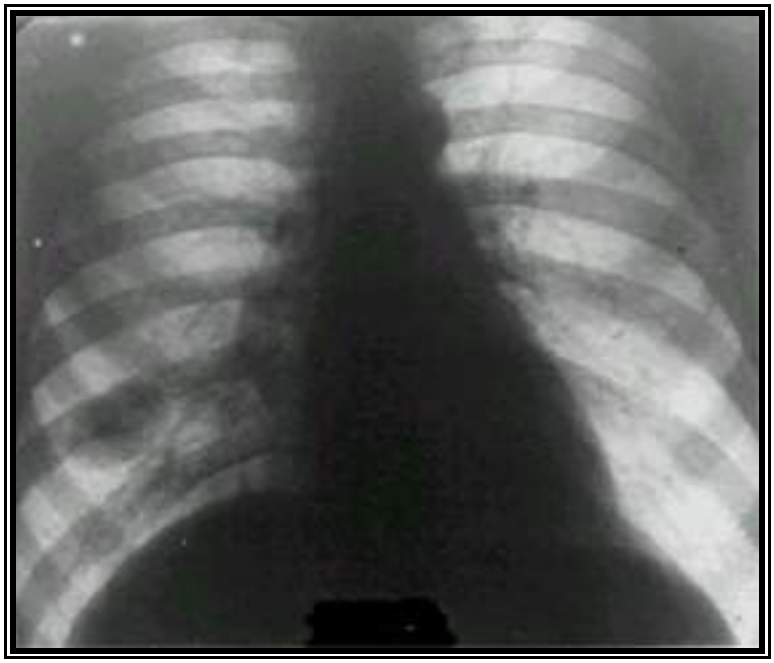

➢ **Stage of petrification of the primary tuberculosis complex** (calcification within the right bronchopulmonary lymph node group) (Fig. 2.1.4)

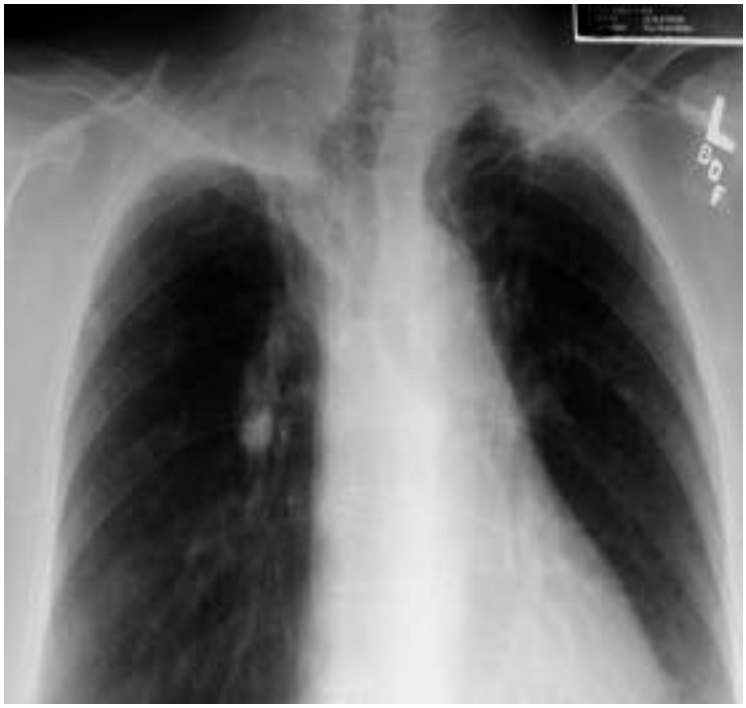

Clinical manifestations of the primary tuberculosis complex (PTC) depend on the phase of the process, the characteristics of its course, and the reactivity of the host organism. The disease may be oligosymptomatic; however, signs of **tuberculous intoxication** are

more common, particularly when the process extends to the serous membranes (pleuritis, polyserositis) or the bronchi.

Two variants of the course are distinguished: **complicated** and **uncomplicated** PTC.

In a complicated course, the specific inflammatory process in the lungs may progress to **tissue breakdown** with the formation of a *primary cavity*, involvement of the bronchi, development of **atelectasis** in other lung segments, and **lymphogenous or hematogenous dissemination**. Paraspesific allergic reactions may occur, along with increased **tuberculin hypersensitivity**.

Under current conditions, in most patients—especially under the influence of modern chemotherapy—the primary tuberculosis complex tends to present with **mild clinical symptoms**, showing a natural tendency toward **resorption, consolidation, and calcification**. Calcification of the primary pulmonary focus and lymph nodes in adults is observed only exceptionally. The classical form with typical bipolarity is now encountered less frequently.

On computed tomography (CT), the pathological process is characterized by the presence of an **inflammatory infiltrate** in the lung parenchyma, **enlargement of regional lymph nodes**, and a zone of **peribronchovascular changes** between the thickened pulmonary focus and the lung root (Figs. 2.1.5–6).

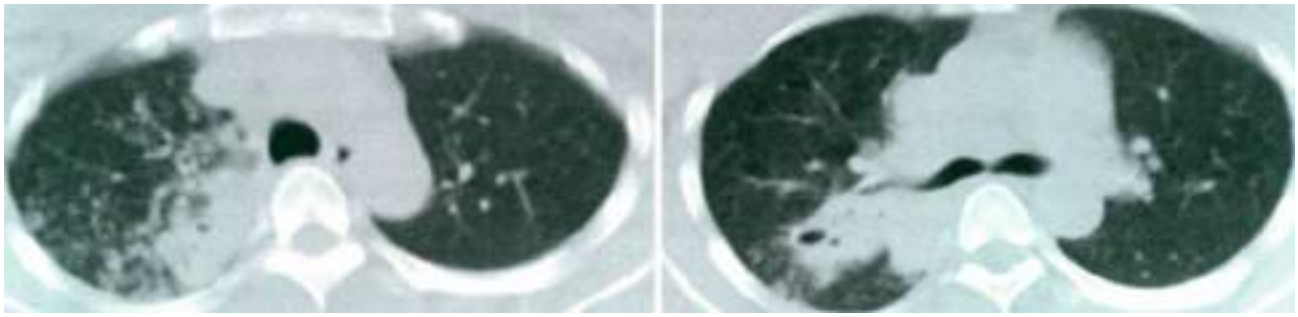

Fig. 2.1.5. Primary tuberculosis complex. Multiple focal and infiltrative lesions are present in the upper lobe of the right lung. Enlarged lymph nodes are visualized in the lung hila. An infiltrate in segment S2 of the right lung contains a cavitary area of breakdown **without an air–fluid**

level.

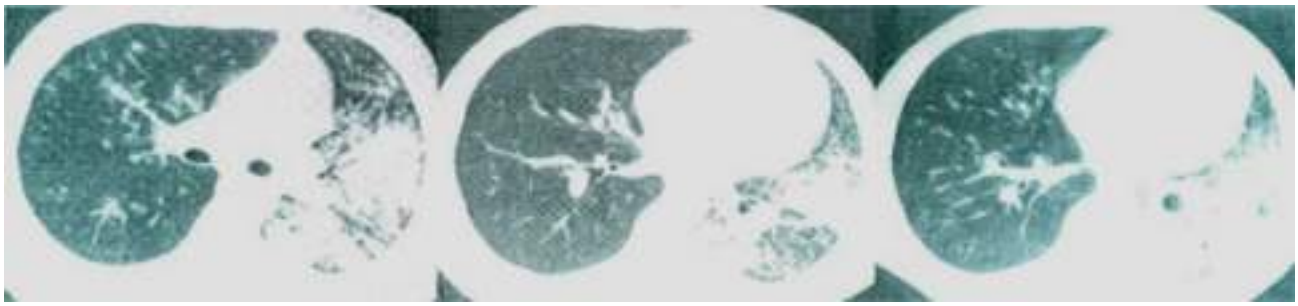

Fig. 2.1.6. Primary tuberculosis complex.

Massive infiltration in the left lung with a cavitary area of breakdown in segment S10 **without an air–fluid level**. Multiple small foci are present in segments S3 and S6 of the right lung. Enlarged lymph nodes are visualized in the left pulmonary hilum.

In modern conditions, with the progression of the HIV epidemic, pediatric phthisiologists increasingly encounter manifestations of the primary tuberculosis complex (PTC) in children born to HIV-infected mothers who did not receive BCG vaccination against tuberculosis in the maternity hospital. In such children, the clinical manifestations of the primary tuberculosis complex are more pronounced, and clinical-laboratory diagnostics may be challenging due to the **atypical course of the disease** (Fig.2.1.7).

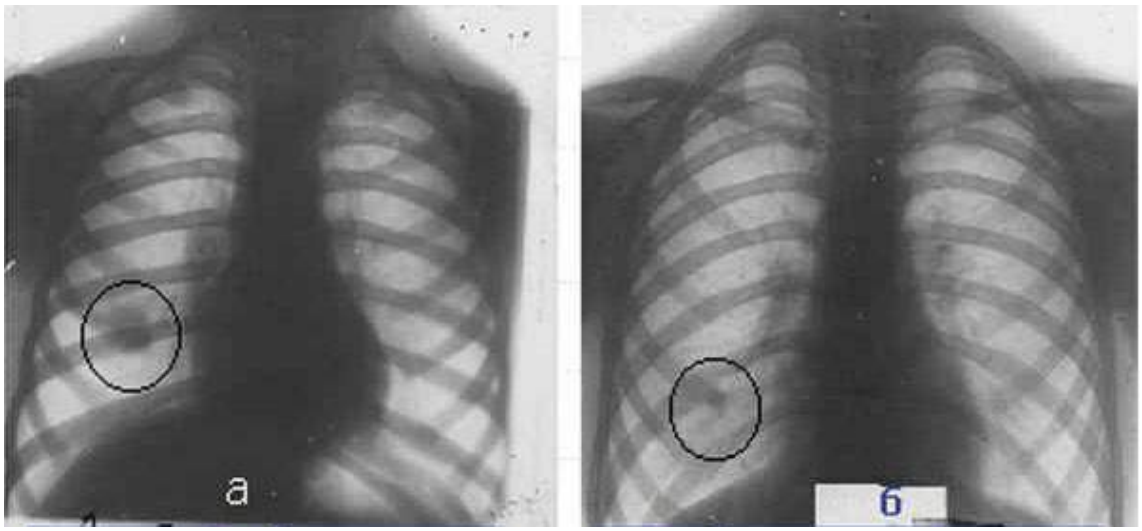

Fig. 2.1.7. Dynamic course of the primary tuberculosis complex.

In an uncomplicated course, the symptoms of the disease resolve rapidly, the hemogram returns to normal, and the specific changes in the lungs and lymph nodes gradually undergo resorption. The macro- and micro-morphological histological changes characteristic of the primary tuberculosis complex are illustrated in Fig. 3.1.8.

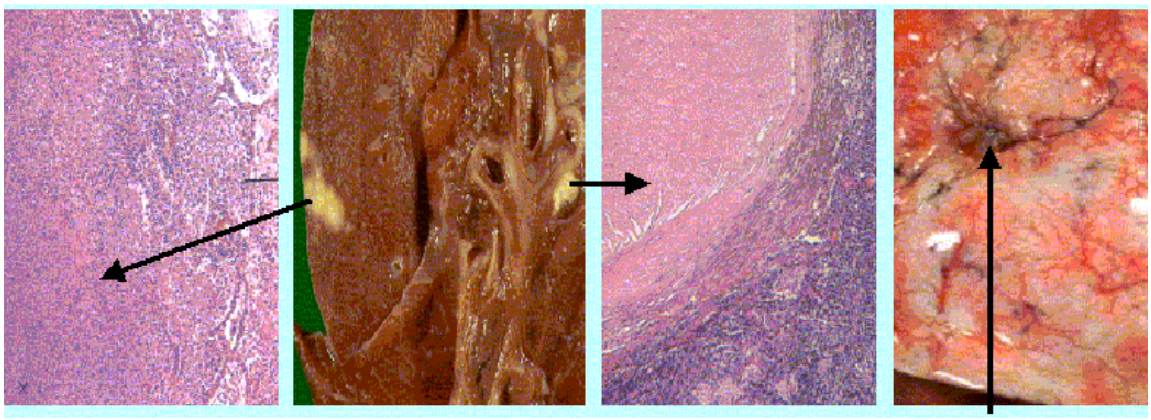

Fig. 2.1.8. Macro- and micro-morphological histological changes in the primary tuberculosis complex.

The most common complications of the primary tuberculosis complex include apical pleuritis, atelectasis, and miliary tuberculosis (Figs. 2.1.9 a, b, c).

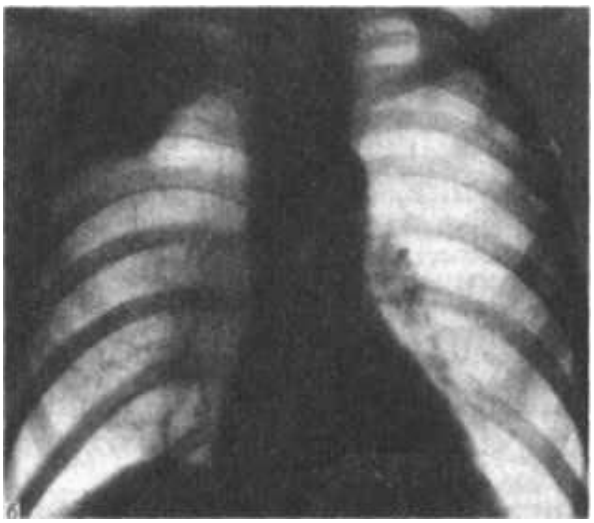

а) Apical pleuritis

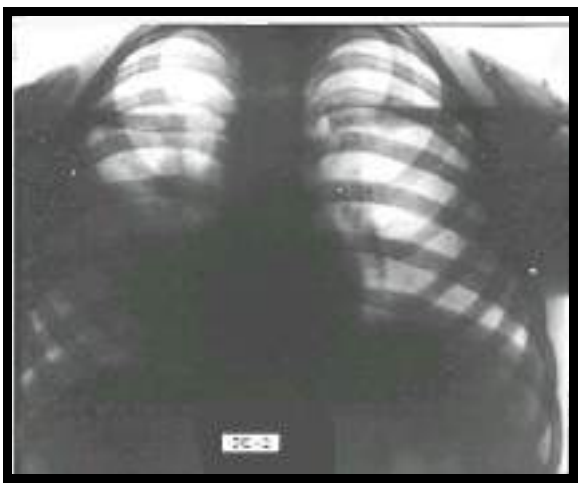

б) Atelectasis

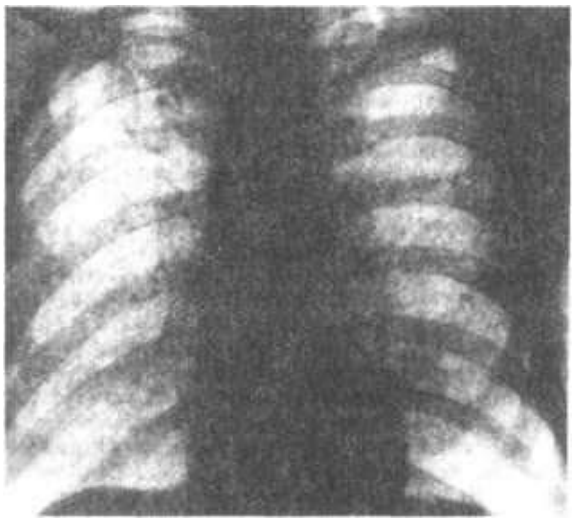

в) Miliary tuberculosis

Fig. 2.1.9. Complications of the primary tuberculosis complex.

2.2. Tuberculosis of the Intrathoracic Lymph Nodes

Tuberculosis of the intrathoracic lymph nodes (ITLN TB) develops as a result of **primary infection** with *Mycobacterium tuberculosis* in children, adolescents, and young adults. Less frequently, it occurs due to **reactivation** of previously existing tuberculous lesions within the intrathoracic lymph nodes.

Three variants are distinguished:

- the **infiltrative** form,
- the **tumor-like** form, and
- the so-called **“minor” forms** of ITLN TB.

The **infiltrative form** of ITLN TB is characterized not only by lymph node enlargement but also by the development of **infiltrative changes** in the perihilar regions of the lung parenchyma. The clinical picture is dominated by symptoms of **intoxication** (Figs. 2.2.1–2).

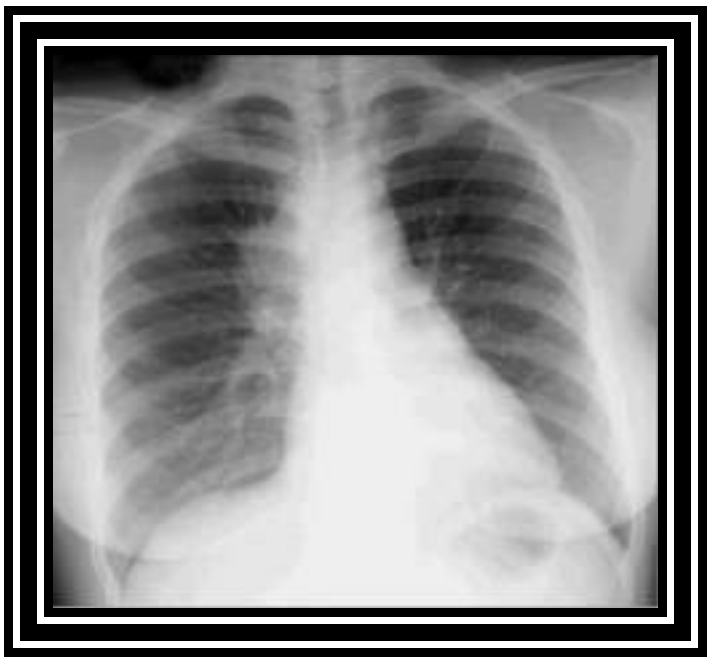

Fig. 2.2.1. Infiltrative form of tuberculous bronchoadenitis on the right in a 27-year-old woman

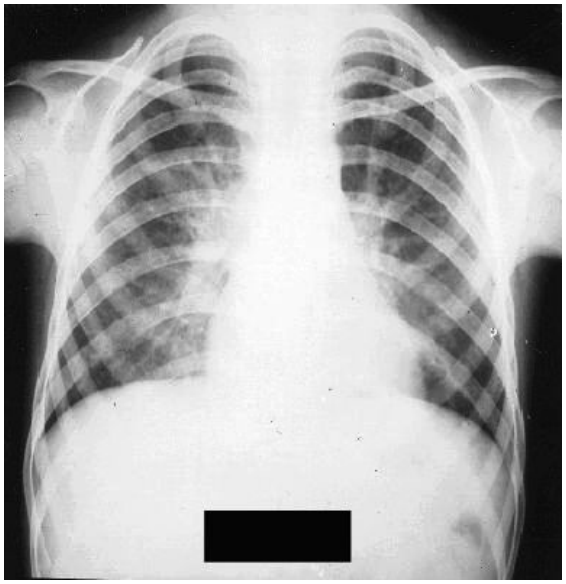

Fig. 2.2.2. Infiltrative tuberculosis on the right in a 33-year-old man.

Tumor-like (tumorous) tuberculosis of the intrathoracic lymph nodes

The **tumor-like (tumorous) form** of ITLN TB is a variant of primary tuberculosis in which **caseous involvement of the lymph nodes predominates**. It manifests as enlargement of individual lymph nodes or entire nodal groups, pronounced clinical symptoms, and a tendency toward a **complicated course** (bronchial involvement, bronchoglandular fistulas, foci of bronchogenic, lymphogenic, and hematogenic dissemination, pleuritis, atelectasis).

The contours of the lymph nodes on radiographs and tomograms are typically **well defined** (Fig. 2.2.3).

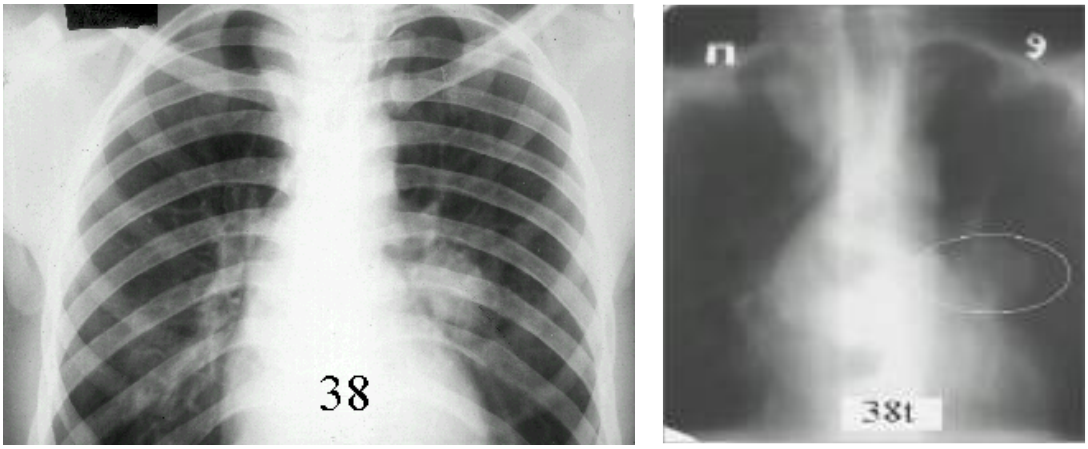

Fig. 2.2.3. Tuberculosis of the intrathoracic lymph nodes (tumorous form).
Enlarged lymph nodes of the left bronchopulmonary group with compression of the lower lobe bronchus and atelectasis of the lower lobe.

The **“minor” forms** of ITLN tuberculosis are characterized by slight enlargement of the lymph nodes and a subtle clinical presentation. Radiological diagnosis of minor forms in the infiltrative phase is possible only through **indirect signs**, such as:

- disturbance of the hilum shadow structure,
- a double contour of the mediastinal shadow,
- accentuation and local enhancement of the pulmonary pattern in a limited perihilar region.

Clinical manifestations typically include **moderate intoxication**.
The hilar shadow appears widened and elongated, convex, with indistinct and blurred margins. Projections of the major bronchi are not visualized, being obscured by inflammatory infiltration. Such a radiological pattern reflects a relatively small enlargement of the lymph nodes (most commonly bronchopulmonary) accompanied by perifocal infiltration of the lung parenchyma (Fig. 2.2.4).

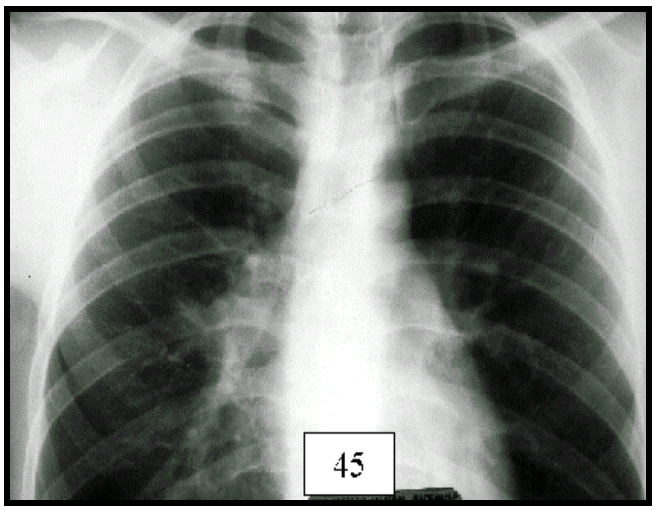

Fig. 2.2.4. Slight enlargement of the lymph nodes (most commonly the bronchopulmonary group) with perifocal infiltration of the lung parenchyma.

The primary CT sign of intrathoracic lymph node tuberculosis (ITLN TB) is **enlargement of the peritracheobronchial lymph node groups**. Typically, the bronchopulmonary lymph nodes at the lung hilum on one side, as well as the higher mediastinal lymph nodes, are affected. **Bilateral hilar involvement is not characteristic** of this form of tuberculosis.

Under normal conditions, lymph nodes do not exceed **10 mm** in size. This value is approximate, as inflammatory changes in lymph nodes may occur even at smaller diameters. Enlargement of the hilar lymph nodes leads to **widening of the lung hilum**, with margins becoming **irregular and undulating**. An important sign is **thickening of the interlobular interstitium** in the lung tissue adjacent to the hilum.

On native (non-contrast) CT scans, it is impossible to reliably differentiate between lymph nodes—even enlarged ones—and branches of the pulmonary artery within the lung hilum. The only usable reference point is the **combined diameter** of the artery and the lymph node. The normal diameter of the lower pulmonary arteries is **15–17 mm**. Considering that enlarged lymph nodes exceed **10 mm**, the **total shadow** of the artery and lymph node in the lung hilum should measure **over 25 mm**.

In ITLN TB, isolated involvement of the hilar lymph nodes **without mediastinal lymph node involvement** is extremely rare. On conventional radiography, mediastinal changes may remain

unrecognized; however, on CT scans, **lymph node enlargement** is the most important diagnostic feature (Fig. 2.2.5).

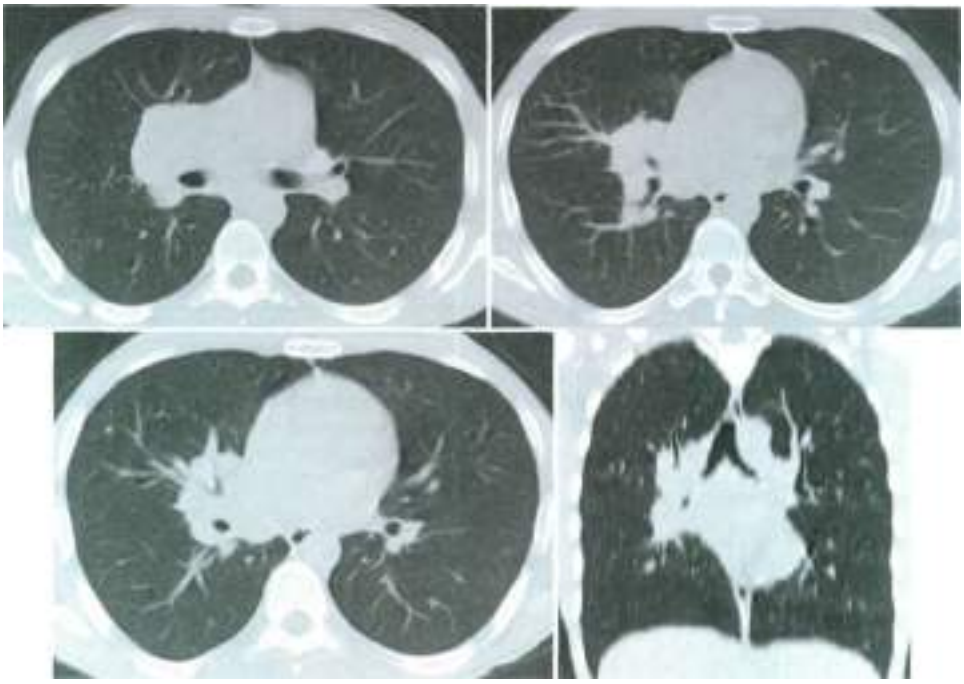

Fig. 2.2.5. Intrathoracic lymph node tuberculosis, GIST+.
Enlargement of the para-aortic, bifurcation, and right bronchopulmonary lymph nodes.

The detection of enlarged lymph nodes in the lung hilum in tuberculosis on CT requires detailed knowledge of normal anatomy. Large blood vessels—particularly the left pulmonary artery, the orifice of the middle-lobe artery, and the upper pulmonary veins—are often mistakenly interpreted as enlarged lymph nodes. When the CT findings are insufficiently clear, CT angiography must be performed.

The use of CT angiography allows not only confident differentiation between enlarged lymph nodes and major mediastinal or hilar vessels but also the identification of important features of lymphadenopathy in intrathoracic lymph node tuberculosis. The contrast agent accumulates actively in the capsule of the affected nodes, while the density of the caseous-necrotic masses remains unchanged. Increased density of the capsule is considered the most important differential diagnostic sign of tuberculous lymphadenopathy. Such a contrast-enhancement pattern is very rarely observed in other diseases, including metastases of small cell lung cancer, sarcoidosis, or lymphomas.

Using CT angiography, four stages of ITLN tuberculosis can be distinguished. In the initial stage, caseous necrosis of the lymph node

stroma develops while the integrity of the capsule is preserved. Tomograms reveal the characteristic **ring sign**, which reflects uniform accumulation of contrast material in the capsule of the nodes (Fig. 2.2.6).

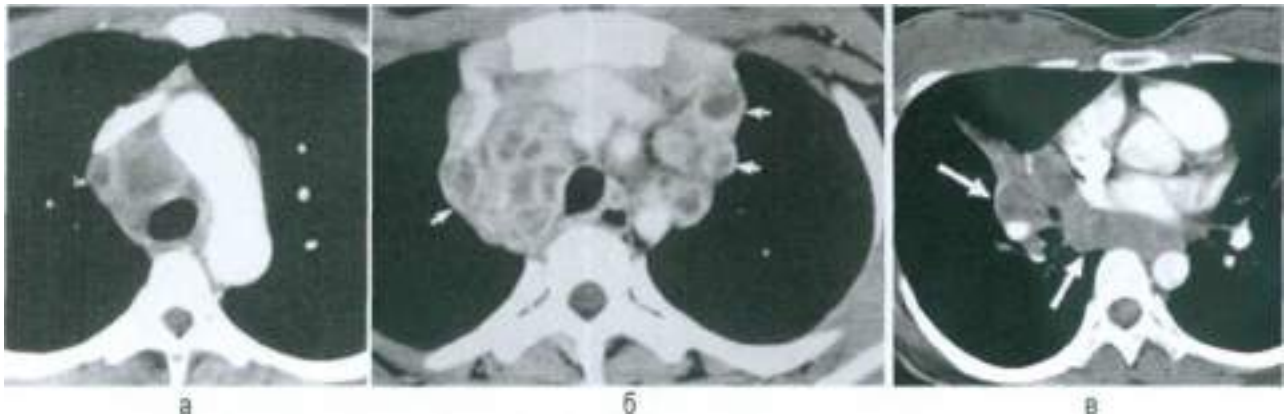

Fig. 2.2.6. Intrathoracic lymph node tuberculosis, developmental stage. CT angiography.

The second stage is characterized by partial destruction of the capsule and the leakage of caseous–necrotic material into the mediastinal fat. In this stage, the contours of the lymph nodes become irregular and indistinct, the adjacent fat tissue becomes densified, and contrast medium accumulates unevenly within the nodal capsule.

The third stage develops when there is substantial or complete destruction of the lymph node capsule, with fusion of the nodes into a single conglomerate. The lymph nodes exhibit a heterogeneous internal structure with areas of reduced attenuation (+10 to +25 HU), corresponding to purulent liquefaction of the caseous–necrotic material. After contrast administration, the capsules of the nodes are no longer visible.

In the final stage, caseous material ruptures through the wall of the adjacent bronchus into the airways, forming a **bronchoglandular fistula** (Fig. 3.2.7). A small cavity containing air typically forms within the lymph node. In the lung parenchyma, foci of dissemination may occur as a result of bronchogenic spread of the infection through the airways.

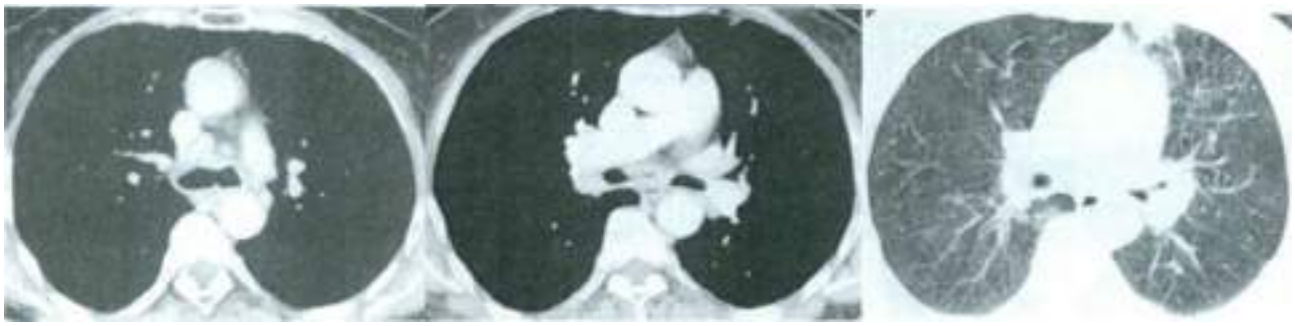

Fig. 2.2.7. Tuberculosis of the intrathoracic lymph nodes (Stage IV).
The bifurcation lymph node is located adjacent to the inner wall of the intermediate bronchus and is connected to it by a fistulous tract.
Numerous small foci of bronchogenic dissemination are present in the lung parenchyma.

The course of ITLN TB may be complicated by the development of hematogenous or lymphogenous dissemination, pleuritis, compression of the adjacent bronchus, and the formation of a broncho-glandular fistula.

Compression of a major bronchus leads to the development of obstructive atelectasis of the corresponding lung segment. A conglomerate of enlarged lymph nodes is visualized around the narrowed bronchus, resembling a neoplastic mass. In children and adolescents, such changes are most often caused by tuberculous involvement, whereas in adults over 40 years of age, a similar appearance is more commonly associated with central lung cancer. Verification of the nature of root changes is possible through histological examination following fibrobronchoscopy. However, CT provides a more detailed assessment of the degree and length of bronchial narrowing than bronchological examination.

Differential diagnosis.

Mediastinal neoplasms are extremely diverse in morphological forms and origin. They may be primary or secondary, benign or malignant, solid or cystic, and may arise from true mediastinal tissues, from ectopic tissues located within the mediastinum, or from the organs situated in the mediastinum. The most common are thymomas, neurogenic tumors, and benign cysts, which together account for up to 60% of all mediastinal masses. There are significant differences between adults and children: in adults, primary tumors of the thymus and thyroid gland

and malignant lymphomas predominate, whereas in children, neurogenic tumors, teratodermoid formations, and congenital cysts are more common.

The clinical manifestations of mediastinal neoplasms depend on their nature, location, and size. More than 80% of incidentally detected masses are benign, while over 50% of tumors presenting with clinical symptoms are malignant.

Each type of mediastinal tumor tends to have a characteristic, preferential localization, which greatly aids in determining its nature on radiography and CT.

In the anterior mediastinum, the upper part most often contains intrathoracic goiters extending from the neck. Lower, in the middle anterior mediastinum, thymomas, lymphomas, and teratodermoid masses are usually found. In most cases, thymomas and lymphomas are located anterior to the aortic arch and the main pulmonary artery, while teratomas lie slightly lower. The upper and lower margins of such masses depend on tumor size. Large tumors of lymphoid origin may occupy both the middle and upper anterior mediastinum, completely obliterating the retrosternal fat space. Thymic tumors more often extend inferiorly along the pericardium, spreading along the anterior and lateral surfaces of the heart and sometimes reaching the diaphragm.

In the lower anterior mediastinum, most retrosternal lipomas and a small portion of pericardial cysts are found. In such cases, the cysts are spindle-shaped formations between the sternum and the anterior wall of the right ventricle. However, the most common condition mimicking a mass in the lower anterior mediastinum is simple accumulation of retrosternal fat.

The middle mediastinum is the preferred location for bronchogenic cysts, often found adjacent to the lateral walls of the trachea in its upper or middle segments. Additionally, peritracheobronchial lymph nodes—frequently enlarged in numerous diseases such as tuberculosis, sarcoidosis, pneumoconiosis, metastatic disease, and other rarer conditions—are also located in this region. The middle mediastinum is also the site of most vascular pathologies such as aneurysms of the aorta and its major branches, dilatation of pulmonary arteries, and congenital variants or anomalies of large vessels.

In the posterior mediastinum, the most common pathological processes include neurogenic tumors located in the costovertebral recesses and bronchoenteric cysts adjacent to the esophagus. In addition, lymphoid masses, meningoceles, and various esophageal abnormalities may be found. At the thoracic inlet, the so-called posterior intrathoracic goiter may develop, representing a portion of an enlarged thyroid extending into the chest behind the trachea and large vessels. In the mid- and lower posterior mediastinum, aneurysms of the descending thoracic aorta and hiatal hernias are localized. Some authors also include paravertebral abscesses due to inflammatory, often tuberculous, spinal involvement as posterior mediastinal pathology.

The localization of pathological formations within specific mediastinal compartments usually allows a preliminary assumption of their nature. The difficulty is that many tumors and cysts may extend across multiple compartments, particularly mesenchymal tumors such as fibromas, lipomas, schwannomas, and lymphomas. Conversely, different pathological lesions may appear in the same mediastinal compartment—for example, thymoma, lymphoma, teratoma, and lipoma may all be located in the same portion of the anterior mediastinum—making differentiation by conventional radiography often impossible. CT and MRI supplement radiographic findings with valuable information about the internal structure of the lesion. The presence of calcifications, fluid, fat, air, or the lesion’s enhancement characteristics after contrast administration are critical features that should be determined before performing any invasive diagnostic or therapeutic procedures.

Calcification is one of the key differential diagnostic features of mediastinal masses. CT is the most effective method for detecting calcifications. Coarse calcifications are typical of teratodermoid formations, intrathoracic goiters, and hematomas. Diffuse, fine, or lamellar calcifications in lymph nodes are observed in tuberculosis and pneumoconiosis, and may also appear after radiotherapy in patients with malignant lymphomas. “Eggshell” calcifications of lymph nodes are characteristic of pneumoconiosis. Large (over 1.0 cm) calcified paratracheal lymph nodes—residuals of past primary tuberculosis—are often found in the mediastinum and are referred to as mediastinal tuberculomas. Linear calcifications are seen in the capsules of cystic

lesions (dermoid, parasitic, congenital cysts, encapsulated hematomas). Linear calcifications in the walls of large vessels, especially the aorta, indicate advanced atherosclerosis or aneurysms.

Teratodermoid formations are embryonic-origin neoplasms—germ cell tumors composed of various tissues not characteristic of the anatomical region in which they arise.

According to their histological structure, they are classified into teratomas, seminomas, embryonal cell tumors, choriocarcinomas, yolk sac tumors, and mixed neoplasms.

The most common germ cell tumors in the mediastinum are teratomas, which account for up to 75% of all lesions in this group. They may be solid (teratomas), cystic (dermoid cysts), mixed (teratodermoids), or malignant (teratocarcinomas, about 25%).

On CT, teratodermoid formations appear as round pathological masses typically located in the anterior mediastinum, more often in its middle portion, with displacement to the right or left (Fig. 3.2.8). Occasionally, teratodermoid lesions may occur in the posterior mediastinum (its middle or lower sections).

Benign teratomas have smooth, well-defined contours, whereas malignant ones more often display lobulated and indistinct margins. A definitive sign confirming the teratoid nature of the lesion is the presence of bone structures and teeth within the tumor.

Long-standing teratomas, especially those exhibiting transmitted pulsation, may cause erosion of the sternum and ribs.

In dermoid cysts complicated by rupture into the bronchus or esophagus, accumulation of air and a fluid level may be noted.

The major advantage of CT over conventional radiography is its ability to detect areas of low attenuation within dermoid formations corresponding to accumulations of fatty tissue and fluid.

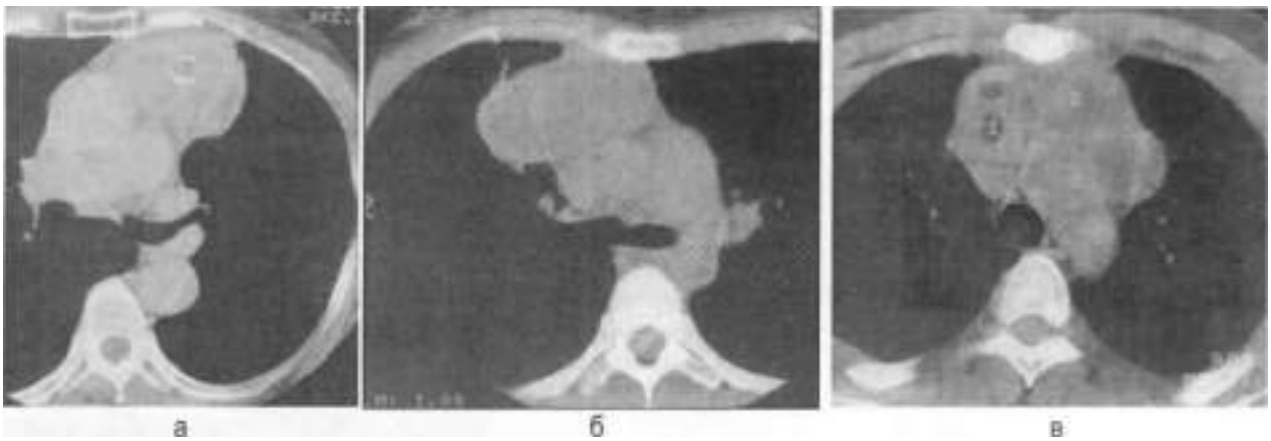

Fig. 2.2.8. Variants of teratodermoid formations.
A dermoid cyst located anteriorly and to the left of the ascending aorta, in the anterior mediastinum, with a heterogeneous structure due to calcium and fat inclusions (a).
A dermoid cyst located anteriorly and to the right of the ascending aorta, with a capsule and a dense internal structure (b).
A teratoma located in the anterior mediastinum, with a capsule and a heterogeneous structure due to fat inclusions (c).

Malignant germ cell tumors most commonly occur in adolescents, and almost half of these neoplasms are seminomas. These tumors also tend to localize in the middle part of the anterior mediastinum. On CT, they appear as **large masses of homogeneous soft-tissue density**, without calcifications, fat, or fluid components, often with **ill-defined margins** due to infiltration of adjacent tissues.

Fat-containing lesions in the thoracic cavity generally require differentiation from tuberculosis of the respiratory organs. Fat can be reliably detected on CT due to its **low attenuation values**, ranging from **–70 to –130 HU**. When fat is combined with other tissues, its density increases. In the mediastinum, fat-containing lesions are mostly benign. True lipomas are much less common than **diffuse lipomatosis** and **diaphragmatic fat herniation**.

Diffuse lipomatosis represents an idiopathic increase in the volume of mediastinal adipose tissue. On radiography, smoothing of the contours of the upper mediastinum and slight widening are observed. Fat accumulations **lack a capsule** and do not compress or displace the anatomical structures of the mediastinum. CT enables a definitive diagnosis and eliminates the need for further diagnostic procedures (Figs. 2.2.9–12).

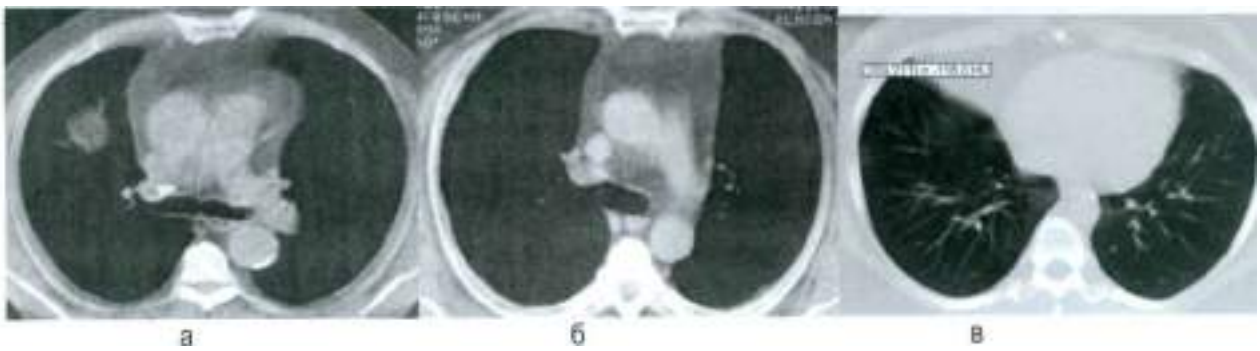

Fig. 2.2.9. Variants of mediastinal lipomatosis.
CT at the level of the tracheal bifurcation (a), lung hila (b), and diaphragm (c).
Excess accumulation of fat (–116 HU) in the anterior mediastinum without signs of encapsulation.

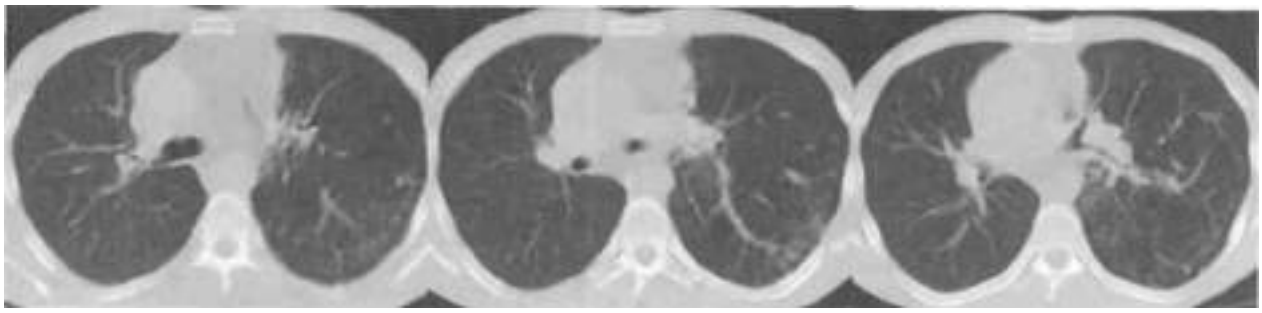

Fig. 2.2.10. Malignant diffuse mediastinal lipomatosis.
Accumulation of fat in the middle–lower mediastinum without a capsule; it does not compress but displaces the mediastinum to the right. In the cortical middle–lower segments of the left lung, multiple areas of parenchymal thickening of the “ground-glass” type are visualized.

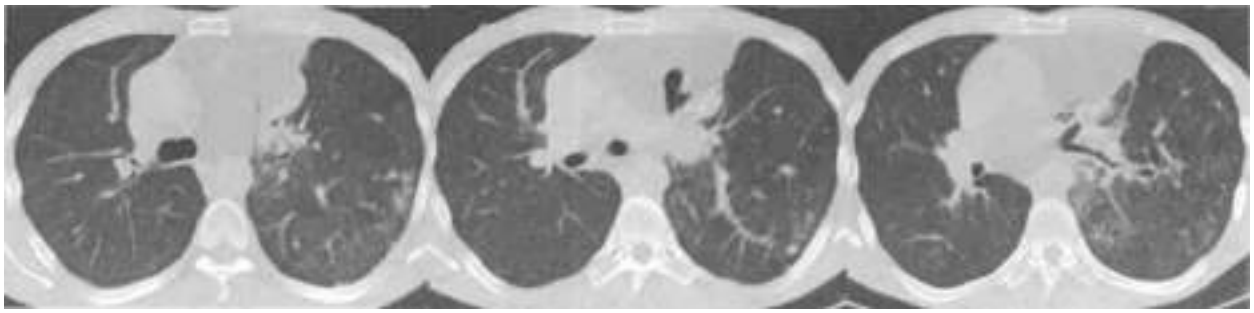

Fig. 2.2.11. The same patient after four years of follow-up. An increase in fat accumulation in the mid-lower mediastinum is observed, along with newly enlarged left bronchopulmonary lymph

nodes and small metastatic foci in the left lung, against the background of diffuse decreased lung transparency of the “ground-glass” type.

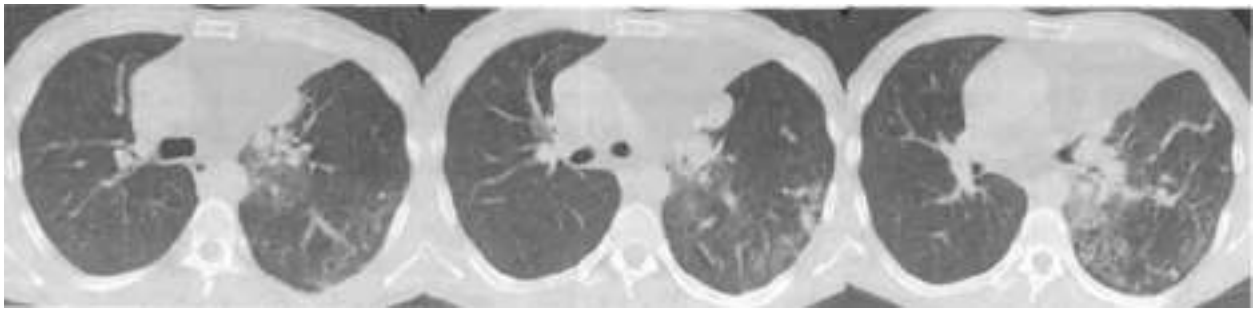

Fig. 2.2.7. Tuberculosis of the intrathoracic lymph nodes (stage IV). The bifurcation lymph node is located adjacent to the inner wall of the intermediate bronchus and is connected to it by a fistulous tract. Multiple small foci of bronchogenic dissemination are present in the lung parenchyma.

Fat that penetrates into the mediastinum from the abdominal cavity through the Morgagni or Larrey diaphragmatic apertures is often visualized on radiographs as a pathological mass in the cardio-diaphragmatic angle. Such formations usually need to be differentiated from coelomic pericardial cysts**.** On CT, these hernias demonstrate characteristic densitometric features, and the use of multiplanar reconstructions makes it possible to determine the anatomical continuity between fat collections in the thoracic and abdominal cavities (Fig. 2.2.13).

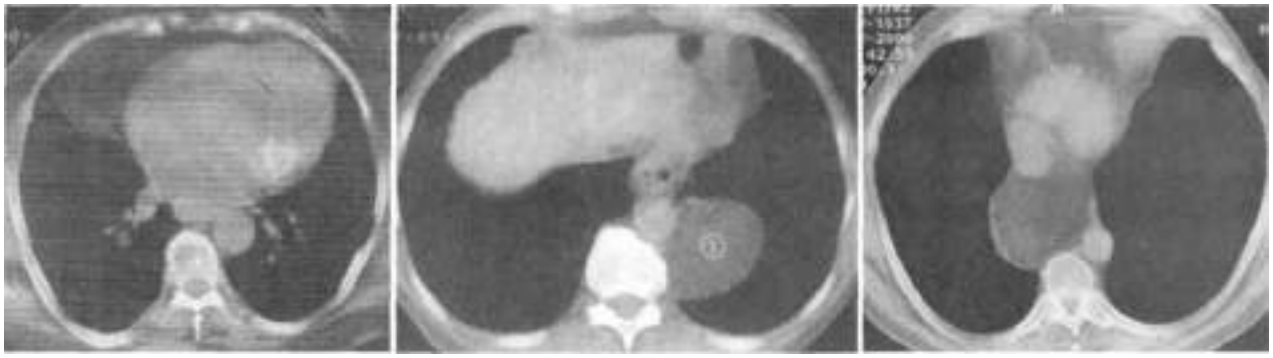

Fig. 2.2.13. Variants of diaphragmatic hernias (CT at the level of the diaphragm). Fat-containing hernias of the anterior (a), posterior (b), and esophageal (c) diaphragmatic openings.

Lipomas and liposarcomas of the mediastinum account for up to 1% of all primary mediastinal masses. Lipomas are benign, fully encapsulated tumors originating from mature adipose tissue. They are located either entirely within the mediastinum or may extend into two adjacent

anatomical regions (the mediastinum and the neck, or the mediastinum and the preperitoneal fat). Sometimes they arise from the adipose tissue of thymic remnants (thymolipomas). On CT, true lipomas have a thin capsule, a homogeneous structure, typical densitometric characteristics, and do not cause compression of mediastinal anatomical structures(Fig.2.2.14a).

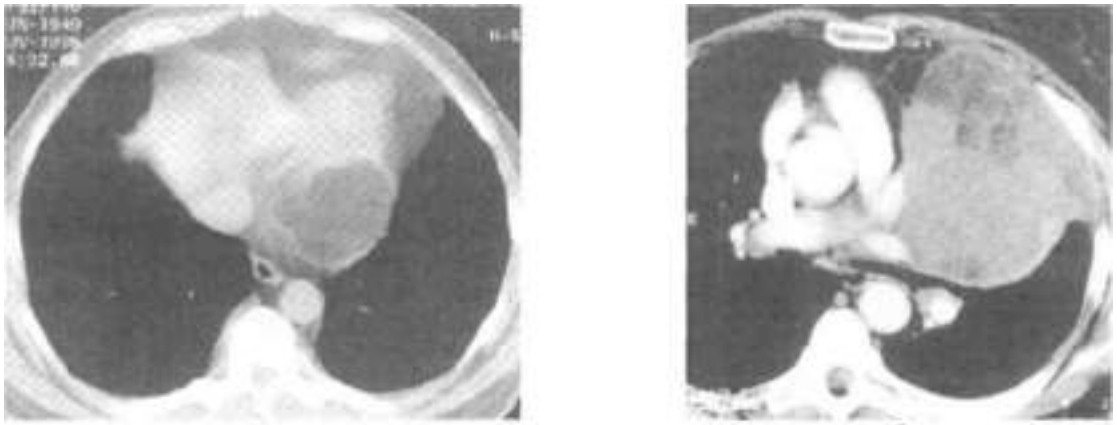

Fig. 2.2.14. Lipoma of the posterior mediastinum located adjacent to the posterior wall of the left ventricle (a). Liposarcoma of the anterior mediastinum (b). A pathological mass of heterogeneous structure with multiple fat inclusions (b).

Clinical manifestations of lipomas, even those of considerable size, are most often absent. Only occasionally may mild compressive symptoms be noted. Lipomas have a slow growth rate and very rarely undergo malignant transformation.

The most common are parasternal lipomas, which may be purely mediastinal or abdomino-mediastinal. The latter should be differentiated from herniation of the preperitoneal fat. Regardless of type, parasternal lipomas appear as oval or irregularly shaped masses closely adjacent to the heart, diaphragm, and anterior chest wall.

Cervico-mediastinal lipomas are characterized by one part of the tumor located in the cervical region and the other in the upper mediastinum, protruding toward one or the other hemithorax, more often to the right. With larger tumor size, displacement of adjacent anatomical structures (esophagus, trachea, aortic arch) may occur. The radiographic appearance is quite similar to that of a cervico-mediastinal goiter. Distinguishing features include the immobility of the lipoma during swallowing and the absence of calcifications, while CT provides characteristic densitometric values. Lipomas may reach very large sizes

and, when located anterior to or along the borders of the heart, may lead to an apparent enlargement of the cardiac silhouette on radiography. A discrepancy between radiographic and echocardiographic findings is an absolute indication for CT, which establishes the precise diagnosis.

Liposarcomas differ by exhibiting invasive growth and, at the time of detection, often infiltrate adjacent vessels or cardiac chambers. On CT, liposarcomas show heterogeneous structure due to the presence of fat and denser tissues. Sometimes these lesions demonstrate uneven soft-tissue density (greater than +20 HU), and the nature of the mass can only be determined histologically (Fig. 2.2.14b).

A number of mediastinal tumors may contain fat detectable on CT. These include thymolipomas and teratomas, as well as the rarer angiomyolipomas and hemangiomas.

Bronchogenic cysts are thin-walled, unilocular cystic formations that represent homoplastic dysembryomas, with walls similar in structure to the bronchi and trachea. They are located in the middle or upper parts of the central mediastinum, in close proximity to the trachea and the main and lobar bronchi.

On CT, bronchogenic cysts appear as oval lesions with a homogeneous structure, smooth and well-defined margins, and a broad base abutting the airway (Fig. 2.2.15). Displacement of the trachea, unlike in mediastinal goiter, is minimal. Cysts located in the region of the carina usually do not extend beyond the mediastinal contours and are typically detected only by CT. When a bronchogenic cyst ruptures into the tracheobronchial tree, a fluid level is visualized within it.

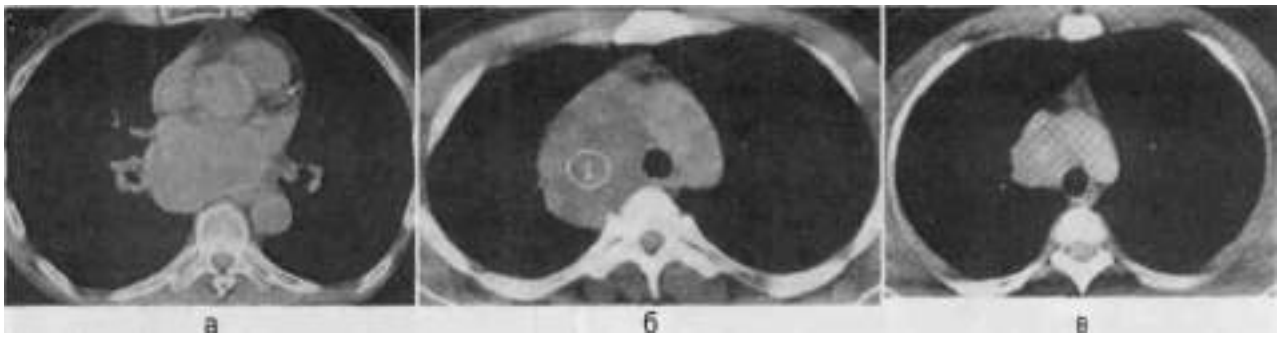

Fig. 2.2.15. Variants of bronchogenic cysts.
A large pathological lesion with a thin capsule is located in the central mediastinum, beneath the tracheal bifurcation.

Enterogenic cysts are also homoplastic dysembryomas, but their walls have a structure similar to that of various segments of the digestive tract (esophagus, stomach, intestine). The radiographic, CT, and MRI appearance of enterogenic cysts is identical to that of bronchogenic cysts; however, unlike the latter, they are usually located in the lower part of the posterior mediastinum, lying directly adjacent to the esophagus and causing its displacement and compression. Enterogenic cysts may develop complications such as infection, ulceration, or perforation into the esophagus, bronchi, or pleural cavity.

CT and MRI provide the most objective information regarding the cystic nature of a mediastinal lesion. CT reveals a thin, smooth cyst wall and characteristic attenuation values corresponding to fluid. Linear calcifications of the capsule are a common finding in bronchoenterogenic cysts. However, attenuation values vary significantly depending on the cyst content. A high concentration of protein, blood elements, or amorphous calcium may markedly increase density on native scans. In such cases, cysts can be difficult to differentiate from soft-tissue masses or even calcifications. An important CT criterion is the persistence of the cyst’s attenuation after intravenous contrast administration.

Coelomic cysts and pericardial diverticula are strictly benign entities and are genetically identical. Both arise from abnormal differentiation of the primitive embryonic cavity—the coelom—from which the pericardium develops. The distinction lies in the fact that diverticula communicate with the pericardial cavity, whereas cysts do not and are connected to the pericardium by planar adhesions or a stalk-like attachment. Because these lesions share a common origin and demonstrate identical imaging characteristics, they can be considered together. These are thin-walled, fluid-filled lesions of round, oval, or pear-shaped configuration. They are typically located in the anterior cardiophrenic angles, more frequently on the right (Fig. 2.2.16). In 10% of cases, pericardial cysts may be located in the upper mediastinum at the site where the pericardium attaches to the aortic arch, where they appear spindle-shaped. Their size usually does not exceed 4–6 cm. As fluid accumulates, their dimensions may increase, but this occurs very slowly.

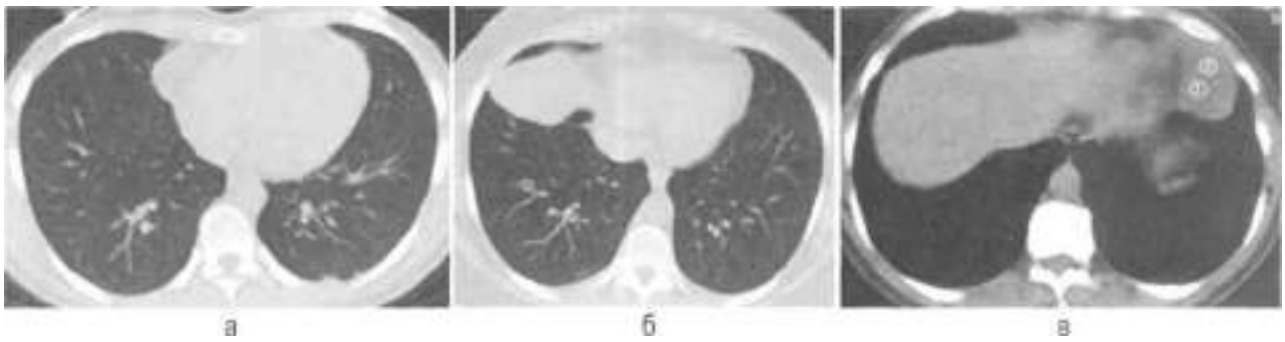

Fig. 2.2.16. Variants of pericardial coelomic cysts.

Clinically, cysts and diverticula are asymptomatic in the vast majority of cases. The complaints observed in some patients (discomfort or pain in the cardiac region, palpitations, arrhythmias, dyspnea) are caused by irritation of the nerve receptors of the pericardium.

Malignant lymphomas relatively often present with pathological changes in the mediastinum. The term *“lymphoma”* refers to primary malignant tumors of the immune system. It encompasses a group of diseases that includes Hodgkin’s disease, or lymphogranulomatosis (LGM), as an independent nosological entity, and a larger group of lymphoproliferative disorders classified as malignant non-Hodgkin lymphomas (NHL).

Lymphomas are the most common mediastinal tumors in patients aged 20–40 years. LGM has a characteristic bimodal age distribution, with peaks in the third and sixth decades of life. NHLs occur four times more frequently than LGM. In two-thirds of patients, the disease is diagnosed on the basis of asymptomatic peripheral lymphadenopathy persisting for 4–6 weeks.

After establishing the histological diagnosis—usually through a biopsy of a peripheral lymph node—imaging studies are required to determine the stage of the neoplastic process.

Lymphogranulomatosis begins with involvement of intrathoracic and peripheral lymph nodes in more than 60% of patients, followed by spread to lymph nodes of other anatomical regions. Typically, the nodes of the anterior superior mediastinum, pericardial nodes of the inferior mediastinum, and para-aortic nodes are affected. The pathological process usually progresses sequentially from one lymph node group to the next.

Malignant non-Hodgkin lymphomas begin in 80% of patients with involvement of abdominal lymph nodes (para-aortic, mesenteric, hepatic and splenic hilum, etc.), and only at a later stage does the disease

extend to thoracic lymph nodes. At the same time, the process is initially multifocal or diffuse and can rapidly involve distant lymph node groups and various parenchymal organs. The liver and spleen are the organs most typically affected.

In LGM, the most characteristic finding is involvement of the lymph nodes of the anterior mediastinum or the prevascular space, followed by the peritracheobronchial nodes and the pulmonary hila. This pattern occurs in more than 80% of patients with stage I–II LGM. The affected lymph nodes may appear as isolated enlarged nodes (Fig. 2.2.17), but more commonly form an irregularly shaped conglomerate with uneven contours, or a solitary soft-tissue density mass.

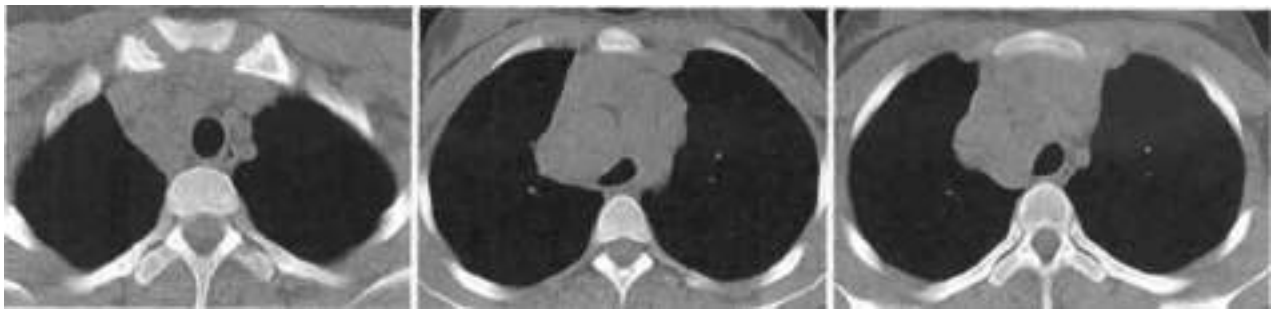

Fig. 2.2.17. Malignant lymphoma (Hodgkin's disease). Enlarged lymph nodes of the anterior and central mediastinum form an irregularly shaped conglomerate with uneven contours.

In non-Hodgkin lymphomas (NHL), involvement of various groups of lymph nodes is more typical, including cases without involvement of the anterior mediastinal nodes. In such situations, the lymph nodes of the central mediastinum, nodes along the trachea and main bronchi, as well as the hilar, posterior mediastinal, and paracardial nodes may be affected.

Thymic involvement is observed in 30% of patients. However, isolated thymic involvement in lymphomas **without mediastinal lymph node disease** occurs extremely rarely. This represents an important differential-diagnostic feature during CT evaluation of patients with anterior mediastinal pathology.

A characteristic sign of malignant growth is **infiltration of the adjacent fatty tissue and mediastinal pleura**, **thickening of the pericardium** (often with fluid accumulation), **pleural effusion**, and **infiltration of the lung parenchyma** (Fig. 2.2.18). Malignant lymphomas may extend to

the mediastinal vessels, which can be identified on CT angiography. After administration of iodinated contrast, the attenuation of tumor tissue increases only slightly, and areas of low-density necrosis are frequently observed.

The use of CT for staging malignant lymphomas has certain limitations. The main radiological sign of thoracic lymph node involvement is an increase in their size to more than 10 mm. However, smaller nodes do not exclude microscopic disease. Significant difficulties arise when assessing treatment response and during follow-up, because distinguishing fibrotic tissue from residual tumor in lymph nodes and extranodal lesions is not possible. More effective methods include MRI and gallium citrate scintigraphy.

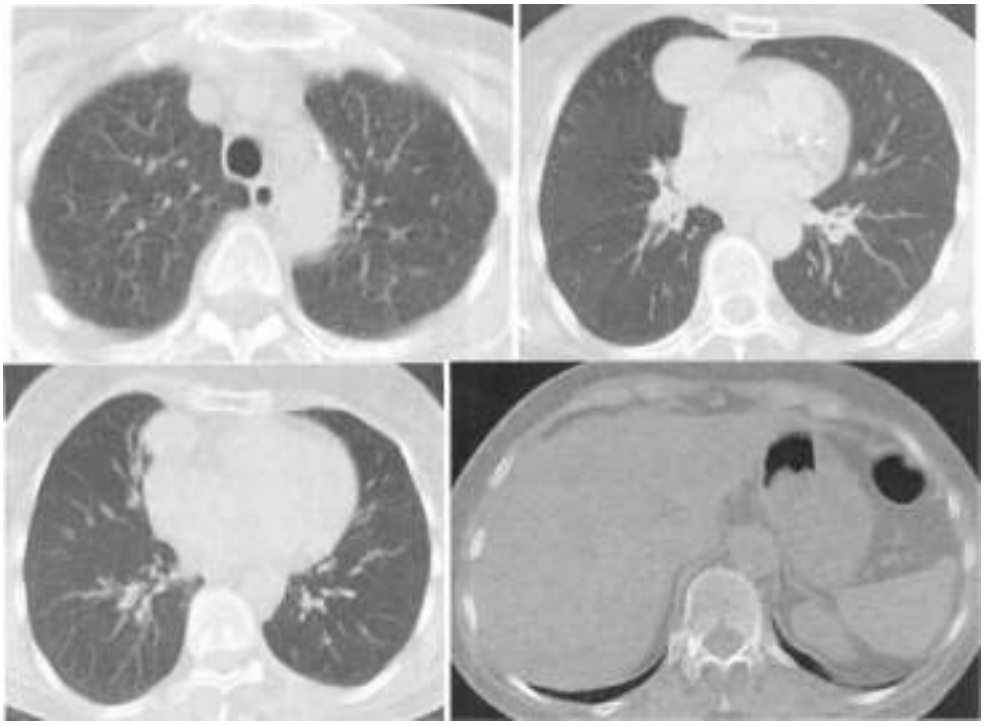

Fig. 2.2.18. Malignant thymoma.

Tumor involvement in malignant lymphomas often spreads from the lymph nodes to the lungs, producing an imaging pattern similar to primary lung cancer. According to various authors, pulmonary involvement occurs in **12–40%** of patients with Hodgkin lymphoma (HL) and in **4–24%** of those with non-Hodgkin lymphoma (NHL). Three CT patterns are distinguished: **nodular**, **bronchovascular-lymphangitic**, and **alveolar-pneumonic**.

A pleural effusion is observed in **6–33%** of patients with Hodgkin lymphoma and in **10–20%** of patients with non-Hodgkin lymphoma. A pericardial effusion is present in **one-third** of cases.

Sarcoidosis is a multisystem granulomatous disease of unknown etiology, relatively benign but prone to chronic progression, characterized by the accumulation of activated T-lymphocytes (CD4+) and macrophages in various organs, with formation of **non-caseating epithelioid cell granulomas**, leading to disruption of the normal architecture of the affected organ(s).

In most cases, the disease develops in individuals aged **20–40 years**. Epithelioid granulomas may form in any organ: lymph nodes, lungs, skin, liver, spleen, kidneys, salivary glands, eyes, heart, muscles, bones, intestines, and the central or peripheral nervous system. The most commonly affected sites are the **intrathoracic lymph nodes (95%)**. In **25–30%** of cases, only the intrathoracic lymph nodes are involved; in **65%**, lymph node involvement is combined with lung lesions; and in **5%**, the process is confined solely to the lungs.

According to the International Consensus (1999), thoracic sarcoidosis is divided into **five stages (0–IV)**, also referred to as “types”:

- **Stage 0** – no abnormalities on chest radiograph;
- **Stage I** – thoracic lymphadenopathy with normal lung parenchyma;
- **Stage II** – thoracic lymphadenopathy with parenchymal abnormalities;
- **Stage III** – parenchymal lung disease without lymphadenopathy;
- **Stage IV** – irreversible pulmonary fibrosis.

In **Stage I sarcoidosis**, CT typically demonstrates mediastinal lymphadenopathy involving the peritracheobronchial and preaortic lymph nodes, the hilar lymph nodes, and the pulmonary ligaments. **Symmetric hilar involvement** is characteristic of sarcoidosis and helps distinguish it from tuberculosis, in which hilar involvement is usually unilateral or at least asymmetric (Fig. 2.2.19). The lymph nodes retain a homogeneous internal structure, smooth and well-defined margins, and often appear as multiple nodes within a group; conglomerates may form, and the nodes can reach considerable size, but **do not cause bronchial obstruction**.

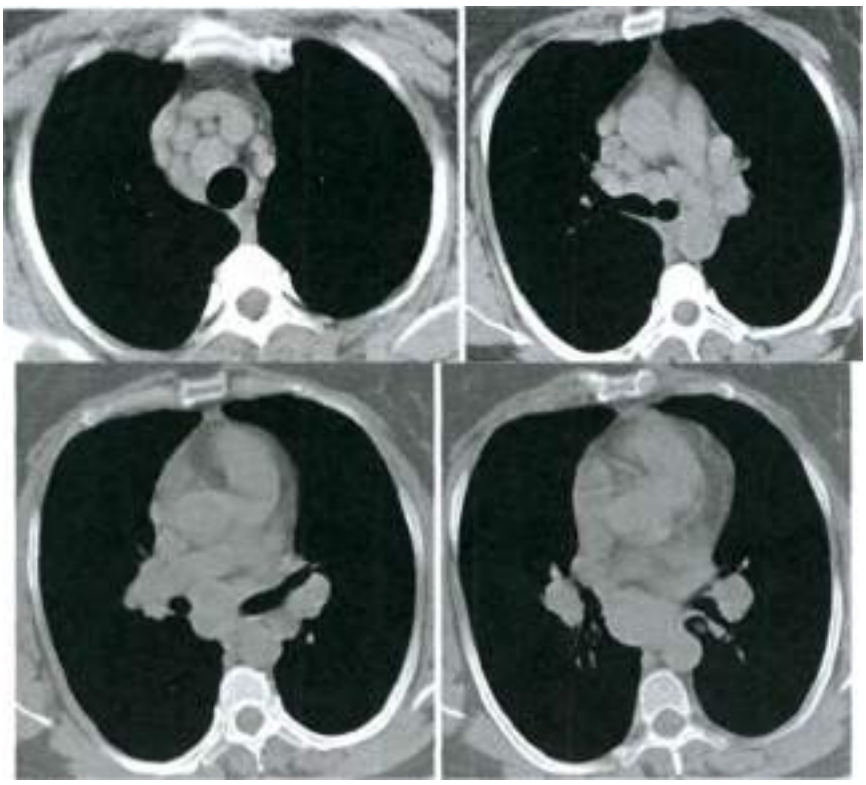

Fig. 2.2.19. Sarcoidosis, stage I.
A characteristic feature of sarcoidosis is the **polycystic (polylobulated) appearance of the lung hila**, caused by conglomerates of lymph nodes closely adjacent to the angle of bifurcation of the major bronchi (the so-called *"boot-shaped" or "clumped" lymph nodes* sign).
After intravenous contrast administration, **no enhancement patterns typical of tuberculosis** are observed (Fig. 2.2.20).

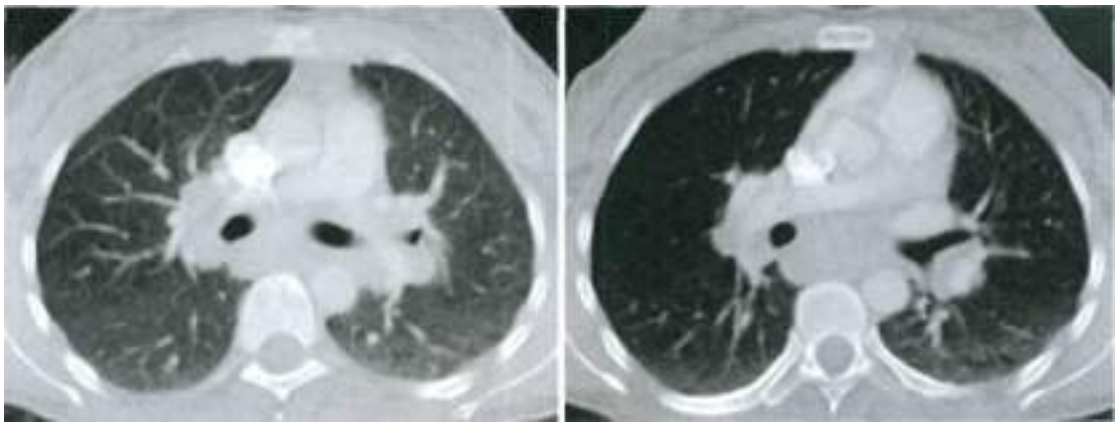

Fig. 2.2.20. Sarcoidosis of the intrathoracic lymph nodes.

Calcifications within the structure of the lymph nodes are observed in 30% of patients with chronic or generalized forms of sarcoidosis. Characteristic features of lymph node calcification in sarcoidosis include:

monolithic appearance, multiple localization, central position within the lymph node, and location distant from the bronchial wall (Fig. 2.2.21).

Fig. 2.2.21. Intrathoracic lymph nodes in sarcoidosis.

A decrease in the number and size of lymph nodes, deformation of their contours, increased structural density, and the absence of conglomerate formations are noted in the regression phase of sarcoidosis. Enlarged abdominal lymph nodes are detected in approximately 75% of cases during progression to the chronic stage, as well as in generalized sarcoidosis.

3.2. Diagnostics and Differential Diagnosis of Disseminated Lung Lesions and Disseminated Pulmonary Tuberculosis

Disseminated (diffuse) lung lesions (DLL) include pathological conditions characterized by widespread changes in both lungs, presenting as diffusely distributed foci, enlargement of the interstitial tissue, or a combination of these processes.

Diffuse lung diseases constitute a large and heterogeneous group of disorders differing in etiology, pathogenetic mechanisms, clinical and radiological manifestations, and pathohistological substrates. They may result from embryopathies and hereditary diseases, exposure of lung tissue to physical and chemical factors, organ-specific immunologic reactions (autoimmune or allergic), disturbances of pulmonary microcirculation (pulmonary hypertension), as well as inflammatory, metabolic, and neoplastic processes.

Disseminated focal lung lesions are characteristic of disseminated tuberculosis, pneumoconioses, sarcoidosis, pulmonary carcinomatosis, pulmonary edema due to acute left ventricular failure, and acute toxic pulmonary edema. Predominantly interstitial lesions with a reticular or

reticulonodular pattern are seen in hematogenous tuberculosis, pneumoconioses, sarcoidosis, pulmonary fibrosis secondary to cardiac defects, exogenous toxic and idiopathic pulmonary fibrosis (Hamman–Rich syndrome), allergic alveolitis, and carcinomatous lymphangitis. “Honeycomb lung” represents the terminal stage of sarcoidosis, Langerhans cell histiocytosis (Histiocytosis X), idiopathic pulmonary fibrosis, and some pneumoconioses.

Overall, widespread disseminated pulmonary involvement occurs in more than 150 diseases. Despite their diversity and significant differences, these disorders share the common feature of **diffuse lung involvement**, with the radiological picture serving as the cornerstone of diagnosis.

In most diffuse disorders, the primary pathogenetic substrate is an alterative-productive reaction of the alveolar septa (alveolitis, granuloma formation), vasculitis, or recurrent interstitial edema, accompanied by secondary productive-sclerotic changes in the lung stroma. Diffuse fibrosis in the lungs leads to gas-exchange impairment due to disruption of gas diffusion across the alveolar–capillary membrane. Thus, another unifying feature of these conditions is the development of **restrictive respiratory failure**, as reflected in pulmonary function testing: a decrease in vital capacity (VC) and maximal voluntary ventilation (MVV) to less than 80% of predicted values (based on height and weight).

Common clinical features of DLL include progressive inspiratory dyspnea, a sensation of chest tightness, mild cough, tachypnea, and auscultatory findings such as fine crackles or fibrotic rales over affected lung areas. In the phase of diffuse pneumosclerosis, when pulmonary arterial pressure rises and the right heart becomes overloaded, congestive heart failure joins the pulmonary insufficiency.

In the comprehensive diagnostic evaluation of DLL—based on history, physical examination, laboratory tests, and instrumental studies—**chest radiography (CXR)** plays a leading role, as it remains the only method of *in vivo* diagnosis of pulmonary dissemination. In latent disease, CXR often detects the condition first; in clinically manifest disease, it allows assessment of the extent and nature of the process, complications, and the status of intrathoracic lymph nodes. To identify DLL, chest X-rays must be obtained in both frontal and lateral projections.

For differential diagnosis—particularly when autoimmune lung diseases, neoplastic or tuberculous dissemination, or rare disorders are suspected—CT and MRI of the lungs are widely used, enabling diagnosis verification in 97% of cases.

The radiological picture of DLL depends on the underlying pathological changes. The alterations invariably involve alveolar epithelium, interstitial tissue, and capillary endothelium, but the nature, extent, and distribution of lesions vary widely. In alveolitis, three phases are observed: interstitial edema, infiltration, and proliferation followed by interstitial fibrosis. The pathomorphological substrate of all granulomatous diseases is granuloma formation. In connective tissue diseases, vasculitis and/or interstitial pneumonitis develop.

According to radiologic manifestations, three radiological syndromes are distinguished:

- **focal or nodular disseminated lung disease**,
- **reticular (interstitial) disseminated lung disease**,
- **reticulonodular (mixed) disseminated lung disease**.

Nodular DLL refers to numerous foci (nodules) in both lungs. Their substrate varies: granulomas, fibrotic nodules in pneumoconioses, proliferating and disseminated tumor tissue, acinar atelectasis, hemorrhages, etc. Depending on their diameter, disseminations are classified as miliary (0.5–2 mm), small-nodular (2–4 mm), medium-nodular (4–8 mm), and large-nodular (8–12 mm). The miliary type occurs in tuberculosis, pneumoconioses (silicosis), Langerhans cell histiocytosis, fungal infections, acute bronchiolitis, and hyaline membrane disease. Small- and medium-nodular DLL are typical for tuberculosis, pneumoconioses, sarcoidosis, fungal infections, pulmonary edema, systemic diseases, and malignancies. Large-nodular changes are mainly associated with neoplastic and parasitic diseases, tuberculosis, sarcoidosis, and silicotuberculosis.

Reticular (interstitial) DLL is characterized by reticular deformation of the lung pattern (“mesh-like” appearance). The substrate is an increased volume of fluid or tissue within the interstitial space. This pattern is typical for alveolitis, chronic bronchitis, pneumoconioses due to weakly fibrogenic dust (asbestosis, anthracosis), etc.

Mixed (reticulonodular) DLL represents a combination of reticular remodeling and multiple diffusely distributed nodular opacities, making the normal lung markings indistinguishable. The terminal manifestation of nodular and interstitial diffuse changes is **honeycomb lung**—a coarse fibrotic distortion with intervening emphysematous spaces resembling “honeycombs.”

An important component in the differential diagnosis of DLL is the **radiologic history**—previous CXR studies. DLL is not a static but a dynamic category of diseases; therefore, serial CXRs objectively reflect disease evolution, assisting in accurate staging, course assessment, and prognosis.

2.3. Diagnosis and Differential Diagnosis of Disseminated Lung Lesions and Disseminated Pulmonary Tuberculosis

2.3.1. Disseminated Pulmonary Tuberculosis

Disseminated pulmonary tuberculosis is characterized by the presence of multiple foci of dissemination—usually in both lungs—of hematogenous, lymphogenous, or mixed origin, varying in duration and demonstrating different proportions of exudative and productive inflammation, with acute, subacute, or chronic clinical courses.

The primary task of a general practitioner, internist, or pulmonologist is to exclude disseminated pulmonary tuberculosis, which is characterized by signs of intoxication: fever, pronounced night sweats, progressive weight loss, general weakness, and a significant decrease in working capacity; dyspnea even with minimal physical exertion; a mild productive cough with purulent sputum; on auscultation—harsh vesicular breathing and diffuse crepitations; and positive tuberculin tests (Mantoux test—papule or hyperemia at the site of administration of 2 TU).

Chest X-ray reveals symmetrical, relatively dense and unevenly distributed foci of various sizes and shapes (0.5–2 mm in diameter) in both lungs; their margins are indistinct, and the opacities vary in density, superimposed on a fine reticular pattern. A characteristic feature is the “sprinkling” phenomenon—an increase in the number of focal shadows over time—predominantly involving the upper lung zones (apical, posterior segments and the superior segment of the lower lobe). The pulmonary vascular pattern is diminished, as it is replaced by

disseminated lesions; hilar shadows remain unchanged. Common additional findings include fibrotic changes in the apical–subclavian regions and thickening of the interlobar and parietal pleura (Fig. 2.3.1.1).

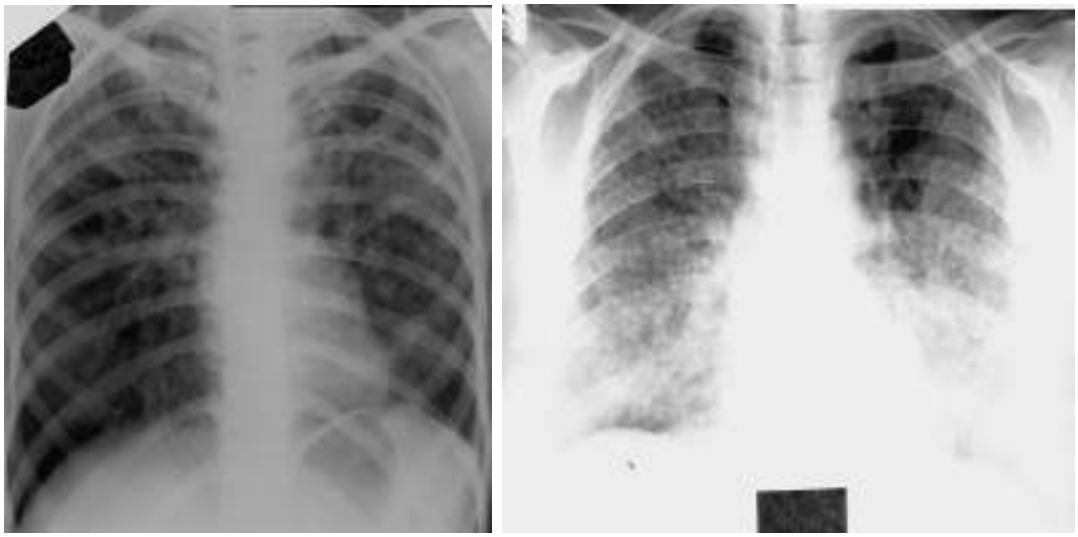

Fig. 2.3.1.1. Disseminated pulmonary tuberculosis.

During laboratory examination, signs of latent intoxication may be detected (elevated intoxication indices and ESR at a temperature of 37°C), positive immune tuberculin tests (RSAL, PPN, RBTL, RUK, etc.), and detection of mycobacteria in sputum. Bronchoscopy reveals characteristic bronchial changes and lymphocytosis in the bronchoalveolar lavage cytogram.

On CT, all forms of disseminated pulmonary tuberculosis are characterized by a combination of focal and interstitial changes in the lungs. The presence of foci of various shapes and sizes is an obligatory element of the CT picture in all patients. The severity and character of interstitial changes depend significantly on the duration of the disease and the pathogenic variant of its development.

Hematogenous tuberculous disseminations are distinguished by a predominance of focal changes in the lungs. Changes in disseminated pulmonary tuberculosis are characterized by the appearance of multiple uniform or polymorphic foci in both lungs. The foci are distributed throughout the lung fields; however, their distribution is not as uniform as in miliary tuberculosis. Lesions predominate in the upper lobes of the lungs, especially in the apical segments, where not only larger foci but

also small infiltrates with tiny cavities of destruction and isolated thin-walled cavities may be detected.

In the lower lobes, particularly in the basal segments, the number and size of foci are smaller than in the upper lobes. A characteristic feature is the uneven and asymmetric involvement of individual lobes and segments, with the appearance of areas exhibiting more or less pronounced changes. Interstitial changes in this group of patients are also significantly expressed; however, they do not display the uniformity seen in patients with miliary forms. Changes predominantly involve larger interstitial structures such as interlobular septa, while the overall increase in lung tissue density is minimal. Thickening of interlobular septa and walls of small bronchi results in a characteristic reticular deformation of the pulmonary pattern, most pronounced in areas of focal clustering.

Chronic hematogenous disseminations are characterized by predominant focal changes in the upper lobes of the lungs, primarily in the apical and posterior segments. In the basal segments and middle lobes, foci are absent or present in small numbers. At sites of maximal focal concentration, as well as within infiltrates, cavities of destruction of varying diameter develop. These cavities have a regular round shape, thin walls, and contain no fluid.

Interstitial changes include marked thickening of interlobular septa and bronchial walls, and the appearance of coarse fibrous strands within the lung parenchyma extending toward the pleura. A typical feature is a reduction in upper-lobe volume with a simultaneous increase in the volume of the lower lobes.

Lung tissue density in the basal segments may decrease significantly to −900...−950 HU, indicating the development of emphysema. At the same time, emphysematous bullae and areas of paraseptal emphysema appear in the upper lobes along the costal, mediastinal, and interlobar pleura. Multiple air-filled cavities displace the foci and infiltrates deeper into the lung tissue toward the lung root. In the final stage of the process, these changes can be described as a **“honeycomb lung”** (Figs. 2.3.1.2–8).

Fig. 2.3.1.2. Subacute hematogenous-disseminated pulmonary tuberculosis, MBT+.
Fine bilateral dissemination with a chaotic distribution of foci in the lung parenchyma, predominantly in the upper lobe of the right lung.

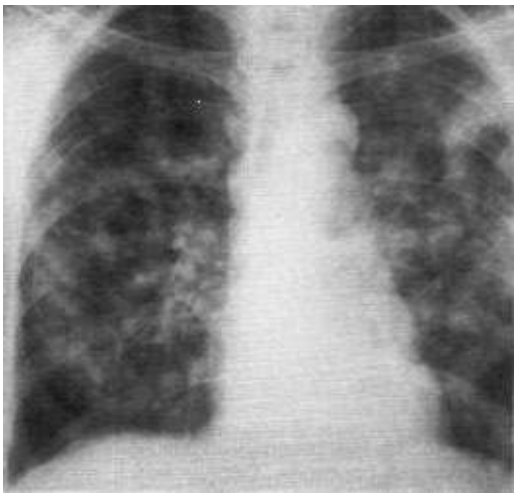

Fig. 2.3.1.3. Chest X-ray of patient N., 35 years old, frontal projection.
Large polymorphic opacities without clear borders, showing a tendency to merge, predominantly in the perihilar region and in the middle and upper lung fields—producing a **“snowstorm” pattern**. Subacute

hematogenous-disseminated pulmonary tuberculosis.

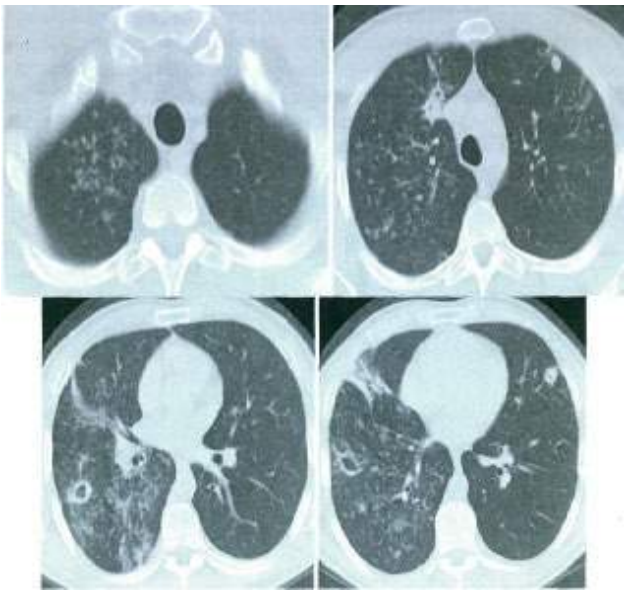

Fig. 2.3.1.4. Subacute hematogenous-disseminated pulmonary tuberculosis in the phase of destruction, MBT+.
Uneven and asymmetric involvement of the lungs. Multiple polymorphic peribronchial foci and small infiltrates containing tiny cavities of breakdown.

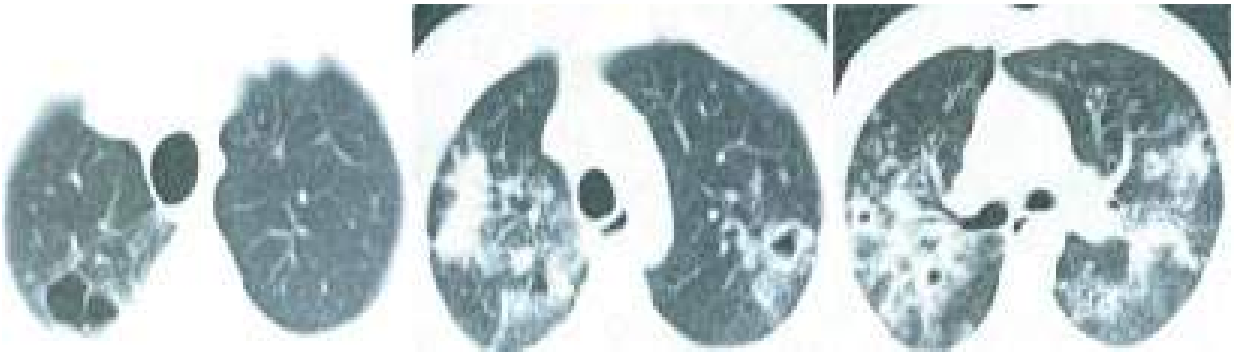

Fig. 2.3.1.5a. Subacute hematogenous–disseminated pulmonary tuberculosis in the destructive phase, MBT+ (before initiation of treatment).
Uneven and asymmetric involvement of the lungs. In the upper segments, large foci and small infiltrates with minute destruction cavities as well as isolated thin-walled cavities are present. In the lower lung lobes—particularly in the basal segments—the number and size of foci are smaller than in the upper regions.

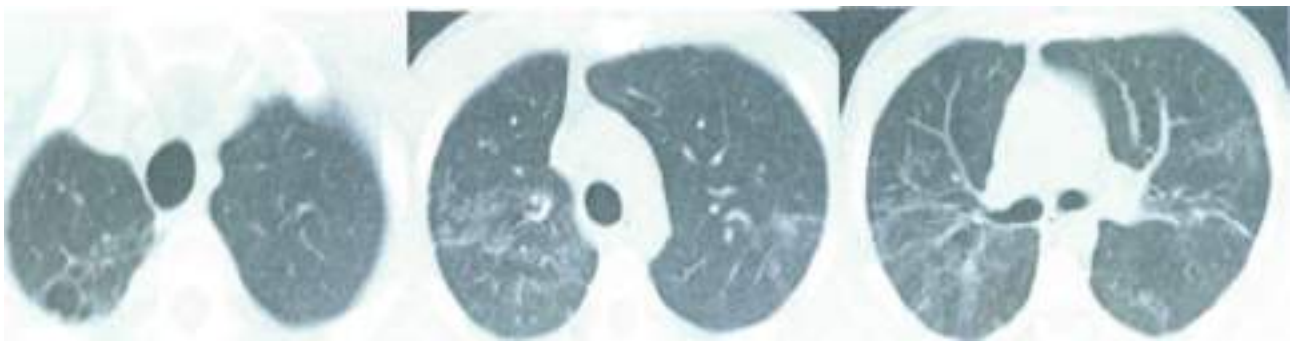

Fig. 2.3.1.5 b. The same patient, after 4 months of treatment. Marked resorption and consolidation of infiltrative and focal opacities, with scarring of most cavitary lesions.

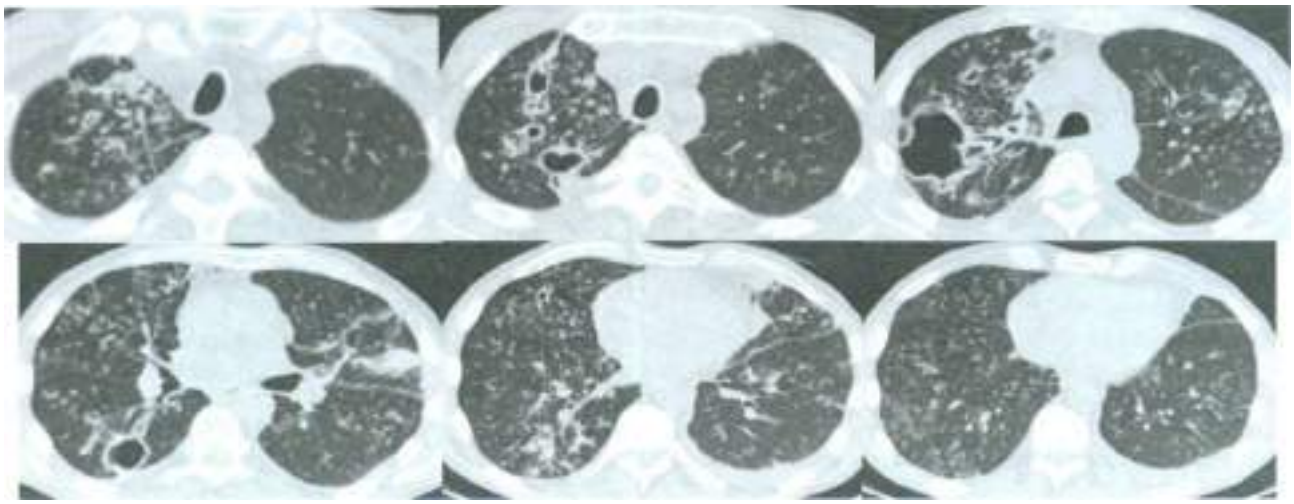

Fig. 2.3.1.6. Disseminated pulmonary tuberculosis in the phase of cavitation, MBT+.
Irregular and asymmetric lung involvement. Numerous typical cavitary lesions of varying size and shape are present in the right lung, with walls of uneven thickness and **no fluid level**. Multiple polymorphic foci and infiltrates are predominantly located in the upper and middle lung zones. A small amount of fluid is present in the left pleural cavity.

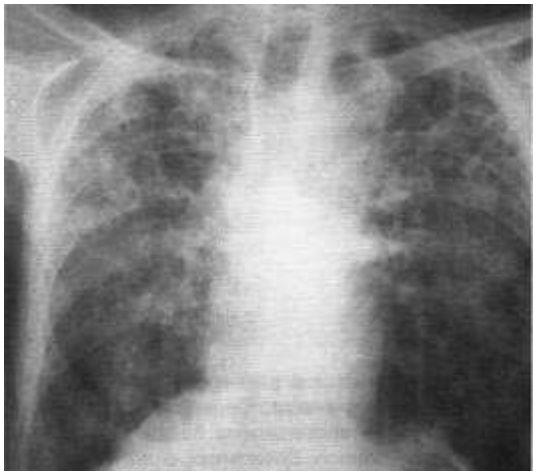

Fig. 2.3.1.7. Chest radiograph of patient S., 43 years old, frontal projection.

In both lungs, predominantly in the upper and middle lung fields, polymorphic focal opacities of varying intensity are identified with a tendency to coalesce. Several cavitary lesions are forming in the upper lobes.

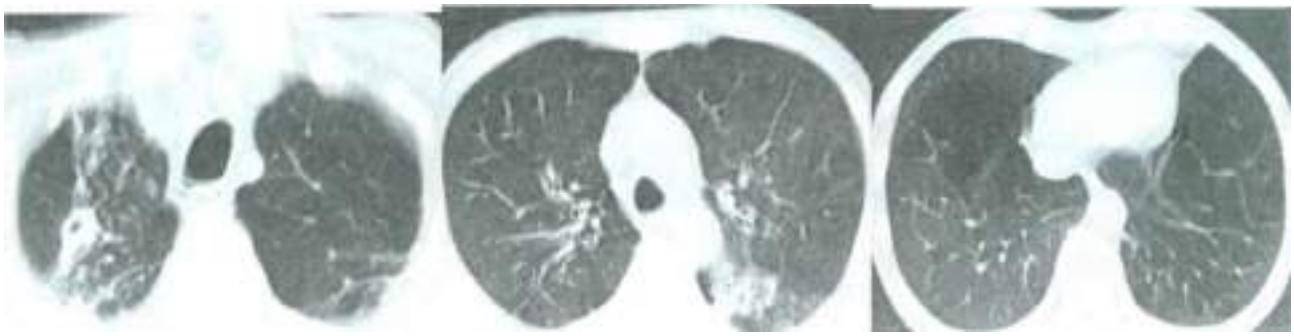

Fig. 2.3.1.8. Disseminated pulmonary tuberculosis in the breakdown phase, MBT+ (“honeycomb lung”).

In both lungs — predominantly in the upper regions — there are numerous polymorphic foci, some with a confluent pattern, isolated small cavities of destruction, pronounced fibrotic and bullous-dystrophic changes, and panlobular emphysema mainly in the lower regions.

Lymphogenous tuberculous disseminations differ by several important features that allow the clinician to assume the pathogenetic mechanism of the disease. These include the predominance of changes in the **middle lung zones at the level of the lung roots**, with less pronounced involvement of the apical and basal segments. The most significant abnormalities are found in the **anterior and posterior segments of the upper lobes**, the **apical segments of the lower lobes**, as well as in the **lingular segments** and the **middle lobe**.

Another distinguishing feature of lymphogenous dissemination is the **marked heterogeneity of lung involvement**, with alternating areas of altered and preserved parenchyma. The distribution of nodules and interstitial changes corresponds to the anatomical boundaries of a specific lymphatic drainage pathway — **either the deep or superficial lymphatic network**. A characteristic feature of lymphogenous dissemination is the **predominance of interstitial changes**, within which small nodules are located.

In most cases, the pathological process involves the **deep lymphatic network of the lung**, resulting in lesions predominantly situated deep within the lung parenchyma, along the vessels and bronchi. Each lobe may contain one or several isolated regions of parenchymal

consolidation of irregular shape, with a **broad base facing the pleura** and the **apex directed toward the lung root**.

Against the background of unevenly increased lung density, nodules of various diameters can be seen — sometimes **large, irregular, and poorly marginated**. Numerous small nodules are typically distributed around them. Also present are **markedly thickened walls of small bronchi**, **densified interlobular and interacinous septa**, vessels with **poorly defined contours**, and **Kerley lines**. Together with the characteristic pulmonary changes, **enlarged lymph nodes** of the lung roots and mediastinum — mainly bifurcational and paratracheal groups — are detected.

The **extent of involvement** within each lobe and the **number of affected lobes** may vary considerably. In some patients, the entire deep lymphatic network of the lungs is affected; in others, the process is limited to several small intraparenchymal infiltrates. Multiple small nodules are located within the walls of the lobules and acini, with local increases in lung density at their sites.

In cases where pathological changes are localized predominantly in the **cortical (subpleural) zones** of the lungs — at the junction of the superficial and deep lymphatic networks — nodules are arranged in a **broad band** along the chest wall and mediastinum. Meanwhile, the deeper lung regions and perihilar zones remain relatively unaffected (Fig. 2.3.1.9).

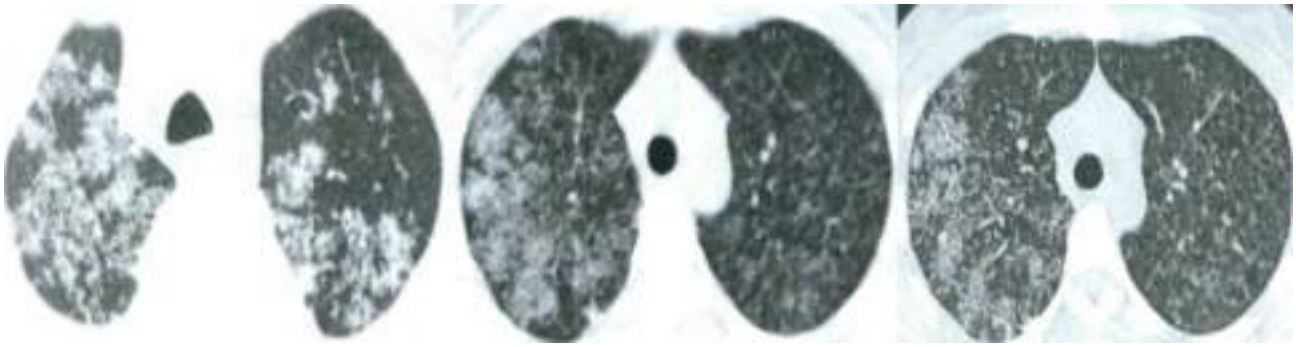

Fig. 2.3.1.9. Variants of lymphogenous disseminated pulmonary tuberculosis.

Multiple small nodules are seen in both lungs against the background of pronounced interstitial changes. The distribution of the nodules within the lung parenchyma is uneven, with predominant involvement of the deep lymphatic system in the pathological process.

2.3.2. Differential Diagnosis of Disseminated Lung Lesions of Various Genesis

The differential diagnosis of disseminated processes in the lungs, and in particular disseminated tuberculosis, may present significant challenges. A large number of diseases and pathological conditions can have a similar clinical and radiological presentation. However, the most common among them in phthisiatric practice include: bronchogenic spread in different forms of tuberculosis, pneumonias, metastatic cancer, sarcoidosis, and pneumoconiosis. It should be emphasized once again that the assessment of pulmonary changes in disseminated processes must be based on high-resolution computed tomography (HRCT).

2.3.2.1. Bronchogenic tuberculous dissemination and mycobacteriosis

Bronchogenic tuberculous dissemination usually occurs in the presence of a cavitary lesion in the lung, as well as in tuberculosis of a major bronchus or tuberculosis of the intrathoracic lymph nodes with the formation of a broncho-glandular fistula. According to the current classification, such changes are interpreted as the *dissemination phase* within a specific form of respiratory tuberculosis (Fig. 2.3.2.1.1).

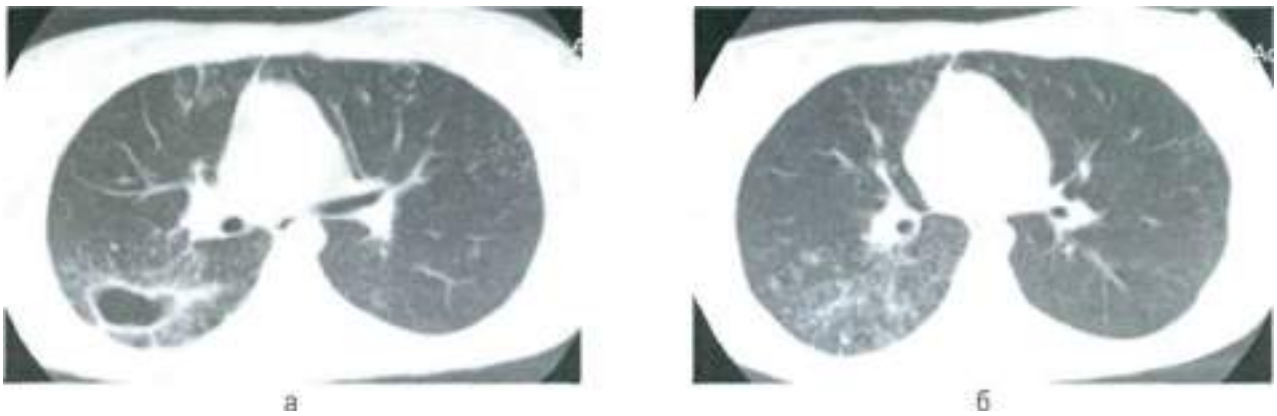

Fig. 2.3.2.1.1. Infiltrative tuberculosis of segment S2 of the right lung, in the phase of cavitation and bronchogenic spread, MBT+. In segment S2 of the right lung, a cavity of destruction with a zone of perifocal infiltration and fibrous–focal changes is present (a). In the lower lobe of the right lung — multiple polymorphic foci of bronchogenic dissemination (b).

Characteristic features of bronchogenic dissemination include a pronounced predominance of focal changes over interstitial ones. Polymorphic foci measuring 2–7 mm are located mainly in the subpleural regions of the lungs, usually in the lower and middle lobes. Some of them merge, forming larger foci of irregular shape. The contours of the small foci are typically clear and smooth, and their shape is regular, round. Larger foci more often have indistinct borders and are located close to the visceral pleura. On thin CT slices, the lumen of a small bronchus or a small cavity of destruction may be visible within them.

Fresh disseminations show moderately increased lung density in the affected area, with thickened interlobular septa commonly seen. Chronic disseminations are accompanied by areas of intralobular or bullous emphysema around the foci.

Mycobacteriosis is an infectious disease of humans and animals caused by various nontuberculous mycobacteria. The most common causative agents are members of the *Mycobacterium avium–intracellulare* complex (MAC), *M. kansasii*, *M. xenopi*, *M. fortuitum*, *M. scrofulaceum*, *M. gordonae*, *M. abscessus* and *M. chelonae*.

The disease has clinical and radiological features similar to classical tuberculosis.

On chest CT, one may observe acinar, nodular, and miliary opacities, as well as lymphadenopathy. Bronchiectasis is also common. However, upper-lobe predominance is not typical, and cavities are rare (see Fig. 2.3.2.1.2–3).

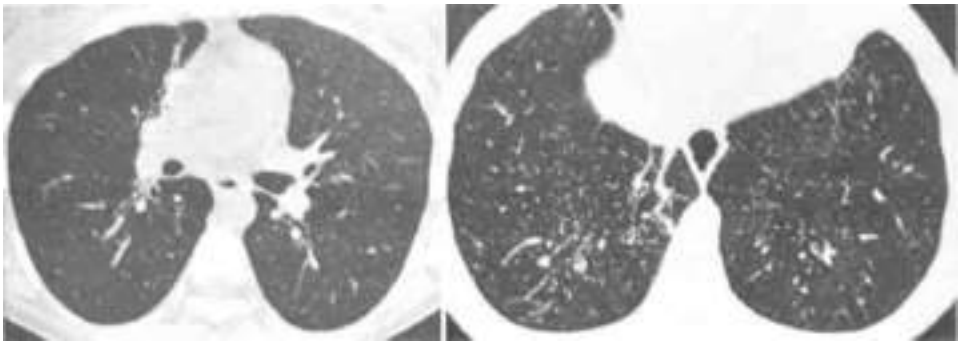

Fig. 2.3.2.1.2. Pulmonary mycobacteriosis (disseminated form), MAC+.

Both lungs demonstrate numerous polymorphic foci predominantly in the middle and lower zones, arranged chaotically, with areas of confluent

lesions. In segment S5 of the right lung, cylindrical bronchiectasis is observed. In the lower lobe of the right lung, the *“tree-in-bud”* sign is present.

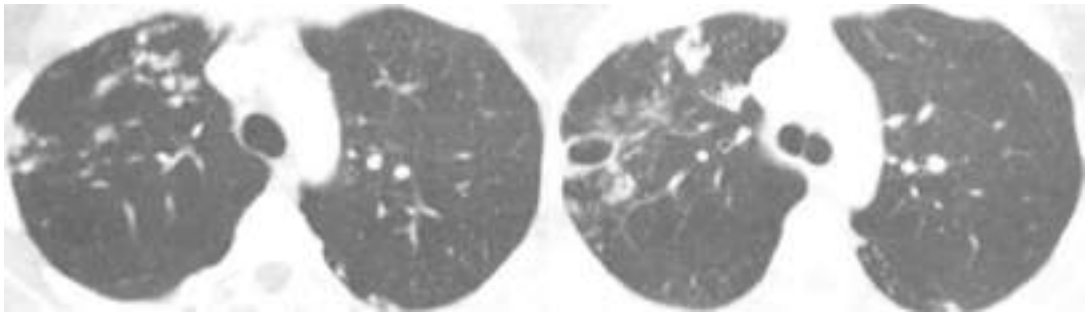

Fig. 2.3.2.3. Pulmonary mycobacteriosis (infiltrative form in the phase of cavitation).

In the upper lobe of the right lung, numerous polymorphic foci—some of them confluent—and areas of infiltration are visualized. In segment S2, a cavity of destruction with a zone of perifocal infiltration without an air–fluid level is present. In segment S6 of the left lung, multiple polymorphic foci of bronchogenic seeding are identified.

2.3.2.2. Pulmonary Embolism

Pulmonary embolism (PE) is one of the most common and life-threatening complications of numerous diseases. It is known that among therapeutic patients PE most frequently occurs in stroke (65%), myocardial infarction (22%), acute medical conditions (more than 15%), and in the elderly (9%). According to the Framingham study, mortality due to PE accounts for 15.6% of all in-hospital deaths (18% in surgical diseases and 82% in therapeutic cases).

PE is a widespread disorder: in the United States it affects about 200,000 people annually, and 10–15% of patients die from it (if left untreated, mortality reaches 30%).

PE is a partial or complete occlusion of the main trunk, large, medium, or small branches of the pulmonary artery, most commonly by thrombotic masses (blood clots). This leads to the development of pulmonary hypertension and compensated or decompensated pulmonary heart disease. PE is one of the most difficult conditions to diagnose; therefore, mortality remains high.

Radiological criteria for PE (Fig. 2.3.2.2.1):

• Reduction in pulmonary vascular markings (a pathognomonic sign); increased lung transparency (Westermark sign)

• Deformation or enlargement of one of the lung roots
• Prominence of the pulmonary artery cone
• Cardiac enlargement due to right ventricular dilation
• In pulmonary infarction – a wedge-shaped opacity pointing toward the lung root
• Elevated hemidiaphragm on the affected side
• Possible presence of pleural effusion

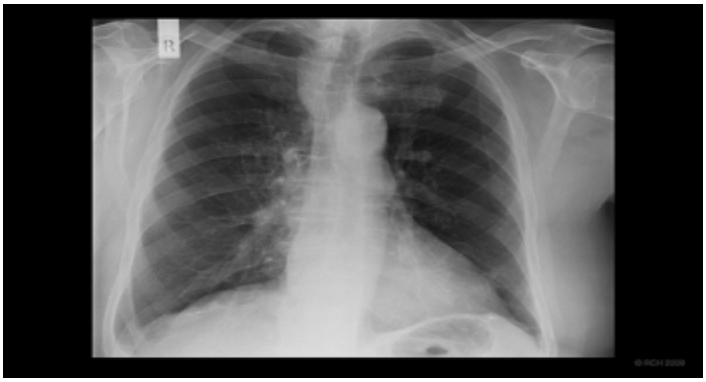

Fig. 2.3.2.2.1. Chest radiograph in pulmonary embolism.

“Criteria of lung computed tomography (CT) (Fig. 3.3.2.2.2) or selective angiography: the presence of a thrombus, vascular occlusion, or a filling defect (oligemia – decreased peripheral lung perfusion).”

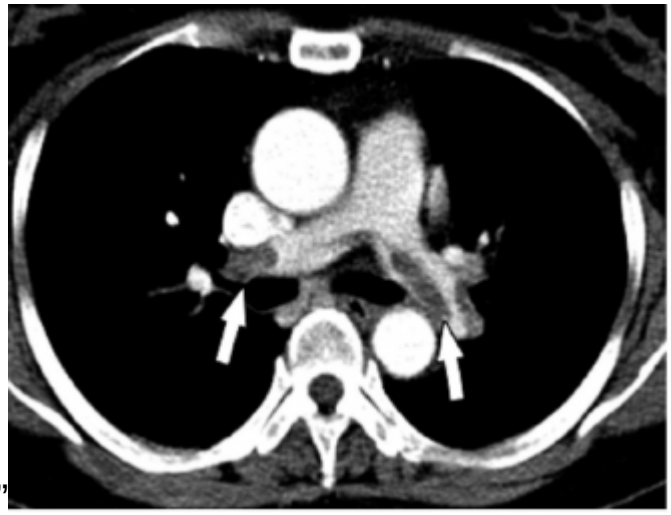

Fig. 2.3.2.2.2. CT appearance of thromboembolism of the main pulmonary arteries on CT-angiography.

The radiological picture of septic emboli has specific features; however, differential diagnosis with disseminated pulmonary tuberculosis is sometimes required. Multiple infiltrates measuring 1–2 cm appear in the lungs; they are usually round or wedge-shaped, have relatively well-

defined margins, and a homogeneous internal structure. Most of these infiltrates are located subpleurally.

Within several days (or even hours), purulent destruction of lung tissue and small bronchi develops at the sites of involvement. As a result, round infiltrates rapidly transform into thin-walled cavities, some of which contain a small amount of liquid pus. After a few days, these thin-walled cavities undergo scarring. At the same time, new infiltrates and cavities may appear in the lungs, creating a characteristic polymorphic pattern (Fig. 2.3.2.2.3–4).

Dynamic radiological follow-up makes it possible to trace the entire spectrum of changes in the lungs. The most common complications of septic pulmonary emboli include pneumothorax, pleural or pericardial effusion, or pyopneumothorax.

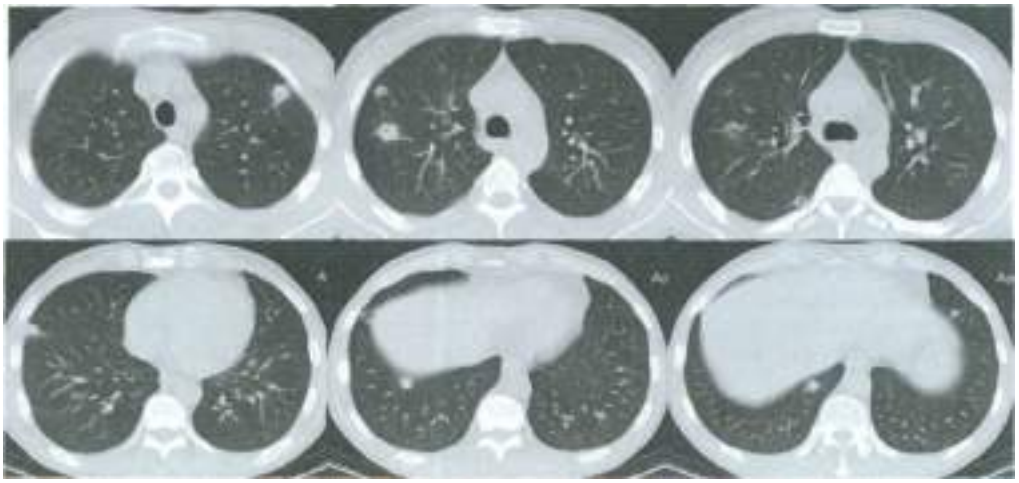

Fig. 2.3.2.2.3. Multiple septic emboli in the lungs.

In both lungs, predominantly in the right one, numerous small round focal opacities associated with arterial vessels are visualized; some of them contain small cavities.

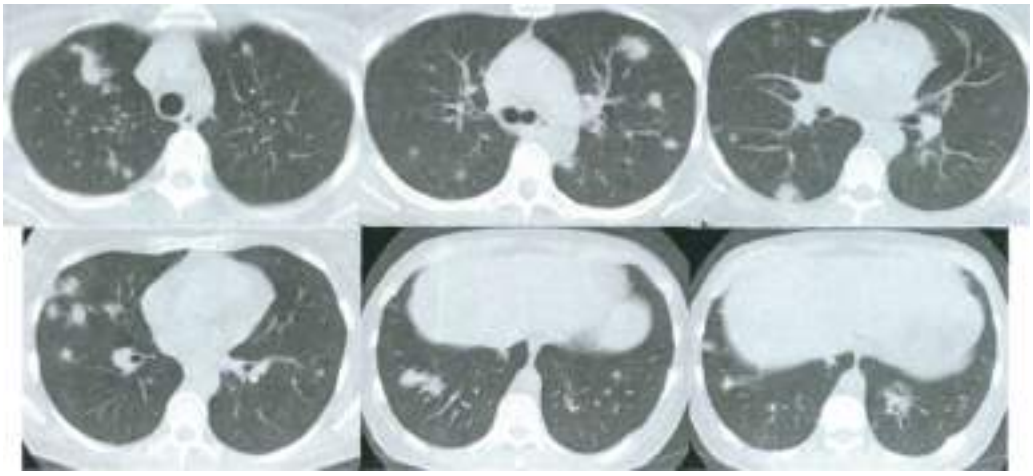

Figure 2.3.2.2.4.
Multiple septic emboli in the lungs.
In the subcortical regions of the lungs, numerous predominantly round, poorly defined nodules and focal opacities are visualized, some of which contain small cavities.

2.3.2.3. Pneumonias

Pneumonias caused by typical pathogens (*Streptococcus pneumoniae*) rarely require differentiation from disseminated tuberculosis due to significant differences in the clinical–radiological picture and CT semiotics (Fig. 2.3.2.3.1). In so-called atypical pneumonias, whose etiological agents are *Mycoplasma pneumoniae*, *Chlamydia pneumoniae*, and *Legionella spp.*, the radiographic and CT appearance may resemble disseminated tuberculosis. In addition, they do not respond to standard antibacterial therapy and differ in their clinical course from bacterial pneumonias (fever without chills, nonproductive cough, extra-thoracic symptoms such as right upper-quadrant abdominal pain, headache, myalgia, diarrhea).

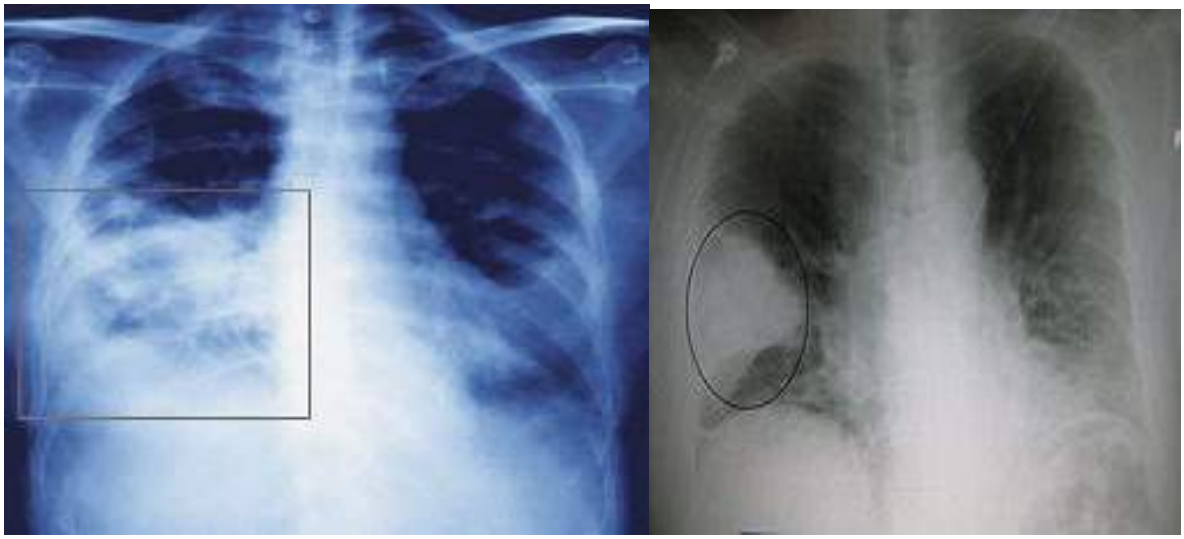

Fig. 2.3.2.3.1. A variant of community-acquired pneumonia localized in the right lower lobe.
Mycoplasma pneumonia is characterized by bronchiolitis that progresses to bronchopneumonia.
The dominant CT finding is centrilobular nodules (the “tree-in-bud” sign), along with features of bronchial obstruction such as expiratory air-trapping and mosaic perfusion adjacent to areas of ground-glass

opacities and patchy lobular consolidation (Fig. 2.3.2.3.2). In children, CT signs of bronchial obstruction may persist in previously affected regions for 1–2 years.

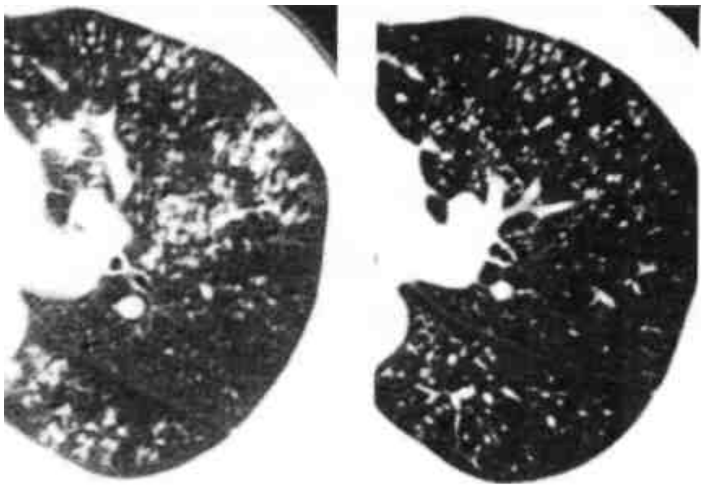

Fig. 2.3.2.3.2. *Atypical pneumonia. Multiple centrilobular nodules with a "tree-in-bud" pattern caused by bronchiolitis due to* **Mycoplasma pneumoniae**.

Viral pneumonias.

Primary respiratory viruses include the parainfluenza and influenza groups (the most common pathogens of viral pneumonia in adults), respiratory syncytial virus (the most common pathogen in children), adenovirus, and picornavirus. The infection begins in the central airways and involves the lung parenchyma only after the peribronchial and peribronchiolar alveoli become affected. Small airways are predominantly involved, especially in children, leading to their obstruction.

Viral respiratory infection progresses in a predictable sequential pattern. After inhalation of the pathogen, the inflammatory process begins in the airways. CT demonstrates patchy areas of heterogeneous parenchymal attenuation (**Fig. 2.3.2.3.3 a, b**), as well as a diffuse *tree-in-bud* pattern indicating bronchiolar filling with pathological secretions.

In the subacute phase, there is accentuation of the interlobular septa due to dilation of lymphatic vessels that participate in the resorption of intraalveolar exudate, as well as thickening of the central peribronchovascular interstitium and pathological changes of the bronchioles.

As the infection progresses further, the walls of the alveoli become involved, with development of intraalveolar edema and hemorrhagic inflammation. Filling of the peribronchiolar airspaces results in patchy areas of consolidation corresponding to a broncho-pneumonic pattern. Peribronchiolar acinar-type consolidation may also be observed. Perifocal hemorrhage produces less dense peripheral zones with a *halo* appearance (**Fig. 2.3.2.3.3 c**).

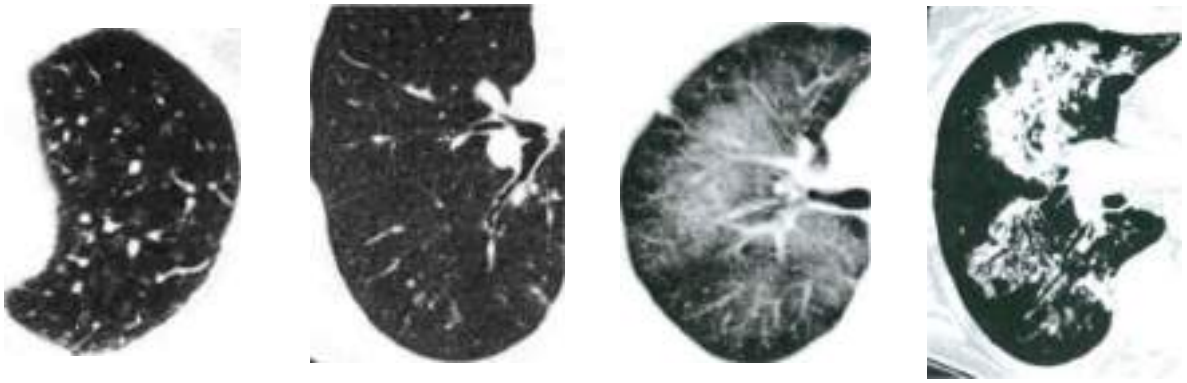

a b c d

Fig. 2.3.2.3.3. In viral pneumonias, various imaging patterns may be detected, ranging from focal to diffuse ground-glass opacities or areas of consolidation.
Cytomegalovirus pneumonia with ill-defined peribronchial focal–patchy opacities (a) and ground-glass foci (b).
Diffuse ground-glass opacity in cytomegalovirus infection (c). Influenza pneumonia with patchy confluent areas of consolidation, air bronchograms, and a peripheral halo caused by hemorrhage (d).

Influenza pneumonia is most commonly complicated by **bacterial pneumonia**, and therefore a more widespread consolidation of the lung parenchyma may develop (Fig. 2.3.2.3.4 a, b; 2.3.2.3.5).

The **radiographic appearance of adenoviral pneumonia** is very similar to that of **bacterial (pneumococcal) pneumonia**.

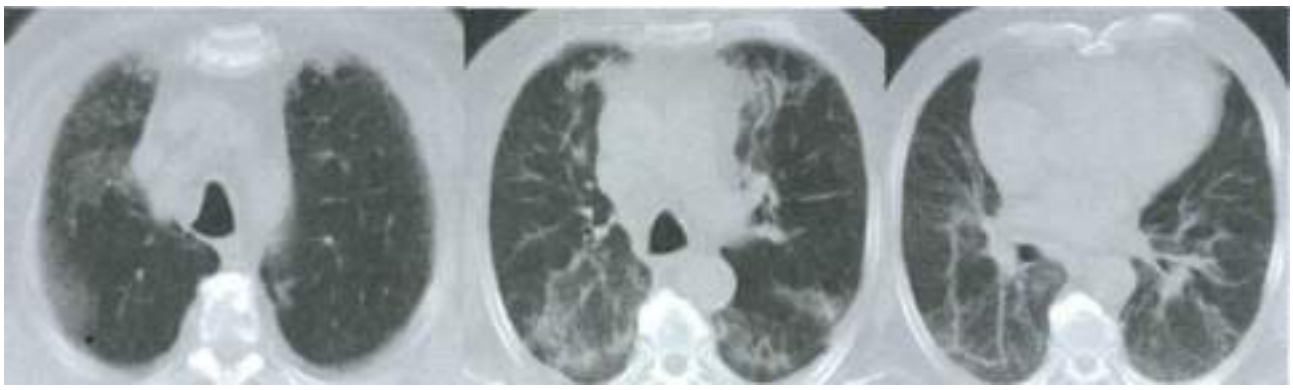

Fig. 2.3.2.3.4 a. **Influenza pneumonia.** Diffuse ground-glass opacities and areas of consolidation predominantly in the middle and lower lung zones.

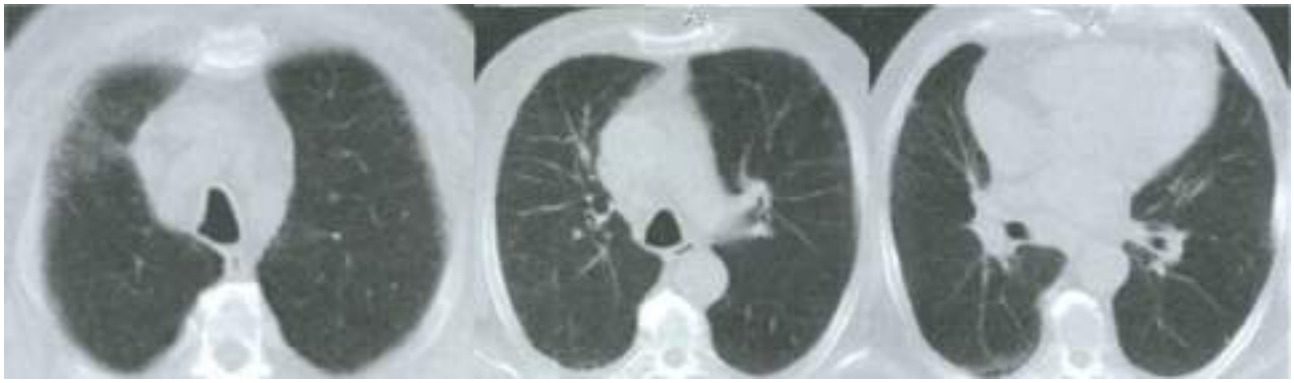

Fig. 2.3.2.3.4 b. The same patient after six months of treatment and follow-up. Marked resorption of changes in both lungs; signs of panlobular emphysema.

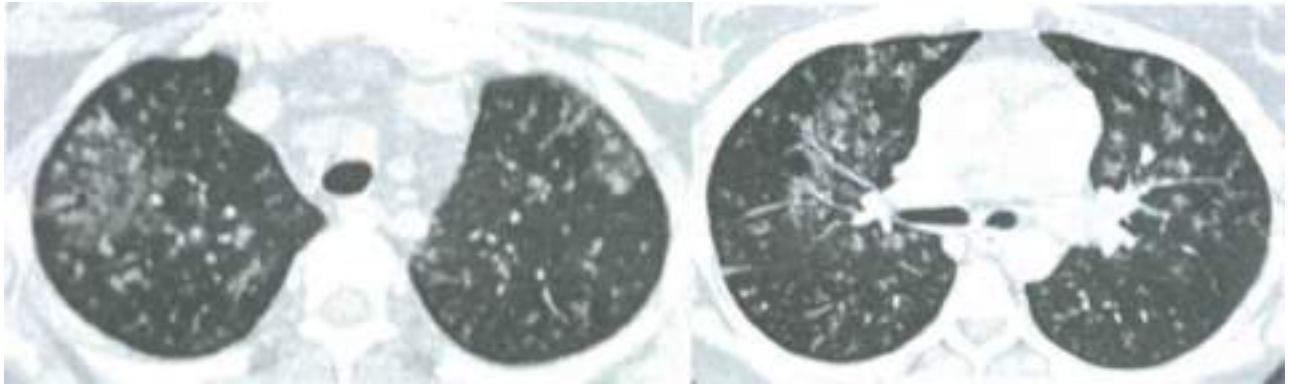

Figure 2.3.2.3.5. Influenza pneumonia. In both lungs, predominantly in the upper and middle zones, multiple poorly defined centrilobular nodular opacities and areas of diffuse decreased lung transparency of the “ground-glass” type are visualized.

Infections caused by cytomegalovirus (CMV) often occur in patients undergoing chemotherapy or within the first four months after organ transplantation (in more than 50% of cases, particularly after kidney or liver transplantation). CMV pneumonia also occurs in patients with AIDS (when CD4 < 100 cells/mm^3).

The CT pattern of CMV pneumonia includes signs of airway involvement: bronchial wall thickening, the “tree-in-bud” sign, and bronchiectasis. In the stage of alveolar involvement, ill-defined granular opacities are noted, and less commonly — consolidation. Focal or nodular opacities up to several centimeters in diameter have also been described (in approximately 60% of cases). In fact, the most common pattern is a combination of alveolar opacities and interstitial changes. There is a tendency toward bilateral and symmetric involvement (Fig. 2.3.2.3.6).

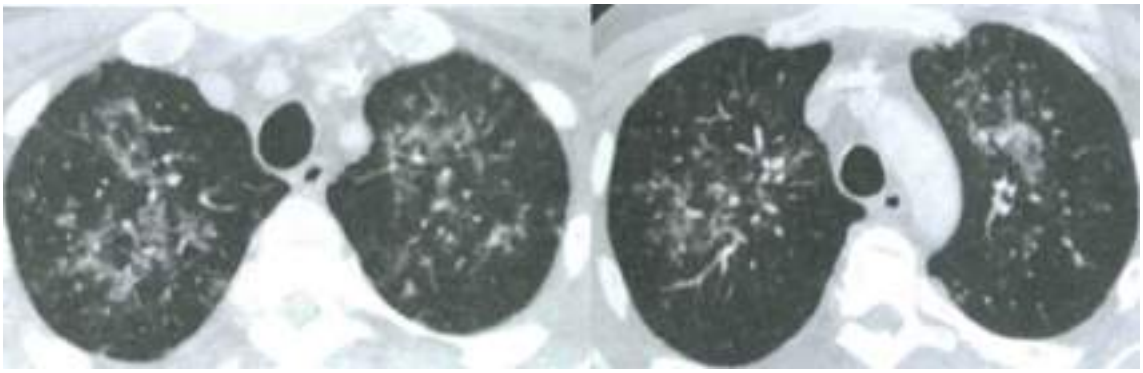

Fig. 2.3.2.3.6. Cytomegalovirus pneumonia. In both lungs, predominantly in the mid-zones, multiple poorly defined peribronchial focal–patchy opacities and areas of diffuse decreased lung transparency of the “ground-glass” type are visualized.

Pneumonia caused by the *Herpes simplex* virus is rare and usually occurs after pronounced skin and mucosal lesions have already appeared. Chickenpox (varicella) can cause severe pneumonia in adults. It manifests as diffuse, poorly defined acinar nodules (4–6 mm) (Fig. 2.3.2.3.7). This pattern persists for several weeks and may resolve with the formation of dense foci and calcifications (Fig. 2.3.2.3.8–9). In 40% of cases, lymphadenopathy in the lung hila is detected.

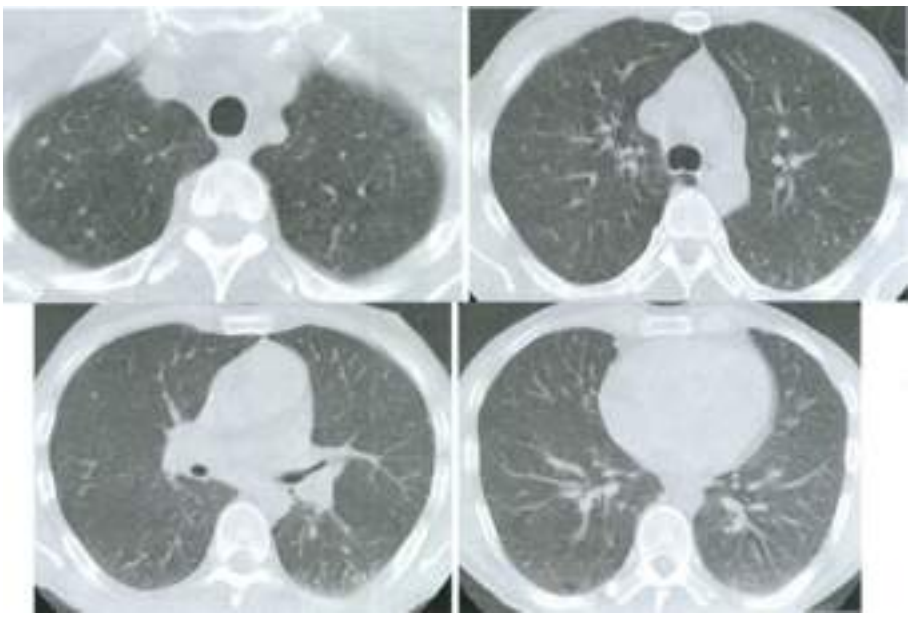

Fig. 2.3.2.3.7. Pneumonia complicating varicella on the 2nd week of observation in a 32-year-old patient. Numerous small (1–3 mm) poorly defined acinar nodules of low density are chaotically distributed predominantly in the middle and lower lung zones, against a background of diffuse ground-glass opacity. An azygos lobe is present in the right upper lobe.

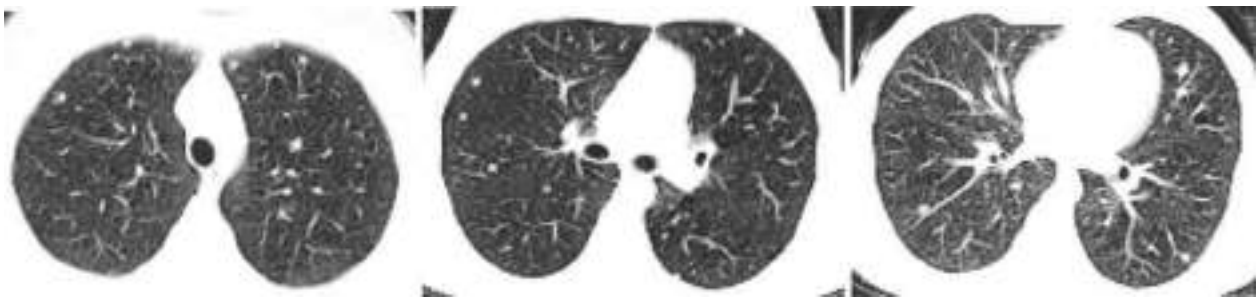

Fig. 2.3.2.3.8. Condition after pneumonia complicated by chickenpox in an HIV-infected patient. Multiple small (1-3 mm) high-density focal shadows (calcifications) in the middle and lower parts of the lungs.

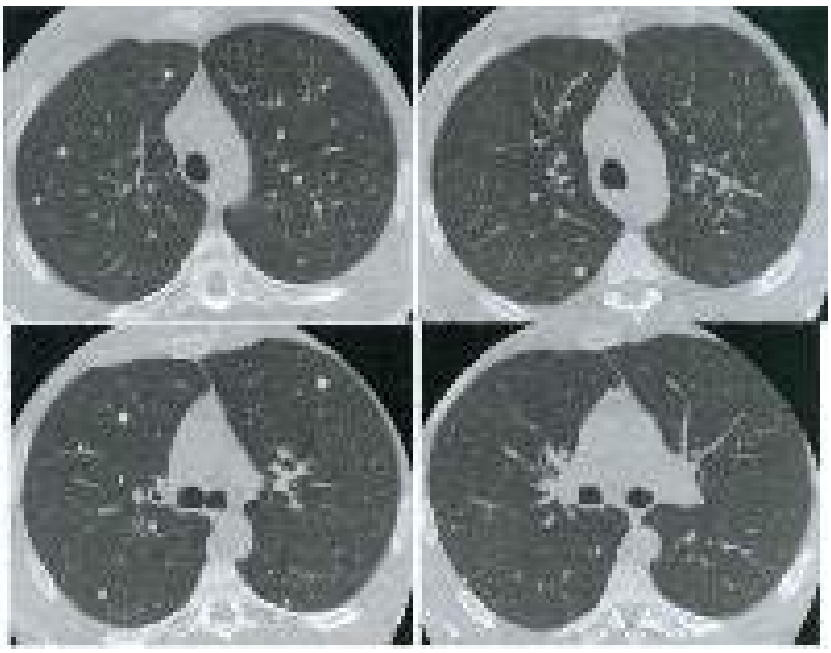

Fig. 2.3.2.3.9. *Condition 6 months after pneumonia that complicated varicella in an HIV-infected patient.* HRCT. Both lungs demonstrate chaotically distributed multiple focal opacities up to 5 mm in diameter, some of which contain centrally located calcifications, while others are completely calcified.

Pneumonias caused by *Pneumocystis* (*Pneumocystis carinii* pneumonia) frequently occur in patients with impaired cell-mediated immunity. *Pneumocystis carinii* is the most common etiological agent of pneumonia in HIV-infected individuals (60–75% of all patients experience at least one episode of pneumocystis pneumonia).

The initial imaging pattern of pneumocystis pneumonia is predominantly alveolar involvement with patchy **ground-glass opacities**, more often with a diffuse bilateral distribution (75%), primarily within the perihilar regions of the lungs (Fig. 2.3.2.3.10 a, b). With further progression of the infection, patients with immunodeficiency develop extensive pulmonary consolidation with the **air-bronchogram sign**, whereas those receiving treatment may demonstrate a **granulomatous reaction with interstitial fibrosis and nodular changes** (Fig. 2.3.2.3.10 c, d). Pleural effusion and mediastinal lymphadenopathy are uncharacteristic.

The dynamics of ground-glass opacities allow monitoring of the pharmacotherapeutic response (Fig. 2.3.2.3.11–13).

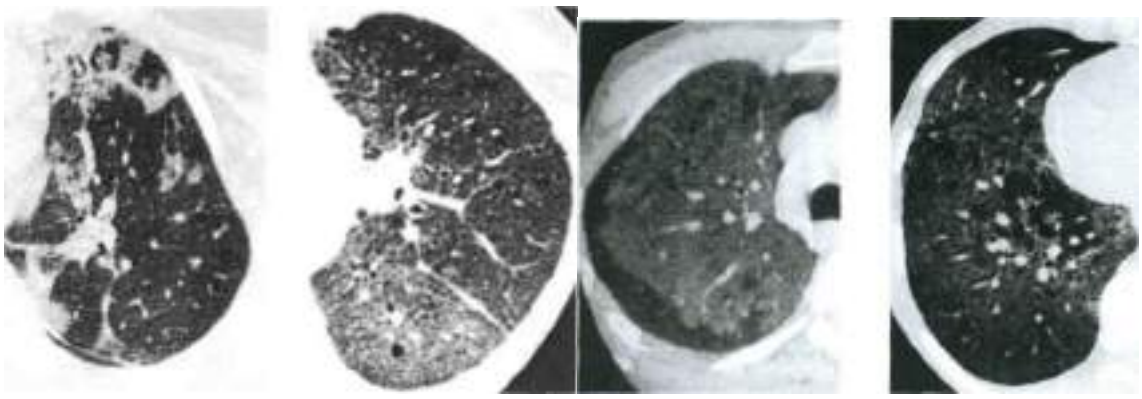

a b c d

Fig. 2.3.2.3.10. Variants of pneumocystis pneumonia. Acute form with diffuse patchy ground-glass opacification (a). Acute form with diffuse ground-glass opacification and thickened interlobular septa (b). Fibrosing form with signs of pulmonary parenchymal distortion (c). Cystic changes (d).

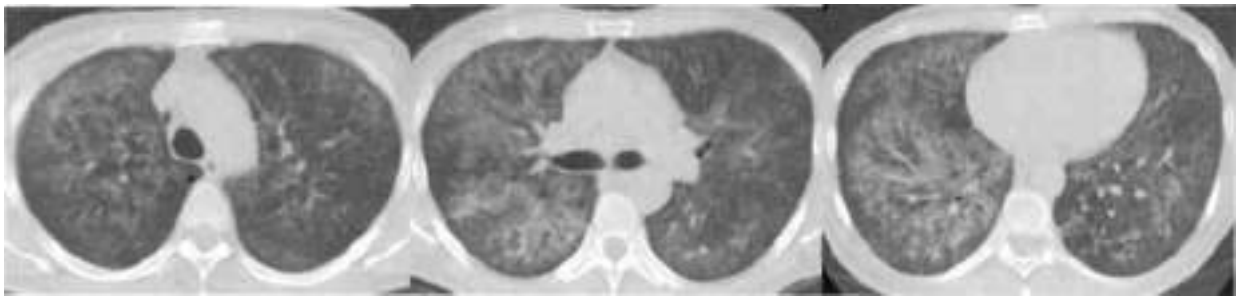

Fig. 2.3.2.3.11. Pneumocystis pneumonia in an HIV-infected patient. Acute form with heterogeneous ground-glass opacification and thickened interlobular septa.

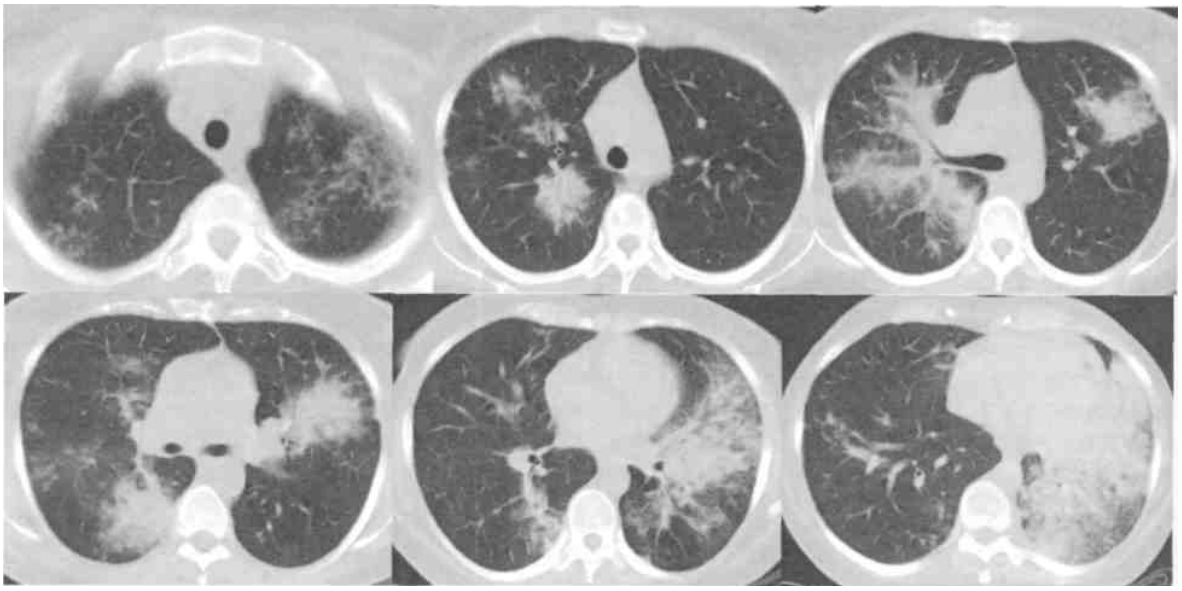

Fig. 2.3.2.3.12. Pneumocystis pneumonia in an HIV-infected patient. Progressive course with the development of widespread heterogeneous infiltrates with an air-bronchogram sign, accompanied by interstitial fibrosis and nodular changes.

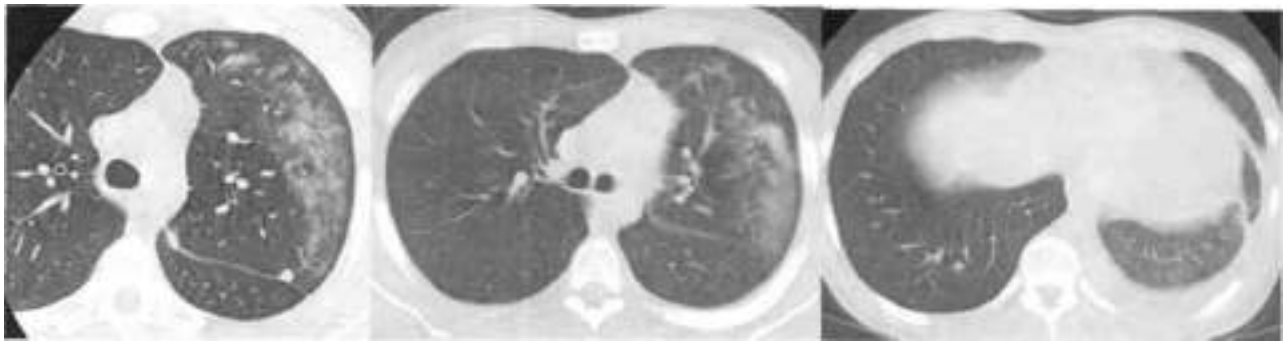

Fig. 2.3.2.3.13. Pneumocystis pneumonia in an HIV-infected patient. Rare form with diffuse ground-glass consolidation in the upper lobe of the left lung, pericarditis, and right-sided pleural effusion.

Possible development of destructive cystic changes in the lungs (pneumatoceles or thick-walled cysts), which are predominantly detected in the upper lobes and apical segments of the lower lobes (7%). Initially, small cysts appear within areas of consolidation and subsequently merge into larger ones. In cases with cysts, differential diagnosis with pulmonary tuberculosis is required (Fig. 2.3.2.3.14–15). Subpleural cysts may be complicated by pneumothorax. These changes may almost completely resolve under antiretroviral therapy.

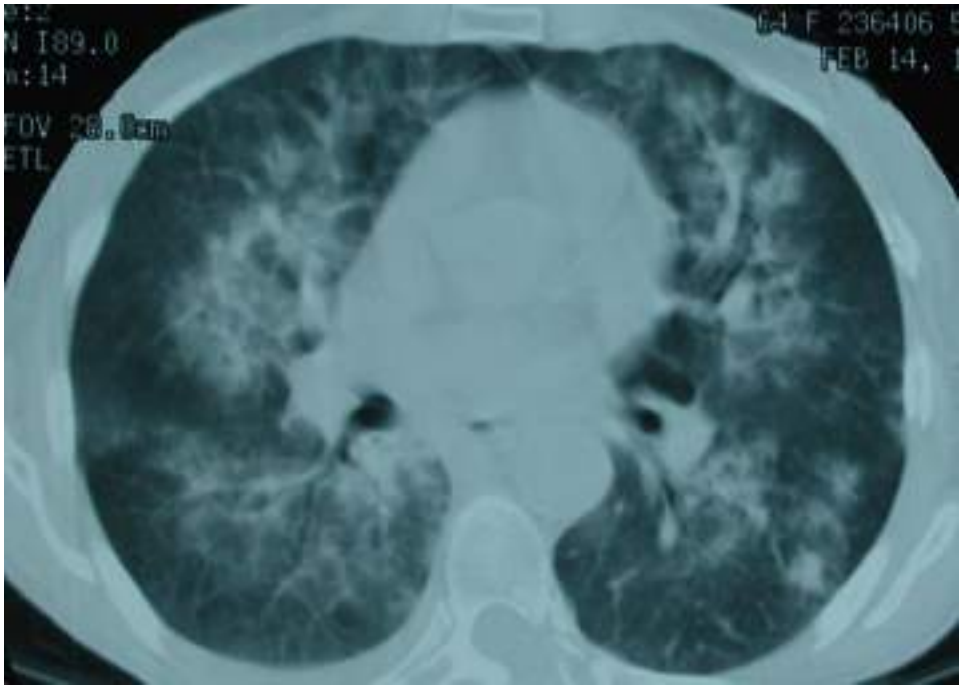

Fig. 2.3.2.3.14. Pneumocystis pneumonia.

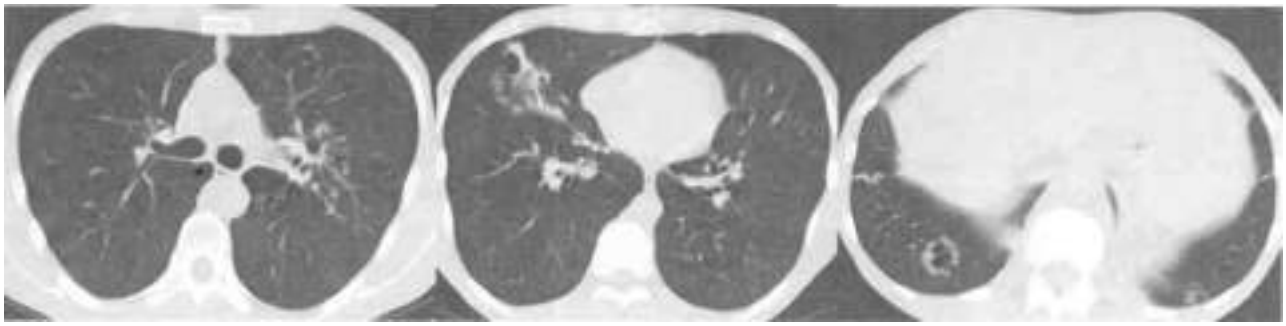

Fig. 2.3.2.3.15. Pneumocystis pneumonia in an HIV-infected patient. Patchy bilateral ground-glass opacities; in segment S10 of the right lung, a thick-walled cyst is present.

Eosinophilic pneumonia (EP) is usually accompanied by peripheral blood eosinophilia and responds rapidly to steroid therapy (regression within several days and complete recovery within months). In 50% of patients, there is a genetically determined increased sensitivity to environmental allergens, and in 40%—bronchial asthma. The involvement may be idiopathic or represent a secondary immunologic reaction to drugs, parasites, or other agents.

The dominant feature is **ground-glass opacification** (100%) and **consolidation** (92%) of a diffuse nature without any preferred localization (Fig. 2.3.2.3.16–19). Transient and migratory infiltrates occur. Other frequent findings include poorly defined nodules (54%), septal thickening (70%), and thickening of the central bronchovascular bundles (60%). Bronchiectasis and lymphadenopathy are rare. Pleural effusion develops in two-thirds of cases.

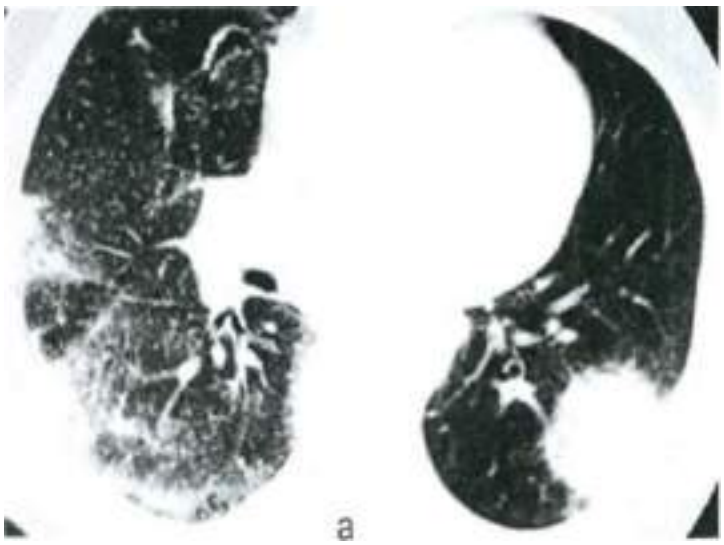

Fig. 2.3.2.3.16. Variants of eosinophilic pneumonia with subpleural infiltrates of varying density.

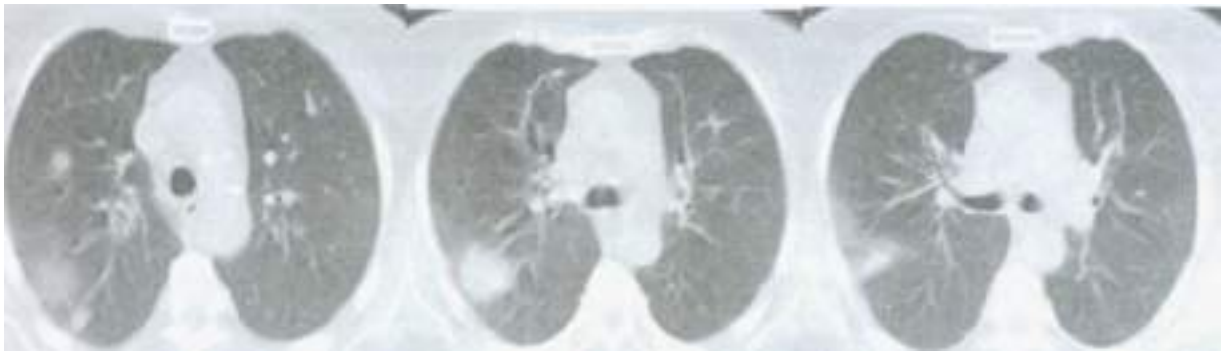

Fig. 2.3.2.3.17. Eosinophilic pneumonia. Subpleural infiltrates of varying density and ground-glass opacification.

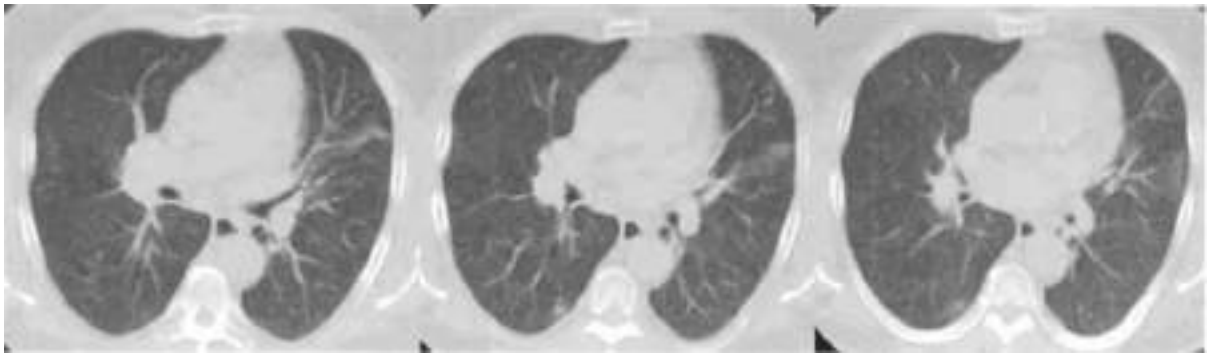

Fig. 2.3.2.3.18. Eosinophilic pneumonia. Ground-glass opacification in segment S4 of the left lung, thickening of the central bronchovascular bundles, and subpleural poorly defined nodules in segment S10 of the right lung.

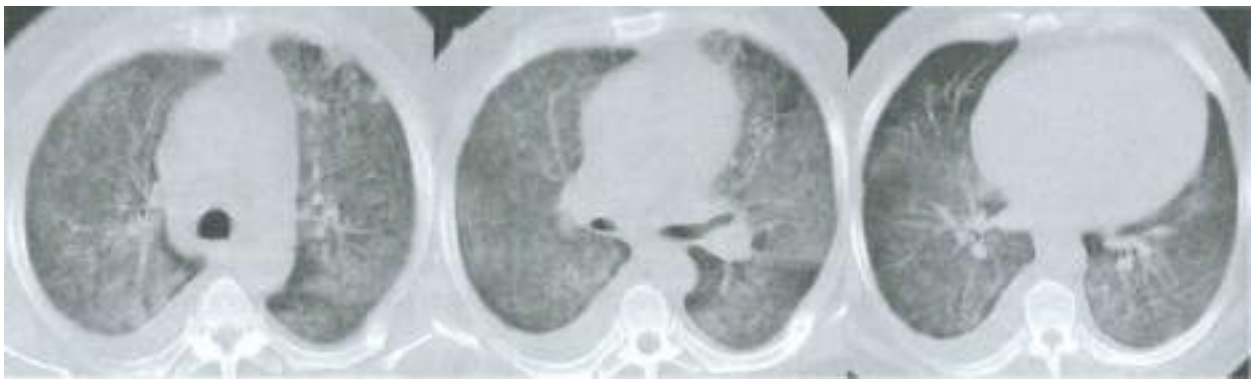

Fig. 2.3.2.3.19 a. Eosinophilic pneumonia. Diffuse ground-glass opacification of the lung parenchyma and right-sided pleural effusion.

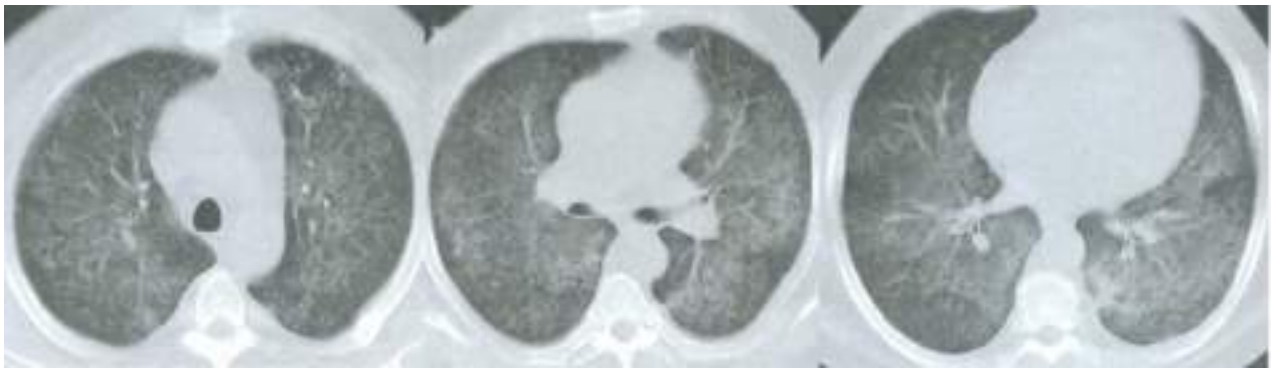

Fig. 2.3.2.3.19 b. The same patient after 10 days of glucocorticosteroid therapy. Positive dynamics in the form of a reduction in ground-glass areas, appearance of poorly defined nodules, thickened septa, and thickening of the central bronchovascular bundles; pleural effusion is not detected.

In chronic EP, ground-glass opacification (88%) and consolidation (100%) also predominate, but with a predominantly subpleural distribution of involvement in the upper and middle lung regions. Nodules (38%), septal thickening (18%), thickening of the central bronchovascular bundles (38%), and pleural effusion (10%) occur less frequently than in the acute form (Fig. 2.3.2.3.20).

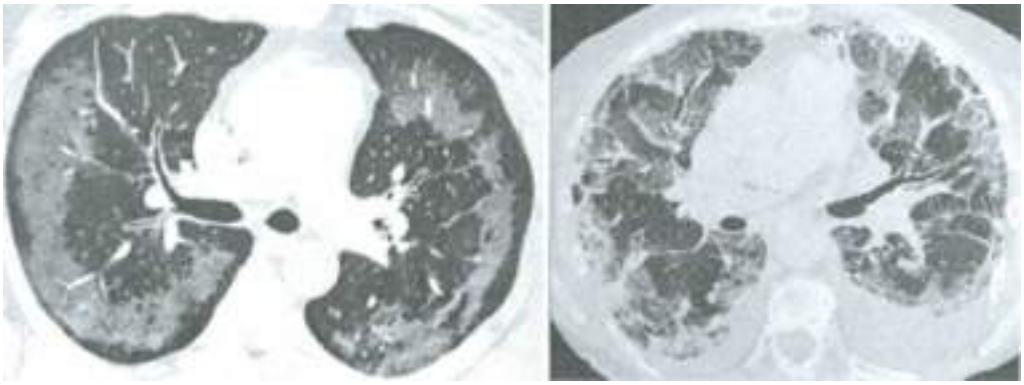

Fig. 2.3.2.3.20. Variants of chronic eosinophilic pneumonia.

2.3.2.4. Fungal lung infections.

Opportunistic fungal infection is a common cause of morbidity and mortality in immunocompromised patients, such as those with chemotherapy-induced neutropenia, AIDS, or immunosuppression after organ and bone marrow transplantation. The most important opportunistic fungi include *Cryptococcus neoformans*, *Candida*, and *Aspergillus*. Clinical and radiologic manifestations are nonspecific and highly variable. Because many of these microorganisms can colonize the upper respiratory tract, sputum cultures are considered diagnostically unreliable. A definitive diagnosis requires identification of the fungus within infected tissue through microscopy and/or culture.

Pulmonary candidiasis is uncommon and occurs only in patients with severe immunodeficiency. It may develop due to aspiration of microorganisms from the upper airways, hematogenous spread from the gastrointestinal tract, or from an infected central venous catheter. Diffuse endobronchial dissemination of the fungus may produce a rare miliary form of candidiasis. Candidiasis is characterized by subtle patchy or nodular opacities (septic foci, emboli), predominantly in the lower lobes, which may also be surrounded by a halo. Pleural effusion occurs in 25% of cases, and cavitation is rare. In most patients, candidiasis represents a superinfection.

Cryptococcus neoformans is minimally pathogenic in immunocompetent individuals but can cause severe, often disseminated infection in immunocompromised patients.

Fungal infections with a tendency for vascular invasion (invasive aspergillosis, mucormycosis) are characterized by nodular opacities with features typical of pulmonary infarction.

Early signs of invasive aspergillosis include solitary or multiple pulmonary lesions ranging from a few millimeters to several centimeters in size, with a surrounding halo of ground-glass density (Fig. 2.3.2.4.1–2 a, b, c). Although the halo sign is nonspecific (it also occurs in tuberculosis, CMV and herpetic infection, candidiasis, and legionellosis), its presence in immunocompromised patients should raise suspicion of fungal infection when signs of infection (fever, C-reactive protein, etc.) persist despite broad-spectrum antibacterial therapy.

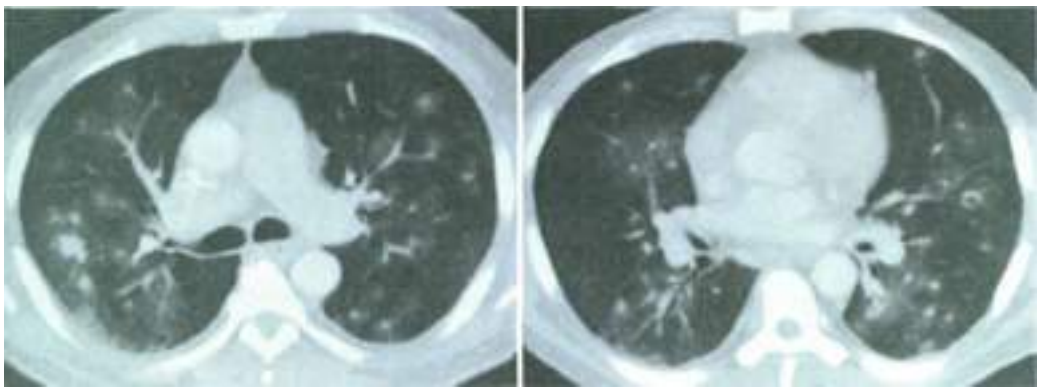

Fig. 2.3.2.4.1. Angioinvasive aspergillosis. Multiple infiltrative opacities in both lungs with areas of central consolidation.

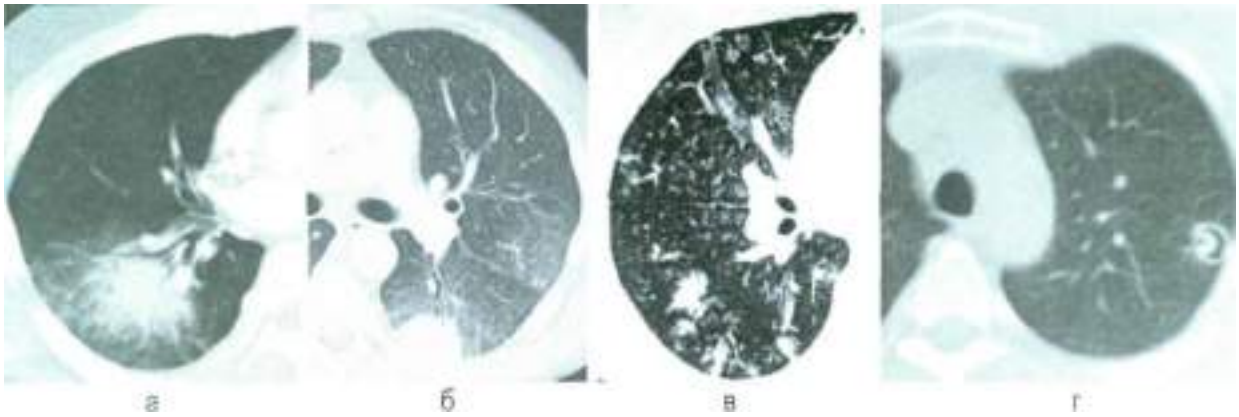

Fig. 2.3.2.4.2. Pulmonary aspergillosis. Angioinvasive aspergillosis: a dense infiltrate in segment S9 of the right lung with a ground-glass halo (a). Wedge-shaped subpleural infiltrate caused by pulmonary infarction due to mycosis (b). Invasive airway aspergillosis: “tree-in-bud” sign with patchy peribronchiolar opacities (c). The “air crescent” sign is pathognomonic for aspergillosis (d).

Mycotic infiltration of blood vessels with their occlusion leads to wedge-shaped infarcts (Fig. 2.3.2.4.2 d), in which post-contrast CT reveals a non-enhancing center and a peripheral ring of enhancement (the wall composed of granulation tissue). A non-dilated bronchus entering the infiltrated region and abruptly tapering within it is often seen.

Progression of the infection is initially characterized by fine punctate patchy opacities resembling disseminated tuberculosis. Later, these foci merge and may form large areas of consolidation. Cavitation is a later finding, appearing after 2–3 weeks. Cavities typically contain the “air crescent” sign, which indicates a necrotic process and improvement of the patient’s immune status (Fig. 2.3.2.4.2 d). These changes must be

differentiated from cavitary lesions of other etiologies (tuberculosis, Wegener's granulomatosis, etc.).

Lymphadenopathy, pleural effusion, and soft-tissue infiltration are very rare. Intrapulmonary mycotic aneurysms are life-threatening complications due to their potential to rupture after resolution of pneumonia (Fig. 2.3.2.4.2 d).

In obstructive tracheobronchial aspergillosis, CT reveals large mucus-filled branching bronchi, usually in the lower lobes, along with areas of pulmonary consolidation or distal atelectasis (Fig. 2.3.2.4.3).

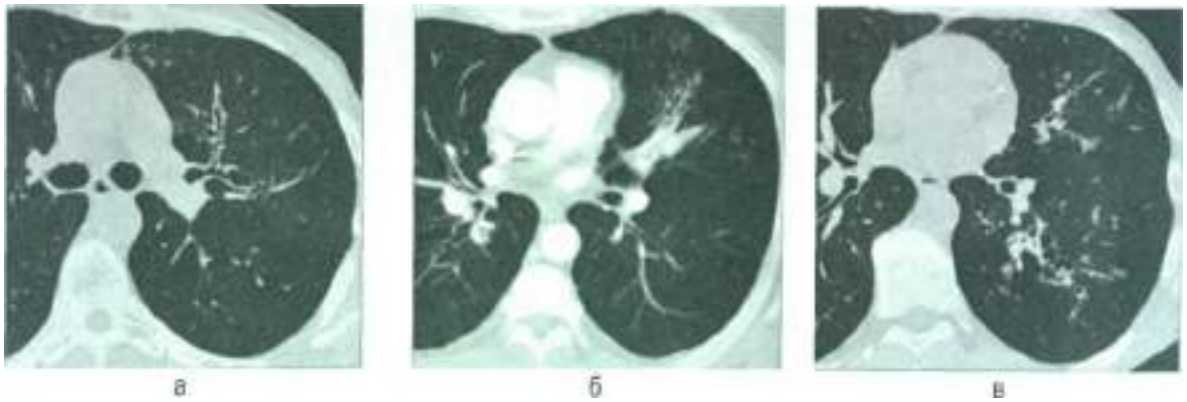

Fig. 2.3.2.4.3. Variants of obstructive tracheobronchial aspergillosis. Bronchiectasis in the left upper-lobe segmental and subsegmental bronchi, with a "tree-in-bud" sign (a). Lingular bronchi are ectatic and filled with secretions; small bronchi are filled with secretions forming a "tree-in-bud" pattern (b). Cylindrical bronchiectasis in the segmental and subsegmental bronchi of the left lower lobe and lingular bronchi, filled with secretions and appearing as focal opacities (c).

Chronic necrotizing aspergillosis typically affects the upper lobes and manifests as slowly progressive pulmonary consolidation with cavitation. In more than 50% of cases, mycetomas are found within the cavities (Fig. 2.3.2.4.4–5).

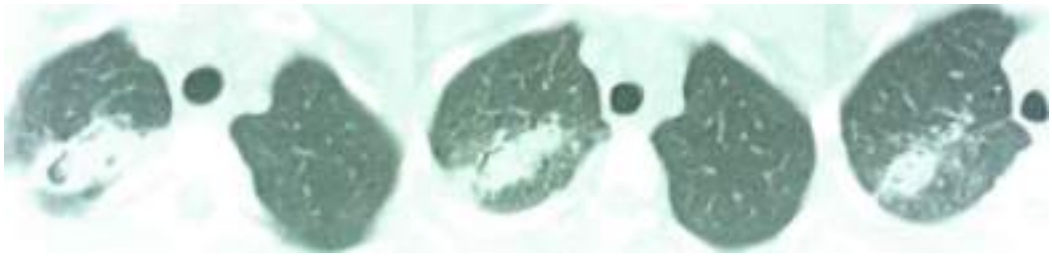

Fig. 3.3.2.4.4. Secondary pulmonary aspergillosis that developed in a cavitary lesion in patients with a history of tuberculosis. A sequestrum within the cavity is caused by the presence of a mycetoma (fungal ball, fungal mycelium).

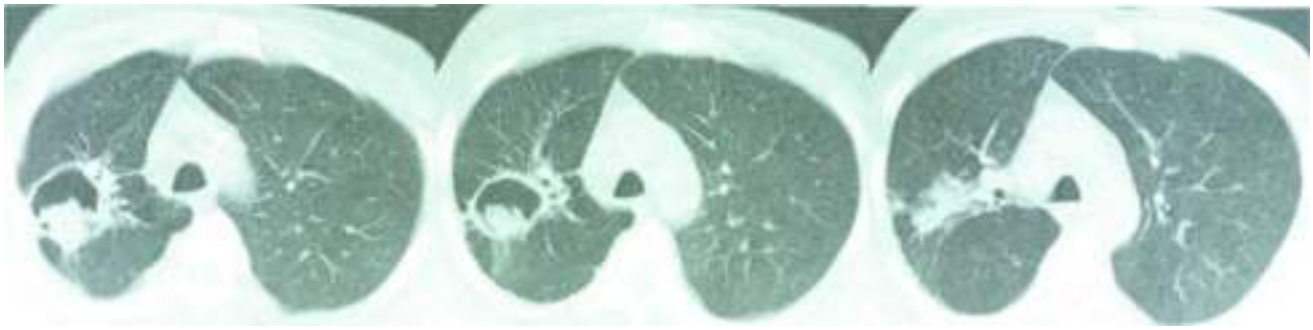

Fig. 2.3.2.4.5. Secondary pulmonary aspergillosis that developed in a residual cavitary lesion after tuberculosis treatment. A sequestrum within the cavity is caused by the presence of a mycetoma.

Pulmonary mucormycosis, similar to aspergillosis, has a tendency for arterial invasion. Pathomorphologically and radiologically, it resembles invasive aspergillosis. Pulmonary consolidation is observed, often with cavitation.
Radiologic manifestations of cryptococcosis include solitary or multiple nodules and focal opacities. Diffuse small nodular lesions, cavitation, lymphadenopathy, and pleural effusion are more frequently observed in immunocompromised patients.

2.3.2.5. Diffuse neoplastic lung lesions.

Benign tumors may occasionally present as pulmonary dissemination (Fig. 2.3.2.5.1).

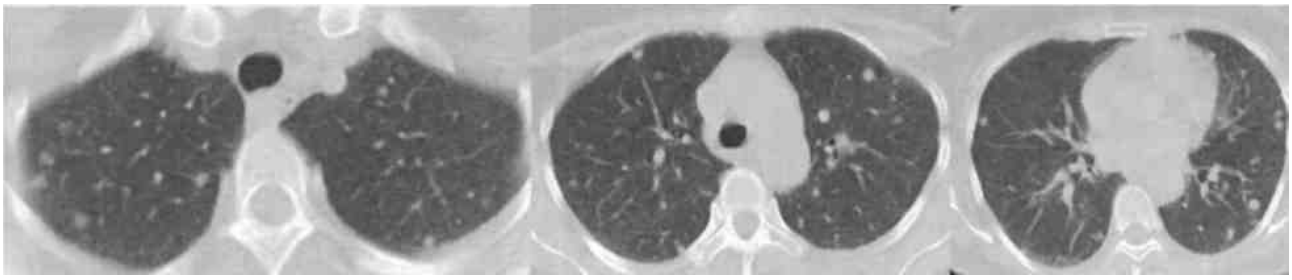

Fig. 2.3.2.5.1. Sclerosing hemangioma, GIST+. Multiple polymorphic lesions and small focal opacities chaotically distributed in both lungs (“coin lesion” sign).

Metastatic carcinoma. The most common primary tumors metastasizing to the lungs are breast cancer, renal cell carcinoma, colorectal cancer, gastric cancer, and pancreatic cancer. Metastases from seminoma and sarcoma may also occur.
CT is the most sensitive method for detecting metastases during tumor staging. CT can reveal nodules as small as 2–3 mm.

All pulmonary focal lesions not related to vessels are suspicious for nodules. Linear opacities without a focal center are not considered nodules and usually represent small (post-inflammatory) scars. Small nodules visualized on thick CT slices may show a gradual decrease in density toward the periphery due to partial volume averaging.
Metastatic nodules typically have smooth, well-defined margins. Lesions with ill-defined contours should raise suspicion for peripheral bronchogenic carcinoma. However, metastatic nodules with indistinct borders may occur due to local lymphogenic edema, intranodular hemorrhage (angiosarcoma, choriocarcinoma), or scarring after chemotherapy.
Solitary metastases are uncommon (approximately 5% of all solitary pulmonary nodules). The likelihood of a pulmonary nodule being metastatic increases as the number of nodules increases. Metastases are most frequently found in the outer third of the lungs (90%) and near the pleura. They predominate in the lower lobes (66%). Up to 40% of metastases are accompanied by the “feeding vessel” sign (Fig. 2.3.2.5.2).
CT is so sensitive in detecting pulmonary nodules (2–3 mm) that it frequently identifies benign lesions such as granulomas, intrapulmonary

lymph nodes, and focal scars. This creates challenges in differential diagnosis during preoperative tumor staging.

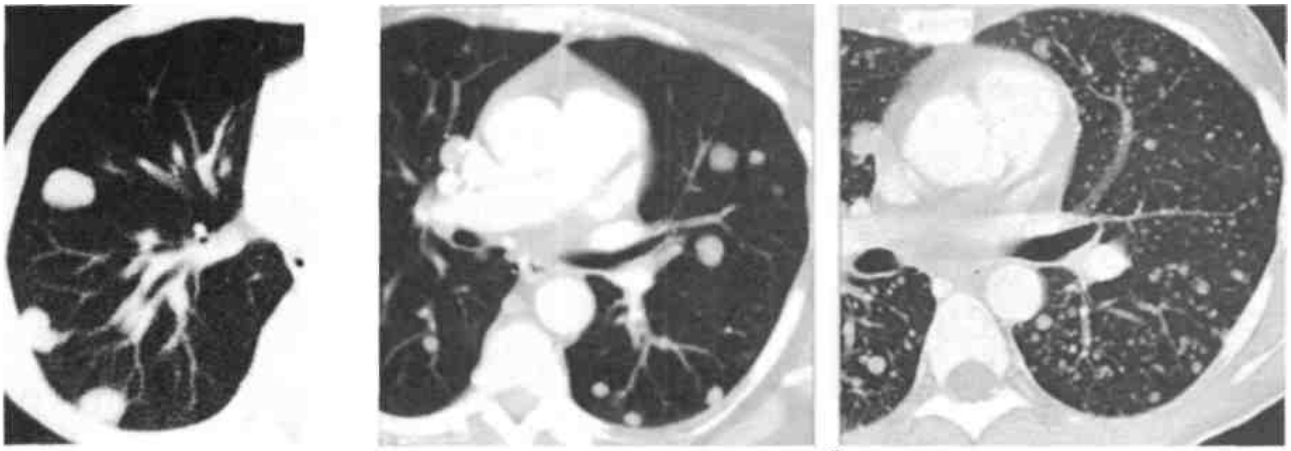

Fig. 2.3.2.5.2. Predominantly subpleural hematogenous metastases with the feeding-vessel sign (a). Chaotically distributed hematogenous metastases (b).

Since a specific histological diagnosis cannot be established by CT for all these findings, another differential diagnostic strategy must be chosen-either performing follow-up imaging after 3–6 months or defining minimal sizes (3–5 mm) of focal lesions that require further evaluation. Currently, there is no convincing evidence to support this approach. Some tumors, such as thyroid carcinoma, often produce miliary pulmonary metastases measuring only a few millimeters.

Cavities typical for septic emboli (septic and metastatic pneumonia) are rarely encountered in metastases (although they may occur, for example, in metastases of squamous cell carcinoma). Fat within pulmonary nodules usually indicates a hamartoma but may also be seen in metastases of liposarcoma.

Hematogenous metastases must be differentiated from acute and subacute hematogenous-disseminated tuberculosis. Hematogenous spread is most characteristic of tumors of the head and neck, breast, pancreas, stomach and colon, kidneys, uterus and gonads, and prostate.

On CT, hematogenous metastases are characterized by multiple uniform or polymorphic nodules of varying diameters in the lungs, typically round or oval in shape with smooth, well-defined margins. Most

metastases are located in the peripheral lung regions, subpleurally, but do not contact the visceral pleura. Tumor nodules are chaotically distributed in the lung parenchyma, without association with interstitial structures (Fig. 2.3.2.5.3–4). The number of lesions increases caudally, from the lung apices toward the diaphragm. In many patients, nodules are absent in the apical segments.

A characteristic CT sign of hematogenous origin of metastatic lesions is their connection with small arterial vessels. In such cases, vascular branches terminate directly at the nodules (Fig. 2.3.2.5.5–6).

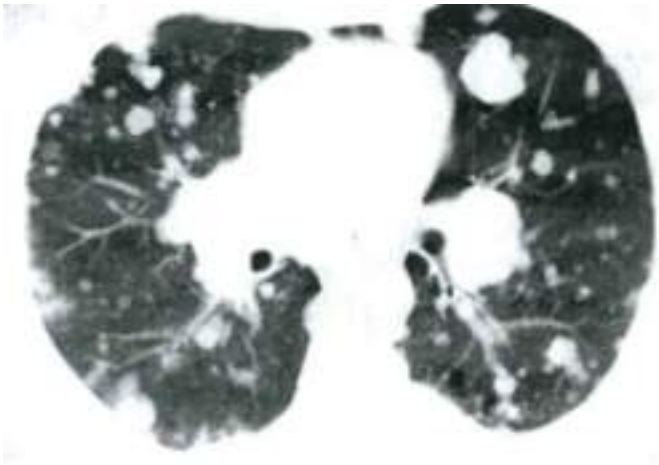

Fig. 2.3.2.5.3. Hematogenous metastases in the lungs and intrathoracic lymph nodes of gastric carcinoma. Multiple polymorphic lesions and focal opacities are chaotically distributed, some of them connected with pulmonary arterial vessels; enlargement of bronchopulmonary lymph nodes.

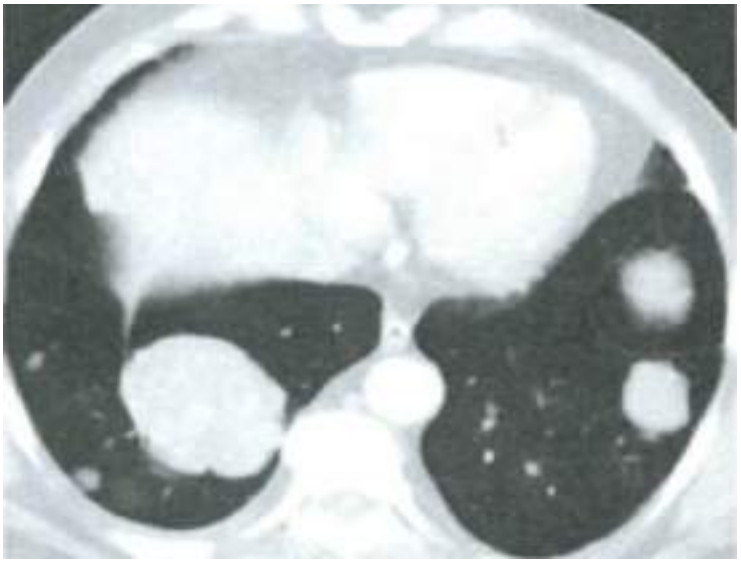

Fig. 2.3.2.5.4. Hematogenous metastases in the lungs and intrathoracic lymph nodes from thyroid carcinoma. Multiple polymorphic lesions and large focal opacities chaotically distributed.

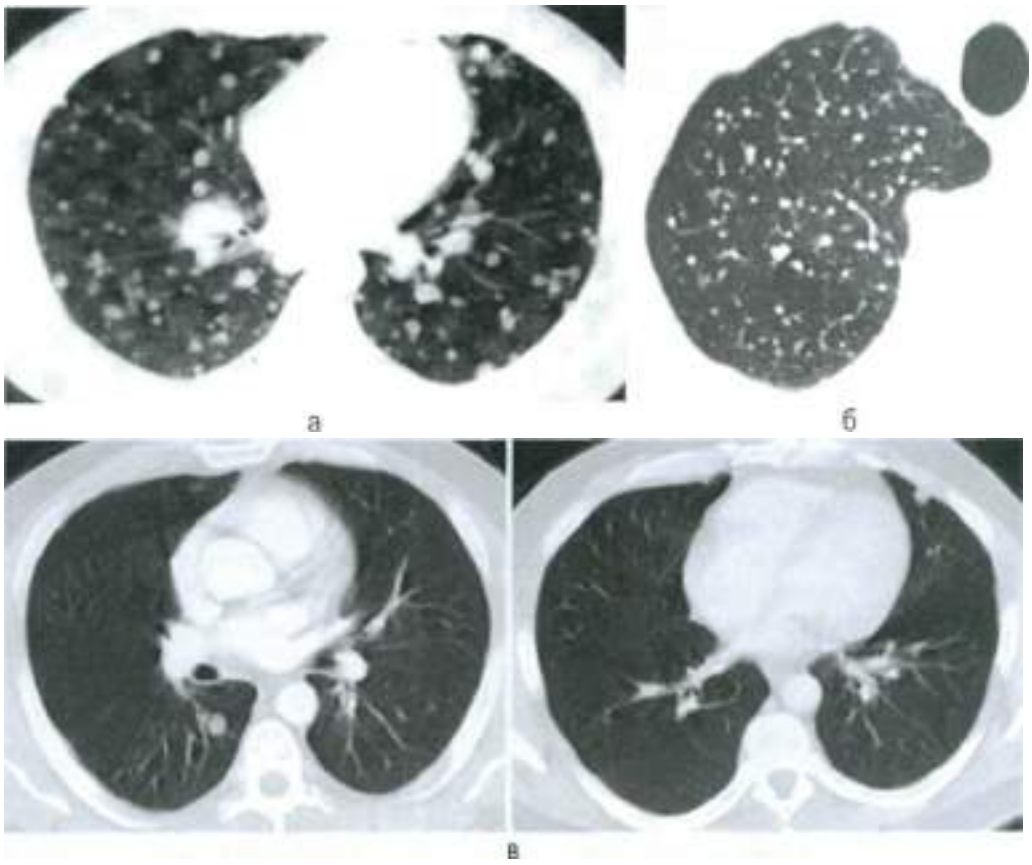

Fig. 2.3.2.5.5. Variants of hematogenous pulmonary metastases from colorectal carcinoma. Multiple small metastatic lesions of varying size (“coin lesion” sign) (a, b). Solitary small metastatic lesions in segment S6 of the right lung and segment S5 of the left lung (c).

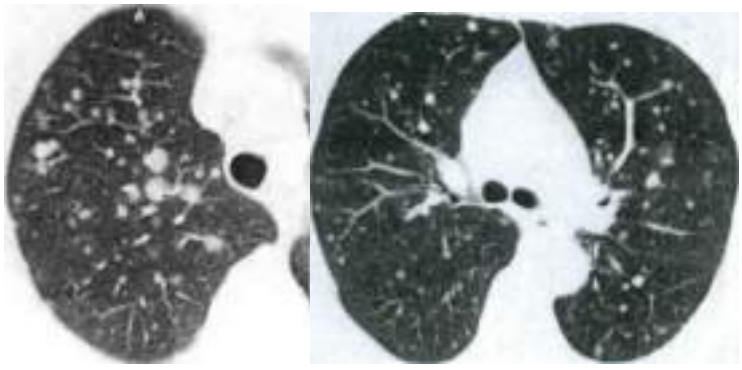

Fig. 2.3.2.5.6. Variants of hematogenous pulmonary metastases from pancreatic carcinoma. A clear connection of some lesions with arterial vessels is visible.

Interstitial changes in the lung parenchyma are not typical of hematogenous metastases, which is an important differential diagnostic feature (Fig. 2.3.2.5.7). Occasionally, an area of decreased density may be seen distal to a tumor nodule, with a broad base adjacent to the pleura. Its occurrence is associated with obstruction of an arterial vessel by tumor cells.

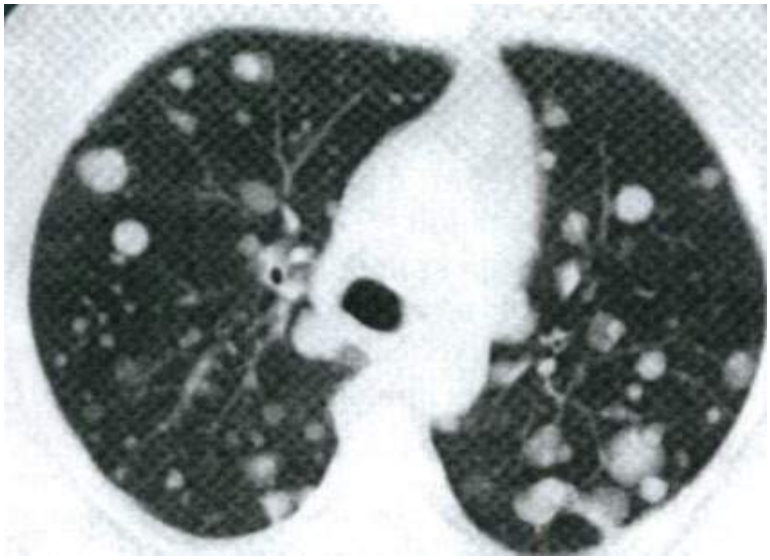

Fig. 2.3.2.5.7. Hematogenous pulmonary metastases from renal carcinoma. Interstitial changes in the lung parenchyma are absent.

Less commonly, large metastatic nodules, which also have a rounded shape, directly abut the visceral pleura with a broad base (Fig. 2.3.2.5.8). An arterial vessel often terminates at the apex of such nodules. Their origin is associated with embolization of small pulmonary arteries by tumor fragments, resulting in infarction.

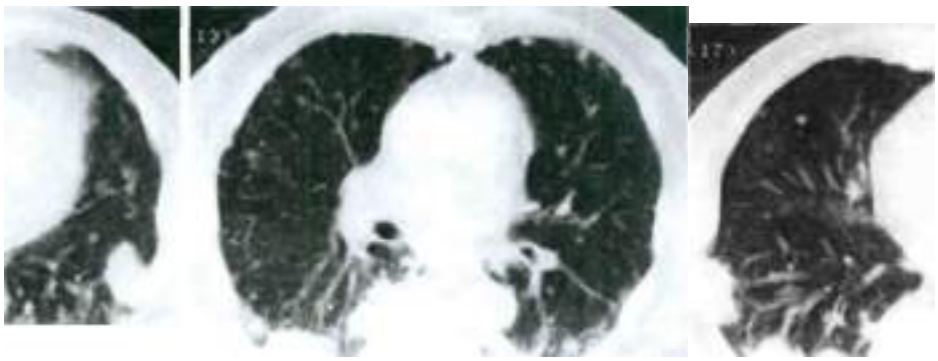

Fig. 2.3.2.5.8. Hematogenous metastases of renal carcinoma. Metastatic lesions are located subpleurally, with a broad base adjacent to the costal pleura, resembling pulmonary infarcts. A clear connection of the lesions with arterial vessels is visible.

In some patients, metastases have ill-defined margins and are surrounded by a more or less wide zone of infiltration (halo). The morphological substrate of this zone is hemorrhage and hemorrhagic edema of the adjacent lung tissue. Such changes may occur, in particular, in metastases of choriocarcinoma and pancreatic tumors (Fig. 2.3.2.5.9–11).

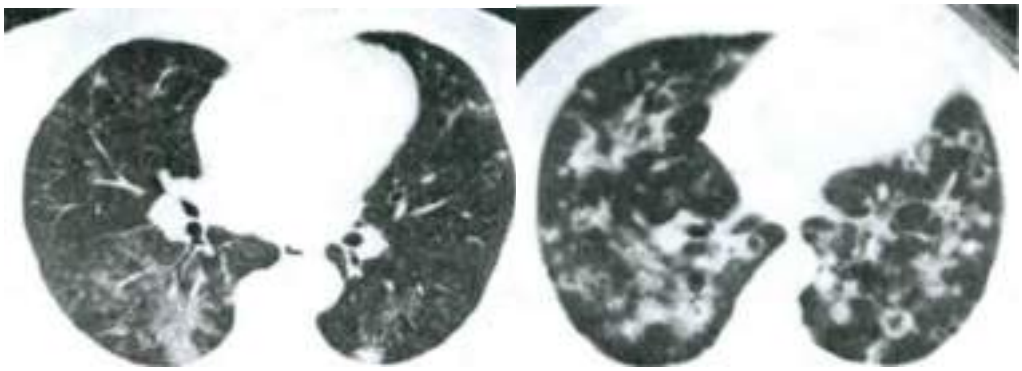

Fig. 2.3.2.5.9. Variants of hematogenous metastases of pancreatic carcinoma. Metastatic lesions have ill-defined, blurred margins, with cavitation visible in some of them (a). Small lesions in the anterior segments of both lungs merge with large areas of ground-glass pulmonary consolidation in the posterior segments (b).

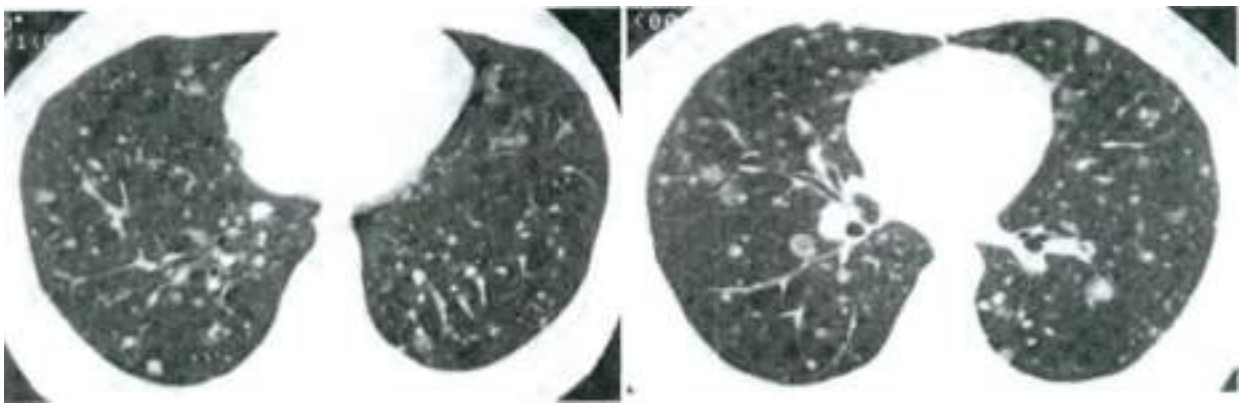

Fig. 2.3.2.5.10. Hematogenous metastases of breast carcinoma. Multiple small and medium-sized focal opacities.

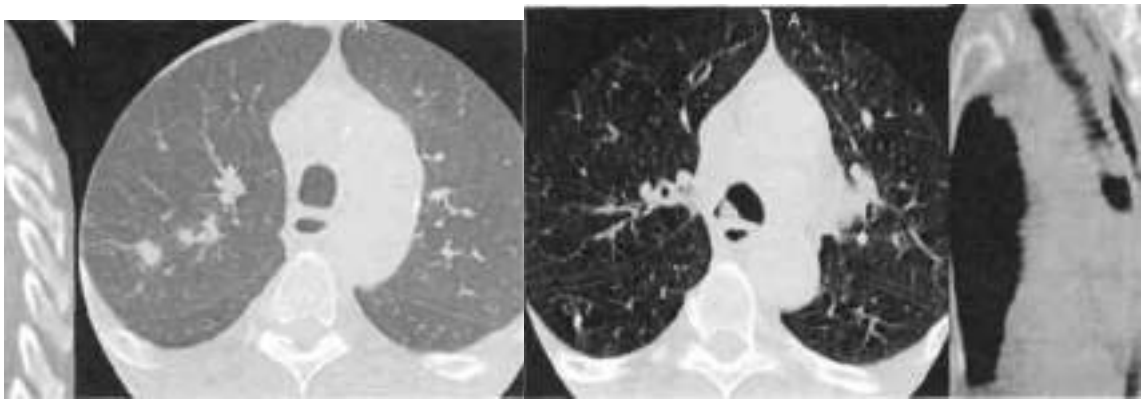

Fig. 2.3.2.5.11. Hematogenous metastases of tracheal carcinoma. The metastases have ill-defined margins and an irregular shape.

The shape and size of metastatic nodules usually have no differential diagnostic significance. However, certain tumors exhibit characteristic patterns of pulmonary involvement. Thus, diffuse miliary dissemination resembling miliary tuberculosis occurs more frequently in medullary thyroid carcinomas (Fig. 2.3.2.5.12). Large solitary metastatic nodules are typical of melanomas, choriocarcinomas, hypernephromas, and tumors of the central nervous system. Calcifications occur in metastases of osteogenic sarcomas (Fig. 2.3.2.5.13) and, less commonly, adenocarcinomas (Fig. 2.3.2.5.14). Calcification may also result from chemotherapy.

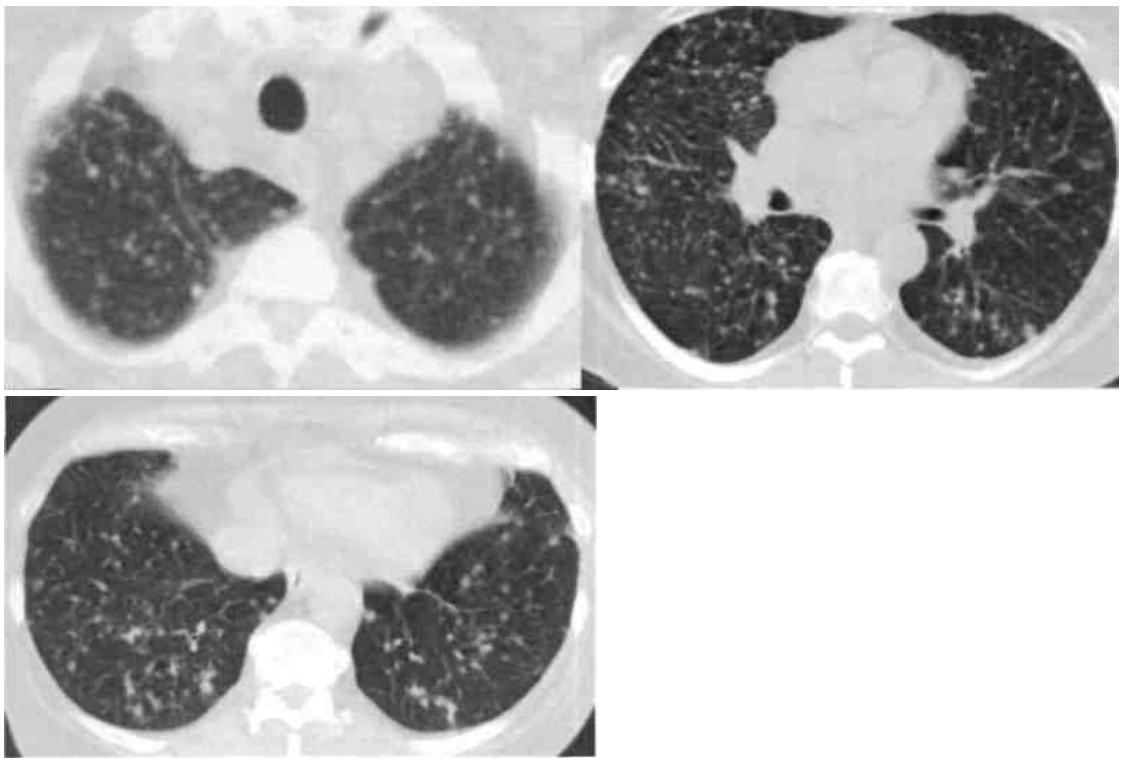

Fig. 2.3.2.5.12. Hematogenous metastases of thyroid carcinoma. Multiple small and miliary lesions throughout both lungs.

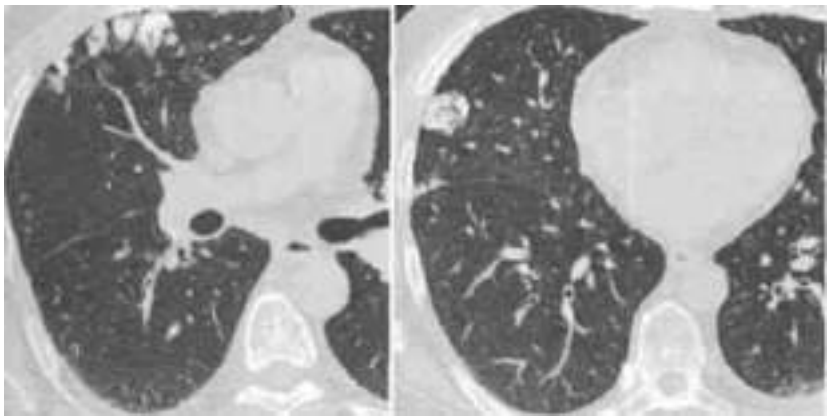

Fig. 2.3.2.5.13. Hematogenous metastases of osteogenic sarcoma. Multiple polymorphic focal opacities with uneven calcification, located subpleurally. In some large lesions, the air-bronchogram sign is present.

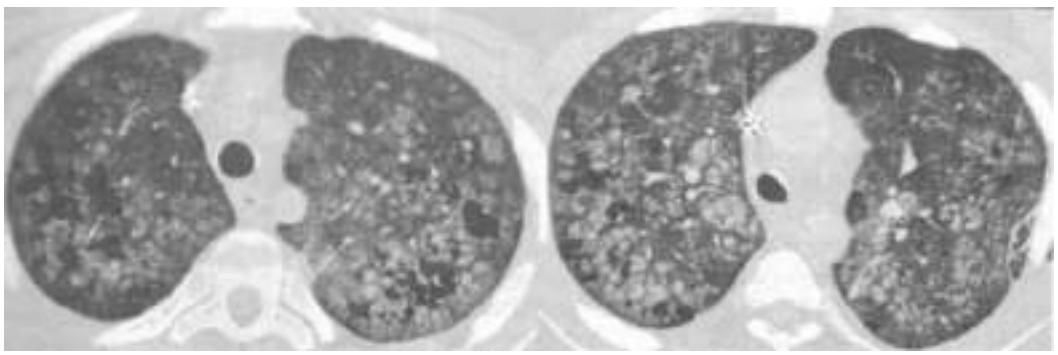

Fig. 2.3.2.5.14. Hematogenous metastases of adenocarcinoma. Multiple polymorphic focal opacities chaotically and centrilobularly distributed, surrounded by areas of emphysema.
Calcifications are present in some lesions.
Cavitary destruction develops in 4–7% of patients with hematogenous metastases, usually in large lesions. Cavities occur more frequently in metastases of squamous cell carcinomas originating from head and neck tumors and female genital tract tumors (Fig. 2.3.2.5.15–16). Cavitary destruction has also been described following chemotherapy for sarcomas.
Hematogenous metastases often remain asymptomatic for a long time or present with nonspecific clinical symptoms. A characteristic feature is the discrepancy between extensive pulmonary involvement and minimal clinical manifestations. Severe dyspnea may result from embolization of large pulmonary arteries by tumor fragments. CT angiography allows detection of a filling defect or complete occlusion of a lobar or segmental pulmonary artery. However, tumor emboli do not show specific CT features compared with ordinary blood clots in pulmonary thromboembolism. Pulmonary tumor emboli are more frequently observed in primary cardiac neoplasms or when a primary tumor invades large vessels and cardiac chambers.

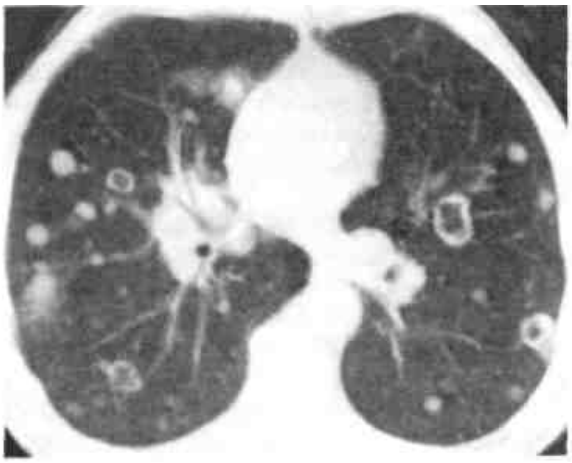

Fig. 2.3.2.5.15. Hematogenous metastases of uterine carcinoma. Cavities of necrosis are visible in some lymph nodes.

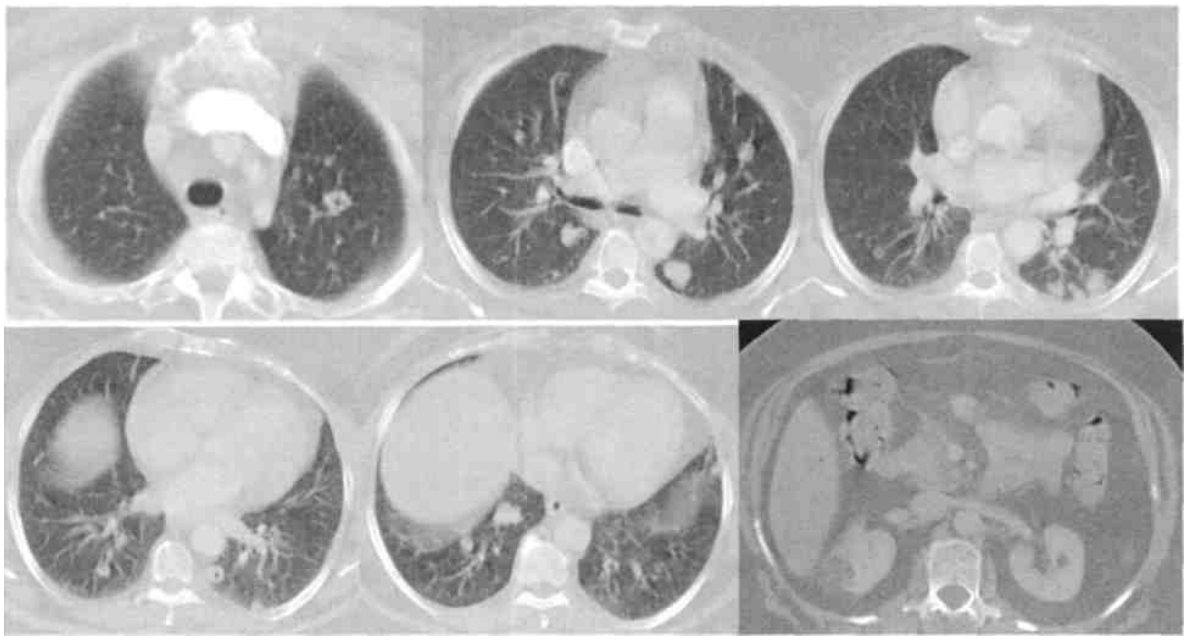

Fig. 2.3.2.5.16. Hematogenous metastases of uterine carcinoma in the lungs and kidneys. Cavities of necrosis are visible in some metastatic nodules. Hypodense nodules are present in both kidneys.

Thus, widespread small and medium-sized metastatic disseminations may produce an imaging pattern resembling disseminated tuberculosis. Overall, localization of lesions in the middle and lower lung regions, absence of interstitial changes, and the characteristic association of nodules with arterial vessels allow differentiation of hematogenous metastases from disseminated tuberculosis.

Lymphangitic carcinomatosis arises from the spread of tumor cells through the lymphatic vessels of the lungs. Lymphogenous metastases occur in 6–8% of oncology patients. The most common primary tumor sites in these cases are the lungs, breast, stomach, pancreas, and rectum. In malignancies of these organs, the rate of lymphogenous metastases increases to 24–56%.

Lymphangitic carcinomatosis may develop in two ways. The first and most common mechanism involves initial hematogenous spread of tumor cells, which subsequently invade the vessel wall and disseminate through lymphatic channels from the peripheral lung regions toward the hilum. The second mechanism is characterized by primary involvement of mediastinal lymph nodes with subsequent retrograde spread of tumor cells through the lymphatic vessels from the lung root toward the cortical regions.

On CT, lymphangitic carcinomatosis is characterized by isolated interstitial (reticular) changes or a combination of focal and interstitial abnormalities. These changes may be generalized, bilateral, or unilateral. Unilateral involvement, including involvement limited to a single lung lobe, is typical for lymphogenous metastases of lung cancer and breast cancer. A characteristic feature is thickening of all components of the pulmonary interstitium, including axial, peripheral, and septal structures.

Thickening of the axial interstitium leads to the appearance of peribronchial cuffs and enlargement of the surrounding arterial structures. The margins of vessels and bronchi become indistinct. These findings are especially noticeable in the perihilar region. Changes in the walls of small intralobular arteries and bronchi are accompanied by centrilobular nodules in the cortical regions. Interlobular septa in these areas become uniformly thickened and appear as numerous polygonal structures. The larger interlobular septa, arranged perpendicular to the costal and mediastinal pleura, correspond to Kerley lines.

The CT appearance of lymphangitic carcinomatosis in its early stages depends significantly on the mechanism of tumor spread. In antegrade spread—from the pleura toward the hilum—changes of the peripheral (interlobular) and intralobular interstitium predominate, often in combination with pleural effusion (Fig. 2.3.2.5.17). Retrograde spread from the hilar lymph nodes is characterized by predominant involvement of the central (peribronchovascular) interstitium and more frequent lymph node enlargement.

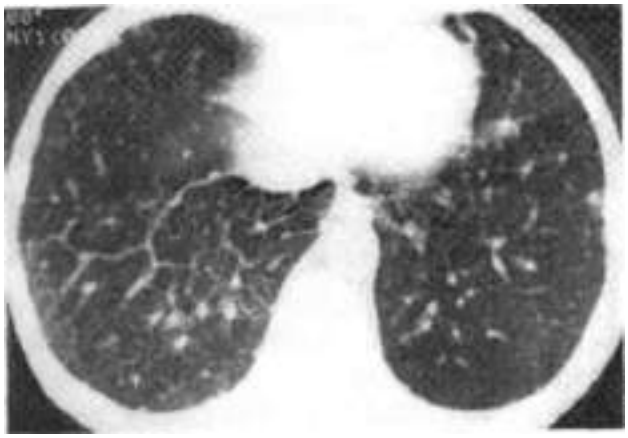

Fig. 2.3.2.5.17. Lymphangitic carcinomatosis, gastric carcinoma metastases to the lungs. Changes predominate in the right lower lobe and are characterized by diffuse, uniform thickening of the interlobular septa with the formation of typical polygonal structures.
With deeper involvement of the pulmonary interstitium, alterations of the intralobular structures occur, with sequential thickening of the interacinar and interalveolar septa and filling of the alveoli with exudate (Fig. 2.3.2.5.18).

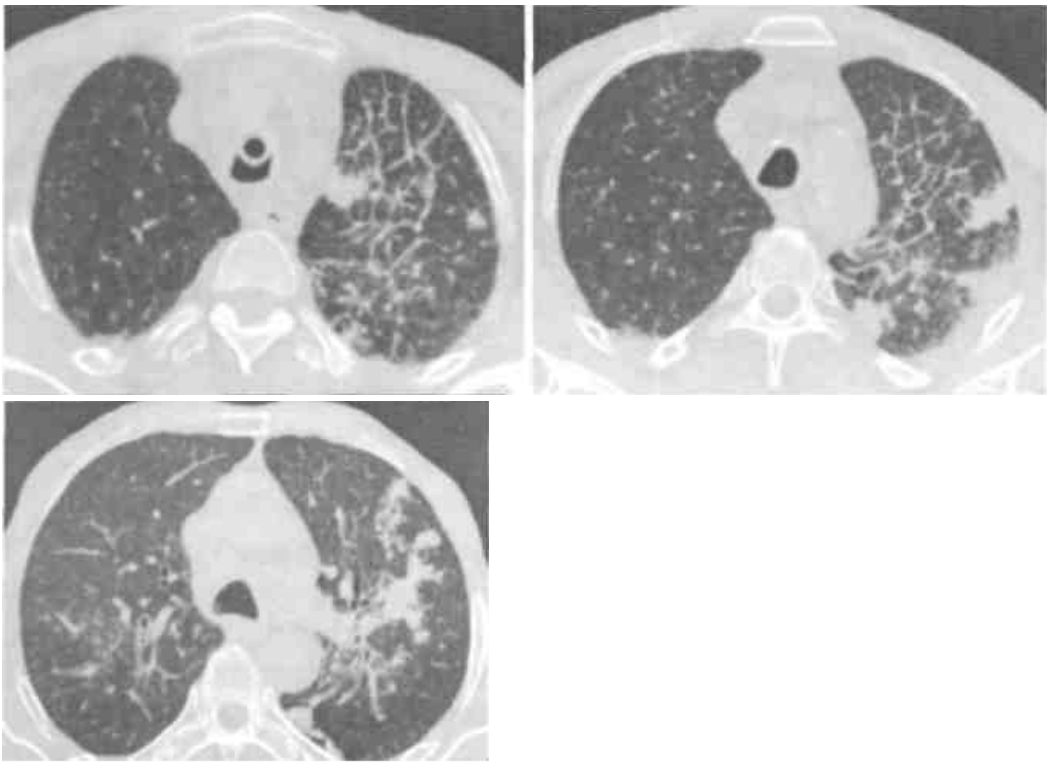

Fig. 2.3.2.5.18. Lymphangitic carcinomatosis, laryngeal carcinoma metastases to the lungs, GIST+. Changes predominate in the upper lobe of the left lung; typical uniform thickening of the interlobular septa; areas of pulmonary consolidation of the alveolar infiltration type; thickened costal pleura; increased number and size of intrathoracic lymph nodes. A ring-shaped shadow of the tracheostomy is visible in the trachea.

On radiographs and computed tomography, small intralobular septa appear as tiny nests measuring 2–5 mm in diameter. Involvement of the alveolar walls in the pathological process results in diffuse increased density of the lung parenchyma of the “ground-glass” type. Within the consolidation zone, altered interstitial structures and intrapulmonary

vessels are clearly visible. Accumulation of exudate in the alveoli leads to complete loss of aeration of the lung parenchyma (Fig. 2.3.2.5.19).

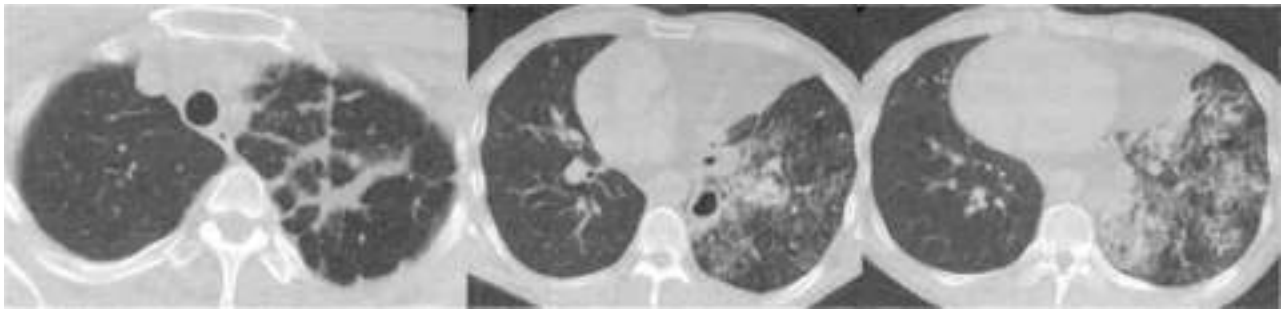

Fig. 2.3.2.5.19. Lymphangitic carcinomatosis, metastases of mediastinal lipoma to the lungs. Thickening and infiltration of the interlobular septa in the upper lobe of the left lung; thickened costal pleura; areas of pulmonary consolidation of the alveolar infiltration type in the middle and lower regions of the left lung; cavitation within a metastatic nodule; increased number and size of intrathoracic lymph nodes.

The lesions observed in lymphangitic carcinomatosis have different origins, which can be clearly distinguished only on CT. Some lesions represent proliferation of tumor tissue along the lymphatic vessels. Such lesions are small (1–2 mm) and are located perilymphatically—that is, within the thickened walls of secondary pulmonary lobules, along vessels and bronchi, and in the interlobular pleura. Less commonly, lesions are found outside the interstitial structures, directly within the lung parenchyma; their origin is associated with simultaneous hematogenous metastasis. Finally, centrilobular lesions result from thickening of the walls of small intralobular arteries and bronchi.
Thickening of the walls of large lobar and segmental arteries and bronchi, representing the so-called central interstitium, is the most important distinguishing feature of lymphangitic carcinomatosis. These changes are most pronounced during retrograde spread of tumor cells from the mediastinal lymph nodes into the lung tissue. In such cases, the walls of the large bronchi are markedly thicker than normal, the bronchial lumen is reduced, and the external bronchial contour becomes indistinct, often with a radiating appearance. The caliber of adjacent arteries is also increased, and their margins may be ill-defined. These changes are frequently accompanied by peribronchial consolidation of the lung parenchyma due to lymphatic stasis (Fig. 2.3.2.5.20).

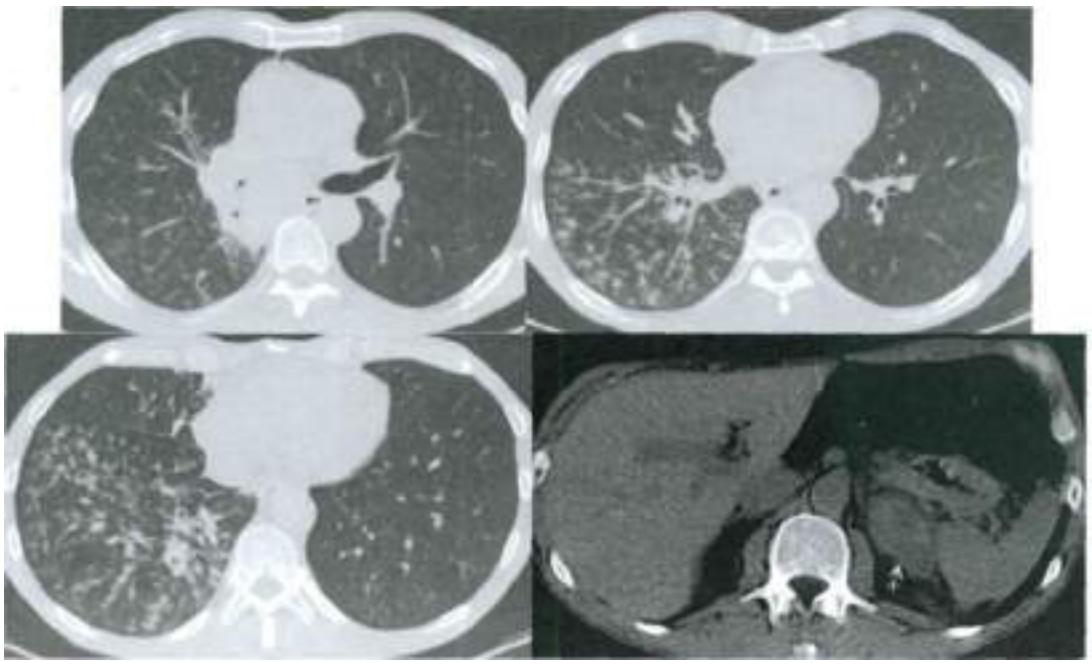

Fig. 2.3.2.5.20. Lymphangitic carcinomatosis, metastases of right adrenal carcinoma (arrow) to the lungs and intrathoracic lymph nodes, GIST+. Changes predominate in the right lung, with typical uniform thickening of the interlobular septa and areas of alveolar-type pulmonary consolidation; enlargement of intrathoracic and right bronchopulmonary lymph nodes.

Characteristic features of lymphangitic carcinomatosis include pleural effusion and enlargement of the hilar and mediastinal lymph nodes. Fluid typically accumulates in both pleural cavities and may be inapparent on routine chest radiographs. Mediastinal lymph node enlargement is not present in all patients with lymphangitic carcinomatosis, particularly in the early stages of the disease. CT allows reliable differentiation of lymphangitic carcinomatosis from hematogenous and lymphogenous tuberculous disseminations (Fig. 2.3.2.5.21).

The development of lymphangitic carcinomatosis is generally accompanied by pronounced clinical symptoms, including progressive dyspnea, weakness, and dry cough. This fundamentally distinguishes lymphogenous metastases from hematogenous ones. However, detection of lymphangitic carcinomatosis, even at early stages, has virtually no impact on the disease outcome. More than half of patients with these changes die within the following three months. Therefore, the

primary role of imaging lies in preventing unnecessary surgical intervention when signs of lymphangitic carcinomatosis are identified.

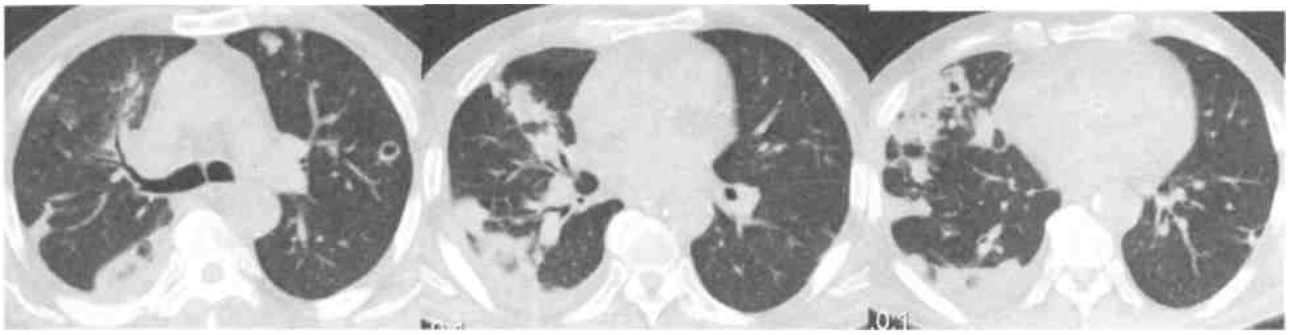

Fig. 2.3.2.5.21. Lymphangitic carcinomatosis, gastric carcinoma metastases to the lungs. In segment S3 of the right lung, areas of ground-glass pulmonary consolidation, multiple perilymphatic and centrilobular nodules, and confluent focal opacities with fine cystic elements predominantly on the right. In segment S2 of the left lung, a metastatic lesion with cavitation. Right-sided pleural effusion and enlargement of the hilar and mediastinal lymph nodes.

Bronchioloalveolar carcinoma presents clinically with minimal symptoms (complaints of weakness, fatigue, progressive dyspnea, dry cough, often chest pain, slight fever) and nonspecific auscultatory findings. The development of bronchioloalveolar carcinoma may be accompanied by abundant production of clear, frothy sputum. Malignant dissemination is possible in patients with a history of present or past cancer of the breast, stomach, kidney, thyroid, cervix, or pancreas. In cases of hematogenous metastasis, the lungs demonstrate fine dissemination resembling acute hematogenous disseminated tuberculosis. Over time, these opacities enlarge while maintaining smooth margins, with progressive increase in reticular changes.

Cancerous lymphangitis is associated with the spread of tumor cells along the lymphatic pathways. In the retrograde form, metastases initially involve the hilar lymph nodes and subsequently spread against the direction of lymph flow into the lung parenchyma. On radiographs, hilar lymph node conglomerates are seen, from which linear shadows radiate along the bronchi and vessels, creating a reticular pattern. In the antegrade form, the tumor spreads from subpleurally located small

metastases through the lymphatic vessels toward the lung hila. Thin, tortuous, poorly defined linear opacities directed toward the lung hilum are identified in the lower and middle lung regions. Adenopathy in this form is absent or appears late. In the lower outer lung regions, narrow septal lines are often visible. When carcinoid nodules develop along the pathways of lymphatic dissemination, focal opacities appear on imaging against the background of a reticular pattern. Reliable diagnostic clues include an oncologic history, persistently elevated ESR, anemia, and detection of atypical cells in sputum.

The disseminated form of bronchioloalveolar carcinoma (BAC) has two major patterns of presentation. The first and more common variant is characterized by multiple polymorphic pulmonary nodules, most often large or medium-sized, with smooth, well-defined margins (Fig. 2.3.2.5.22). Interstitial changes are not prominent, and lymph node enlargement is uncharacteristic. Even with extensive bilateral lung involvement, clinical symptoms may be minimal, making diagnosis challenging. In some CT examinations, a large primary tumor nodule with typical features of peripheral carcinoma may be identified, which allows a more confident interpretation of the nature of the dissemination.

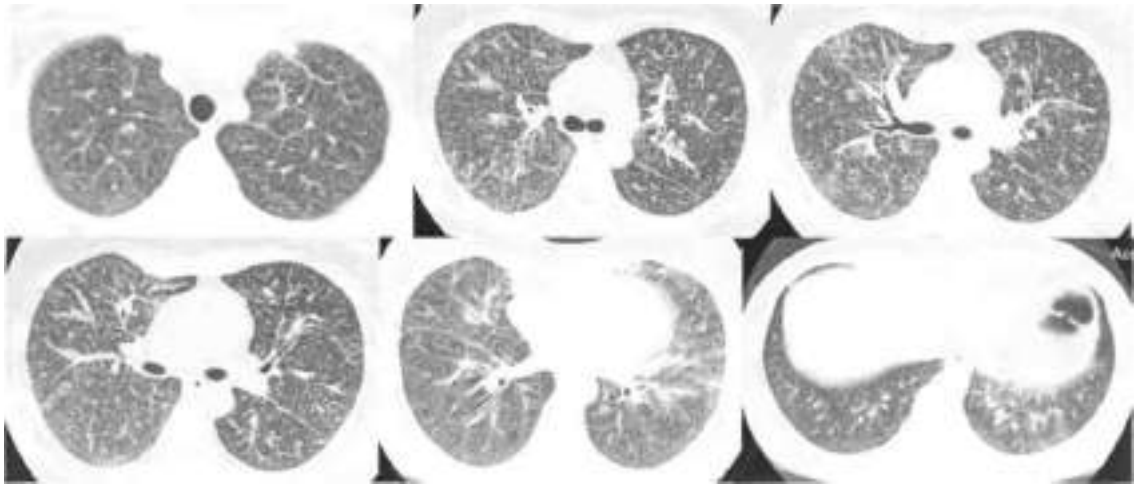

Fig. 2.3.2.5.22. Bronchioloalveolar carcinoma, disseminated form. Multiple polymorphic, predominantly small, round nodules.

The second variant of bronchioloalveolar carcinoma is characterized by predominance of interstitial changes that resemble alveolitis or lymphangitic carcinomatosis (Figs. 2.3.2.5.23–24). In such patients, dyspnea and general symptoms of tumor intoxication are significantly more pronounced. The optimal method for verifying the tumor process in

the disseminated form of bronchioloalveolar carcinoma is bronchoalveolar lavage. Examination of bronchial washings allows detection of tumor cells in the majority of patients.

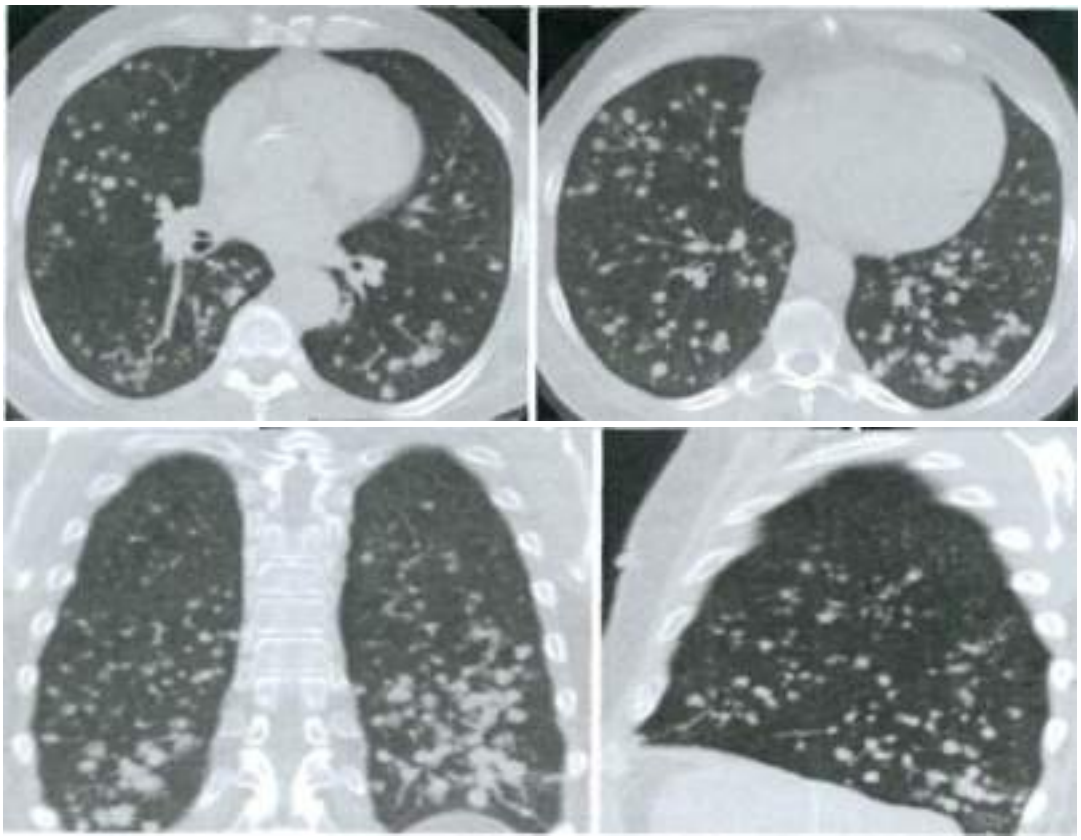

Fig. 2.3.2.5.23 a. Bronchioloalveolar carcinoma, disseminated form, GIST+. Multiple polymorphic, predominantly medium and large round nodules with no interstitial changes.

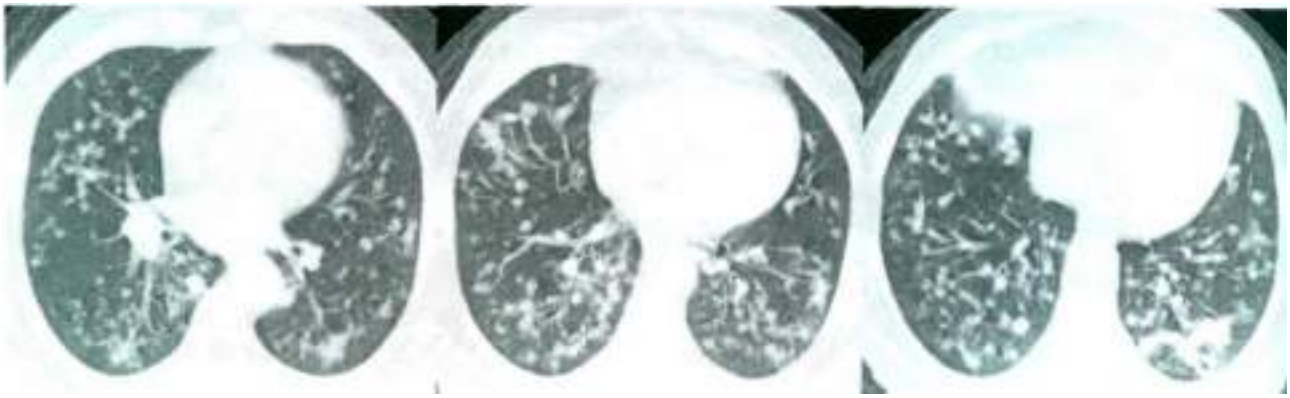

Fig. 2.3.2.5.23 b. The same patient after five months of follow-up. Focal and interstitial changes have progressed.

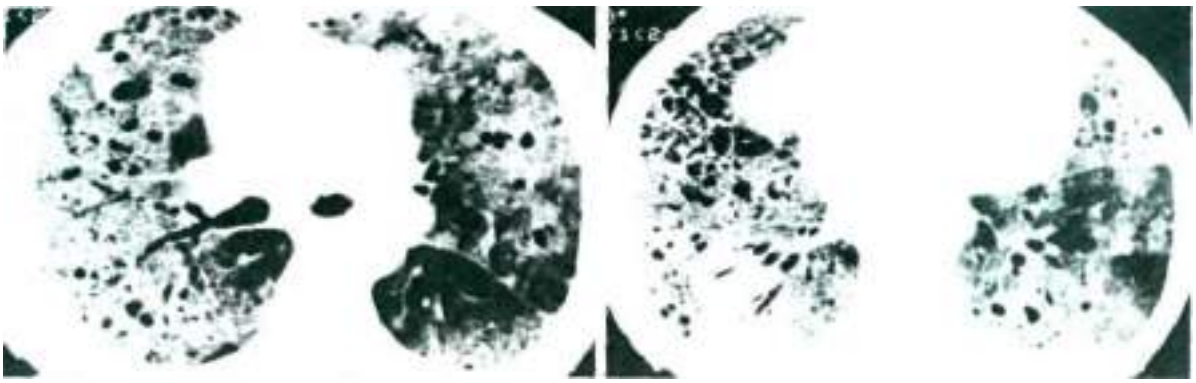

Fig. 2.3.2.5.24. Bronchoalveolar carcinoma, infiltrative (pneumonia-like) form. Diffuse infiltration and areas of ground-glass opacity in both lungs.

Kaposi sarcoma in HIV-infected patients can involve the lungs along with the skin and gastrointestinal tract. The radiologic presentation may resemble disseminated tuberculosis. The overall incidence of Kaposi sarcoma is currently decreasing (from 60% to 15–20%).

CT typically reveals ill-defined nodular lesions or patchy opacities predominantly located in the perihilar regions (bilateral, often asymmetric), oriented along the vascular–bronchial structures. They may be accompanied by nodular thickening of the interlobular septa, producing an image reminiscent of carcinomatous lymphangitis. The lesions have poorly defined margins due to infiltration of the surrounding interstitial tissue (local lymphangitis), resulting in a spiculated appearance or flame-shaped opacities. Similar changes are observed in angiosarcoma (Fig. 2.3.2.5.25).

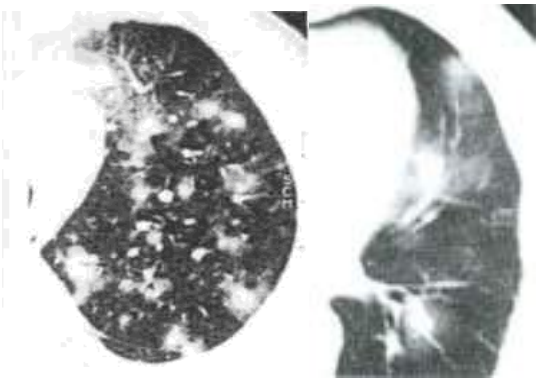

a b

Fig. 2.3.2.5.25. Kaposi sarcoma. Multiple perivascular foci of consolidation caused by perifocal hemorrhage (a). Perifocal hemorrhages are also seen in pulmonary angiosarcoma.

Endobronchial tumor spread may lead to atelectasis. This highly vascular tumor enhances intensely after intravenous contrast

administration. Massive pleural effusion and mediastinal lymphadenopathy are frequently observed.

2.3.2.6. Sarcoidosis.

Sarcoidosis (Bénier–Beck–Schaumann disease) is a systemic disorder characterized by productive inflammation with formation of epithelioid-cell granulomas without caseous necrosis, which subsequently resolve or undergo hyalinization and fibrosis. Clinically, the disease is characterized by enlargement of intrathoracic lymph nodes, diffuse involvement of the lungs, bronchi, serous membranes, and other organs (hepatomegaly, skin and bone lesions).

Diagnosis. It is now well established that the diagnosis of “sarcoidosis” can only be made when clinical, radiologic, and laboratory findings are confirmed histologically by the presence of noncaseating granulomas. In 35–40% of patients, the diagnosis is established by characteristic clinical–radiologic features; in the remaining cases, verification is achieved by histologic examination of biopsy specimens from affected organs. Radiologic evaluation plays a leading role in the diagnosis of sarcoidosis:

• chest radiography and tomography through the hilar region;
• CT as a clarifying method.

Chest radiography remains the most widely used, accessible, and inexpensive technique for assessing lung status; however, it has several limitations, including low contrast resolution and summation effects. Depending on the predominant pattern of mediastinal and parenchymal abnormalities, four principal radiologic (imaging) variants of sarcoidosis are distinguished:

• mediastinal (intrathoracic adenopathy);
• disseminated;
• parenchymal (pneumonic);
• interstitial.

A characteristic finding in sarcoidosis is bilateral enlargement of intrathoracic lymph nodes, predominantly the bronchopulmonary groups (rarely unilateral involvement) (Figs. 2.3.2.6.1–2). Adenopathy may be isolated or combined with pulmonary changes in the form of

dissemination. Pulmonary dissemination appears as scattered nodular opacities, 2–7 mm in diameter, superimposed on a background of fine reticular distortion of the lung pattern, more densely distributed in the axillary regions. In rare cases, isolated pulmonary involvement without adenopathy occurs (Figs. 2.3.2.6.3–4). A pneumonic variant of sarcoidosis, caused by infiltration and hypoventilation of a lung region, is also occasionally encountered.

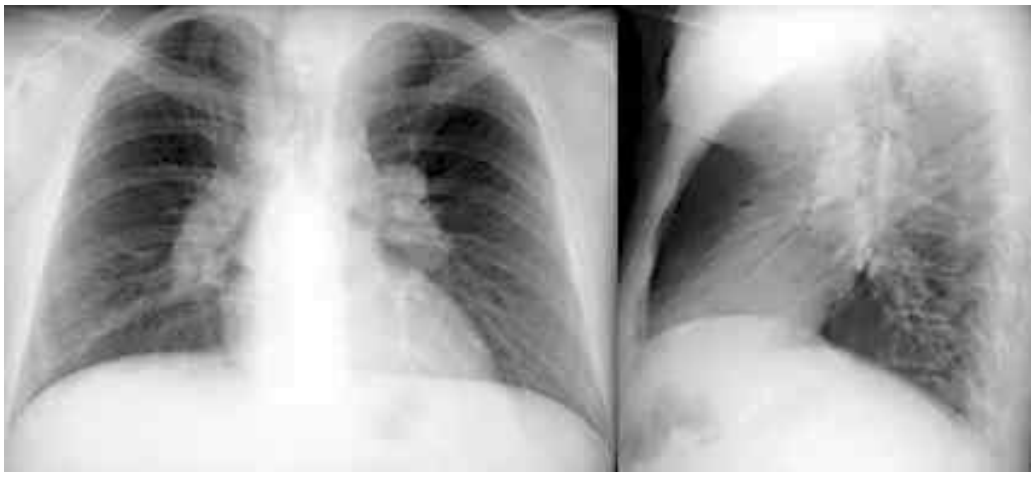

Fig. 2.3.2.6.1. Radiograph: Bilateral perihilar lymphadenopathy.

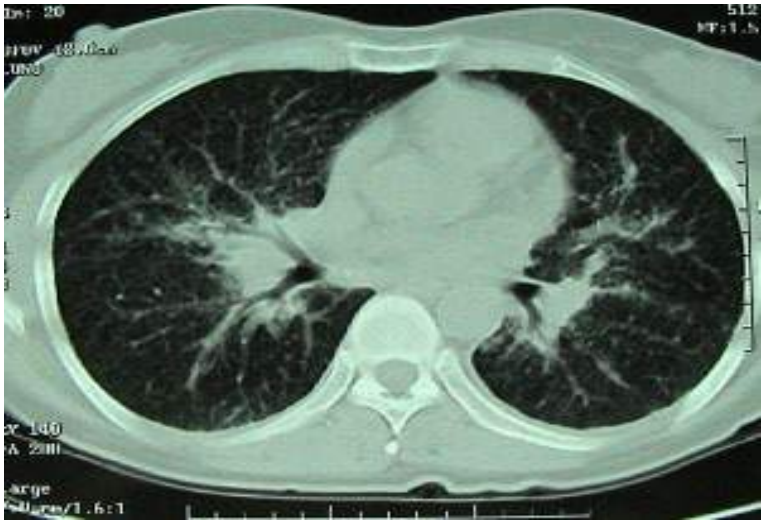

Fig. 2.3.2.6.2. CT: Bilateral perihilar lymphadenopathy combined with pulmonary infiltration.

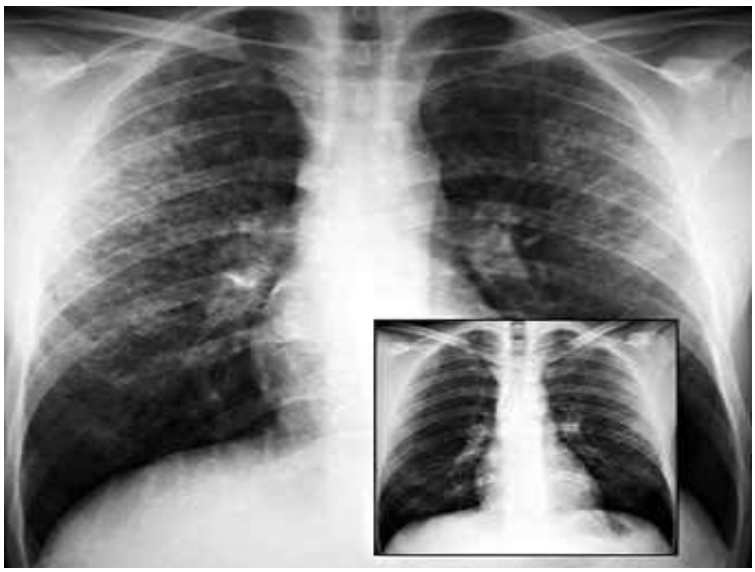

Fig. 2.3.2.6.3. Radiograph: Pulmonary infiltration (without perihilar lymphadenopathy).

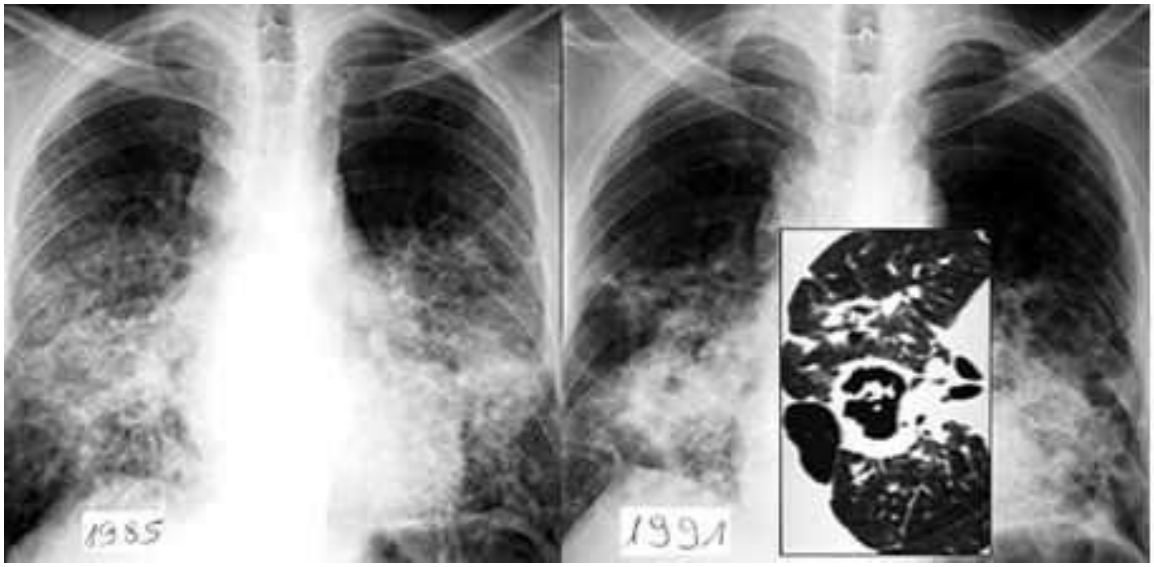

Fig. 2.3.2.6.4. Radiograph: Pulmonary fibrosis.

The radiologic appearance of the mediastinal variant of sarcoidosis is typically characterized by bilateral, symmetric enlargement of the lung hila due to enlargement of the bronchopulmonary lymph node groups (Fig. 2.3.2.6.5). The hila lose their normal structural detail, and their outer (lateral) contours become lobulated. In approximately 5–8% of cases, unilateral lymph node enlargement is observed, which often leads to diagnostic errors (this is explained by the fact that the left hilum is partially obscured by the cardiac silhouette, and therefore mild lymph node enlargement in this region may remain undetected).

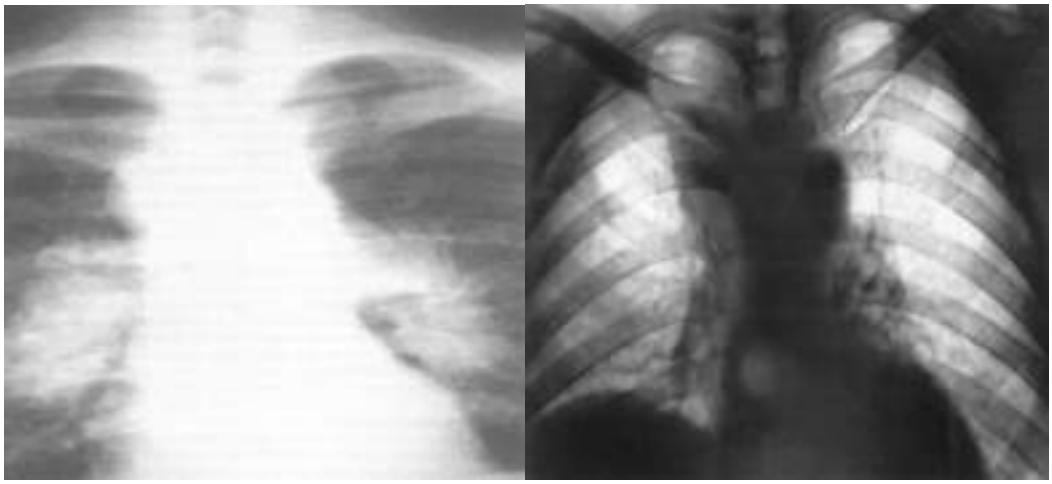

Fig. 2.3.2.6.5. Radiologic appearance of the mediastinal variant of sarcoidosis. Variants of sarcoidosis progression over time (Figs. 3.3.2.6.6–9).

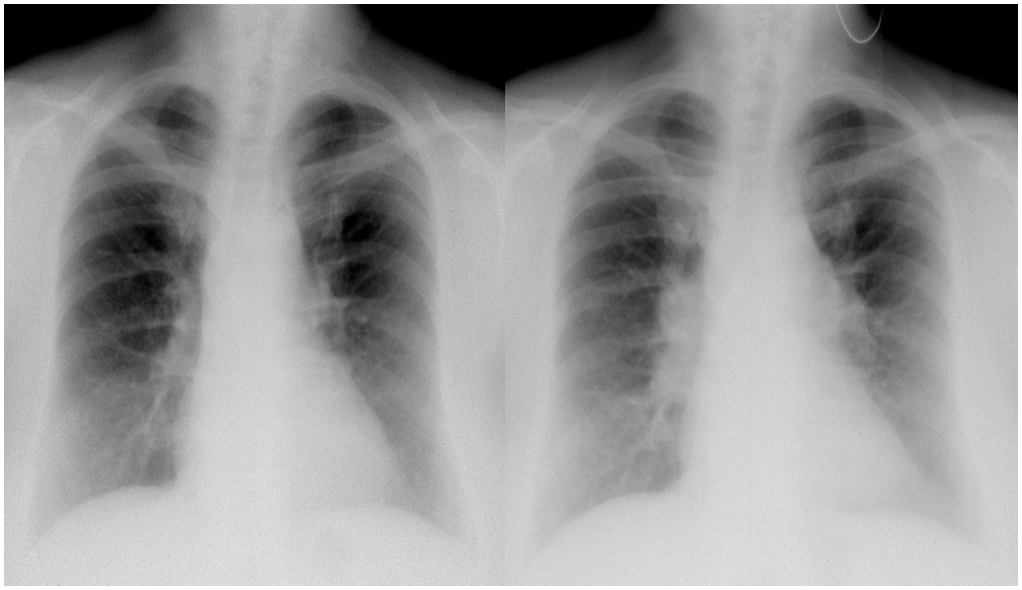

in 1 year

Fig. 2.3.2.6.6. Patient N. Sarcoidosis, Stage I (intrathoracic lymphadenopathy).

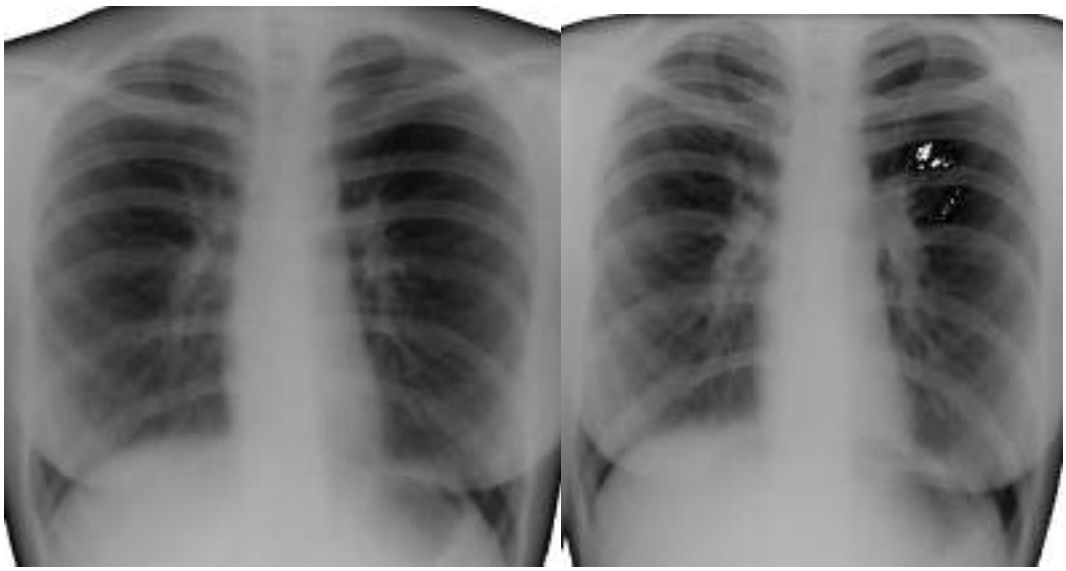

in 5 months

Fig. 2.3.2.6.7. Patient D. Sarcoidosis, Stage I (intrathoracic lymphadenopathy).

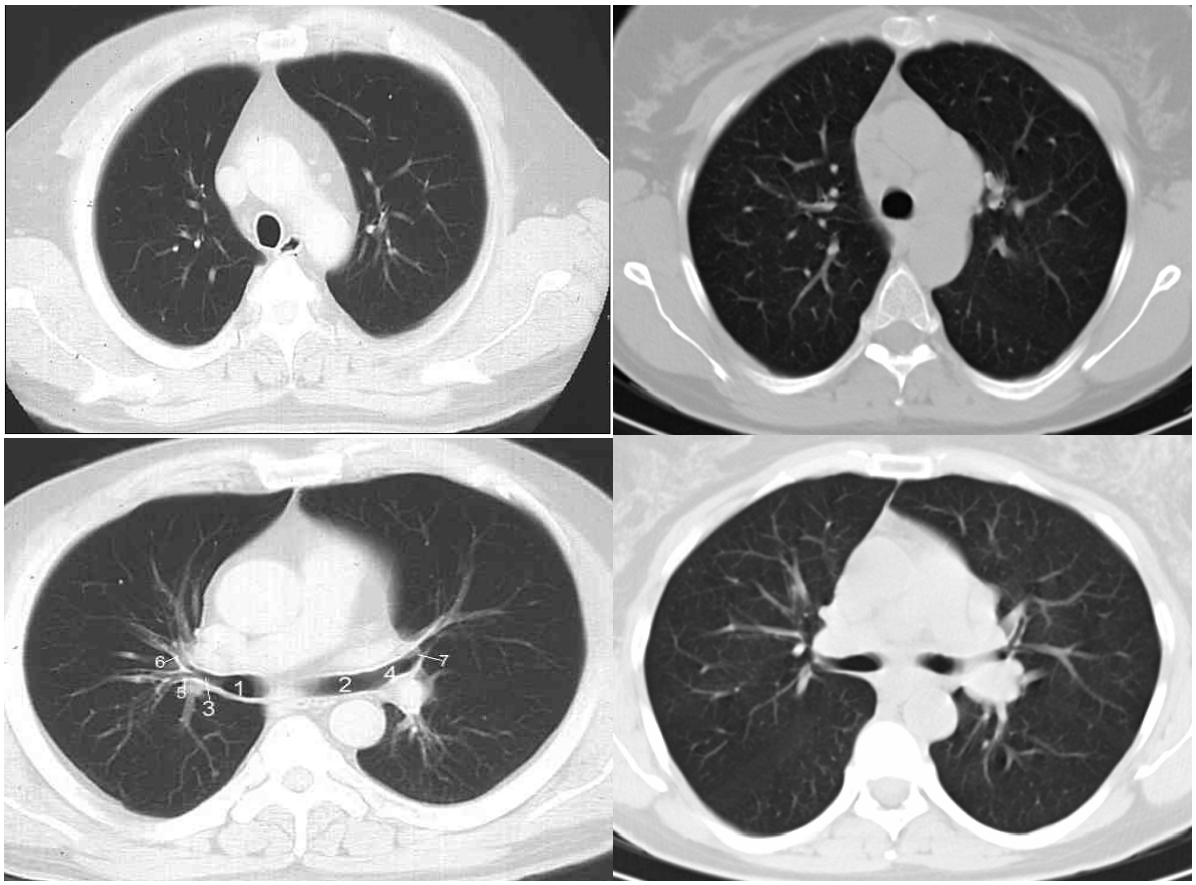

Fig. 2.3.2.6.8. CT of the lungs. Normal CT of the lungs. Sarcoidosis, Stage I (intrathoracic lymphadenopathy).

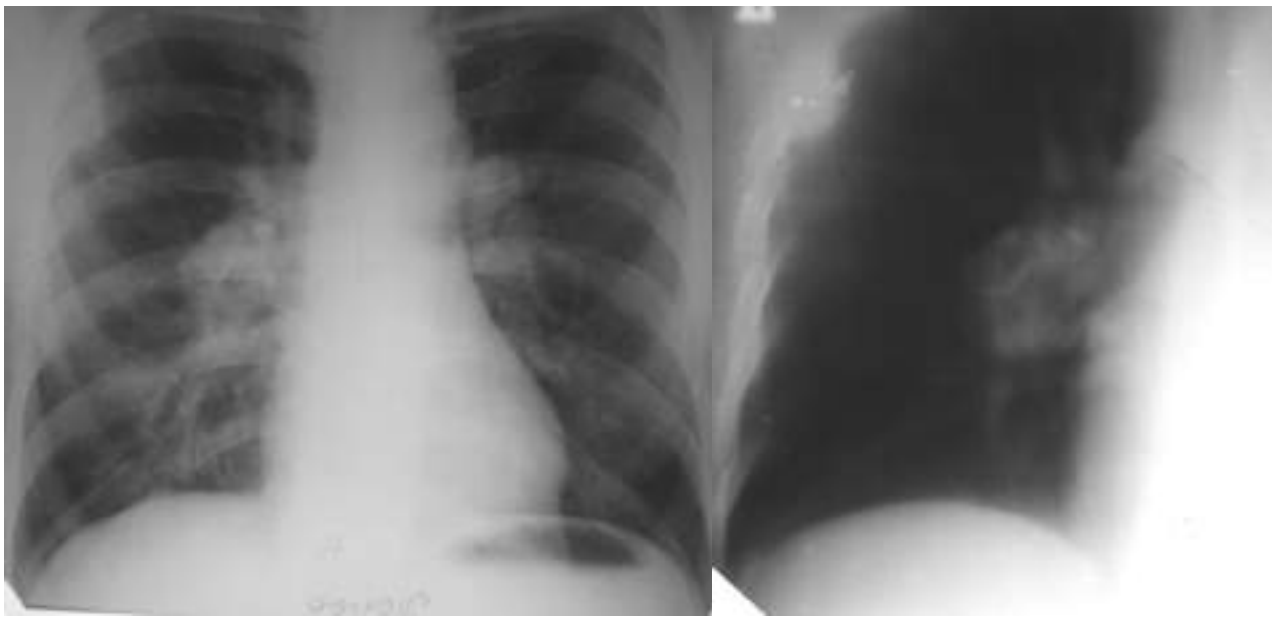

Fig. 2.3.2.6.9. Sarcoidosis, Stage II (intrathoracic lymphadenopathy + pulmonary involvement).

The radiologic symptom complex of dissemination in sarcoidosis is characterized by the presence of multiple scattered pulmonary nodules, ranging from 2 mm to 1 cm in size, detected in 80% of patients with sarcoidosis (Figs. 2.3.2.6.10–12). The nodules predominantly involve the middle and upper lung regions. Reticular–honeycomb (cellular) and looping deformation of the lung pattern is caused by infiltration of interstitial structures. Lymph nodes are enlarged in 10–60% of patients.

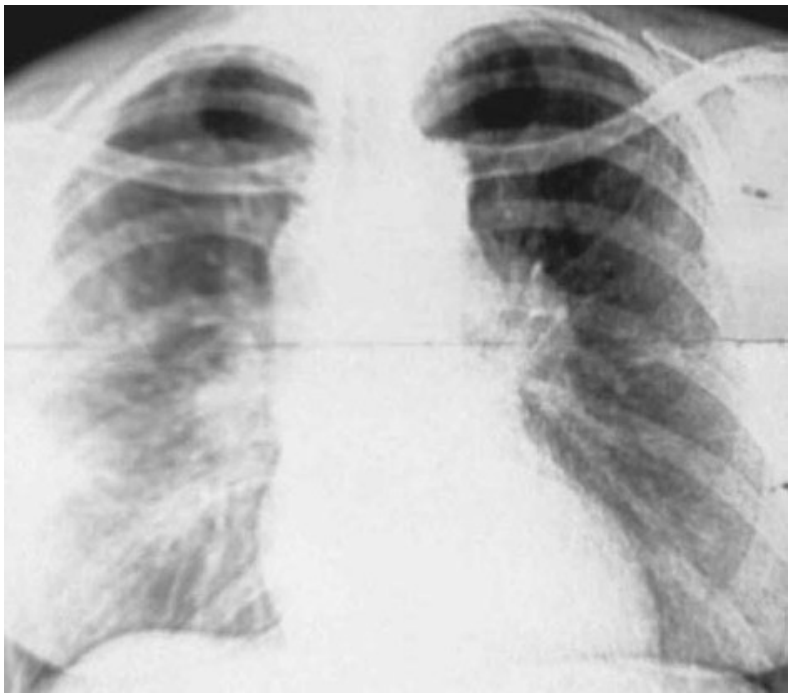

Fig. 2.3.2.6.10. Radiologic symptom complex of dissemination in sarcoidosis.

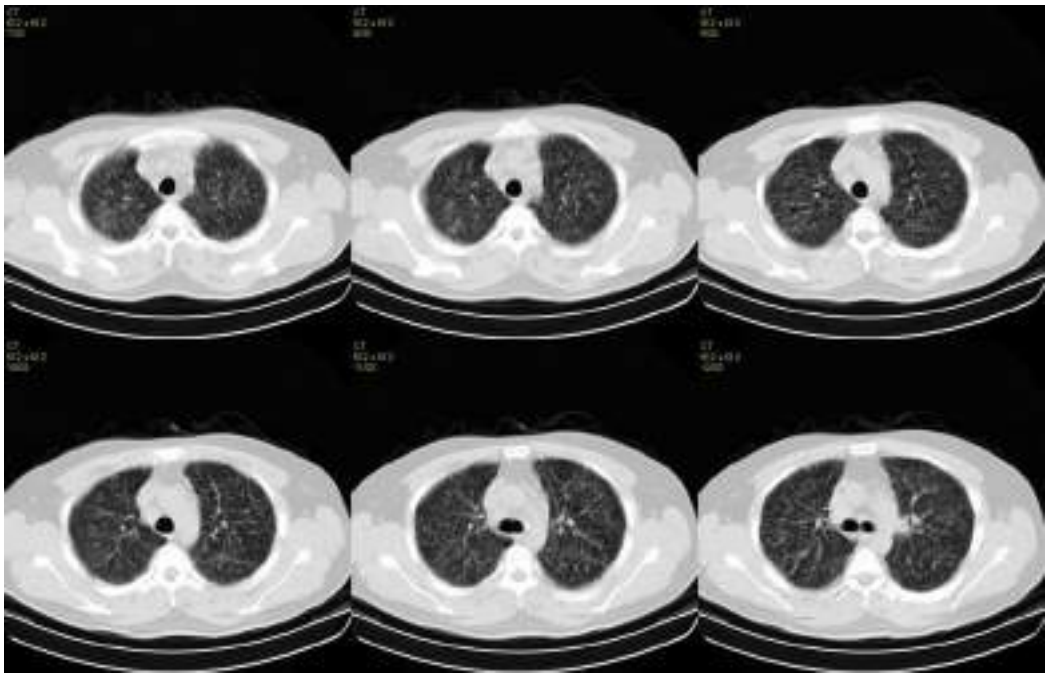

Fig. 2.3.2.6.11. Radiologic symptom complex of dissemination in sarcoidosis.

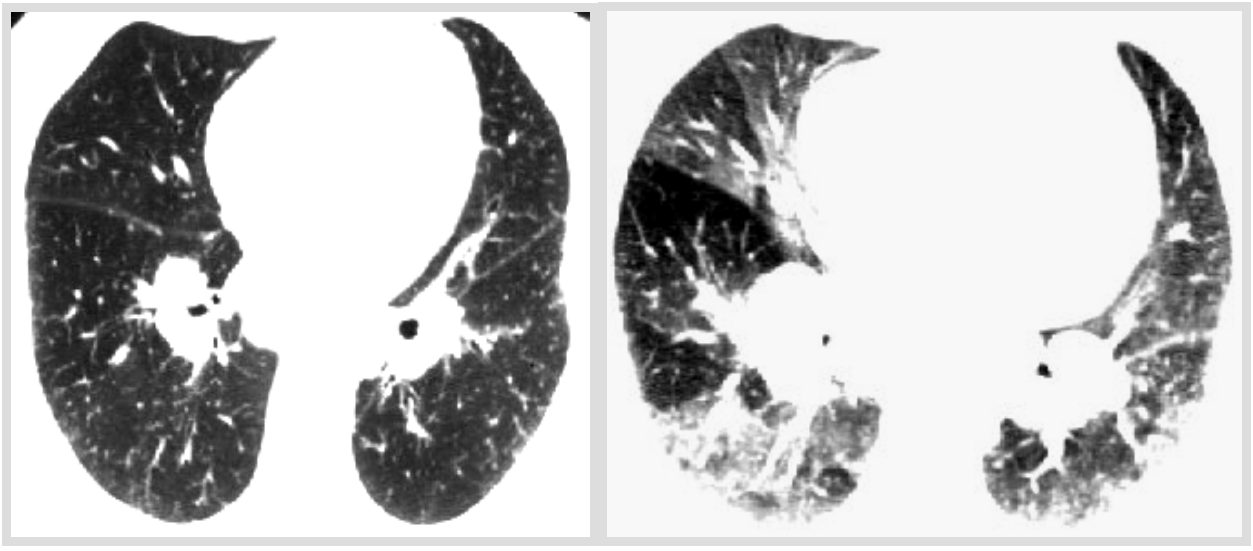

Fig. 2.3.2.6.12. Radiologic symptom complex of dissemination in sarcoidosis.

The parenchymal (pneumonic) radiologic variant of sarcoidosis is caused by areas of infiltration and hypoventilation of the lung parenchyma (Figs. 2.3.2.6.13–15). In this variant, the infiltrative component predominates and is detected in 25–50% of patients with sarcoidosis. The infiltrates often have a bilateral, symmetric distribution, are located in the central regions of the upper lobes (posterior and apical segments), may merge with the hilar area, and partially or completely obscure the lung pattern.

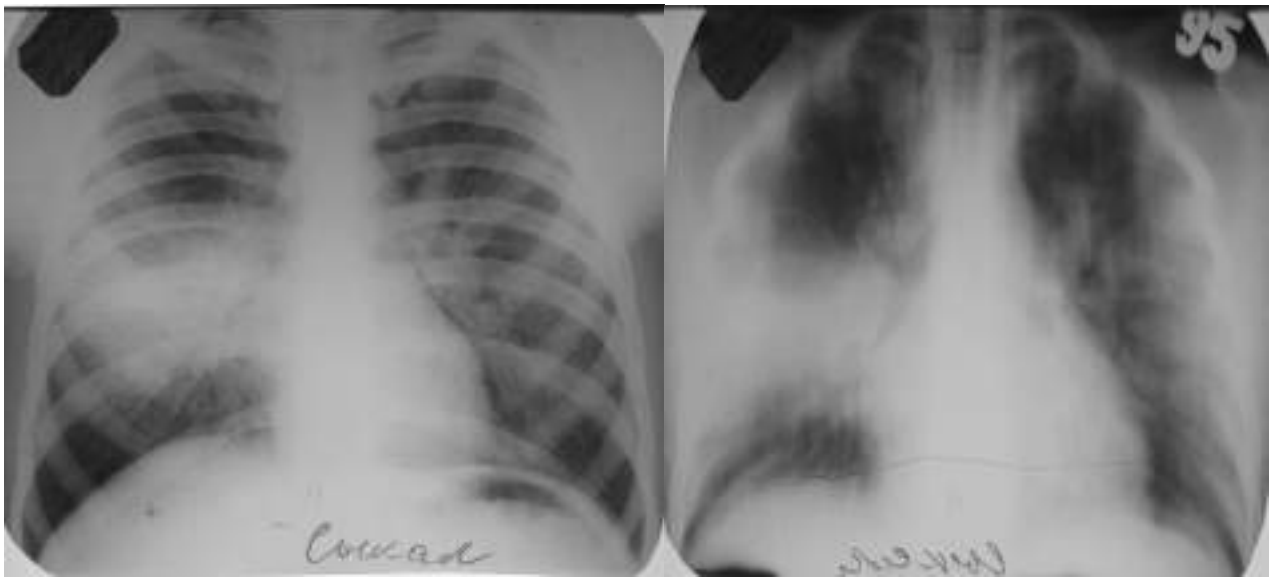

Fig. 2.3.2.6.13. Sarcoidosis, Stage II (intrathoracic lymphadenopathy + lungs). Pneumonic (parenchymal) variant.

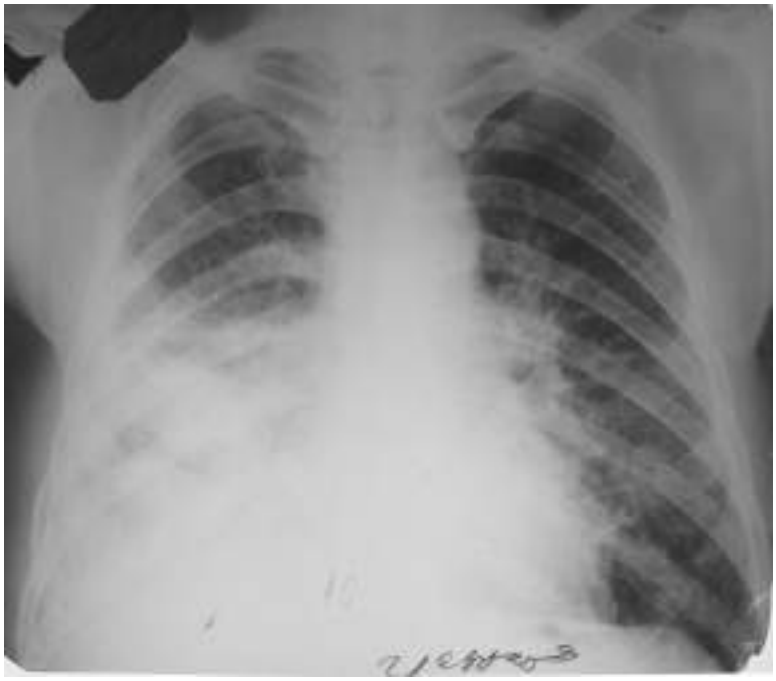

Fig. 2.3.2.6.14. Sarcoidosis, Stage II (intrathoracic lymphadenopathy + lungs). Pneumonic (parenchymal) variant.

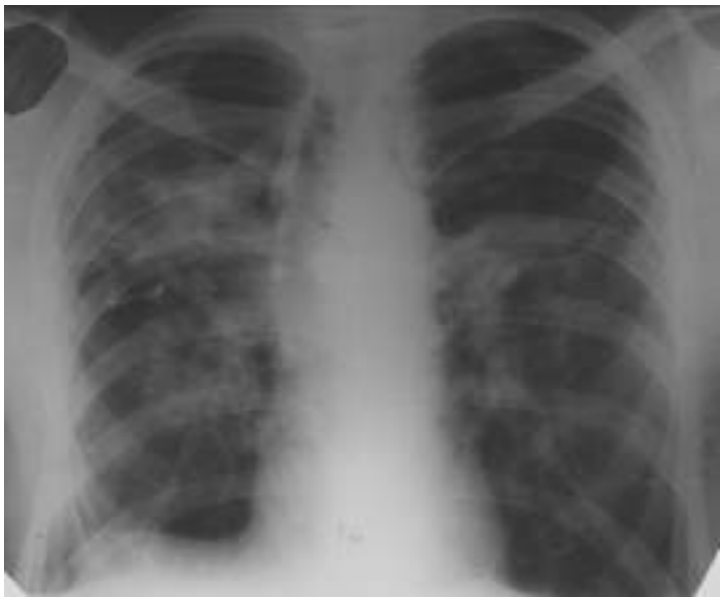

Fig. 2.3.2.6.15. Sarcoidosis, Stage II (intrathoracic lymphadenopathy + lungs). Pneumonic (parenchymal) variant.

Clinically, sarcoidosis may present in several forms: acute, subacute, and primary chronic (with a latent, asymptomatic onset). The clinical picture is dominated by mild fever, migratory joint pain, dyspnea, chest pain, dry cough, weight loss, bilateral mediastinal lymphadenopathy and lymph node enlargement in other locations (nodes are non-tender, not matted, of firm elastic consistency, without ulceration, necrosis, or fistula formation), dry or exudative pleuritis, erythema nodosum on the skin of the shins and forearms, harsh vesicular breathing, and scattered dry rales on lung auscultation.
In the complete blood count, leukocytosis, elevated ESR, and in 50% of patients, absolute lymphopenia are observed. Biochemical testing shows increased acute-phase reactants and elevated γ-globulin levels. Immunologic testing reveals decreased T-lymphocytes due to reduced suppressor populations and increased B-lymphocytes. Pulmonary function testing indicates development of a restrictive pattern of respiratory impairment. Bronchoscopy may reveal nodular elevations on

the bronchial mucosa (sarcoid granulomas) in the form of plaques of varying size, along with ischemic spots (pale areas of mucosa). Pulmonary sarcoidosis begins with alveolitis, characterized by the formation of lymphocytic infiltrates within the pulmonary interstitium. At this stage, fine reticulation of the lung pattern is seen, especially in the perihilar regions. Formation of sarcoid granulomas leads to the appearance of focal opacities on radiographs (conglomerates of granulomas). In most patients, the nodules are small and relatively well defined, although larger areas of consolidation may also occur. In the middle and lower lung zones, they are scattered relatively uniformly and tend to accumulate in medial regions and anterior segments, with fewer lesions in peripheral areas.

The lung hila are enlarged and polycyclic, with clearly delineated, bilaterally enlarged lymph nodes without perifocal reaction. Intrathoracic lymph nodes in the mediastinum and within the lung parenchyma may also be enlarged (appearing as round opacities 4–10 mm in diameter, often projected along the bronchi), contributing to widening of the mediastinal shadow.

As the process transitions into the resorption and consolidation phase, reticular remodeling of the lung pattern predominates, exhibiting a fine honeycombed character. Between the linear and arcuate opacities of the thickened stroma, emphysematous lobules become visible. The number of nodules decreases, they lose their round shape, and their margins become sharp. The lymph nodes in the hila decrease in size, although the hilar shadows remain broadened and polycyclic (Fig. 2.3.2.6.16).

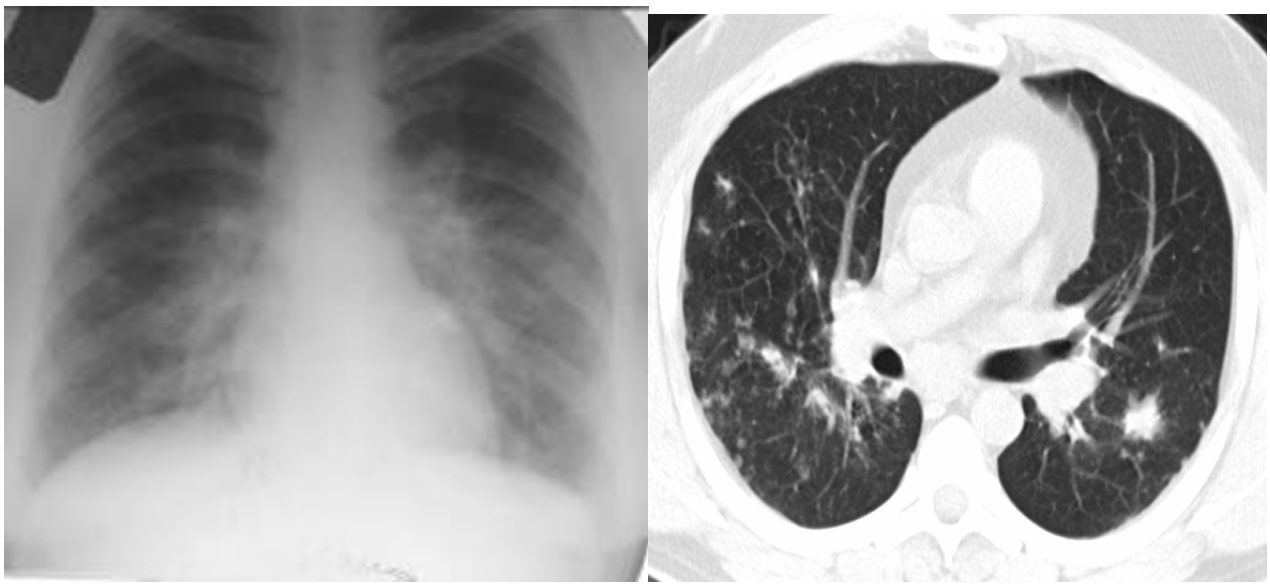

Fig. 2.3.2.6.16. Pulmonary sarcoidosis.

Against the diagnosis of tuberculosis argue the characteristic distribution of focal opacities and their absence in the lung apices, the absence of cavitation, symmetrical bilateral enlargement of the hilar lymph nodes, and early thickening of the interlobar pleura. Radiologic findings are supported by the discrepancy between relatively pronounced morphological and radiographic changes and the mild clinical presentation, negative tuberculin tests, and a positive Kveim test. In approximately one-tenth of sarcoidosis patients, extrathoracic involvement is observed (lacrimal and salivary glands, eyes, nervous system, liver, spleen, kidneys, skin, bones). The diagnosis of sarcoidosis is supported by lymphocyte predominance in bronchoalveolar lavage fluid and significant lung uptake of 67Ga on scintigraphy. Reduction of lymph node size during treatment helps exclude carcinomatosis and hematologic malignancies, provided no specific chemotherapy for those disorders has been administered. In patients treated with corticosteroids, the Kveim test becomes negative.

The disseminated form of sarcoidosis is characterized by mixed focal–interstitial dissemination. The most pronounced changes in sarcoidosis occur at the level of the upper-lobe bronchi, more extensively and earlier on the right side. Particularly marked abnormalities arise in the posterior and anterior segments of the upper lobes, in the apical segments of the lower lobes, in the middle lobe, and in the lingular segments. This pattern of spread along the major interlobar fissure is typical and

consistent. It is clearly visualized not only on CT scans, but also on lateral chest radiographs. Subsequently, these regions are the first to show signs of fibrosis.

CT demonstrates multiple small nodules distributed along the bronchovascular bundles, interlobar fissures, and costal pleura. This perilymphatic distribution of nodules is the most characteristic feature of sarcoidosis. In the perihilar zones, thickening of the peribronchovascular interstitium is clearly visualized, with its contours appearing irregular and beaded in typical cases. Changes in the axial interstitium extend to the intralobular bronchi, resulting in numerous centrilobular nodules.

Thickening of the interlobar pleural layers in sarcoidosis is often irregular and beaded. Multiple small nodules are frequently visible within them (Figs. 2.3.2.6.17–20).

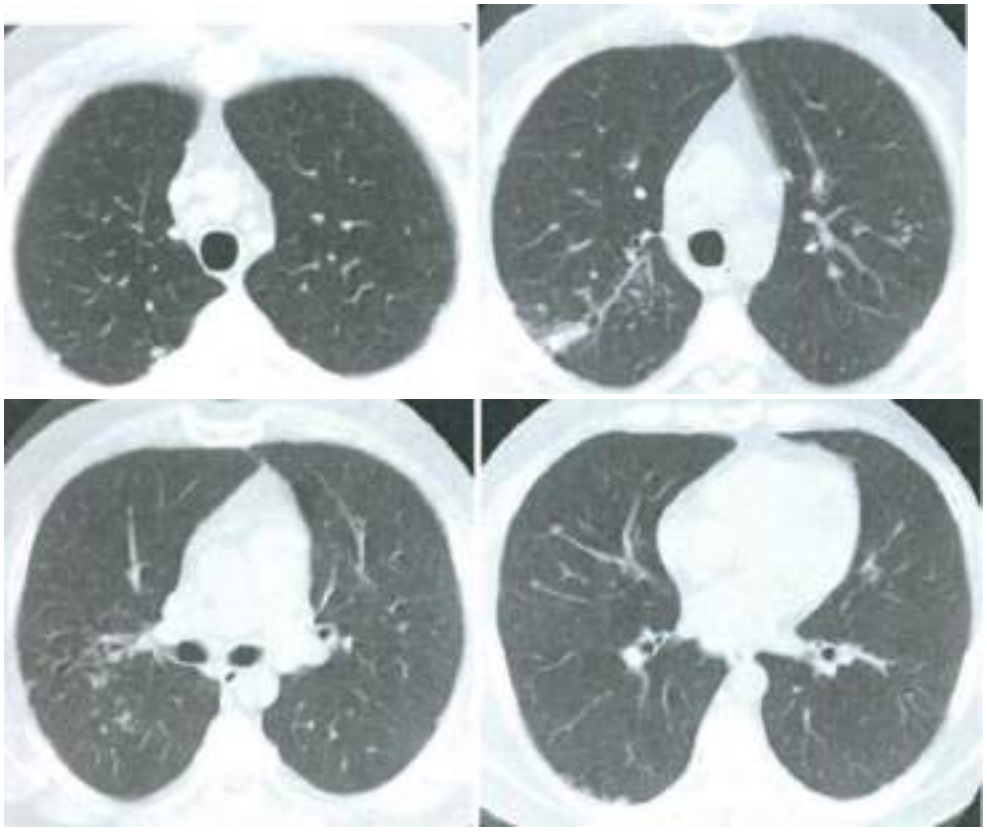

Fig. 2.3.2.6.17. Sarcoidosis of the lungs and intrathoracic lymph nodes. Multiple focal lesions in both lungs.

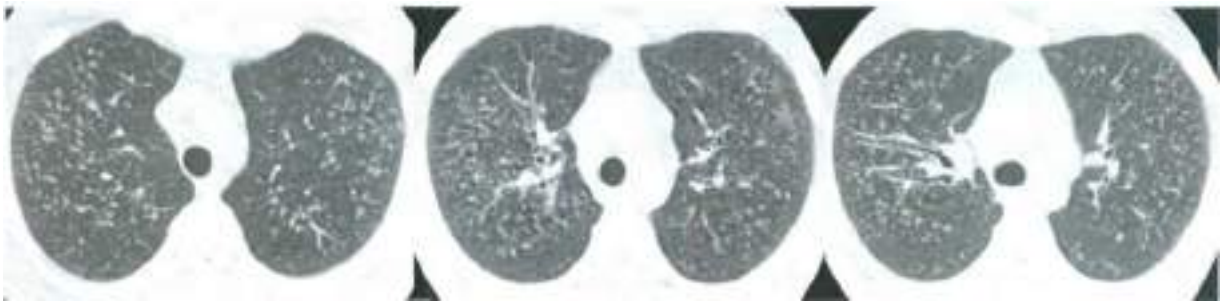

Fig. 2.3.2.6.18. Sarcoidosis of the lungs and intrathoracic lymph nodes. Diffuse changes in both lungs with multiple perilymphatic nodules and peribronchovascular cuffs.

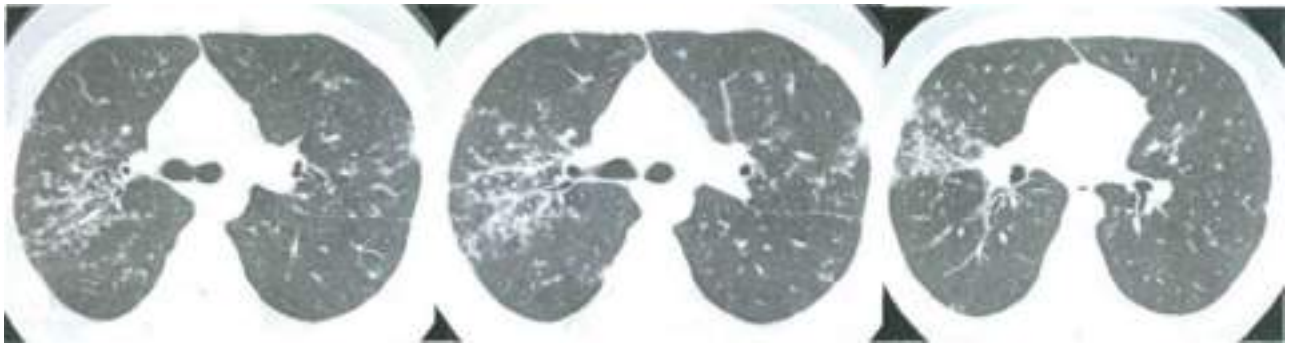

Fig. 2.3.2.6.19. Sarcoidosis of the lungs and intrathoracic lymph nodes. Typical peribronchial and perivascular distribution of small nodules. Some small nodules in the cortical lung regions are arranged in a centrilobular pattern, reflecting diffuse thickening of the entire axial interstitium.

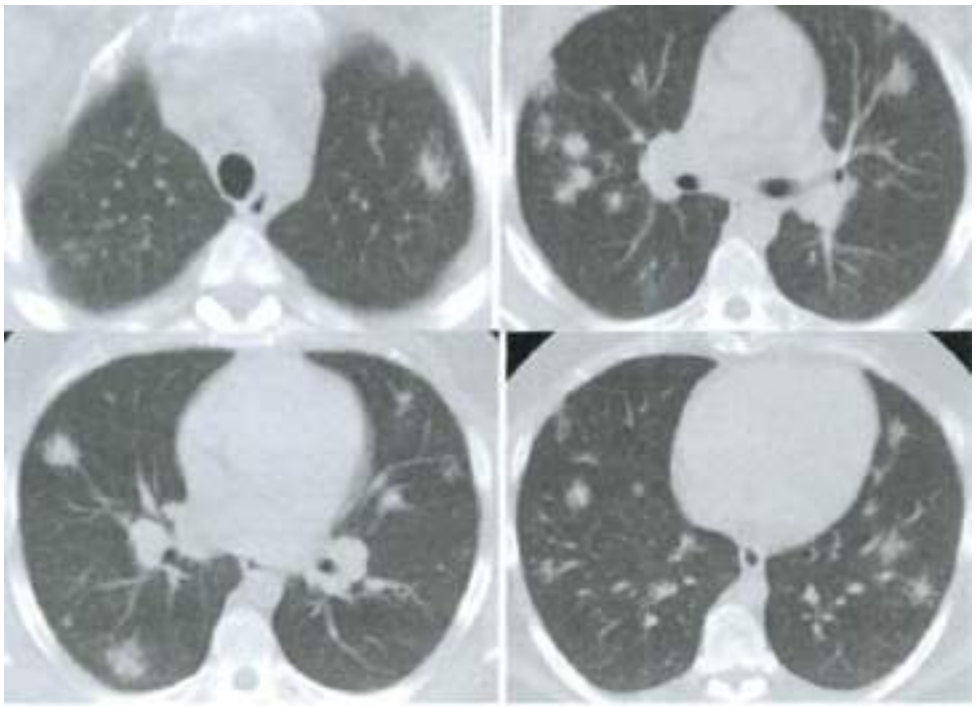

Fig. 2.3.2.6.20. Sarcoidosis of the lungs and intrathoracic lymph nodes. Multiple areas of alveolar infiltration predominantly in the cortical lung regions, with ill-defined contours and a rounded shape. Bronchial lumina are visualized within the areas of consolidation.

In some patients, multiple small nodules coalesce into larger nodules and small-sized infiltrates. Such infiltrates have ill-defined, blurred margins, low density, and sometimes visible bronchial lumina (Figs. 2.3.2.6.21–22). Another form of sarcoid-related changes is the “ground-glass” pattern. These abnormalities vary widely in extent and localization. Morphologic studies show that ground-glass opacities in sarcoidosis are most often due to numerous small nodules not resolvable by high-resolution CT (Figs. 2.3.2.6.23–24). Similarly, larger areas of consolidation (“alveolar sarcoidosis”), which are non-aerated regions of pulmonary density, are formed by multiple coalescent small nodules, edema zones, and cellular infiltration. Such infiltrates are located in the cortical lung regions, with clearly visible bronchial lumina. This pattern may resemble infiltrative tuberculosis, bacterial pneumonia, or bronchioloalveolar carcinoma (Figs. 2.3.2.6.25 a, b). Detection of enlarged mediastinal and hilar lymph nodes provides helpful diagnostic support.

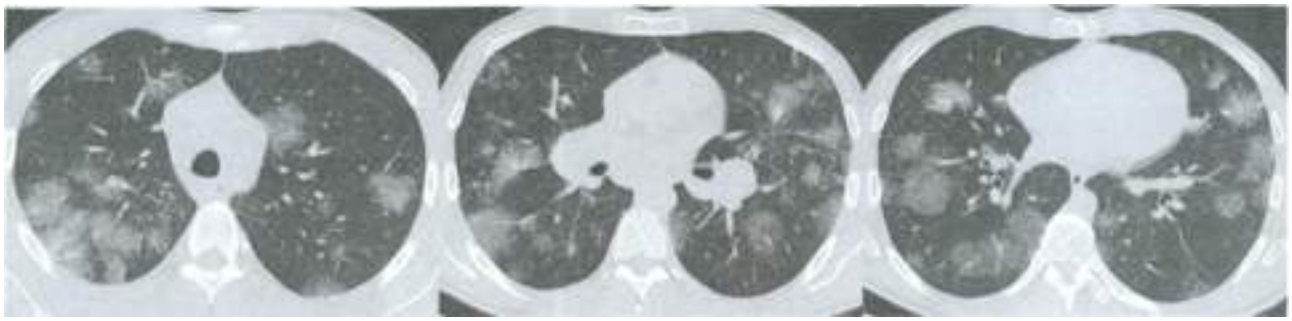

Fig. 2.3.2.6.21. Sarcoidosis of the lungs and intrathoracic lymph nodes. Multiple areas of alveolar infiltration located peribronchially, with ill-defined contours and a rounded shape. Bronchial lumina are visible within the areas of consolidation. Thickening of the bronchial walls in the perihilar region, enlargement of paratracheal, paraaortic, and bronchopulmonary lymph nodes.

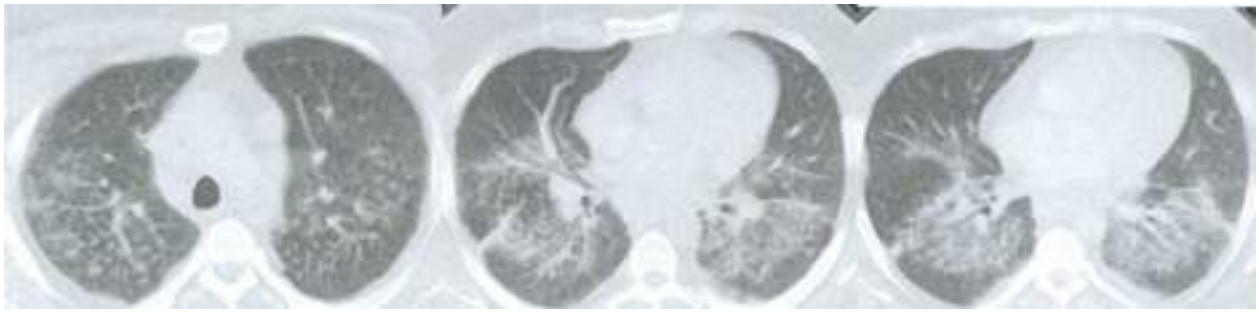

Fig. 2.3.2.6.22. Sarcoidosis of the lungs and intrathoracic lymph nodes. Coalescence of numerous small nodules into larger nodules with ill-defined contours and a rounded shape, as well as infiltrates. Bronchial lumina are visible within the areas of consolidation. Marked thickening of the bronchial walls in the perihilar region. Enlargement of paratracheal and bronchopulmonary lymph nodes.

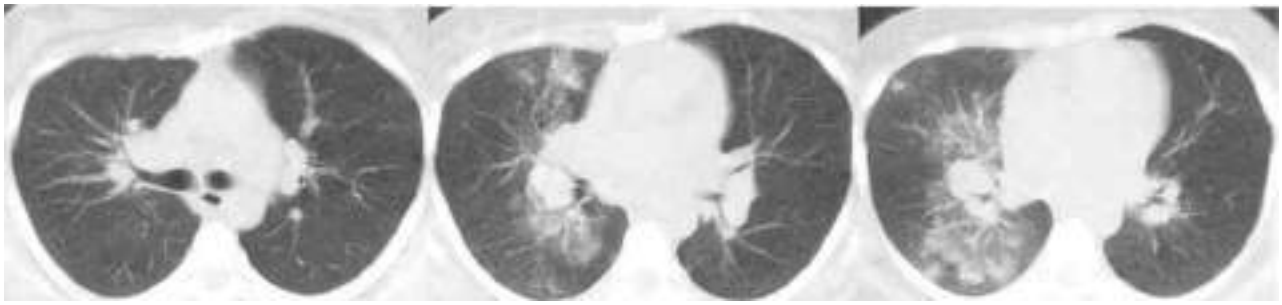

Fig. 2.3.2.6.23. Sarcoidosis of the lungs and intrathoracic lymph nodes. Multiple small nodules predominantly in the middle and lower segments of the right lung form irregularly shaped areas of ground-glass pulmonary consolidation with ill-defined margins. Enlargement of paratracheal and bronchopulmonary lymph nodes.

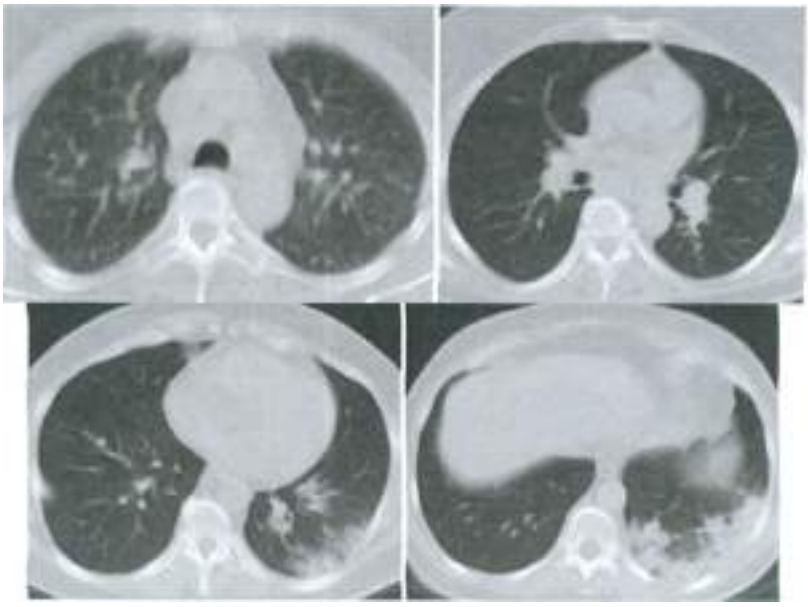

Fig. 2.3.2.6.24. Sarcoidosis of the lungs and intrathoracic lymph nodes. Areas of alveolar infiltration in the cortical regions predominantly of the

right lung. The non-aerated regions abut the chest wall with a broad base, and bronchial lumina are visible within them. Enlargement of paratracheal and bronchopulmonary lymph nodes. Such changes may resemble pneumonia or bronchioloalveolar carcinoma; however, they are typically accompanied by marked enlargement of mediastinal and hilar lymph nodes.

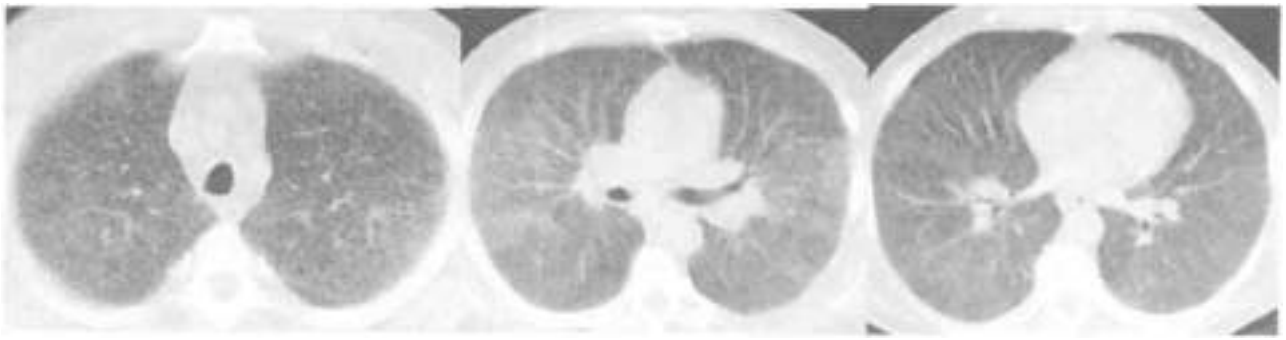

Fig. 2.3.2.6.25 a. Sarcoidosis of the lungs and intrathoracic lymph nodes. Multiple small, low-density nodules in both lungs reflect diffuse thickening of the entire axial interstitium and form irregularly shaped ground-glass areas without well-defined margins. Enlargement of paratracheal and bronchopulmonary lymph nodes.

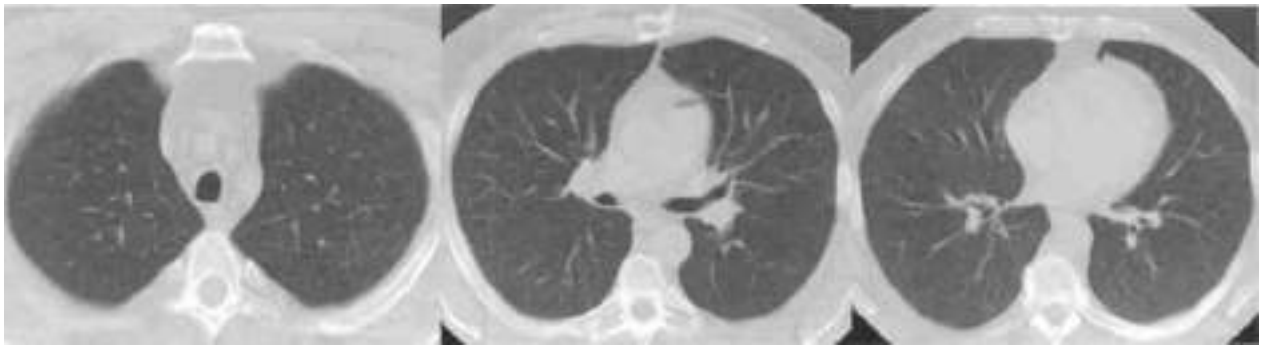

Fig. 2.3.2.6.25 b. The same patient after 12 months of treatment with glucocorticosteroids and delagil. Marked resorption of nodules, disappearance of ground-glass pulmonary consolidations, and reduction in the number and size of intrathoracic and bronchopulmonary lymph nodes.

As fibrosis develops, reticular changes begin to predominate, manifested as uneven thickening of interlobular and intralobular septa. A key sign of early fibrosis is a reduction in the volume of the posterior segments of the upper lobes. In this stage, the upper-lobe bronchi shift posteriorly toward the spine. Simultaneously, the cortical regions of the

lungs become hyperinflated, and subpleural honeycombing begins to form. Reticular changes appear to be displaced from the lung periphery toward the hilum.
Around the upper-lobe bronchi, peribronchially, larger soft-tissue conglomerates form that cannot be separated from the anatomic structures of the hilum. Within these conglomerates, deformed lumina of segmental and smaller bronchi are clearly visible. These soft-tissue masses may extend into the lung parenchyma along the bronchovascular bundles (Figs. 2.3.2.6.26 a, b). Concurrently, deformation and displacement of the interlobar pleura occur, along with the appearance of long linear strands along the costal pleura. All the above-described signs reflect various stages of fibrotic transformation within the lung tissue (Figs. 2.3.2.6.27–30).

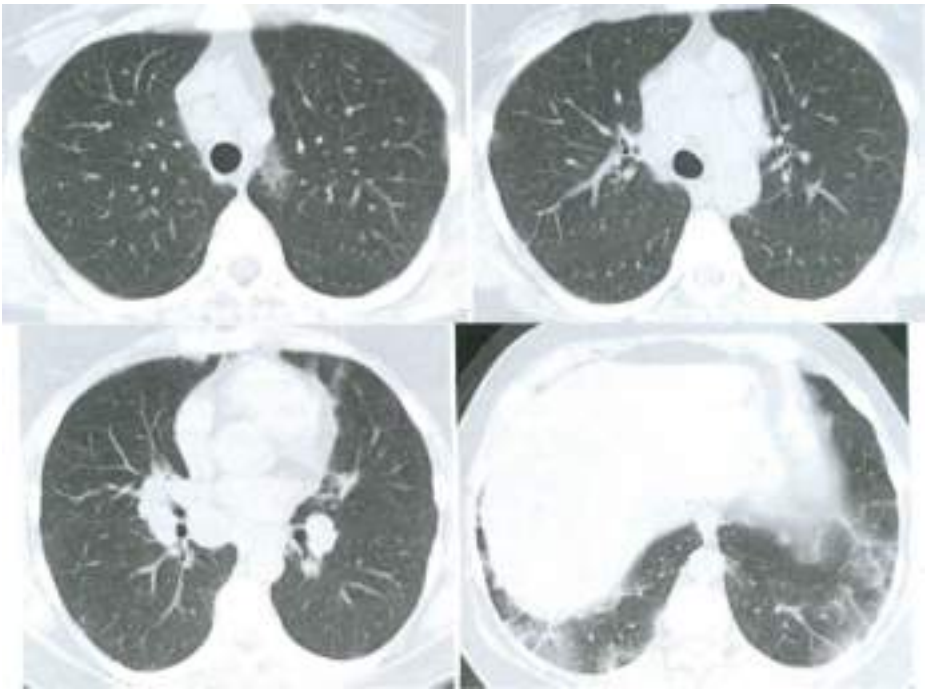

Fig. 2.3.2.6.26 a. Sarcoidosis of the lungs and intrathoracic lymph nodes. Enlargement of paratracheal, paraaortic, and bronchopulmonary lymph nodes. Areas of alveolar infiltration in the cortical regions, predominantly in the supradiaphragmatic zones.

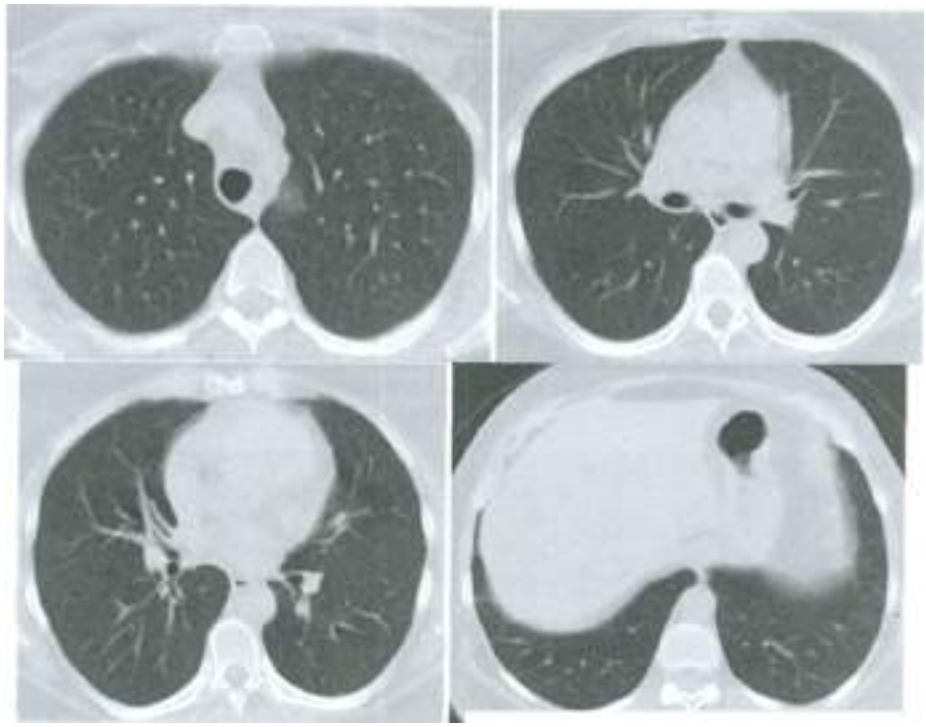

Fig. 2.3.2.6.26 b. The same patient after eight months of treatment with methylprednisolone, delagil, and vitamin E. Enlarged intrathoracic and bronchopulmonary lymph nodes are no longer visualized. Infiltrative changes have resolved.

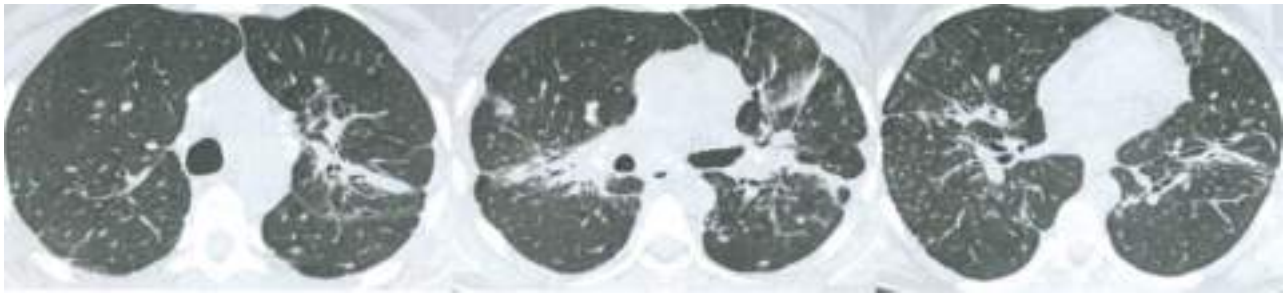

Fig. 2.3.2.6.27. Sarcoidosis, fibrotic stage of the lungs. In the perihilar regions of both lungs, massive soft-tissue conglomerates form around the bronchi, with visible bronchial lumina within them. Lung volume is reduced, and the contours of the mediastinal pleura are irregular. Traction bronchiectasis is present in the lung parenchyma. Calcifications are seen in the mediastinal and bronchopulmonary lymph nodes.

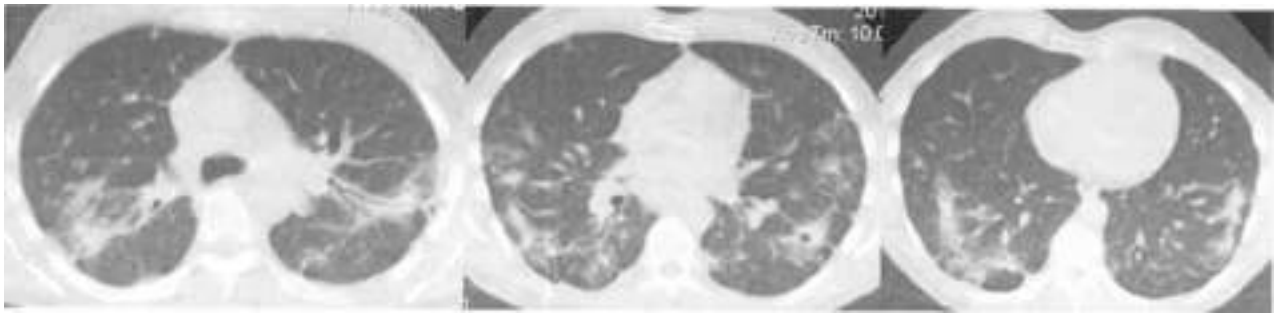

Fig. 2.3.2.6.28. Sarcoidosis, fibrotic stage of the lungs. In the perihilar regions of both lungs, massive soft-tissue conglomerates form around the bronchi, with visible bronchial lumina. Lung volume is reduced, and the contours of the mediastinal pleura are irregular. A cavitary lesion is present in segment S9 of the left lung.

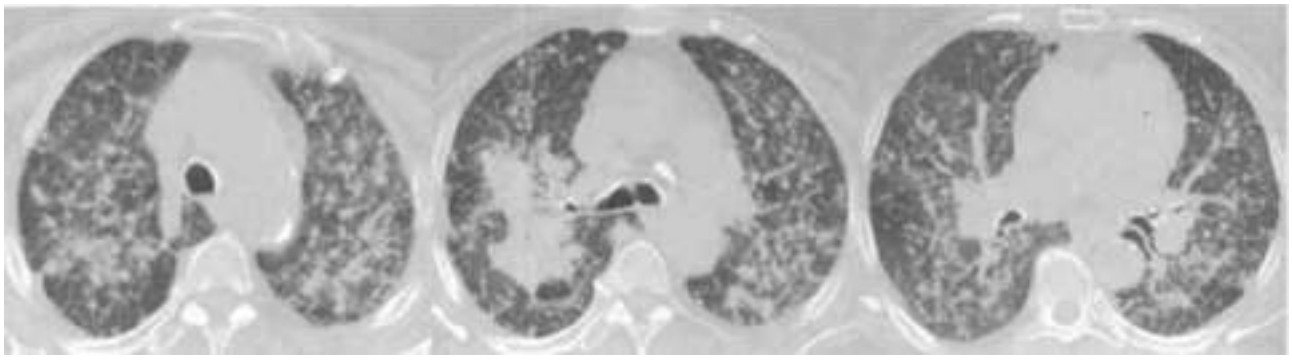

Fig. 2.3.2.6.29. Sarcoidosis, stage of irreversible pulmonary fibrosis. Diffuse consolidation of the lung parenchyma with predominance of changes in the perihilar regions. In non-aerated areas, the lumina of dilated, deformed bronchi are visible. The mediastinal contours are markedly distorted. Calcification of the trachea, major bronchi, and the subcarinal lymph node is present.

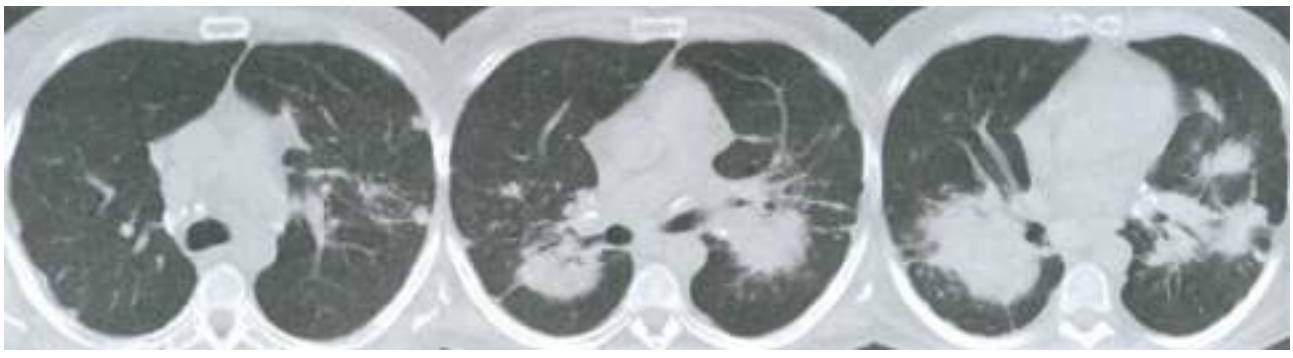

Fig. 2.3.2.6.30. Sarcoidosis, stage of irreversible pulmonary fibrosis. In the perihilar regions of both lungs, massive soft-tissue conglomerates

form around the bronchi, with visible lumina of deformed bronchi. The contours of the mediastinal pleura are irregular. Calcifications are present in the intrathoracic and bronchopulmonary lymph nodes.

2.3.2.7. Dust-Induced Lung Diseases.

Pneumoconiosis is a chronic lung disease that develops as a result of long-term inhalation of industrial dust and is characterized by diffuse aseptic pneumonitis and the formation of pulmonary fibrosis. The diagnosis of pneumoconiosis is based on occupational history indicating prolonged (years to decades) exposure to industrial dust at concentrations exceeding the maximum permissible levels (confirmed by sanitary and hygienic assessment of working conditions) (Fig. 2.3.2.7.1).

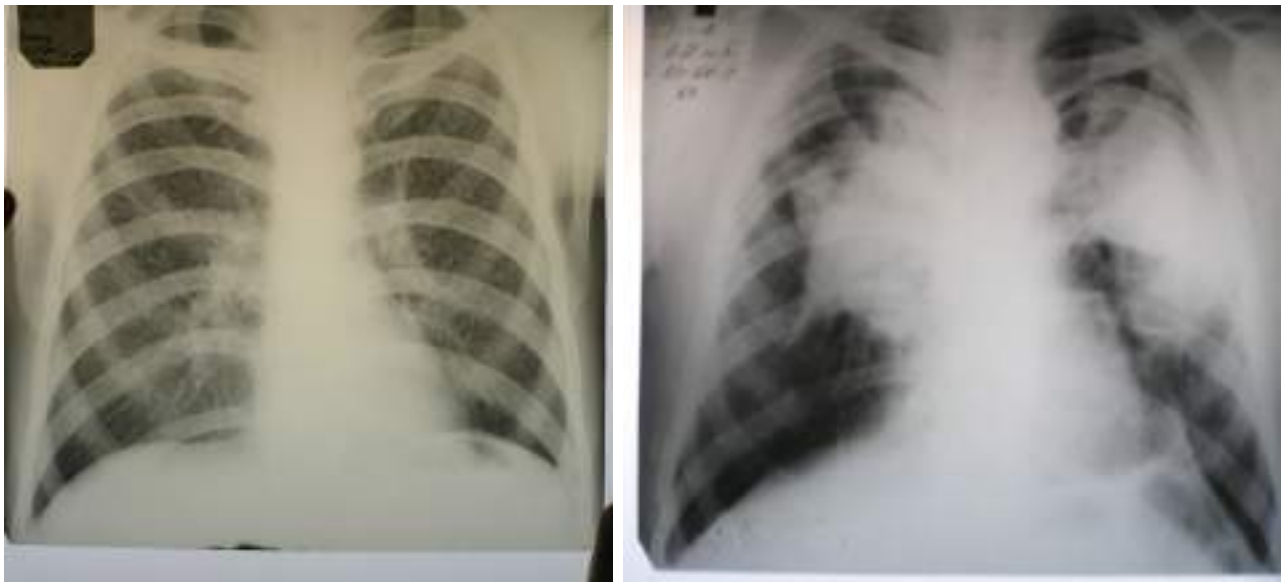

Fig. 2.3.2.7.1. Variant of pneumoconiosis.

The clinical presentation of pneumoconioses is nonspecific: patients report cough—initially dry, later productive with the expectoration of viscous sputum that may be gray or differently colored (depending on the type of dust). Dyspnea is typically inspiratory in nature (mixed inspiratory–expiratory in byssinosis and berylliosis), first occurring on exertion and later at rest. Patients may experience a sensation of chest tightness or sharp, stabbing pain in the lower parts of the thorax (“belt-like constriction”). On auscultation, breath sounds are harsh vesicular; with the development of concomitant dust-related bronchitis, scattered

dry buzzing rales appear, and pneumosclerotic crackles are heard in the lower lung fields.

In addition to these general manifestations, the clinical picture may include specific symptoms depending on the physicochemical properties of the dust, the resorptive effect of dust components dissociating after entry into the body (signs of intoxication, sensitization), the patient's immunologic reactivity, and the presence of accompanying occupational (e.g., vibration disease in miners, occupational hearing loss) or general somatic conditions.

Radiologic findings in pneumoconioses are also diverse. Depending on the fibrogenicity class of the inhaled dust, nodular, interstitial, or nodular–interstitial types of diffuse lung disease may develop.

Taking into account the aggressiveness of the inhaled industrial dust, pneumoconioses are divided into three groups:

I. Pneumoconioses caused by highly and moderately fibrogenic dusts (containing more than 10% free SiO_2 or asbestos): silicosis, silicoanthracosis, silicosilicate pneumoconiosis, silicosiderosis, asbestosis. These are characterized by a nodular or mixed nodular–interstitial pattern of lung involvement.

II. Pneumoconioses caused by weakly fibrogenic dusts (containing less than 10% free SiO_2, bound SiO_2, or no SiO_2): Silicate pneumoconioses (kaolinosis, olivinosis, nephelinosis, mica-related, cement pneumoconioses, talcosis);

Carboconioses (anthracosis, graphitosis, carbon black pneumoconiosis, coke-oven, diamond pneumoconiosis); Metalloconioses (siderosis, stannosis, baritosis, manganoconiosis, aluminosis); Pneumoconiosis of welders, gas-cutters, grinders, polishers, tool sharpeners, foundry workers. These conditions are characterized by interstitial pulmonary fibrosis (t, u).

III. Hypersensitivity pneumonitis (immunoallergic pneumoconioses) caused by toxic–allergic dusts (aerosols):

Berylliosis; pneumonitis due to chromium, nickel, platinum and other rare earth metals or alloys;Pneumonitis from plastic dust, polymer resins, pharmaceuticals (toxic fibrosing alveolitis); Byssinosis, paprika workers' lung, bagassosis, suberosis; extrinsic allergic alveolitis in woodworkers, bird breeders, etc.

These are characterized by fine reticular interstitial lung fibrosis (s, t).

Diagnostic criteria for pneumoconioses caused by highly and moderately fibrogenic dusts include: an occupational exposure history of at least 5 years in conditions with elevated dust concentrations in the workplace air; gradual disease onset; the presence of pneumoconiotic fibrosis with predominance of the nodular form (nodular opacities 1–10 mm in diameter, irregular in shape with well-defined margins, located mainly in the middle and lower lung zones; Stage I – solitary nodules, Stage II – multiple nodules replacing the pulmonary pattern, Stage III – confluent nodules). The lung hila are enlarged and fibrotically altered; the “eggshell calcification” sign (calcified mediastinal lymph nodes, characteristic of Stage II silicosis) may be present. Clinical manifestations of respiratory insufficiency are mild and predominantly restrictive. Signs of systemic intoxication are absent in the early stages. The disease exhibits progressive course with formation of nodular fibrosis and is frequently associated with tuberculosis (development of coniotuberculosis). Further disease progression leads to the formation of extensive fibrotic fields, areas of pulmonary consolidation, and pleuro-mediastinal and pleuro-diaphragmatic adhesions.

Diagnostic criteria for pneumoconioses caused by weakly fibrogenic dusts include: long occupational exposure (more than 5–10 years) to increased dust concentrations in the workplace; gradual development of the disease; predominance of irritative bronchitis as the clinical syndrome; interstitial-type pulmonary fibrosis; absence of intoxication signs; mild to moderate respiratory insufficiency of mixed obstructive–restrictive type; and disease progression due to complications rather than the formation of nodular fibrosis.

Hypersensitivity pneumonitis develops mainly as a result of exposure to toxic-allergic aerosols (aerosols of heavy metals and their alloys, pharmaceuticals, plastics and their degradation products, biologically active substances of animal and plant origin, etc.), leading to activation of cell-mediated and humoral immune responses. In this type of pneumoconiosis, lung injury occurs due to the effects of specific immune complexes containing antigens or haptens. The underlying mechanism of immune disorders in chronic hypersensitivity pneumonitis is delayed-type hypersensitivity. Various patterns of fibrosis are characteristic:

interstitial fibrosis (in extrinsic allergic alveolitis), epithelioid-cell fibrosis (in byssinosis, bagassosis), and granulomatous changes (in berylliosis). Disease onset is gradual and oligosymptomatic. Clinical manifestations range from bronchitis to alveolitis. A pronounced intoxication syndrome, hyperthermia, rapid weight loss, chest pain, and signs of rapidly progressive respiratory failure of mixed restrictive–obstructive type may be present. Progression of hypersensitivity pneumonitis is associated with the development of complications (respiratory and cardiac failure, pulmonary heart disease, bullous emphysema, spontaneous pneumothorax, etc.) and superimposed bacterial infections.

Diagnosis of berylliosis is based on occupational history and is characterized by a clinical picture resembling extrinsic allergic alveolitis, myocarditis, hepatitis, nephropathy, dermatitis, and eczema. A classic reticular remodeling of the lung pattern is observed in the interstitial form of berylliosis, which may at times be accompanied by coarse fibrotic strands. As the process progresses to its granulomatous form, small and later larger (3–4 mm in diameter) focal opacities (beryllium granulomas) appear against the background of thickened walls of small bronchi, moderate emphysema, and slight enlargement of the hilar lymph nodes. Confirmation of the diagnosis is provided by a positive application test with soluble beryllium compounds (sulfate or nitrate) applied to the skin of the forearm (a reaction indicating sensitization to beryllium), as well as by lymph node biopsy (presence of beryllium granulomas).

During bronchoscopy with biopsy of the bronchial mucosa in pneumoconioses, which are often accompanied by dust bronchitis, subatrophic and atrophic changes are found, along with the “tattooing” sign of the airway mucosa (deposition of dust particles in the subepithelial layer), epithelial desquamation, and metaplasia of the ciliated columnar epithelium into stratified squamous epithelium lacking drainage function, as well as glandular atrophy.

Sputum analysis indicates the presence of dust particles, asbestos bodies (in asbestosis), and large quantities of desquamated epithelium.

In pneumoconioses, spirometry reveals the development of a restrictive type of respiratory failure as a result of diffuse pulmonary fibrosis (reduced VC and MVV) and compensatory emphysema (increased residual volume).

In the biochemical blood analysis, changes may be observed that indicate enhanced anabolic processes of collagen and other components of connective tissue: increased levels of protein-bound hydroxyproline, C-reactive protein, sialic acids, seromucoids, fibrinogen, and fibronectin in the blood.

Pneumoconioses, particularly silicosis, are characterized by the formation of multiple granulomas in the lung tissue in combination with moderately expressed changes in the peripheral and septal interstitium. The localization of changes in the lungs and the dynamics of the process bear strong similarity to sarcoidosis. At the initial stage of silicosis, a small number of tiny foci appear in the lung tissue. Their typical localization is the posterior segments of the upper lobes. The foci are located perilymphatically, usually within slightly thickened interlobular septa. Subsequently, the number and size of the foci increase, and the pathological changes spread to the anterior segments of the upper lobes, then to the middle and later the lower lobes of the lungs. In the posterior segments of the upper lobes, the largest foci merge, forming conglomerates of irregular shape. Gradually, they increase in size and merge with the lung hilum, while emphysema develops in the cortical regions of the lung (Fig. 2.3.2.7.2).

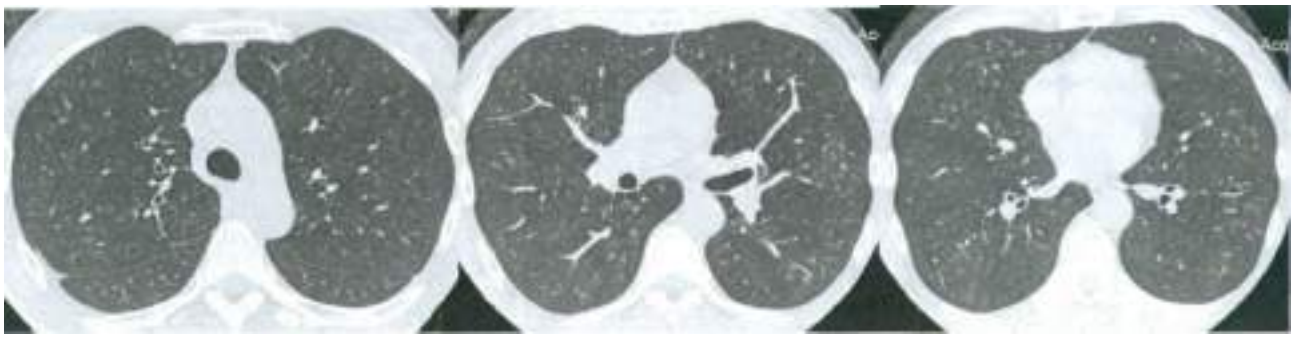

Fig. 2.3.2.7.2. Silicosis, stage I. Diffuse changes in both lungs represented by a small number of fine, monomorphic centrilobular nodules against a background of mildly increased lung parenchymal density**.**

Large silicotic nodules have a regular rounded shape and well-defined margins. Calcifications frequently appear within them, as well as within conglomerates (so-called silicomas) (Figs. 3.3.2.7.3–5). Simultaneously with parenchymal alterations, a gradual enlargement of the hilar and mediastinal lymph nodes develops. Typical findings include

diffuse or ring-shaped (“eggshell”) calcification of the lymph nodes. CT imaging allows detection of characteristic silicotic changes earlier than conventional radiography and provides a more accurate assessment of the stage of the pathological process.

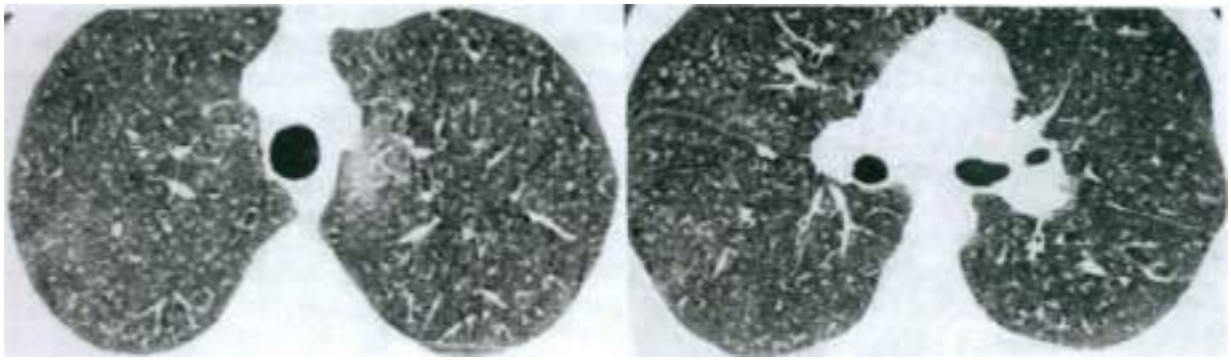

Fig. 2.3.2.7.3. Silicosis, stage I. Diffuse changes in both lungs in the form of small, monomorphic centrilobular nodules against a background of mildly increased lung parenchymal density. Enlarged bronchopulmonary lymph nodes.

Fig. 2.3.2.7.4. Silicosis, stage II. Nodular changes in the upper lobes of the lungs. Nodules of varying size are unevenly distributed within the lung parenchyma. Some of them coalesce, forming larger conglomerate lesions.

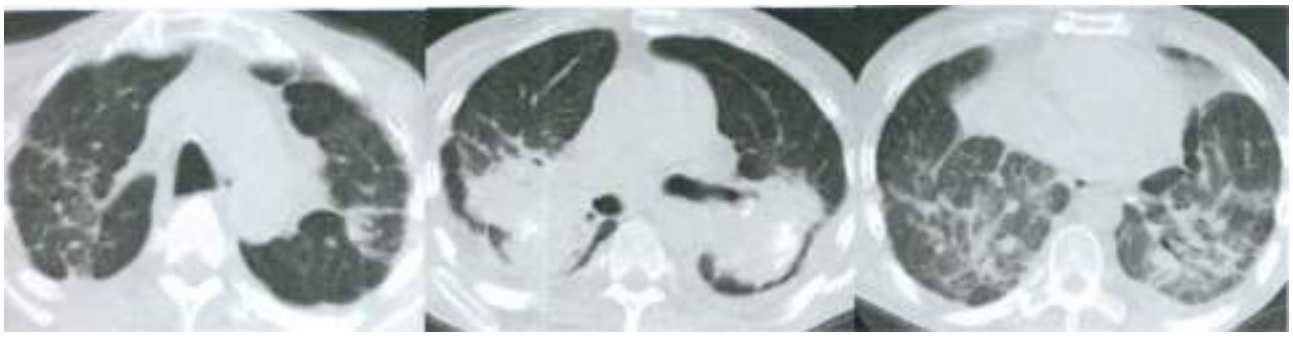

Fig. 2.3.2.7.5. Silicosis, stage III. In the middle lung zones, large soft-tissue masses with indistinct margins and multiple calcific inclusions-silicomas-are visualized. Focal dissemination is present in the upper and lower lung zones.

Focal changes in the upper lobes are typical of stage I. The appearance of conglomerates, most often in the posterior segments of the upper lobes, indicates progression to stage II. The formation of large soft-tissue masses in the perihilar regions, combined with emphysema, occurs in the final, third stage. It should be emphasized that enlargement of nodules in the upper lobes, development of conglomerates, and the presence of calcifications within nodules and lymph nodes are not signs of concomitant tuberculosis. These findings reflect the natural progression of the pneumoconiotic process and are not characteristic of silicotuberculosis. Signs suggestive of superimposed tuberculosis infection include the appearance of pleural effusion, new infiltrates, and cavitary destruction in locations atypical for silicosis. However, the definitive diagnosis of silicotuberculosis relies on the detection of MTB in sputum.

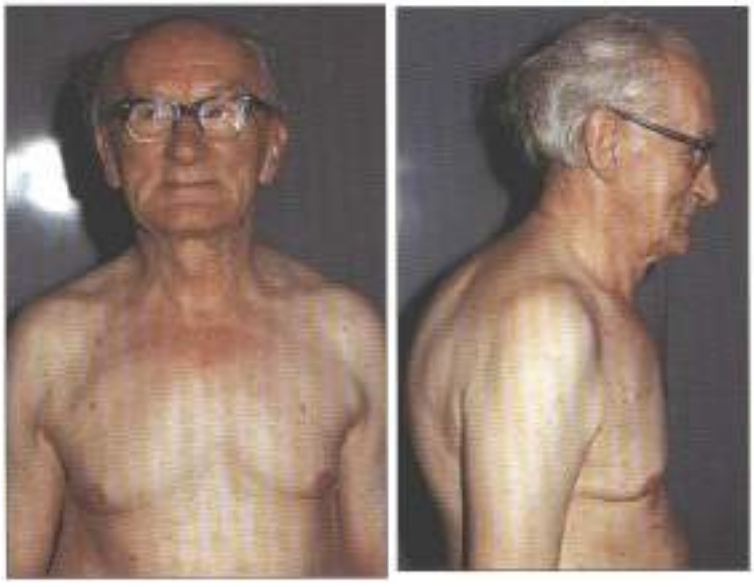

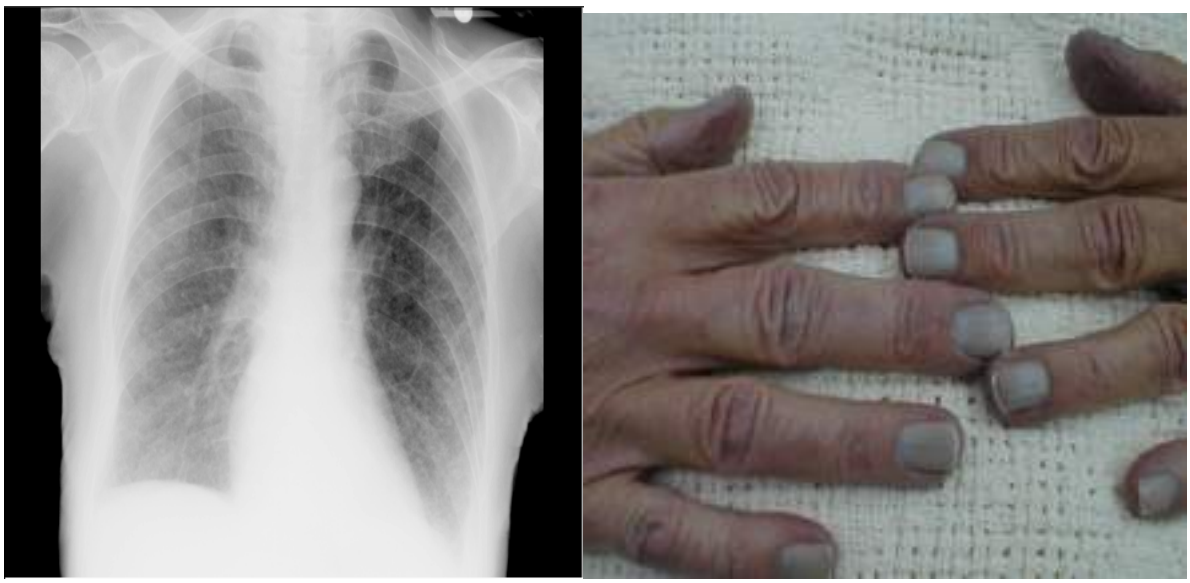

Fig. 2.3.2.7.6. A variant of pulmonary pneumoconiosis.

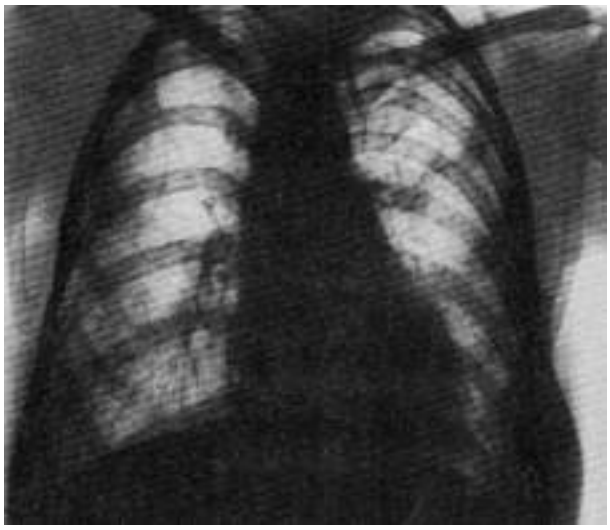

Fig. 2.3.2.7.7. Increased pulmonary markings with solitary nodular shadows in the middle and lower lung zones.

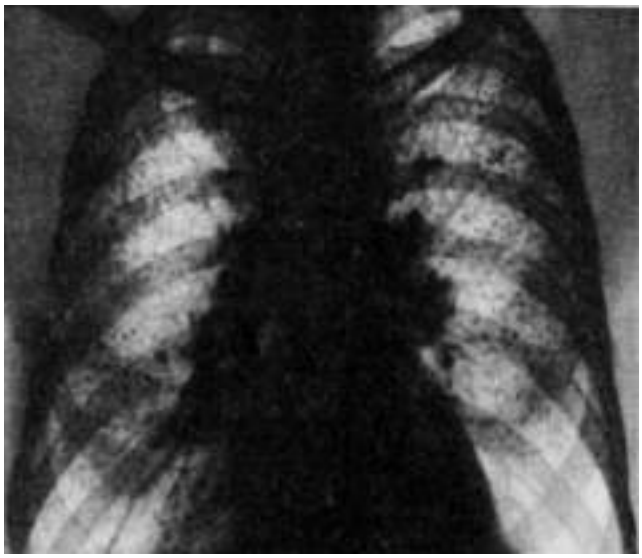

Fig. 2.3.2.7.8. Multiple nodular opacities (p, q, r) replacing the pulmonary pattern throughout all lung zones (“snowstorm” appearance), with the “eggshell”

calcification sign.

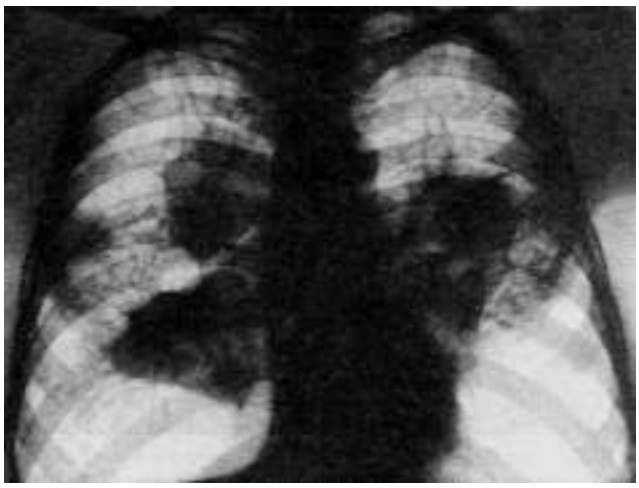

Fig. 2.3.2.7.9. Coalescence of nodules into larger masses, emphysema, fibrotic fields, and pleural adhesions.

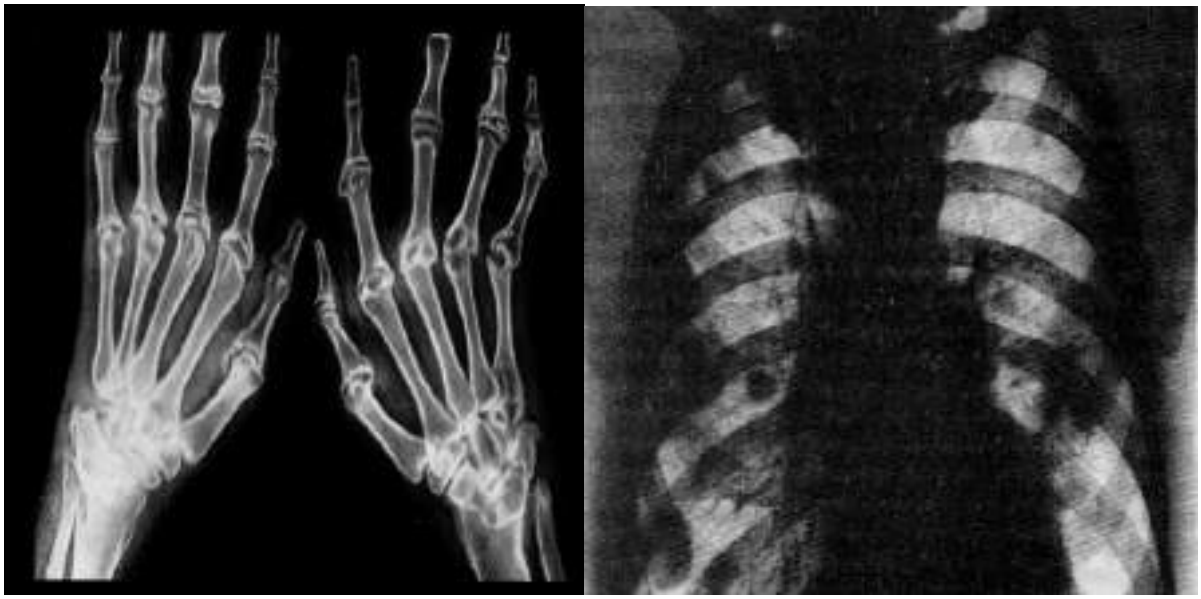

Fig. 2.3.2.7.10. Kaplan–Collinet syndrome.
Rheumatoid silicoarthritis - Rheumatoid silicosis.
Ulnar deviation of the metacarpophalangeal joints.

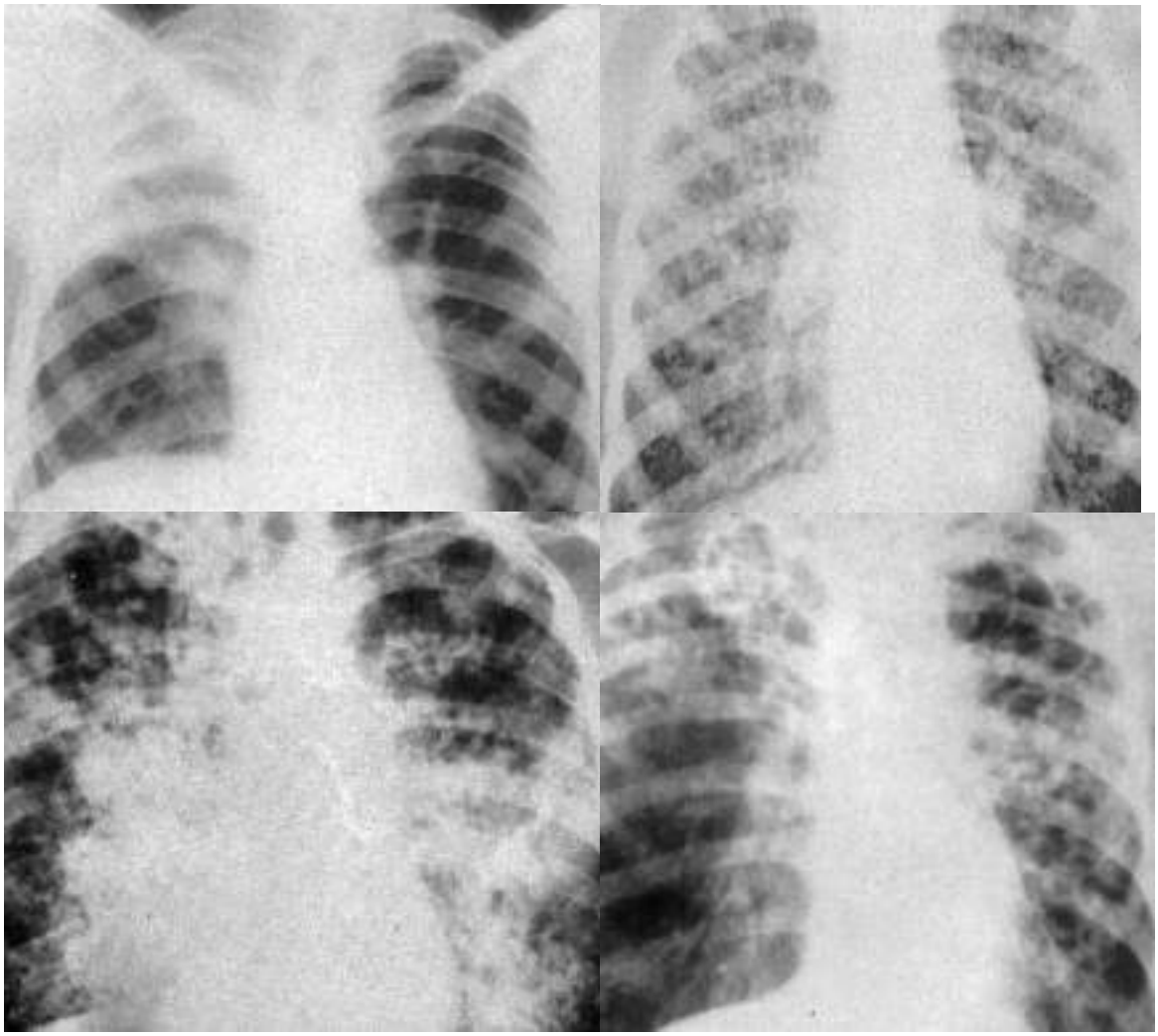

Fig. 2.3.2.7.11. Variants of pneumoconiosis.

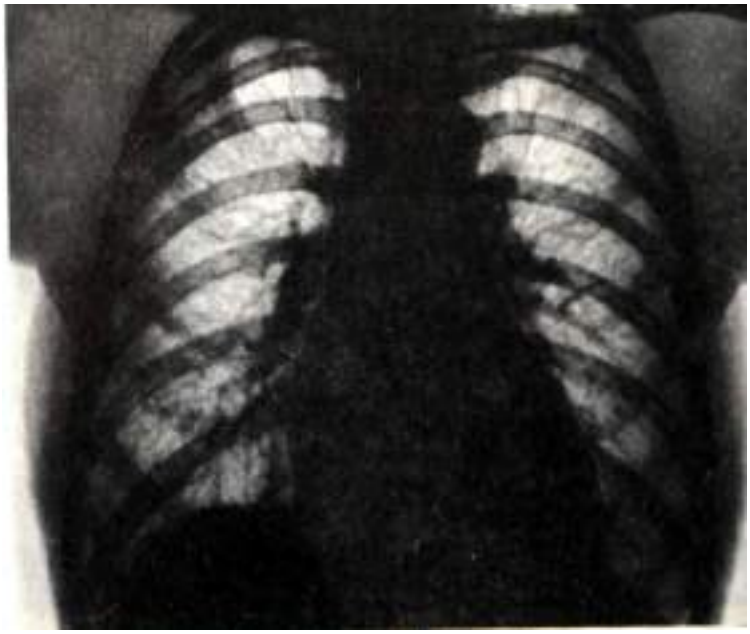

Fig. 2.3.2.7.12. Asbestosis.

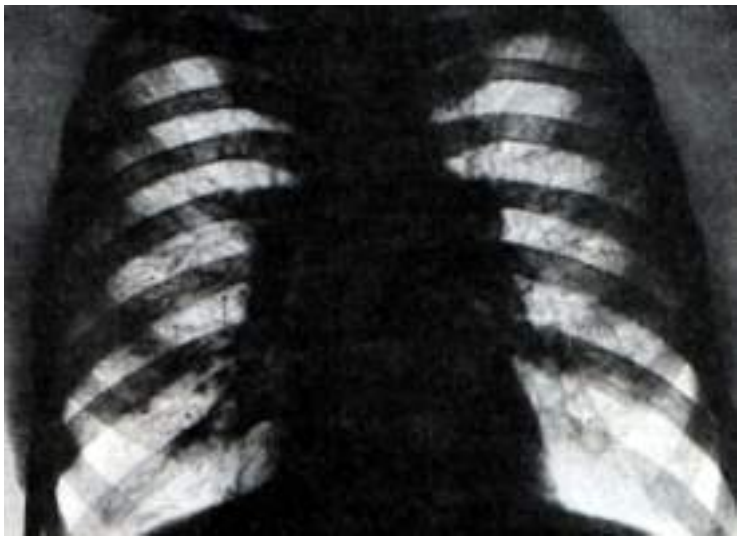

Fig. 2.3.2.7.13. Reticular (t-type) changes with pleural reaction (adhesions).

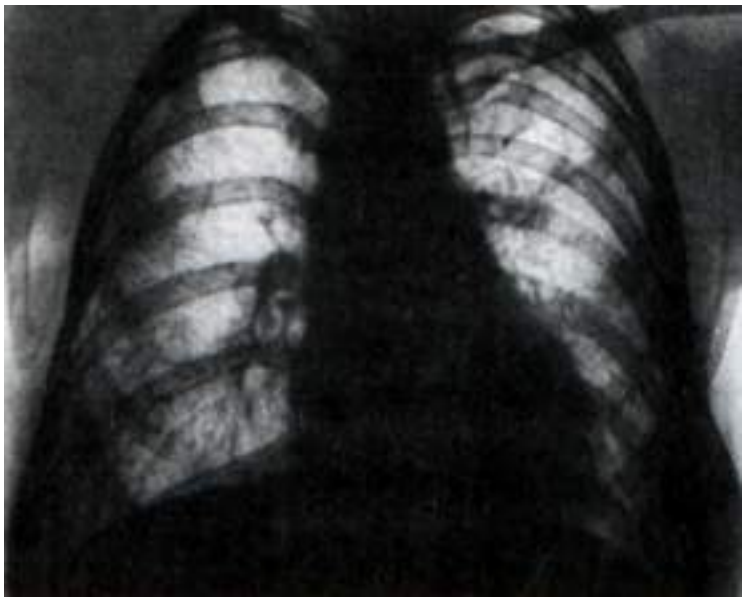

Fig. 2.3.2.7.14. Coarse reticular changes, distortion of the pulmonary pattern, multiple nodular opacities, and the “hairy heart” sign.

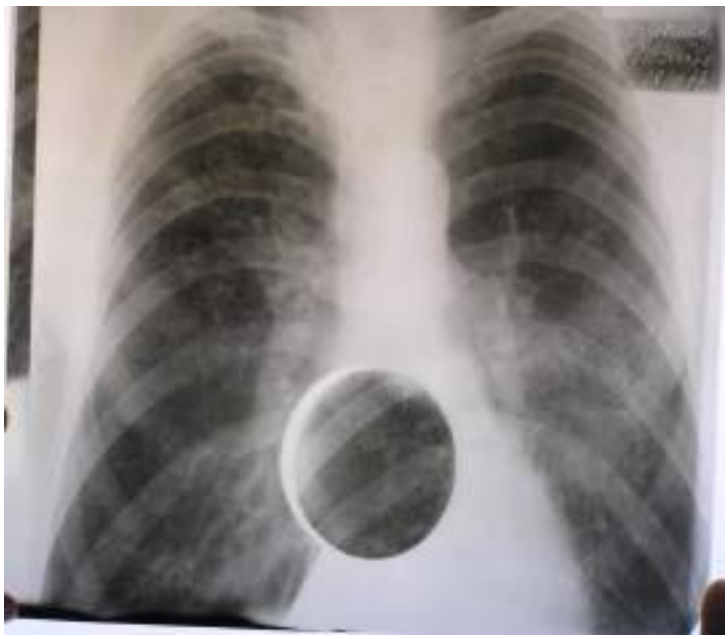

Fig. 2.3.2.7.15. A variant of pneumoconiosis.

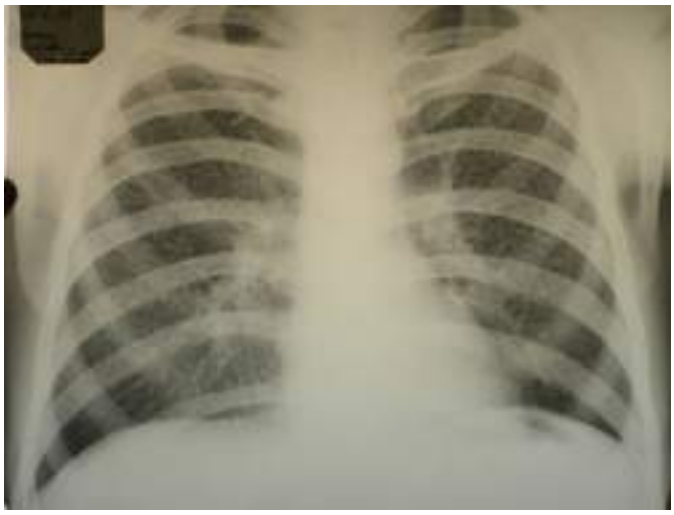

Fig. 2.3.2.7.16. A variant of pneumoconiosis.

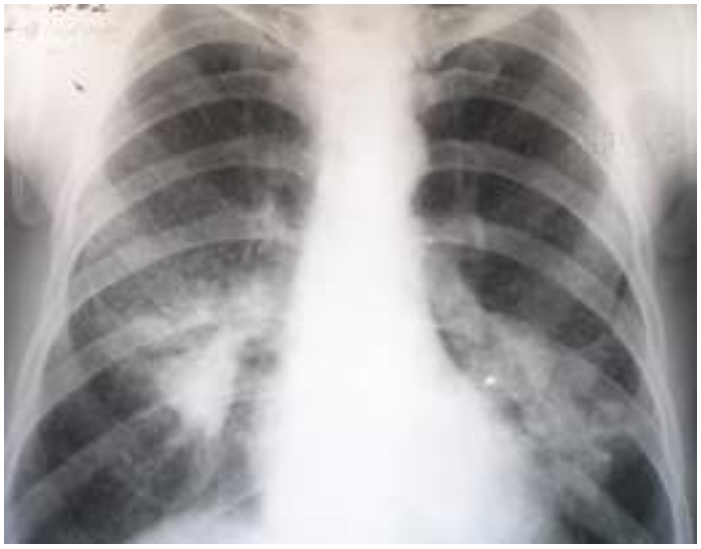

Fig. 2.3.2.7.17. A variant of pneumoconiosis.

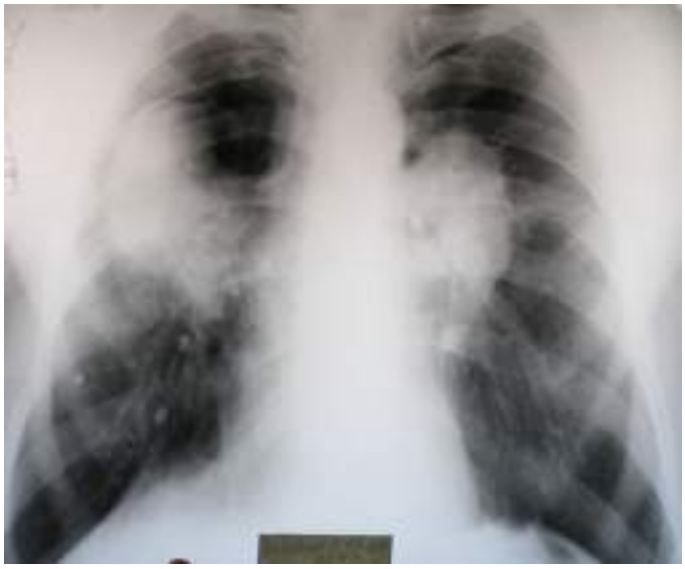

Fig. 2.3.2.7.18. A variant of pneumoconiosis.

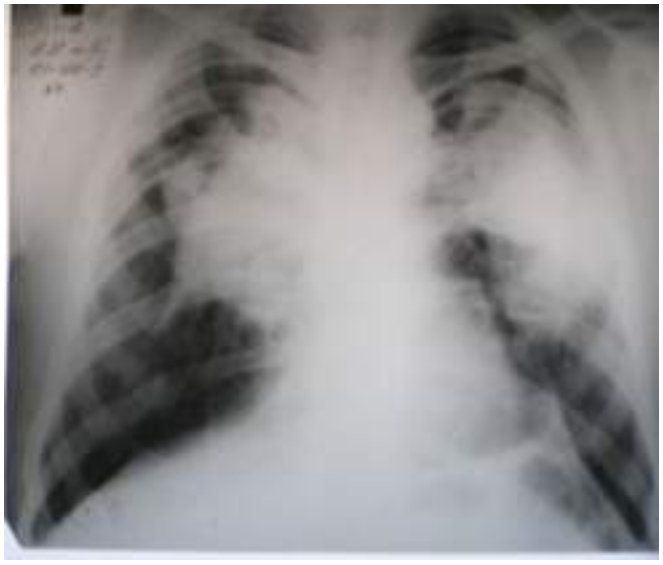

Fig. 2.3.2.7.19. A variant of pneumoconiosis.

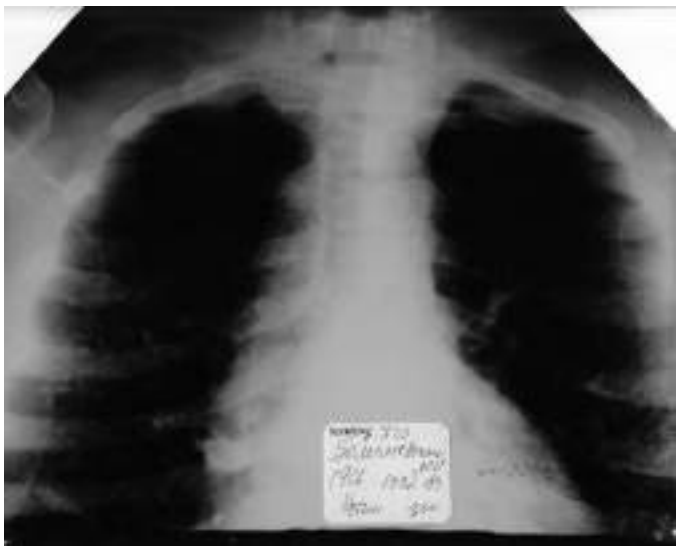

Fig. 2.3.2.7.20. A variant of pneumoconiosis.

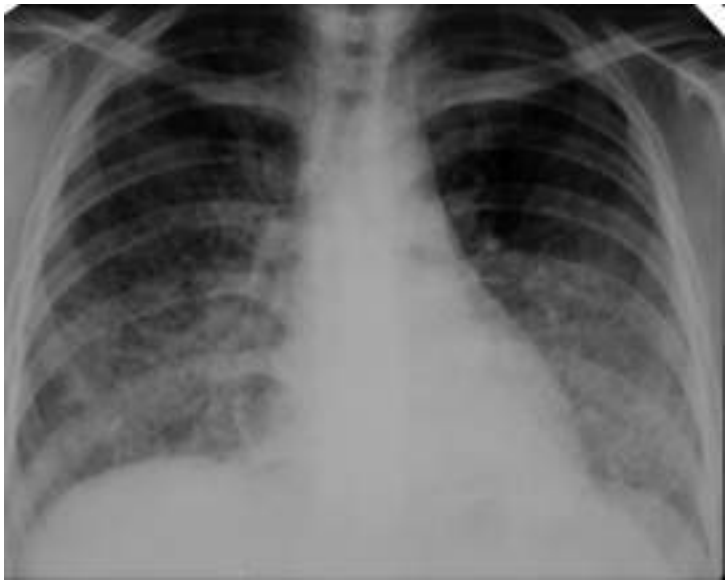

Fig. 2.3.2.7.21. A variant of pneumoconiosis.

2.3.2.8. Idiopathic Interstitial Pneumonias

Idiopathic interstitial pneumonias (IIPs) on radiological examination may mimic disseminated pulmonary tuberculosis and must be differentiated from other diffuse lung diseases (DLDs).

According to the international multidisciplinary consensus on the classification of idiopathic interstitial pneumonias, seven clinico-radiologic-pathologic entities are recognized: idiopathic pulmonary fibrosis; desquamative interstitial pneumonia; nonspecific interstitial pneumonia; cryptogenic organizing pneumonia; acute interstitial pneumonia (Hamman–Rich syndrome); respiratory bronchiolitis–associated interstitial lung disease; and lymphoid interstitial pneumonia.

IIPs have no pathognomonic features. The diseases occur more frequently in patients aged 40–70 years and are more common in men.
On CT, the principal sign of IIP is the presence of fine reticular abnormalities caused by thickening of the intralobular and interlobular interstitium (Fig. 2.3.2.8.1). The most important distinguishing feature of IIPs is the diffuse distribution of abnormalities without clear anatomic localization within individual lobes. Equally important is the predominance of altered areas in the cortical regions of the lungs, mainly in the juxtadiaphragmatic zones, with progression in the craniocaudal direction from the apices toward the diaphragm. A frequent finding is predominant involvement of the posterior, gravity-dependent lung regions. This feature is critical for differentiating IIPs from pulmonary tuberculosis and typical infectious pneumonias.

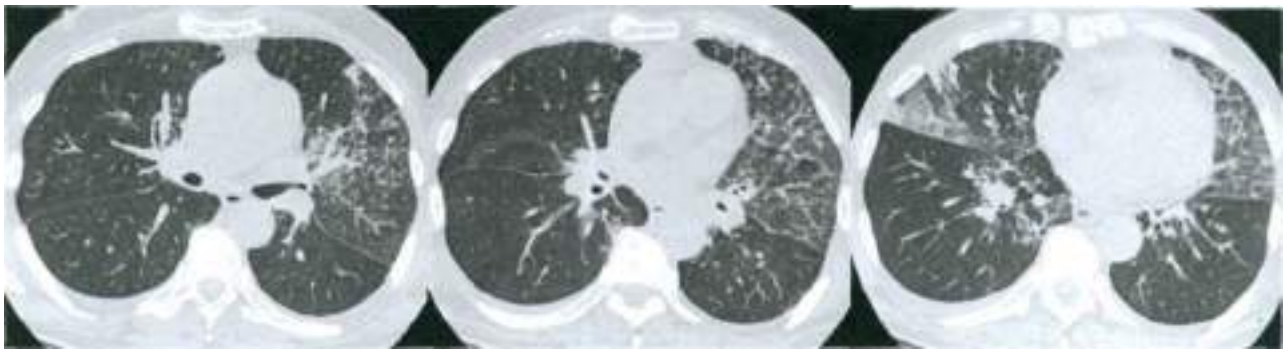

Fig. 2.3.2.8.1. Idiopathic pulmonary fibrosis. Fine reticular abnormalities due to thickening of the intralobular interstitium and areas of ground-glass–type alveolar consolidation are visualized.

CT also demonstrates alterations of the intralobular septa, which morphologically most often correspond to areas of fibrosis and/or cellular infiltration. In addition, typical findings include irregularities of the pleural surfaces, as well as of the vascular and bronchial contours. These anatomical structures acquire uneven and indistinct margins. Collectively, this produces a mosaic pattern with alternating abnormal and normal regions of lung parenchyma.
In later stages, the earliest signs of honeycombing appear in the subpleural zones of reticular abnormalities, in combination with traction bronchiectasis and bronchiolectasis.
Ground-glass opacities are also characteristic of IIPs. They are most frequently localized in areas of reticular abnormalities, within the cortical

regions, and along the diaphragmatic pleural surface. Only exceptionally do such changes involve the entire lung parenchyma, including the perihilar zones. In some patients, ground-glass opacities may predominate over reticular processes. In these zones, regions of consolidation with complete loss of aeration may also occur, typically situated in the most superficial lung regions.

It should be noted that idiopathic pulmonary fibrosis (IPF) is the most common form of IIP, accounting for 80–90% of all idiopathic pneumonias (Fig. 2.3.2.8.2).

Idiopathic pulmonary fibrosis (IPF) is a diffuse lung disease characterized by inflammation and fibrosis of the alveoli and interstitial lung tissue, development of restrictive ventilatory defects, impaired gas exchange, and progressive respiratory failure. According to its clinical course, acute, subacute, chronic, and oligosymptomatic forms are distinguished.

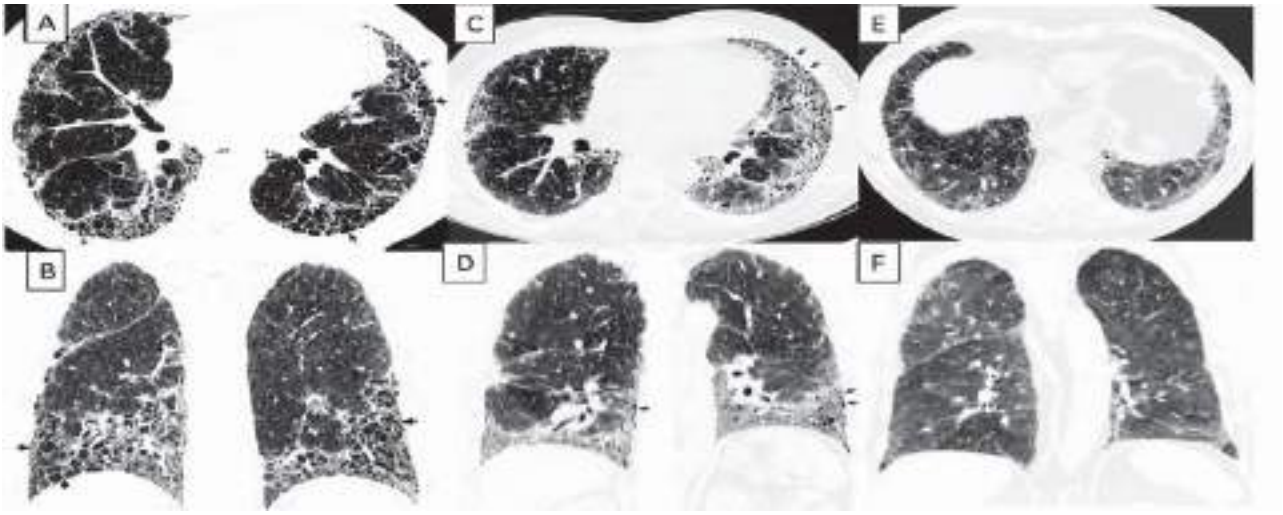

Fig. 2.3.2.8.2. Idiopathic pulmonary fibrosis.

The main clinical symptoms of IPF include persistent inspiratory dyspnea, dry cough, constrictive chest pain, progressive weight loss, general weakness, reduced exercise tolerance, arthralgia, gray-ashen skin cyanosis, and the development of “clubbing.” Percussion reveals dullness over the affected lung zones, most commonly in the lower lobes. Tachypnea is observed. Auscultatory findings include shortened phases of inspiration and expiration, diffusely diminished vesicular breath sounds, and bilateral fine crackles in the interscapular and infrascapular regions, sometimes throughout the entire lung field, resembling “cellophane crackles.” In chronic IPF, a “squeaking” sound

(similar to turning a cork in a bottle) may be heard during inspiration, predominantly in the upper lung fields.

Initial chest radiographs typically show decreased lung transparency with a “ground-glass” pattern (due to thickening of alveolar walls, interstitium, and partial filling of alveoli with cells or fluid) superimposed on a dense, web-like reticular network with small ill-defined nodular opacities. The process is diffuse, though more pronounced in the lower lung zones. Thin, short septal lines may be visible above the diaphragm. As epithelial–cellular granulomas form, the intensity of the reticular pattern increases: the network becomes coarser, with a greater number and size of nodular opacities. In some cases, broad band-like (nodular–linear) opacities predominate along the course of large and medium bronchi and vessels, while in peripheral regions there is an abrupt reduction in fine vascular branches, visualization of thickened interlobular septa, and intervening areas of emphysema. High diaphragmatic position is considered typical for IPF.

Interstitial fibrosis, obliterative arteritis, and involvement of the capillary bed lead to pulmonary hypertension and radiographic signs of cor pulmonale. Angiography demonstrates a reduction and deformation of lobular and terminal branches of the pulmonary artery. Perihilar connective tissue becomes consolidated; mildly enlarged lymph nodes may be detected. As IPF progresses, pronounced pleuro-pulmonary–mediastinal fibrosis develops—thickening of costal and mediastinal pleura, wall consolidation, deformation of the trachea and major bronchi, mediastinal fibrotic infiltration, and displacement of large vessels. Ultimately, IPF evolves into a characteristic “honeycomb lung.” These features are confirmed by CT and MRI imaging (Fig. 2.3.2.8.3–5).

Positron emission lung scanning using inhaled technetium-99m–labeled diethylenetriamine pentaacetate detects reduced alveolar–capillary membrane permeability due to fibrosis (significantly decreased 99mTc half-clearance time).

Complete blood count may reveal erythrocytosis, elevated hemoglobin, left shift of the leukocyte formula, and increased ESR. Biochemical tests show elevated acute-phase reactants, dysproteinemia, hypergammaglobulinemia, increased LDH activity, and elevated surfactant-associated glycoproteins A and D. Immunologic studies show

evidence of an autoimmune component: reduced T-suppressor cells, increased B-lymphocytes, elevated CIC levels, anti-pulmonary antibodies, and mucin antigens such as SSEA-1, KL-6, and 3EG5.
Bronchoalveolar lavage demonstrates an eosinophilic–neutrophilic association with marked lymphocytosis. Pulmonary function tests reveal increased respiratory rate, restrictive ventilatory impairment (reduced tidal volume, VC, MVV, RV, and TLC), decreased diffusing capacity, and absence of airflow obstruction. Oxyhemometry demonstrates hypoxemia without hypercapnia.

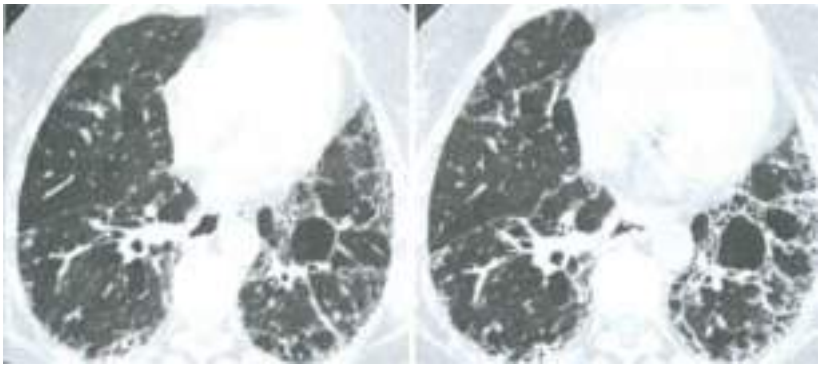

Idiopathic pulmonary fibrosis. Marked diffuse reticular changes in both lungs, with visible lumina of small bronchi on the background of fibrosis.

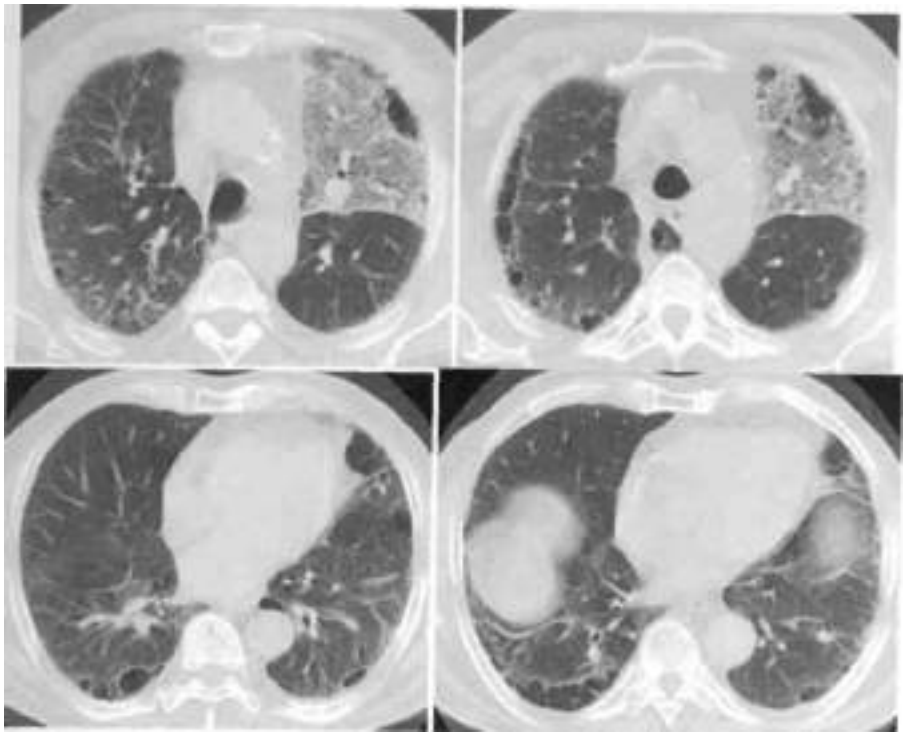

Fig. 2.3.2.8.4. Idiopathic pulmonary fibrosis. Reticular changes along the costal pleura in both lungs. The pleural surface is irregular, and within

areas of increased lung density, multiple small air-containing spaces are visible, corresponding to early “honeycombing.”

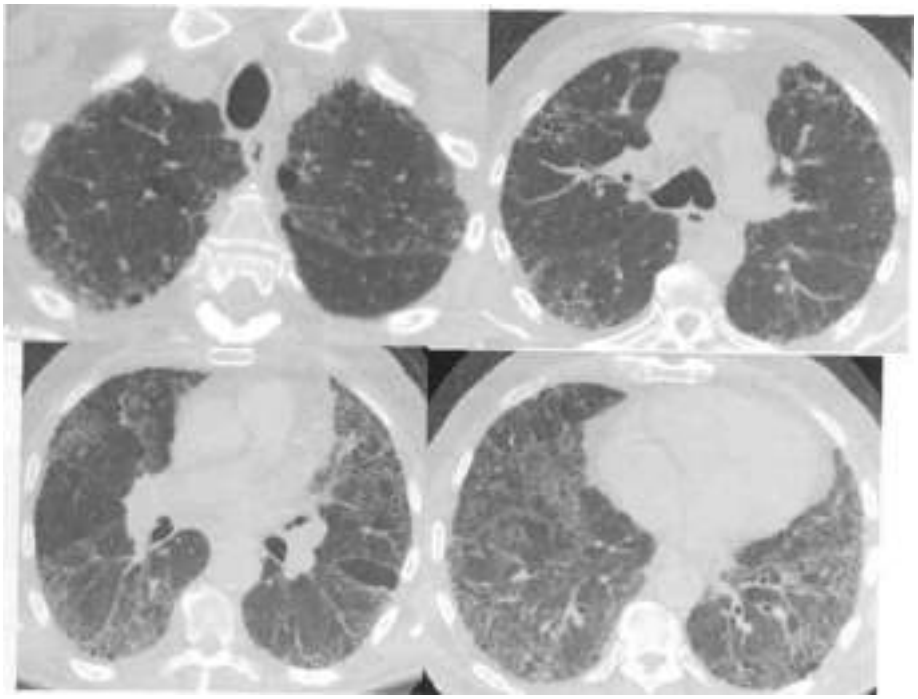

Fig. 2.3.2.8.5. Idiopathic pulmonary fibrosis. Reticular changes in both lungs. The pleural surface is irregular, and within areas of increased lung density, individual air-filled spaces are visible, corresponding to the development of “honeycombing.”

In lymphoid interstitial pneumonia (LIP), when it occurs in HIV-infected patients, in Sjögren’s syndrome, or in Castleman disease, cystic cavities with dense walls are detected. However, their sizes are more uniform, and they are predominantly localized subpleurally. Such cysts may also be scattered throughout the lungs, but they are not a dominant feature (Fig. 2.3.2.8.6–19). Other findings in LIP—poorly defined centrilobular nodules (measuring 3–30 mm, though most are small) and diffuse ground-glass opacification of the lung parenchyma—are key for differential diagnosis.

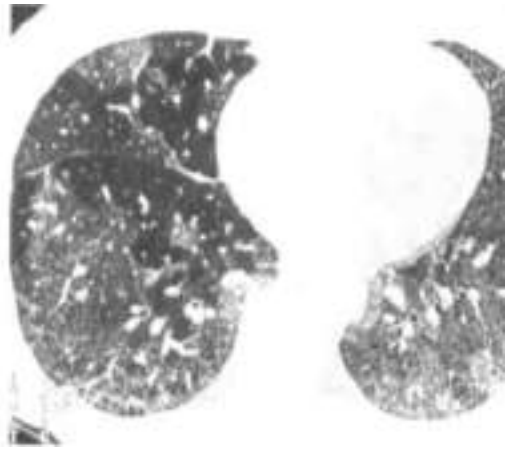

Figure 2.3.2.8.6. Desquamative interstitial pneumonia.

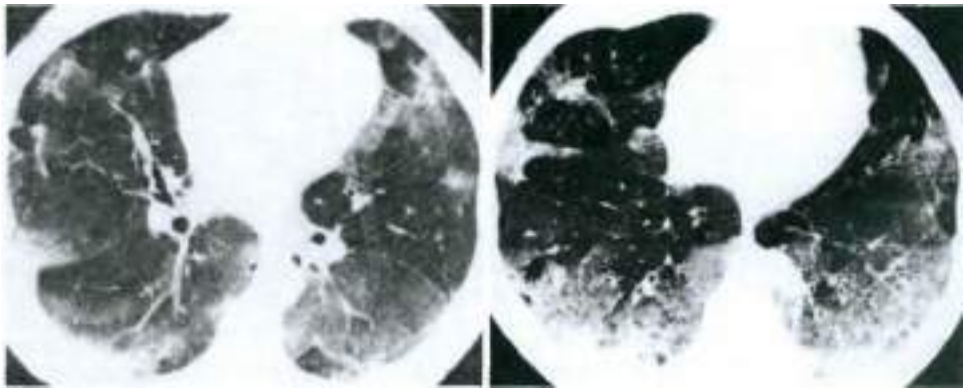

Figure 2.3.2.8.7. Nonspecific interstitial pneumonia. Irregularly shaped areas of increased lung parenchymal attenuation of the “ground-glass” type have indistinct margins and are predominantly localized in the basal segments of the lungs.

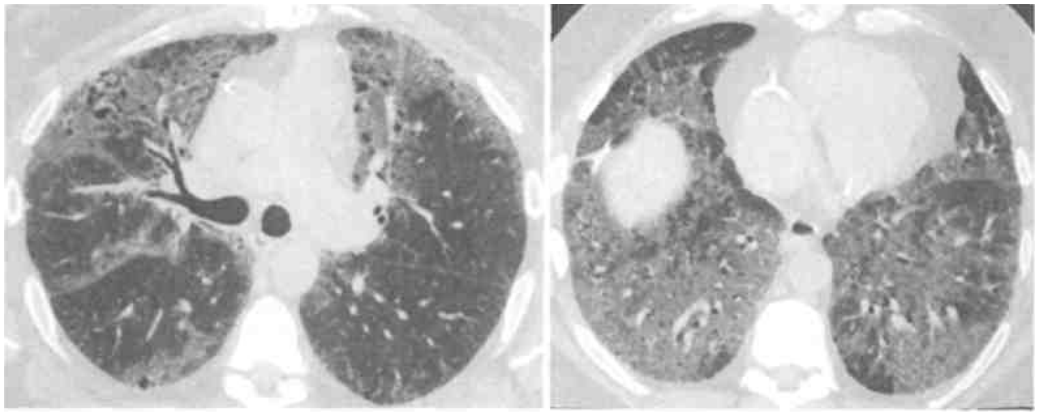

Figure 2.3.2.8.8. Variants of nonspecific interstitial pneumonia. Irregularly shaped areas of increased lung parenchymal attenuation of the “ground-glass” type have indistinct margins and are predominantly localized in the basal segments of the lungs.

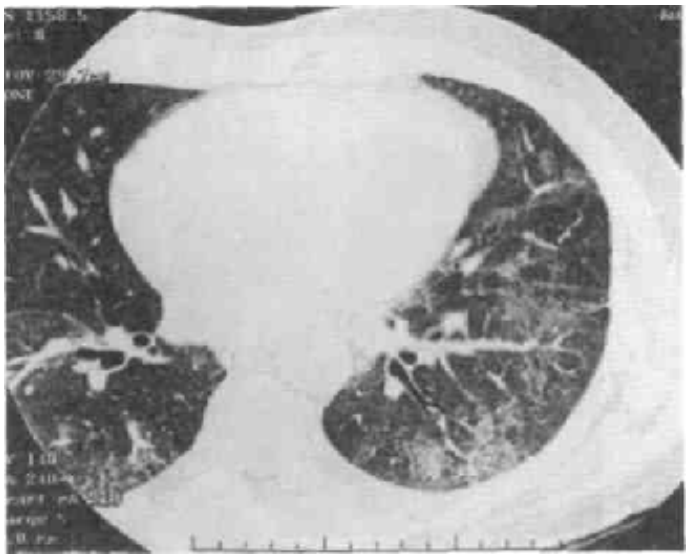

Figure 2.3.2.8.9. Nonspecific interstitial pneumonia – HRCT.

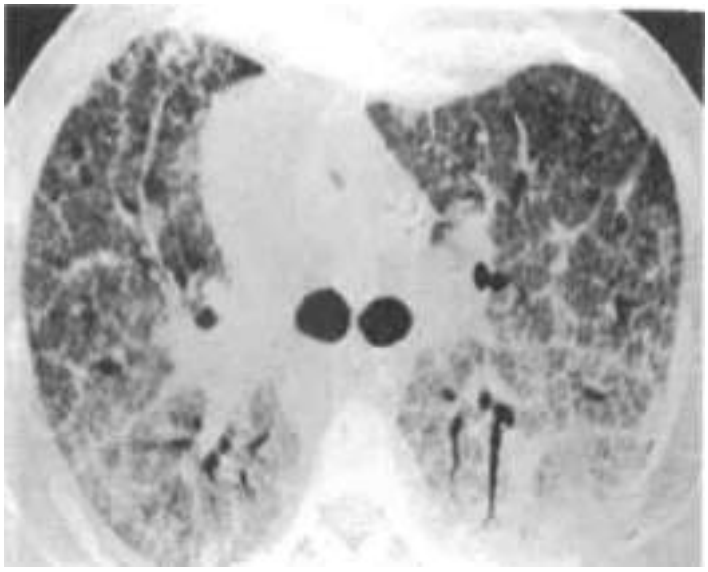

Figure 2.3.2.8.10. Acute interstitial pneumonia (Hamman–Rich syndrome).

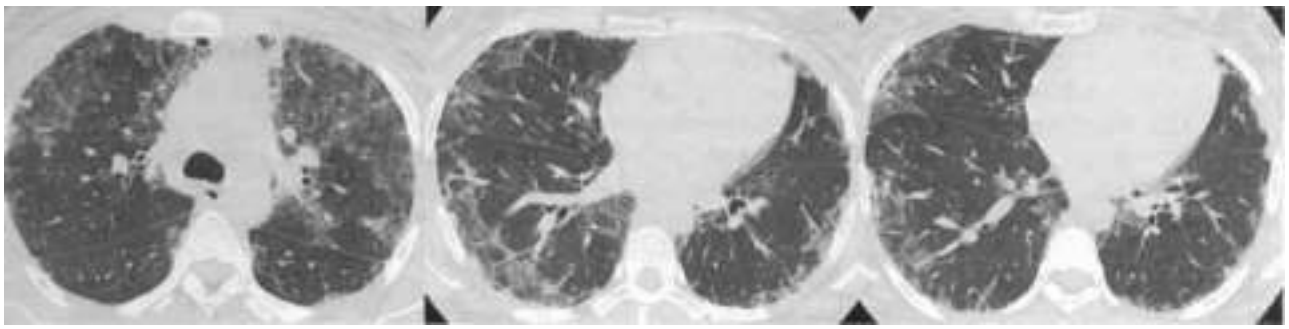

Figure 2.3.2.8.11. Cryptogenic pneumonia. Subpleural and peribronchial areas of ground-glass lung parenchymal consolidation are observed, more pronounced in the lower lobes. Small nodules are present along the bronchovascular bundles.

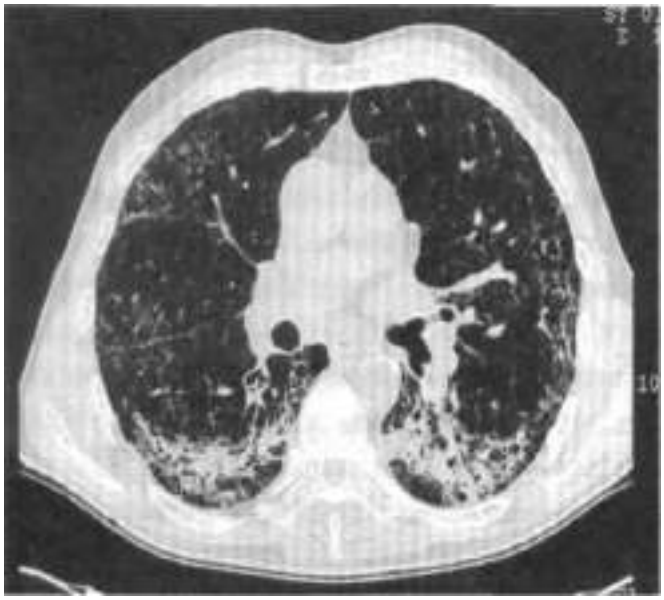

Figure 2.3.2.8.12. Cryptogenic organizing pneumonia.

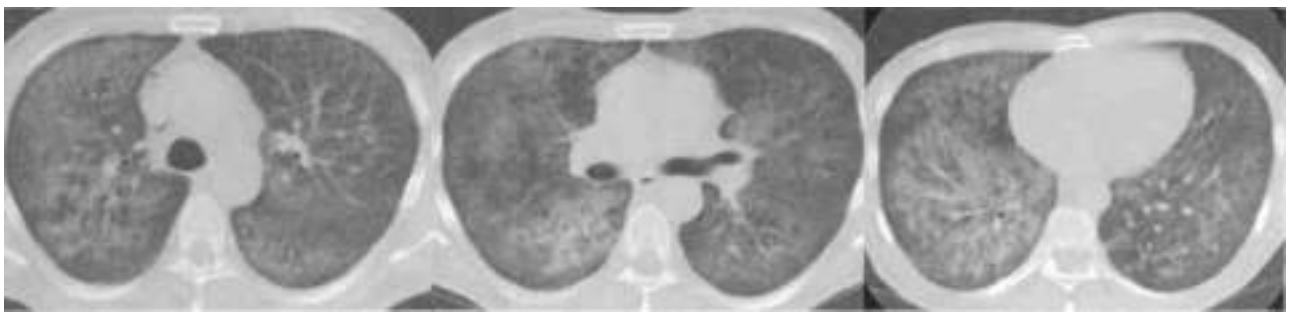

Figure 2.3.2.8.13. Acute interstitial pneumonia (Hamman–Rich syndrome). Diffuse heterogeneous ground-glass opacities, interlobular

septal thickening, and mild bronchiolar dilatation are noted against a background of disrupted normal lung architecture.

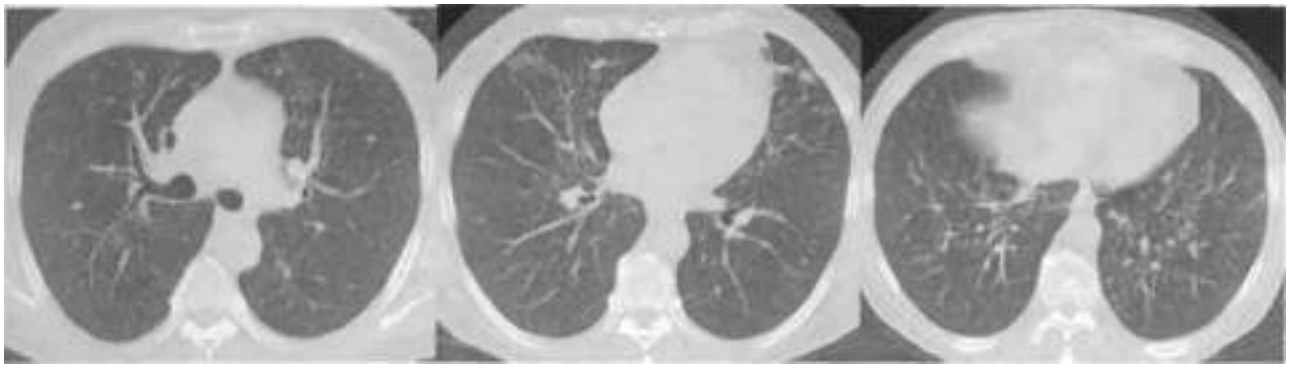

Figure 2.3.2.8.14. Respiratory bronchiolitis–associated interstitial lung disease. Poorly defined centrilobular nodules, diffusely distributed ground-glass opacities, mild fibrosis, and bronchial wall thickening are present.

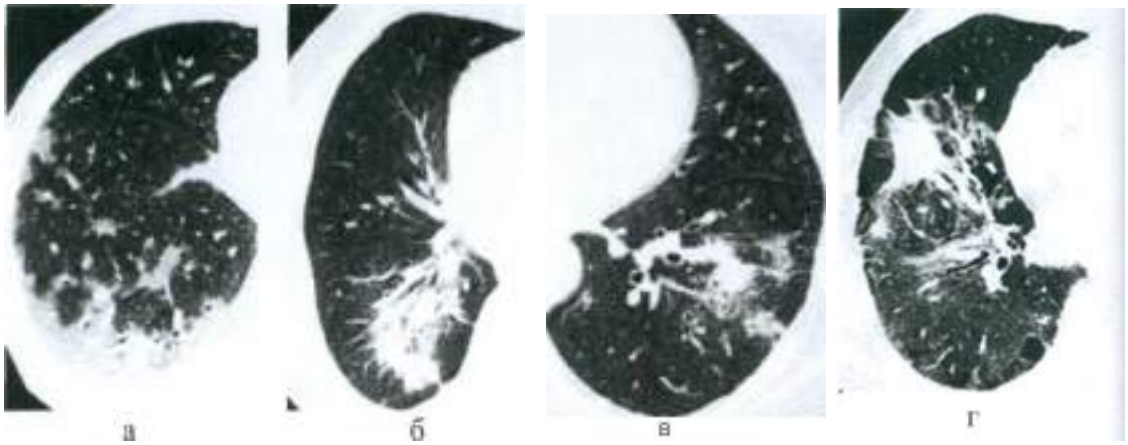

Figure 2.3.2.8.15. Various morphological patterns of respiratory bronchiolitis–associated interstitial lung disease.
Peripheral consolidations broadly abutting the pleura (a).
Peribronchial consolidation with an air bronchogram mimicking pneumonia (b).
Multiple peribronchial nodules (c).
Patchy consolidation with sharp margins and enlarged air-filled bronchial lumina, combined with features of lung architecture distortion and expiratory air trapping in the adjacent lung parenchyma (d).

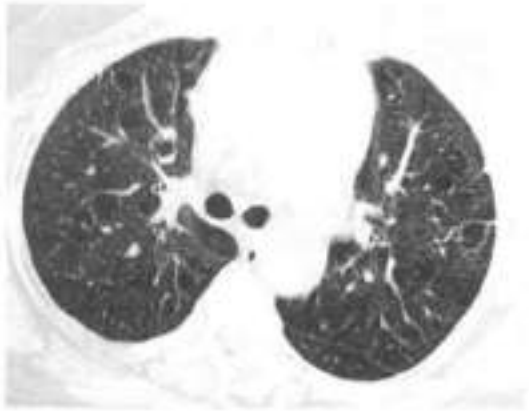

Figure 2.3.2.8.16. Lymphoid interstitial pneumonia.

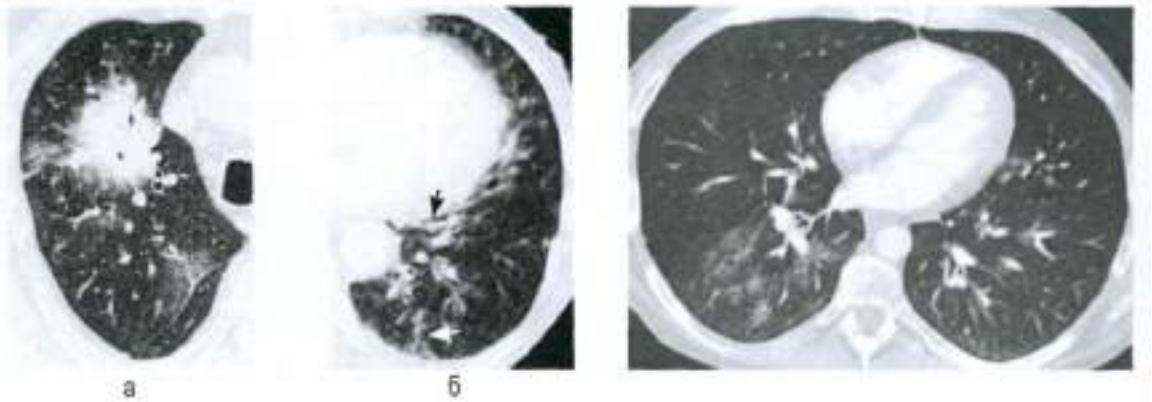

Figure 2.3.2.8.17. Variants of lymphoid interstitial pneumonia.
Poorly defined focal consolidation (a).
Diffuse micronodular consolidation with a “tree-in-bud” pattern (white arrow) and bronchial wall thickening (black arrow), suggesting endobronchial spread of infection (b).
Poorly defined centrilobular ground-glass opacities up to 30 mm in size in the lower lung zones in a patient with HIV infection.

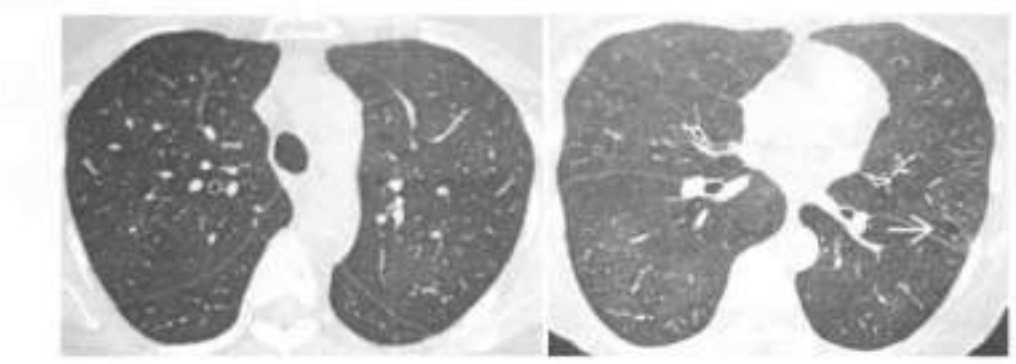

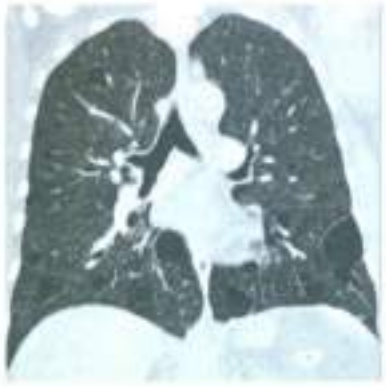

Figure 2.3.2.8.18. Lymphoid interstitial pneumonia. Multiple poorly defined centrilobular nodules, diffusely distributed ground-glass opacities, and numerous cystic air-filled spaces predominantly in the lower lung regions.

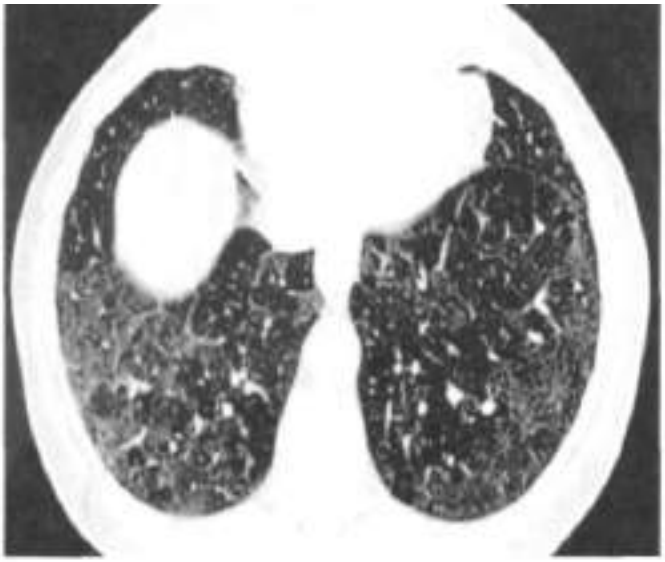

Figure 2.3.2.8.19. Respiratory bronchiolitis–associated interstitial lung disease.

A reticular or reticulonodular remodeling of the pulmonary pattern is caused by a large group of conditions classified as extrinsic allergic alveolitis (EAA) (Fig. 2.3.2.8.20).

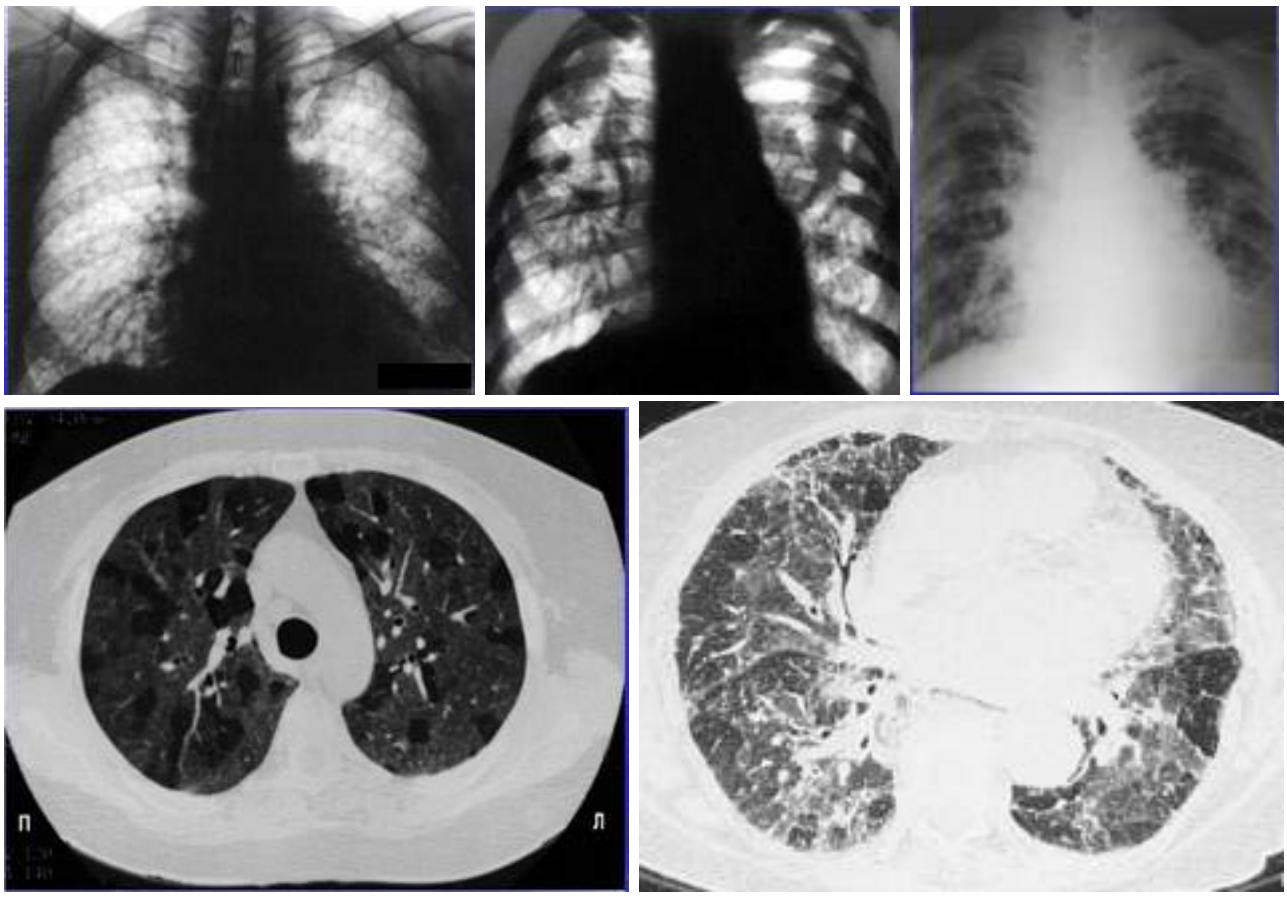

Figure 2.3.2.8.20. Variants of extrinsic allergic alveolitis (EAA).

Extrinsic allergic alveolitis (EAA) is a group of disorders that develop as a result of prolonged and intensive inhalational exposure to organic and inorganic antigens and are characterized by diffuse allergic inflammation of the alveoli and interstitial lung tissue.

Etiological factors capable of inducing EAA are classified into three groups:

1. **Microorganisms** (bacteria, fungi, protozoa) and their metabolic products (proteins, glyco- and lipoproteins, polysaccharides, enzymes, endotoxins);
2. **Biologically active substances of animal and plant origin** (protein antigens of bird feathers, animal wool, fish proteins, milk, saliva, droppings, urine, serum; dust from coffee beans, rice, hemp);
3. **Low-molecular-weight compounds** (diisocyanates, heavy metal salts such as gold, and medications including antibiotics, nitrofurans, antimetabolites such as cyclophosphamide, myelosan, methotrexate, ganglioblockers, and anorectic agents used for obesity treatment).

Acute, subacute, and chronic forms of EAA may all produce detectable radiographic abnormalities. Overall, the disease is characterized by progressive weight loss, sweating, and cough with mucoid sputum. Lung auscultation reveals crepitations, fine crackles, and a “squeaking” sound (in the presence of pleural adhesions and pneumofibrosis). Over time, chronic cor pulmonale develops.

Peripheral blood tests demonstrate leukocytosis, a left shift of the leukocyte formula, eosinophilia, and elevated ESR. Biochemical blood analysis shows hypergammaglobulinemia and increased levels of seromucoids, haptoglobin, and sialic acids. Immunological testing reveals decreased T-suppressor subpopulations, positive lymphocyte blast-transformation reactions, leukocyte migration inhibition in the presence of specific antigen, elevated circulating immune complexes (CIC), and increased titers of antigen-specific IgG detected by Ouchterlony precipitation, passive hemagglutination, and counter-immunoelectrophoresis.

Radiographic evaluation of the chest in acute EAA reveals widespread interstitial lung changes in the form of reticular patterns; patchy infiltrative opacities with indistinct margins may appear in the lower and subpleural lung regions. In subacute EAA, bilateral small nodular opacities measuring 0.2–0.3 cm (granulomatous lung involvement) are observed.

Chronic EAA is characterized by pronounced pulmonary fibrosis: widespread honeycomb-like deformity of the pulmonary pattern, diffuse reticular and linear opacities, a “honeycomb lung” appearance, and signs of lung shrinkage and pulmonary hypertension.

Pulmonary function testing demonstrates restrictive ventilatory defects (reduced vital capacity), and moderate impairment of bronchial patency due to bronchioloalveolitis, with a marked reduction in MEF_{75}%. In the chronic form, a restrictive type of respiratory failure develops, accompanied by arterial hypoxemia.

During transbronchial lung biopsy, the key morphological features of EAA include: lymphocytic infiltration of the alveoli and interalveolar septa; the presence of granulomas; signs of alveolar obliteration; interstitial fibrosis with bronchiolar distortion; areas of pulmonary

emphysema; fragmentation and reduction of elastic fibers; and the detection of immune complexes within the alveolar walls.

The diagnostic criteria for EAA include: a clear association between disease development and a specific etiological factor; disappearance or marked reduction of symptoms after cessation of allergen exposure; positive results of provocative inhalation tests; positive intradermal tests with the causative allergen; detection of specific precipitating antibodies in the blood; bilateral widespread crepitations, predominantly in the basal lung regions; radiographic evidence of nodular pulmonary dissemination or diffuse interstitial changes and “honeycomb lung”; restrictive ventilatory defects on pulmonary function testing in the absence of bronchial obstruction (or with only minimal obstruction); detection of specific lymphocyte stimulation in LBT or LMIT; and characteristic morphological findings in lung biopsy specimens.

Extrinsic allergic alveolitis (EAA), or hypersensitivity pneumonitis, is an allergic reaction of the lung tissue in response to inhalation of various antigens present in organic dust. In acute EAA, radiographic and CT imaging may show no abnormalities or may reveal bilateral lung parenchymal consolidations of varying intensity in the middle and lower lung zones (Figs. 2.3.2.8.21–22). Within a few days, these infiltrative changes resolve and are replaced by delicate reticular changes characteristic of the subacute stage of pneumonitis.

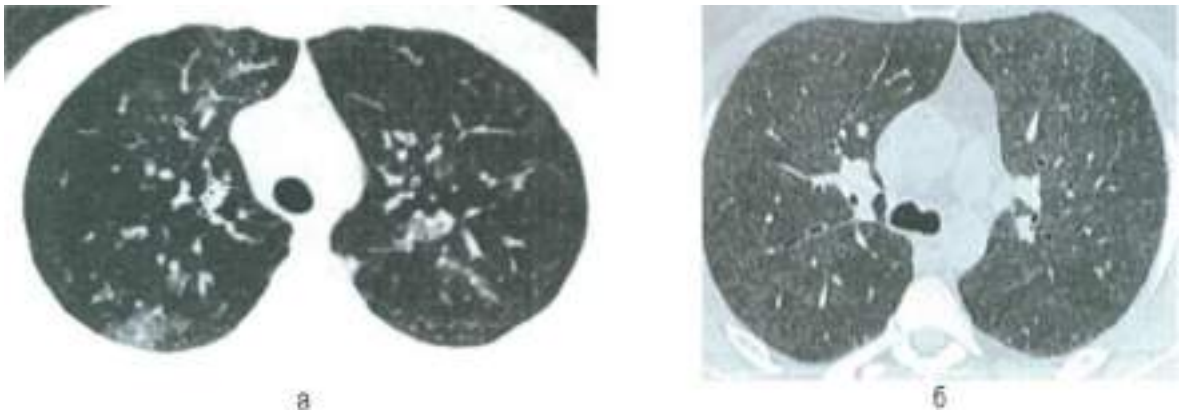

Figure 2.3.2.8.21. Variants of acute EAA.

Isolated areas of ground-glass lung parenchymal consolidation predominantly located in

the cortical regions of the upper lobes (a). Multiple small ground-glass opacities within the lung parenchyma (b).

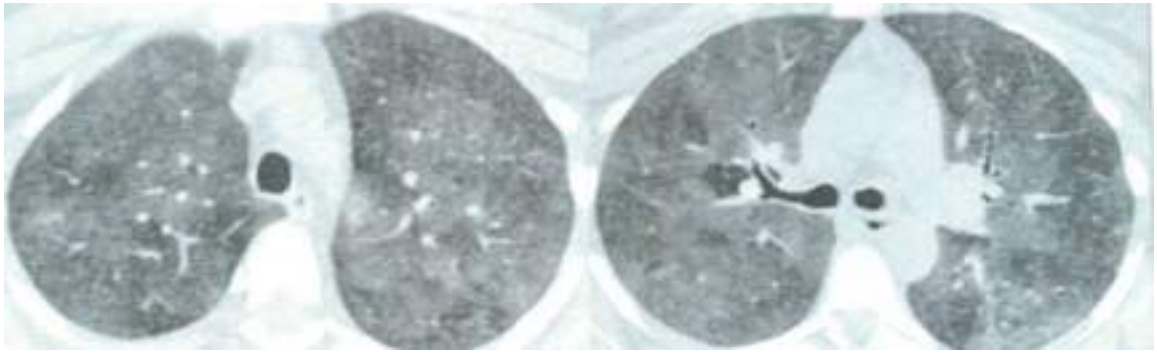

Figure 2.3.2.8.22. Acute EAA. Numerous diffuse ground-glass opacities within the lung parenchyma.

In subacute EAA, CT reveals variably extensive areas of ground-glass lung parenchymal attenuation and a small number of centrilobular nodules. Ground-glass changes may be diffuse and involve the entire lung volume, but are more commonly pronounced in the middle and lower lung zones (Figs. 2.3.2.8.23–25).

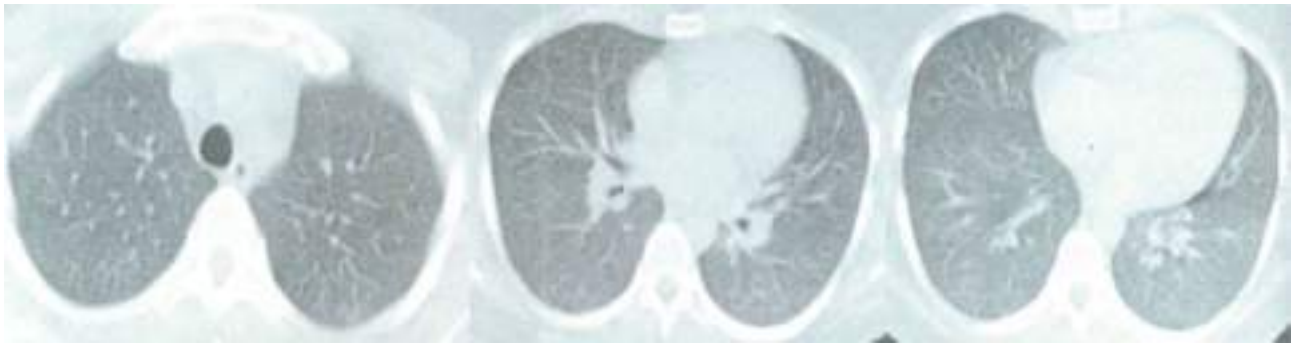

Figure 2.3.2.8.23. Subacute EAA. Diffuse, ill-defined acinar (alveolar) foci of consolidation with a centrilobular distribution (upper lung zones), along with diffuse ground-glass changes more pronounced in the middle and lower lung regions.

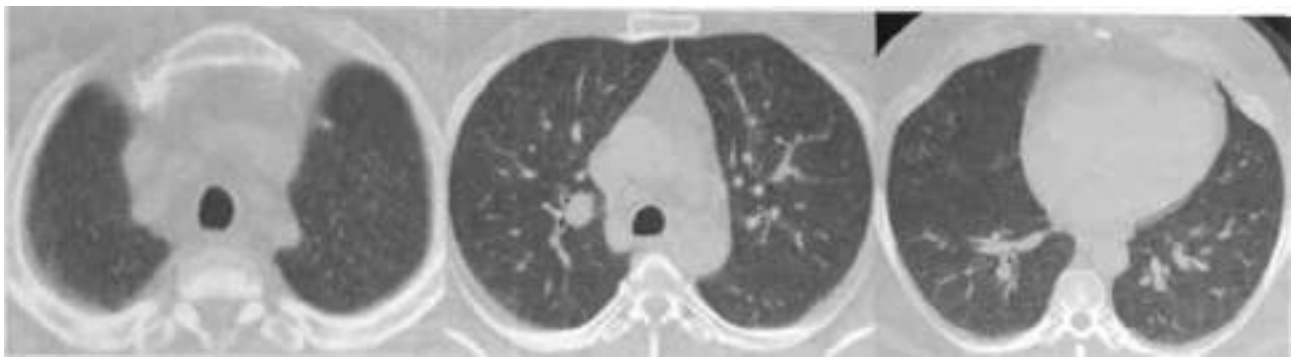

Figure 2.3.2.8.24. Subacute EAA. Diffuse, ill-defined acinar (alveolar) foci of consolidation with a centrilobular distribution, with diffuse ground-glass changes involving the entire lung volume.

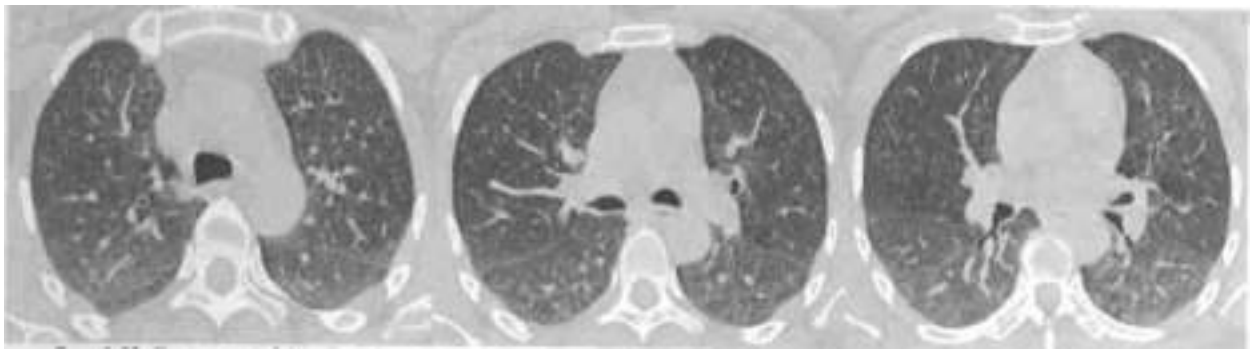

Figure 2.3.2.8.25. Subacute EAA. Diffuse ground-glass changes involving the entire lung volume.

Chronic EAA is distinguished by the presence of fibrosis. On CT, these changes are characterized by the appearance of fine linear structures representing thickening of the intralobular interstitium. As a result, a pattern of delicate reticular changes is formed, supplemented by areas of honeycombing in the cortical regions and distortion of the normal lung architecture (Figs. 2.3.2.8.26–27).

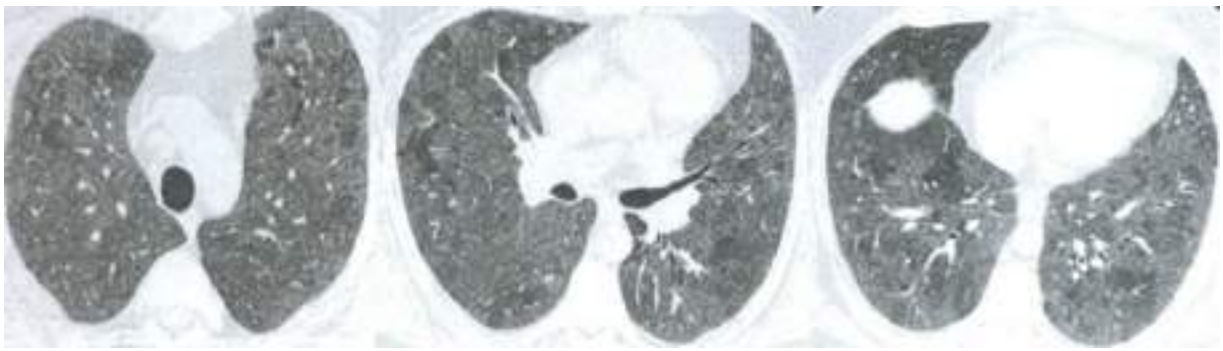

Figure 2.3.2.8.26. Chronic EAA with mixed features of acute alveolitis (ground-glass opacities) and chronic fibrosis, accompanied by regional expiratory air trapping indicating involvement of the airways.

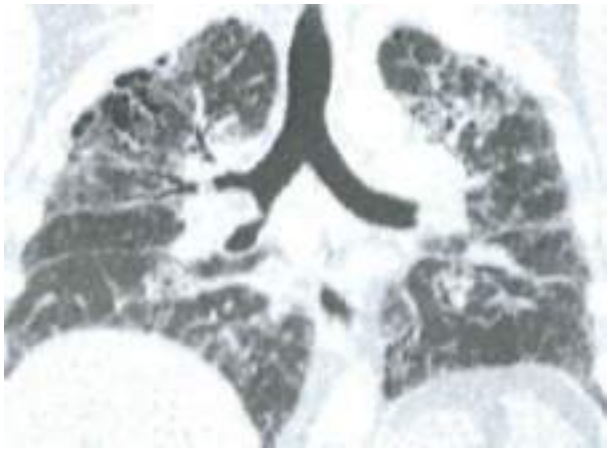

Figure 2.3.2.8.27. Chronic EAA. Extensive areas of ground-glass lung parenchymal consolidation and chronic fibrosis (thickened septa, interstitial tissue thickening, bronchiectasis, and subpleural focal consolidations).

Giant cell interstitial pneumonia is most commonly classified as an occupational lung disease caused by exposure to heavy metals. Pulmonary changes on standard chest radiography closely resemble those of disseminated tuberculosis, while CT findings of the respiratory system mimic the appearance of interstitial pneumonias. The pathological process is characterized by predominant ground-glass pulmonary infiltrates with very fine reticular changes. Lung parenchymal abnormalities are chaotically distributed, involving the cortical regions, mainly in the middle and lower lung zones (Fig. 2.3.2.8.28). Development of honeycomb lung is typical.

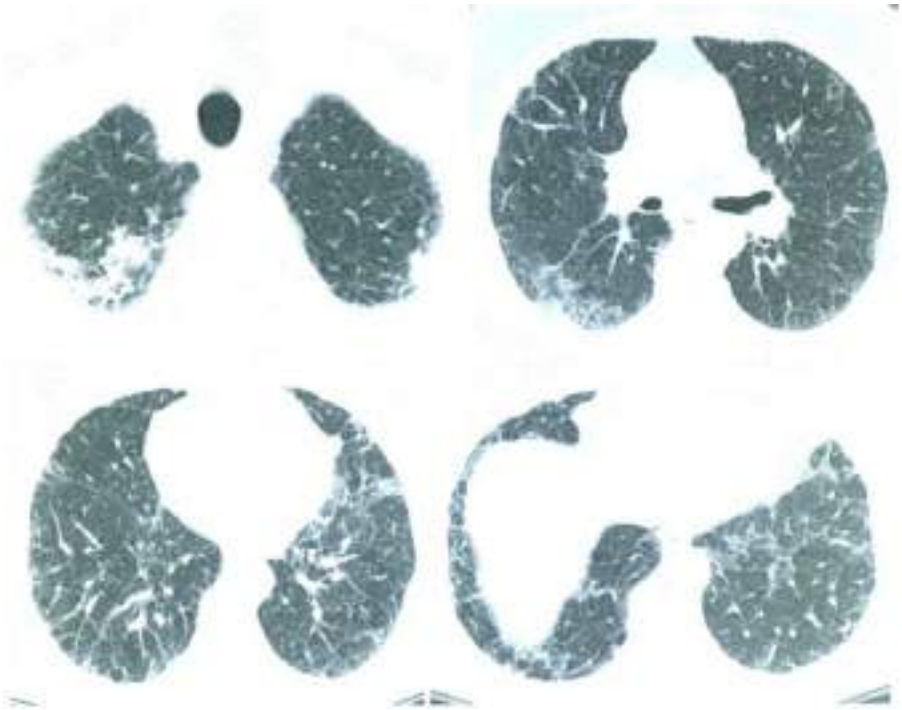

Figure 2.3.2.8.28. Giant cell interstitial pneumonia. In the cortical lung regions, predominantly in the posterior segments, reticular changes are observed in the form of uneven thickening of the intralobular septa and areas of increased attenuation of the ground-glass type.

Acute infectious bronchiolitis most often has a viral (respiratory syncytial virus, adenovirus), mycoplasmal, or chlamydial etiology and on standard chest radiographs may resemble disseminated pulmonary tuberculosis.
The distinguishing CT features of infectious bronchiolitis include small centrilobular nodules with linear branching structures (the “tree-in-bud” pattern), reflecting bronchiolar wall thickening or luminal filling with granulation tissue, mucus, or pus (Figs. 2.3.2.8.29a, b). The “tree-in-bud” sign is most pronounced in the peripheral third of the lung parenchyma. In some cases, it is accompanied by scattered ground-glass opacities or areas of consolidation (complete or near-complete airlessness of the alveolar lung tissue).

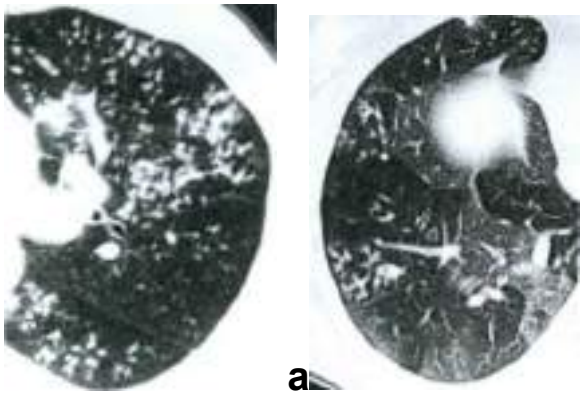

Figure 2.3.2.8.29. CT variants of infectious bronchiolitis.
“Tree-in-bud” pattern and small, well-defined nodules (a).
Expiratory CT - “tree-in-bud” pattern with air trapping, indicating involvement of the small airways.
Autoimmune pneumonitis. Reticulonodular remodeling of the pulmonary architecture may result from endogenous fibrosing alveolitis (autoimmune pneumonitis), which represents a manifestation of systemic connective tissue diseases and primary vasculitides. Alongside diffuse reticular pulmonary fibrosis in rheumatoid arthritis with systemic involvement and systemic lupus erythematosus, pleural involvement (serositis) is more commonly observed.
A distinctive form is so-called rheumatoid silicosis, or **silicoarthritis (Caplan–Colinet syndrome)**—the coexistence of rheumatoid arthritis with silicosis. The articular syndrome (joint pain, stiffness, deformities) of varying severity may precede the development of silicosis, occur simultaneously with it, or appear at different intervals after the diagnosis

of silicosis has been established. Pulmonary findings include changes typical of the interstitial or nodular form of silicosis, with well-demarcated round opacities 0.5–5 cm in diameter, predominantly located in the peripheral regions of both lungs against a background of pronounced interstitial abnormalities.

Morphologically, in the lungs of patients with silicoarthritis, nodules are found—sometimes with necrosis—featuring the concentrically arranged fibers typical of silicosis, surrounded peripherally by a zone of cellular proliferation with vasculitis and palisading fibrocytes characteristic of rheumatoid nodules. The rounded opacities represent accumulations of silica particles and rheumatoid factor. Clinically, either the pulmonary manifestations with progressive restrictive respiratory failure or the symptoms of rheumatoid arthritis may predominate. Detection of high titers of rheumatoid factor in serum (Waaler–Rose reaction) is useful for diagnosing silicoarthritis. In some cases, silicosis may coexist with other collagen vascular diseases (systemic lupus erythematosus, systemic sclerosis—Erasmus syndrome—dermatomyositis, etc.).

Progressive systemic sclerosis (scleroderma) is characterized by basal pneumofibrosis: formation of coarse fibrous strands with a peculiar remodeling of lung architecture in the lower lobes, accompanied by numerous small foci with dense walls, giving the pattern a spongy or “porous” appearance. Small cysts may also be present in the lower lateral regions (cystic pneumofibrosis). Radiographic examination of the esophagus and stomach reveals their dilation, decreased tone and motility, and smoothing of the mucosal folds. Characteristic features of scleroderma include musculoskeletal involvement—osteolysis of distal phalanges, sclerodactyly, and periarticular calcinosis. Raynaud’s phenomenon, Werlhof’s syndrome, and autoimmune hemolytic anemia (Coombs-positive) are also common manifestations.

In nodular polyarteritis, interstitial fibrosis is common. Against the background of diffuse alterations in the pulmonary pattern, areas of consolidation (infarcts) and thin-walled cavities become evident. Pulmonary involvement presents clinically with progressive inspiratory dyspnea, cough with scant sputum production, hemoptysis, and a polymorphic, nonspecific auscultatory picture (moist or dry crackles). Additional diagnostic criteria include: weight loss >4 kg not related to

diet; livedo reticularis—a mottled, net-like discoloration of the skin on the extremities or trunk; testicular pain unrelated to infection or trauma; myalgia, weakness or tenderness of the lower limb muscles; mono- or polyneuropathy; diastolic blood pressure >90 mmHg; elevated blood urea nitrogen (≥10 mmol/L) and creatinine (≥150 μmol/L); and frequently positive hepatitis B markers (+HBsAg). Arteriography reveals aneurysms and occlusion of visceral arteries not caused by atherosclerosis or fibromuscular dysplasia. Biopsy demonstrates granulocytic and mononuclear infiltration of the arterial wall.

In recent years, the incidence of **Gougerot–Sjögren syndrome** has increased significantly. In these patients, chest radiography reveals a downward-intensifying diffuse honeycomb pattern (medium-sized cystic spaces) with no focal opacities, as well as **Goodpasture's syndrome**.

Goodpasture's syndrome (pulmonary–renal hemorrhagic syndrome) is a progressive autoimmune disease of the lungs and kidneys characterized by the formation of antibodies against the basement membranes of renal glomerular capillaries and alveoli, resulting in pulmonary and renal hemorrhages. Diagnostic criteria include: combined lung and kidney involvement (hemoptysis, dyspnea, features of glomerulonephritis), progressive course with development of pulmonary and renal failure, and iron-deficiency anemia. Pulmonary changes in Goodpasture's syndrome consist of multiple focal opacities ("cloudy sky" appearance) against diffuse reticular enhancement of the lung pattern in the middle and lower lung zones (Figs. 2.3.2.8.30–31). Laboratory findings include elevated titers of antibodies to the glomerular and alveolar basement membranes, linear deposits of IgG and complement component C3 along the basement membranes of renal glomeruli and alveoli, and absence of other systemic manifestations.

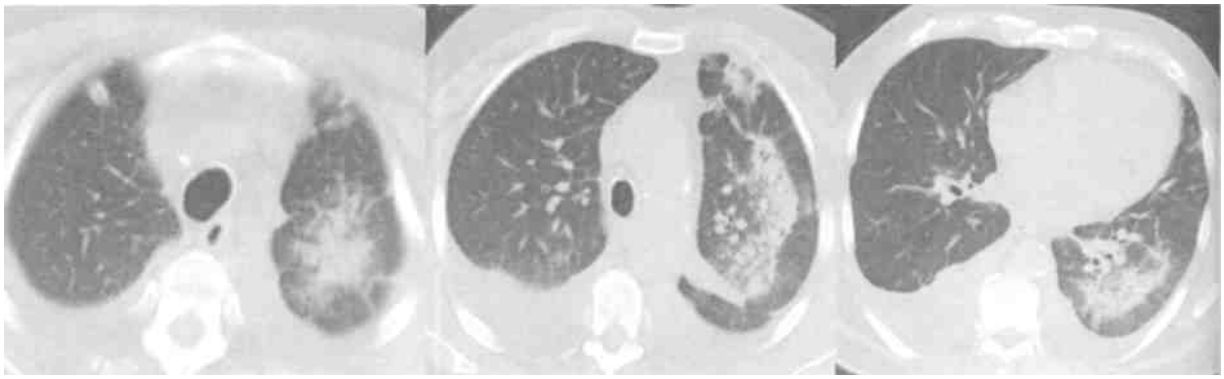

Figure 2.3.2.8.30. Goodpasture’s syndrome. Multiple confluent, densely consolidated acinar foci in the left lung with an air bronchogram sign. Bilateral costal and left-sided interlobar pleural effusion.

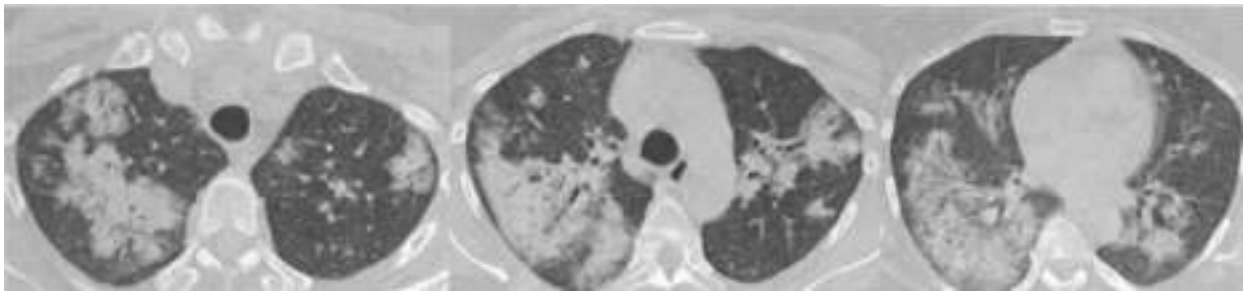

Figure 2.3.2.8.31. Goodpasture’s syndrome. Multiple areas of focal, patchy, and diffuse increased lung parenchymal attenuation ranging from ground-glass opacities to complete alveolar airlessness, with an air bronchogram sign.

Pulmonary changes in systemic connective tissue diseases bear significant similarity to interstitial pneumonias and may sometimes mimic tuberculosis on routine chest radiographs. Such abnormalities may occur in patients with systemic sclerosis (scleroderma) (Fig. 2.3.2.8.32), rheumatoid arthritis (Fig. 2.3.2.8.33), polymyositis (dermatomyositis) (Fig. 2.3.2.8.34), systemic lupus erythematosus, and mixed connective tissue diseases.

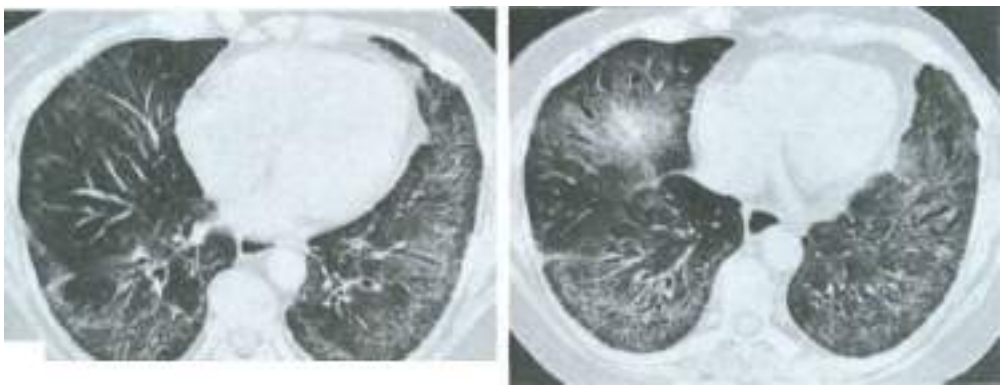

Figure 2.3.2.8.32. Systemic scleroderma. In the cortical lung regions, predominantly in the posterior segments, reticular changes are observed in the form of uneven thickening of the intralobular septa and areas of increased attenuation of the ground-glass type.

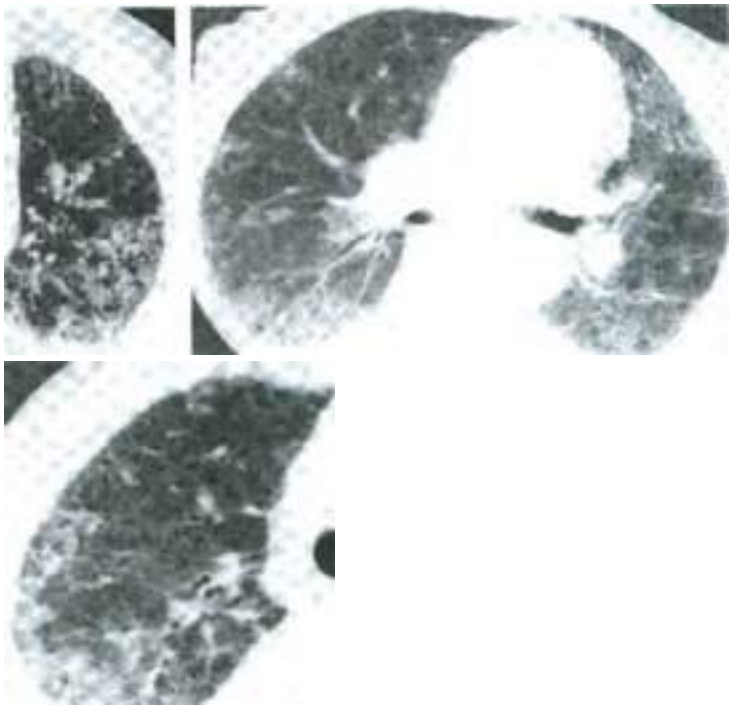

Figure 2.3.2.8.33. Rheumatoid arthritis. In the cortical lung regions, predominantly in the posterior segments, reticular changes are observed in the form of uneven thickening of the intralobular septa and areas of increased ground-glass attenuation.

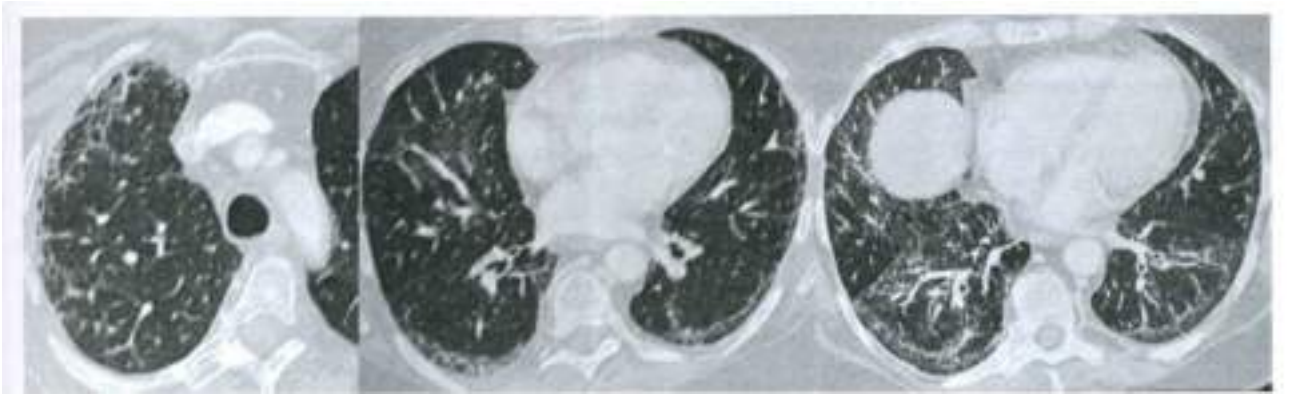

Figure 2.3.2.8.34. Dermatomyositis. Predominantly in the cortical lung regions, reticular changes are observed in the form of uneven thickening of the intralobular septa and areas of increased attenuation of the ground-glass type.

The pathological process in the lungs is characterized by fine reticular changes caused by thickening of the intralobular interstitium. These changes are localized in the cortical lung regions, predominantly in the supradiaphragmatic zones, and are often combined with ground-glass opacities, small centrilobular nodules, and areas of pleural thickening. Focal changes in systemic diseases, especially in rheumatoid arthritis, are due to lymphoid hyperplasia in the bronchiolar walls. Other pulmonary manifestations of rheumatoid arthritis include bronchiectasis and bronchiolectasis, as well as isolated pleural abnormalities such as pleural thickening. Honeycomb lung of similar localization is typical.

Histiocytosis X is a granulomatous disorder of unknown etiology, more commonly occurring in young and middle-aged adults. In more than half of cases, only the lungs are affected; in 20% of cases, combined lung and bone involvement is found; and in approximately 30% of cases, lesions appear simultaneously in several organs. Clinical manifestations are nonspecific and often entirely absent. More than 20% of patients develop spontaneous pneumothorax. The disease course is generally benign, and only rarely does a honeycomb lung pattern develop.

In adults, the primary chronic form of histiocytosis (Hand–Schüller–Christian disease) is most common. The main diagnostic criteria include: recurrent pneumothorax; restrictive and obstructive ventilatory defects; systemic organ involvement (hepatosplenomegaly); formation of small focal opacities against enhanced pulmonary markings (stage I); fine honeycomb-like deformation of the pulmonary pattern (stage II); cystic–

bullous remodeling (“honeycomb lung,” stage III) on chest radiography; and identification of histiocytic granulomas in lung biopsy specimens. Radiographically, histiocytosis manifests as reticular and focal changes in the upper and middle lung zones, which are often interpreted as signs of tuberculous inflammation (Fig. 2.3.2.8.35). Antituberculosis therapy is ineffective. The radiographic appearance differs significantly from CT findings.

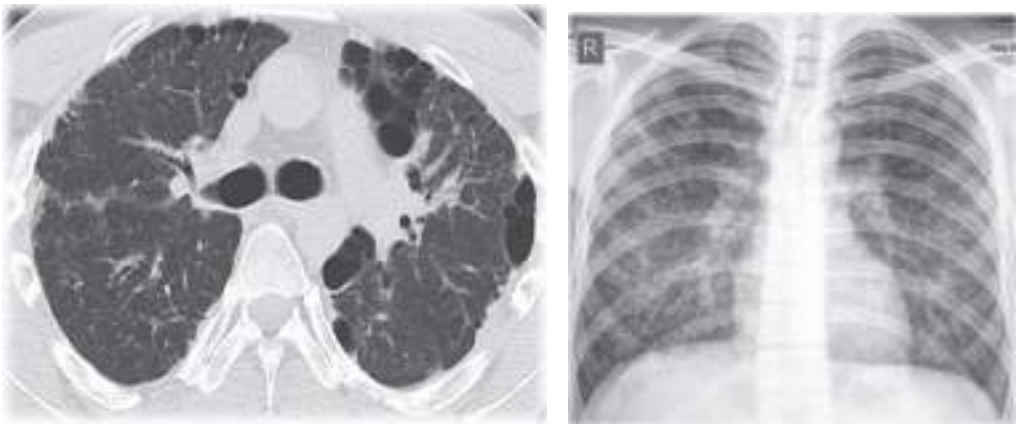

Figure 2.3.2.8.35. Pulmonary histiocytosis X (histiocytic granulomatosis of the lungs).

The principal CT feature of histiocytosis, as a morphological imaging method, is the presence of multiple cysts and small centrilobular nodules (Fig. 2.3.2.8.36).

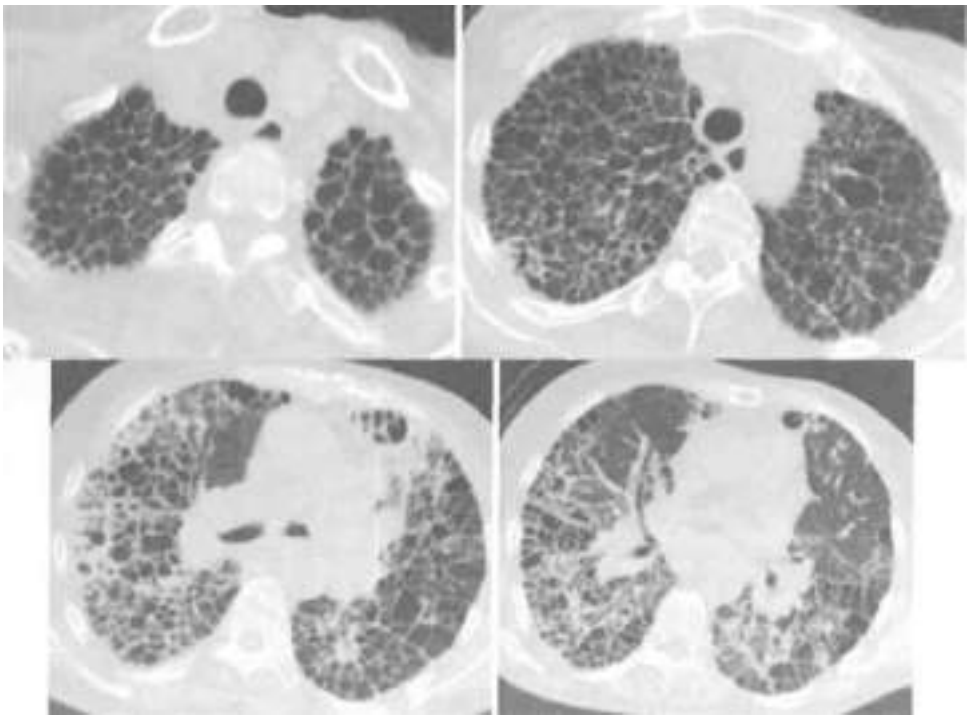

Figure 2.3.2.8.36. Histiocytosis X. Multiple irregularly shaped air-filled cystic spaces with well-defined walls are observed in the lung parenchyma. Scattered small centrilobular nodules are visible between the cystic spaces.

The cysts typically measure less than 10 mm; as they coalesce, they may reach sizes greater than 20 mm and can have either a rounded or bizarre configuration. Their walls are usually barely perceptible, but may reach several millimeters in thickness (Figs. 2.3.2.8.37b, c). Subpleural cysts are prone to recurrent episodes of pneumothorax.

The nodules are usually located in the center of the secondary pulmonary lobule, small in size (up to 5 mm, rarely several centimeters), and like the cysts, are predominantly found in the upper lobes (57%). The basal regions of the lungs and the costophrenic angles are typically spared. Occasionally, small cavitations may be detected within the nodules, although histological examination rarely reveals necrosis within the granulomas. In rare cases, patchy or diffuse ground-glass opacities may be present, although this is not a characteristic feature (Fig. 2.3.2.8.37d). Lung volume is typically increased.

The greatest diagnostic difficulty arises in early forms of histiocytosis, in which pulmonary changes are limited to a small number of centrilobular nodules with no cyst formation. In such cases, diagnosis can only be established by biopsy (Figs. 2.3.2.8.37a, 2.3.2.8.38).

As the disease progresses, the number of nodules decreases, and the lung parenchyma is replaced by thin-walled cysts until intact parenchyma remains only in the basal regions (“vanishing lung”). The size of nodules and the thickness of cyst walls may decrease with treatment.

The combination of intrapulmonary nodules and cysts is considered pathognomonic for pulmonary histiocytosis X. However, a definitive diagnosis can be made only on the basis of lung tissue biopsy.

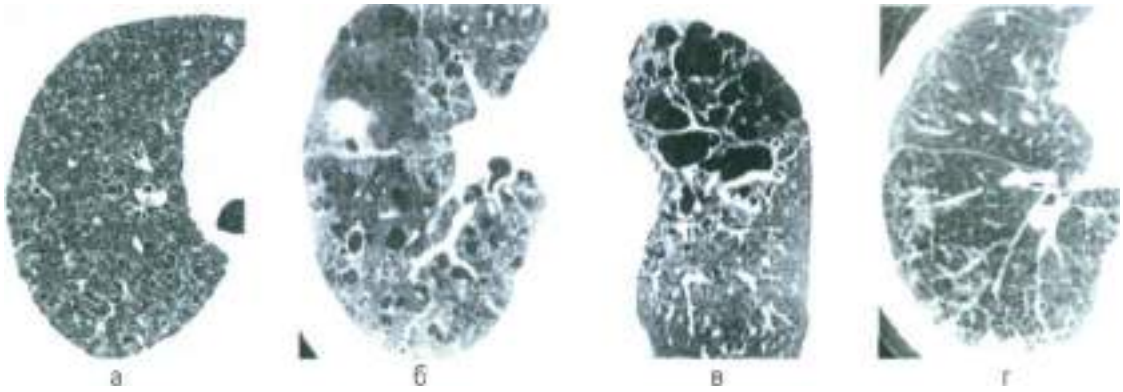

Figure 2.3.2.8.37. CT variants of histiocytosis.
Diffuse centrilobular nodules and microcystic changes (a).
Multiple predominantly small cysts, some confluent, communicating with isolated subpleural nodules; the intervening parenchyma demonstrates ground-glass attenuation (b).
Large confluent cysts, predominantly in the upper lobes (c).
Progressive involvement of the lung parenchyma leading to widespread fibrotic changes (d).

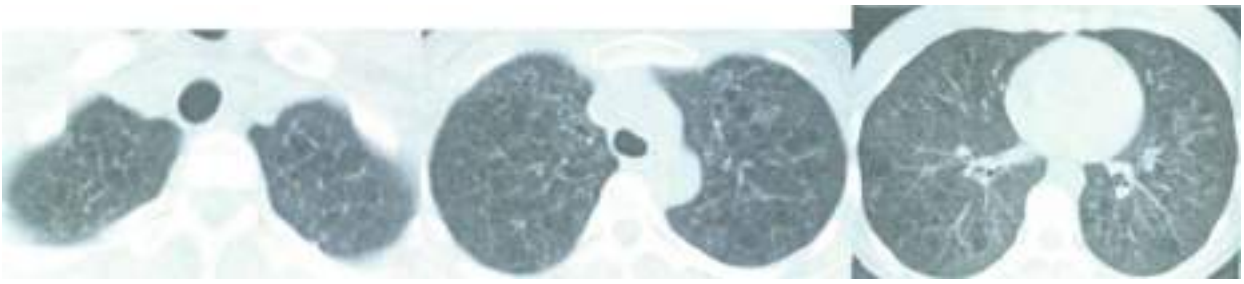

Figure 2.3.2.8.38. Histiocytosis X. Multiple irregularly shaped air-filled cysts with thin walls are visualized within the lung parenchyma; the intervening parenchyma shows ground-glass attenuation.

Pulmonary lymphangioleiomyomatosis (LAM) is a rare disease characterized by proliferation of atypical spindle-shaped cells within the lung parenchyma and walls of lymphatic vessels. Rupture of pulmonary venules leads to episodes of hemoptysis and pulmonary hemorrhage, whereas obstruction of pulmonary lymphatics causes chylous pleural effusion. The condition predominantly affects women of reproductive age, and a hormonal (estrogen-related) etiology is suspected.

The CT appearance is pathognomonic: thin-walled cysts of varying sizes (2–5 cm), mostly small, evenly distributed throughout the lung parenchyma (Fig. 2.3.2.8.39). The cysts tend to enlarge as the disease progresses. They are initially round, with some subsequently coalescing. In most patients, the parenchyma between the cysts remains normal.

However, cases have been described with patchy ground-glass opacities, accentuated interstitial markings between cysts, and—rarely—signs of architectural distortion.

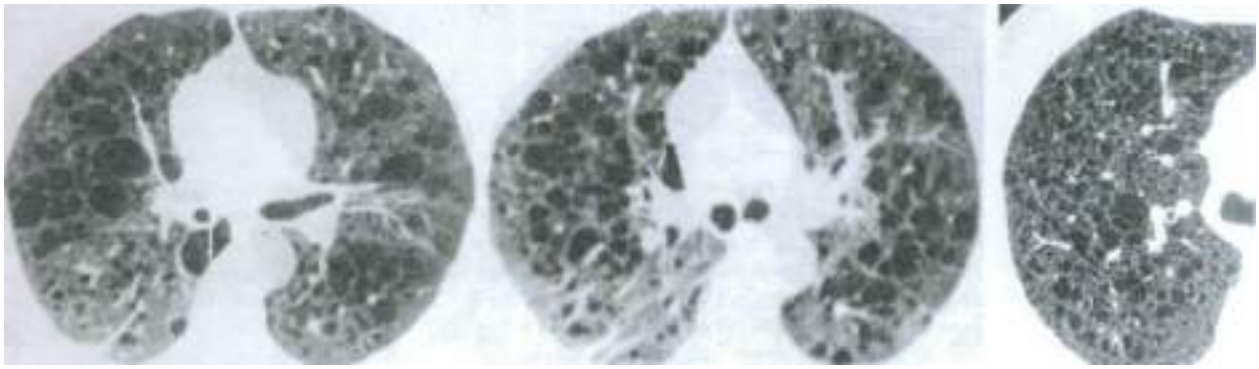

Figure 2.3.2.8.39. Variants of lymphangioleiomyomatosis. Multiple uniform thin-walled air-filled cysts within the lung parenchyma (a).

Complete transformation of the lung parenchymal architecture with relatively homogeneous cysts evenly distributed throughout the lungs (b).

The cysts are diffusely distributed throughout the lungs, with equal involvement of both upper and lower lobes; no regions are spared. Cyst wall thickness ranges from barely perceptible to 4 mm. Only a small number of nodules are rarely detected.

Chylothorax occurs in 60% of cases, and spontaneous pneumothorax in 40%. Mediastinal lymphadenopathy is frequently present (50% of patients). Without treatment, cystic transformation of the lung parenchyma progresses over several years and is accompanied by relatively mild fibrosis. A normal CT scan does not exclude LAM.

Thus, the presence of multiple thin-walled round or complex “geographic” cystic spaces throughout both lungs in young women is pathognomonic for this disease. However, lung biopsy is recommended to confirm the diagnosis.

Pulmonary alveolar proteinosis (PAP) is a diffuse lung disease of unknown etiology, characterized by accumulation of protein-lipid material within the alveoli. In rare cases, a link is established with inhalation of silica dust, use of certain medications, or immunologic disorders. PAP is very uncommon and most often develops in

individuals aged 30–50 years. In addition to a characteristic CT pattern, diagnosis is based on typical findings in bronchoalveolar lavage fluid.
CT demonstrates bilateral ground-glass infiltrative changes combined with uniform interlobular septal thickening. Ground-glass regions often show a characteristic geographic distribution with sharp demarcation between affected and healthy lung tissue (“crazy paving”). Interlobular septal thickening is observed only within the ground-glass regions and morphologically corresponds to moderately expressed edema or fibrosis. The “crazy-paving” pattern is characteristic of PAP and occurs in 100% of cases, greatly facilitating accurate diagnosis (Figs. 2.3.2.8.40–42).

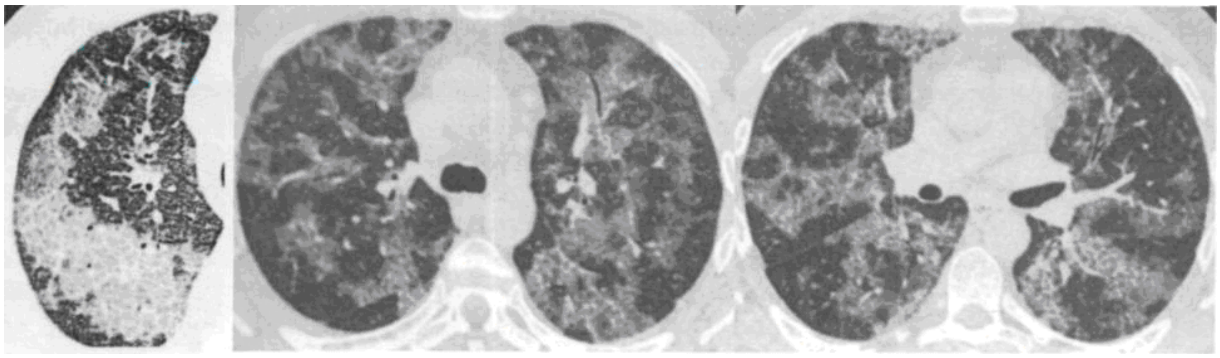

Figure 2.3.2.8.40. Pulmonary alveolar proteinosis. Acute form: ground-glass opacities superimposed on uniform thickening of the intralobular septa (“crazy-paving”) with a geographic distribution and sharply defined margins.

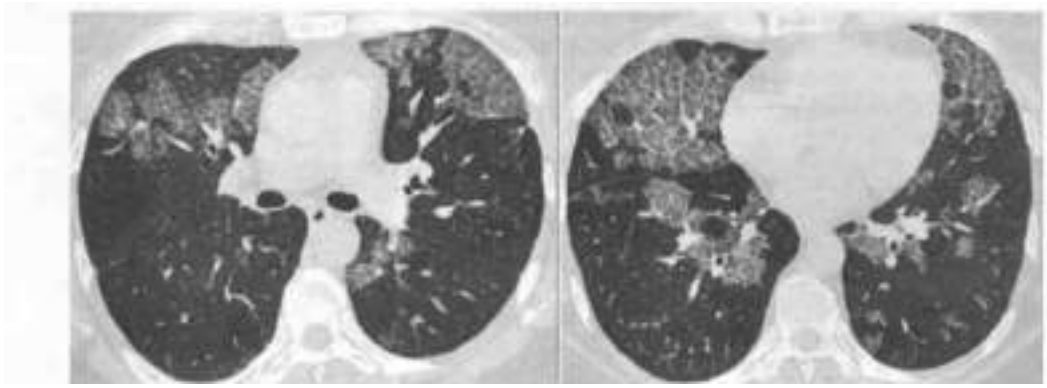

Figure 2.3.2.8.41. Pulmonary alveolar proteinosis. Increased lung parenchymal attenuation with areas of heterogeneous alveolar and interstitial infiltration (the “crazy-paving” pattern).

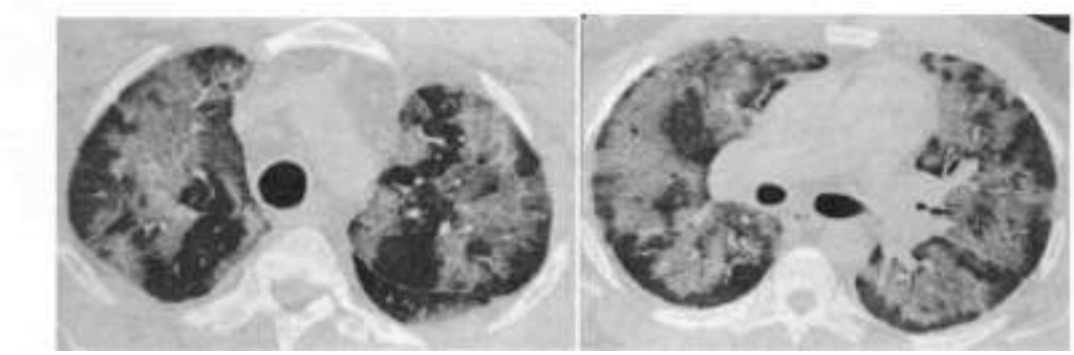

Figure 2.3.2.8.42. Pulmonary alveolar proteinosis. Marked increase in lung parenchymal attenuation with extensive areas of heterogeneous alveolar and interstitial infiltration (the “crazy-paving” pattern).

It should be remembered that the “crazy-paving” pattern may also occur in other conditions (interstitial pneumonias – 30–60%, bacterial pneumonia – 6%, tuberculosis – 1%, mycoplasma pneumonia – 6%, Pneumocystis pneumonia – 7%, chronic eosinophilic pneumonia – 8%).

Pulmonary edema.

On CT, interstitial edema manifests as uniformly thickened interlobular septa, bronchial walls (“cuffing”), and bronchovascular bundles (Figs. 2.3.2.8.43–44). A fine intralobular reticular pattern may also be present. Subpleural lines arise due to obstruction of lymphatic drainage caused by interstitial edema. In mild cases, ill-defined centrilobular nodules are visible, reflecting prominent centrilobular arteries and thickened perivascular interstitium.

Alveolar edema appears as focal, patchy, or diffuse increased attenuation of the lung parenchyma, ranging from ground-glass opacities to complete alveolar airlessness. Lung attenuation is often diffusely increased (the “dark bronchus” sign). Subpleural regions may be less affected. Vessels become enlarged and can be traced to the subpleural space.

All transitional forms between stages may occur, with various combinations of septal line thickening and patchy ground-glass opacification. Pleural effusion may also be present.

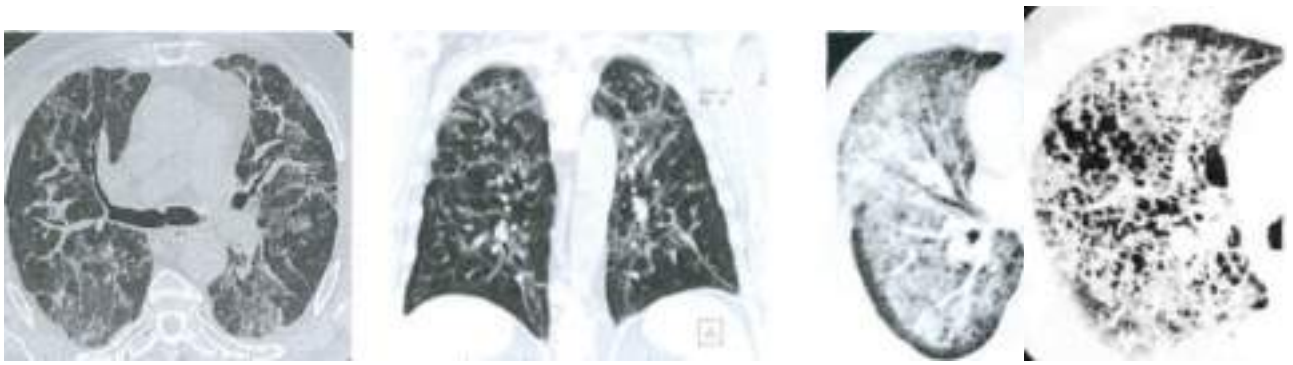

a **b** **c** **d**

Figure 2.3.2.8.43. Pulmonary edema.
Interstitial edema with well-defined interlobular septa and an anterior–posterior gradient of parenchymal attenuation (a). Thickened interlobular septa with smooth margins and alveolar filling with exudate (frontal plane) (b). Parenchymal edema with patchy centrilobular ground-glass opacities (c). Atypical manifestations in coexisting pulmonary emphysema, presenting as a reticular pattern with ground-glass attenuation (d).

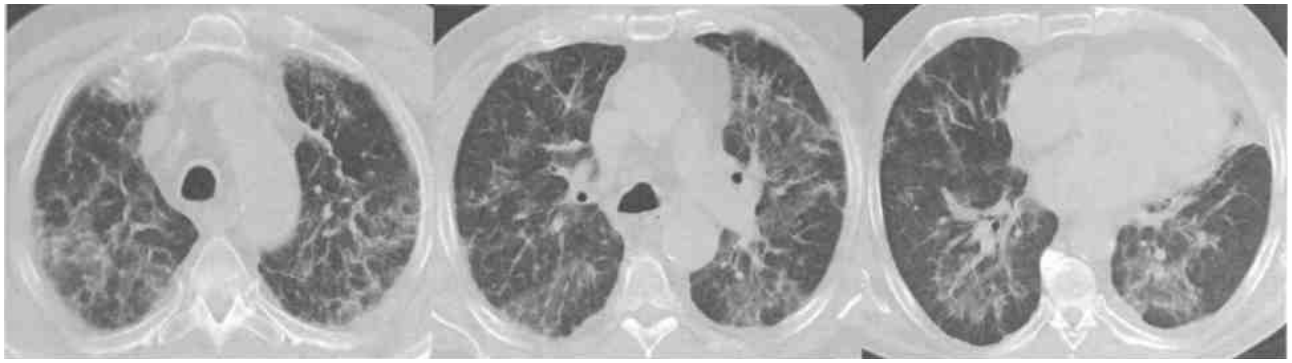

Figure 2.3.2.8.44a. Pulmonary edema in a patient with stage III cardiovascular insufficiency. Interstitial edema with thickened interlobular septa, focal and patchy ground-glass parenchymal opacities, and an anterior–posterior gradient of parenchymal attenuation.

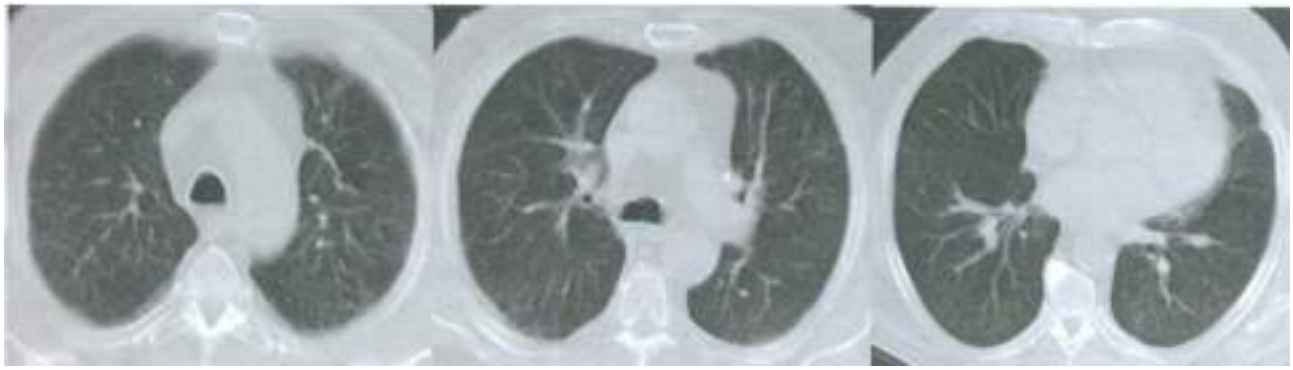

Figure 2.3.2.8.44b. The same patient after three months of treatment. Areas of increased lung parenchymal attenuation have resolved; well-defined thickened interlobular septa remain.

2.3.2.9. Other Types of Disseminations.

Disseminated tuberculosis must often be differentiated from pulmonary conditions that do not belong to the group of disseminative lung diseases. The most common of these is widespread bronchiectasis. On standard radiography, multiple bronchiectases may produce a combination of interstitial and focal abnormalities that mimic disseminated tuberculosis. CT allows reliable differentiation between parenchymal and bronchial abnormalities, assessment of disease extent, and evaluation of the morphological type of bronchiectasis.

Bronchiectasis represents a localized dilatation of the bronchial tree. These changes may be focal or widespread, and in some cases only minimally expressed. Currently, bronchiectasis is most frequently observed in patients with cystic fibrosis, mucociliary dysfunction, and immunodeficiency disorders. Reversible bronchiectases may occur following pneumonia and can completely regress within 4–6 months.

One diagnostic criterion for bronchiectasis is an increased internal bronchial diameter relative to the diameter of the corresponding artery. Normally, the artery is slightly larger than the bronchus. However, the bronchus-to-artery ratio varies (0.8–1.4), therefore two additional criteria are used:

• lack of bronchial tapering toward the periphery (the bronchus maintains the same diameter as its parent branch for more than 2 cm), and
• visualization of bronchi within 1 cm of the costal pleura or in the mediastinal pleura.

A bronchus-to-artery diameter ratio may be considered a reliable standalone criterion only if it is at least 1.5. Ratios between 1.0 and 1.5 should be noted in several bronchi or accompanied by other findings (bronchial wall thickening and absence of luminal tapering). The diameters of small bronchi on cross-sectional images must be evaluated carefully, avoiding measurements near bronchial or vascular bifurcations and avoiding overestimation of bronchial width in areas of localized vasoconstriction. On 10-mm slices, normal bronchi are seen only in the

inner third of the lungs, whereas on high-resolution CT they are visible in the inner two-thirds.

Three morphological types of bronchiectasis are distinguished: cylindrical (tubular, spindle-shaped), varicose, and cystic. Depending on the orientation of the bronchi relative to the imaging plane, cylindrical bronchiectases may appear on CT as a **“signet-ring”** configuration on cross-sectional images or as **“tram-track”** lines on longitudinal sections. The “tram-track” sign can often be followed far into the periphery (Fig. 2.3.2.9.1a, c).

The rare varicose form is recognized by noticeable fluctuations in bronchial caliber on longitudinal sections (Fig. 2.3.2.9.1a).

In cystic bronchiectasis, secretions often accumulate with the formation of horizontal fluid levels (Fig. 2.3.2.9.1c, d). Air-filled cystic structures in areas of atelectasis resemble a **cluster of grapes**.

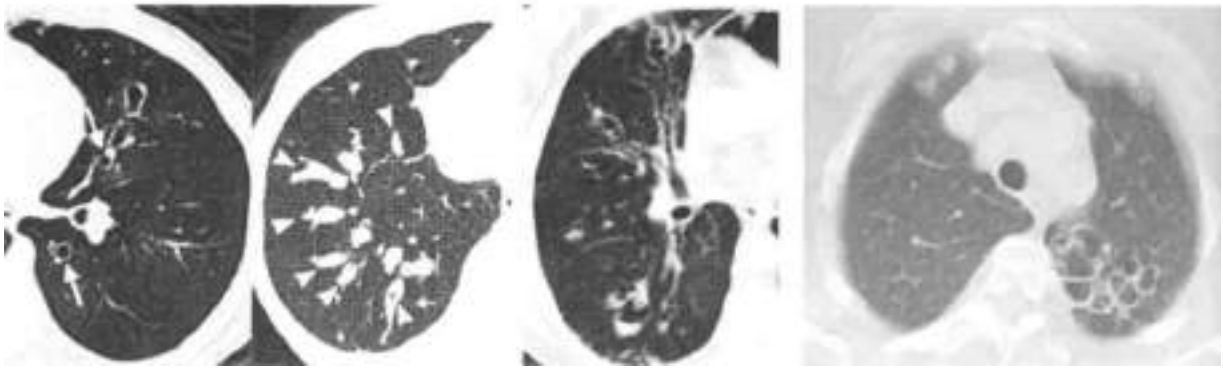

a b c d

Figure 2.3.2.9.1. Bronchiectasis.

Cylindrical bronchiectasis (a). Widespread bronchiectasis with mucus plugging in the right lower lobe; bronchi wider than the accompanying arteries (b). Varicose and cystic bronchiectasis with horizontal fluid levels (c). Cystic bronchiectasis in the left upper lobe without fluid levels (d).

Dilated bronchi filled with secretions appear as V- or Y-shaped soft-tissue–density structures (Fig. 2.3.2.9.2). Bronchial wall thickening indicates a bronchitic component or mucosal edema. Retention cysts frequently accompany bronchiectasis in cystic fibrosis and allergic bronchopulmonary aspergillosis.

Bronchiolectasis is detected only when dilated bronchioles are filled with mucus. CT demonstrates thin branching soft-tissue–density structures in

the subpleural zone (0.5–1 cm from the pleura) with small bulbous endings — the **“tree-in-bud”** pattern (Figs. 2.3.2.9.3–4).
Isolated, localized dilation of a mucus-filled bronchus may be an indirect sign of a small endobronchial tumor.

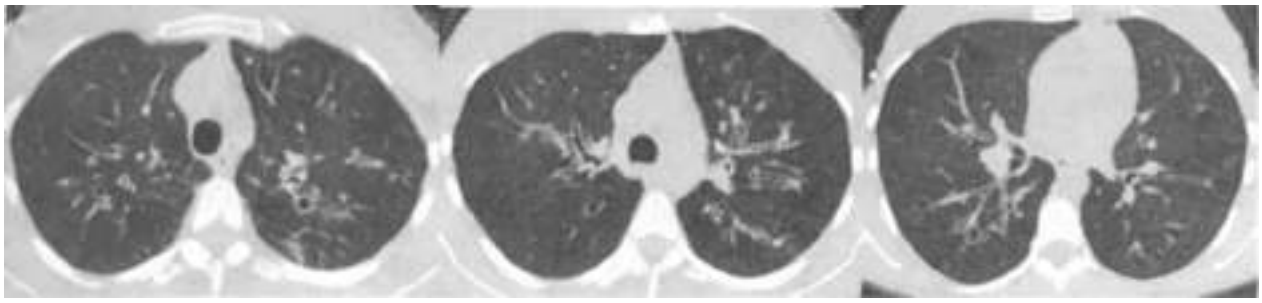

Figure 2.3.2.9.2. Bronchiectasis. Widespread cylindrical and cystic bronchiectasis (signet-ring sign) with mucus plugging and characteristic V- and Y-shaped configurations. Bronchial wall thickening is noted.

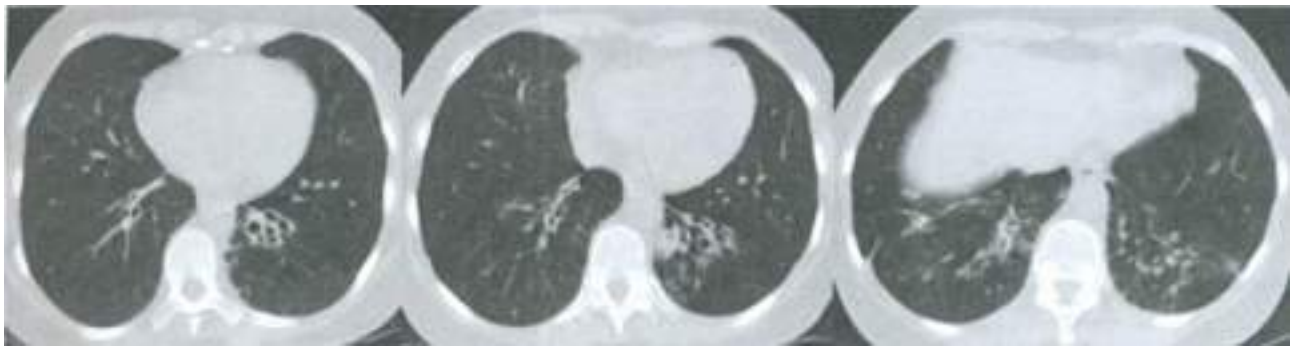

Figure 2.3.2.9.3. Bronchiectasis of the lower lobes. Cylindrical and cystic bronchiectasis with mucus plugging and characteristic V- and Y-shaped configurations; a “tree-in-bud” pattern is seen in the cortical regions. Bronchial wall thickening is present, accompanied by areas of consolidation in the surrounding lung parenchyma.

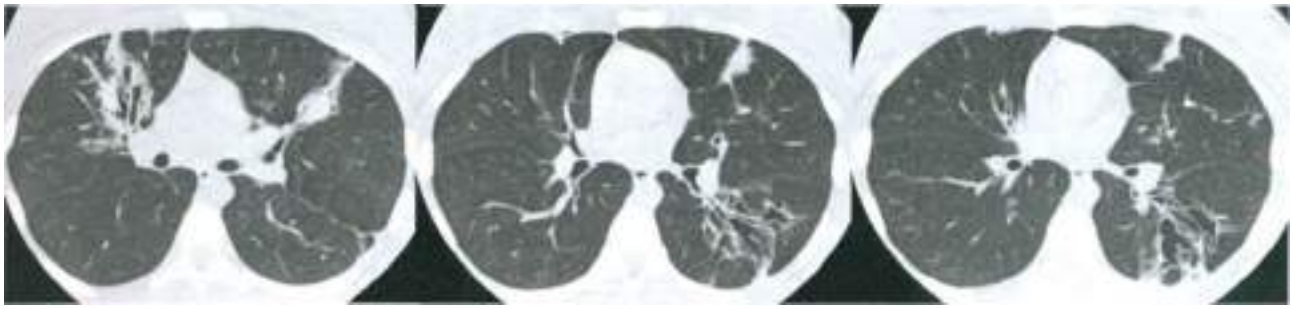

Figure 2.3.2.9.4. Widespread varicose bronchiectasis with thickened, inflamed walls and areas of surrounding parenchymal consolidation in a patient with mucociliary dysfunction.

Pulmonary emphysema. In some cases, pulmonary abnormalities in patients with emphysema may resemble disseminated tuberculosis on routine chest radiography due to multiple areas of hypoventilated lung

parenchyma. Chest CT allows confident differentiation between these conditions (Figs. 2.3.2.9.5–6).

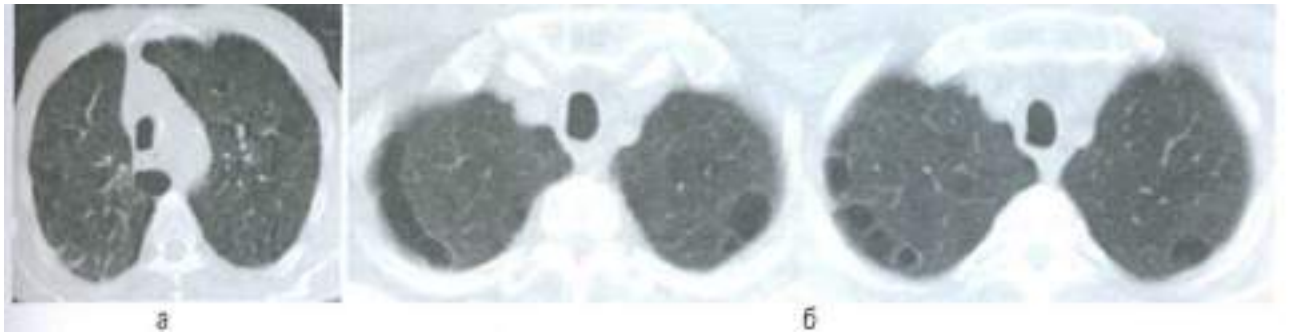

Figure 2.3.2.9.5. Forms of pulmonary emphysema. Centrilobular emphysema with small localized areas of overinflation within intact lobular peripheries (commonly seen in smokers). Associated paraseptal emphysema with a subpleural bulla (a).
Paraseptal emphysema with multiple subpleural bullae (b).

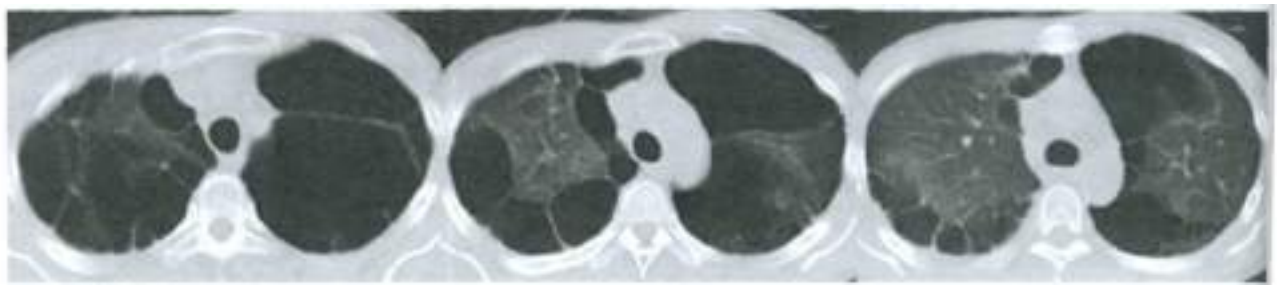

Figure 2.3.2.9.6. Panlobular emphysema with destruction of all intralobular alveoli, reduced vascularization, and progressive loss of lung tissue.

Pulmonary hemorrhage. The CT appearance ranges from small, subtle acinar opacities to diffuse ground-glass attenuation and widespread homogeneous consolidations with an air bronchogram sign (Fig. 2.3.2.9.7). These changes typically resolve within 2–3 days; however, some patchy irregular opacities or linear structures may persist longer.

In chronic recurrent hemorrhage, the amount of hemosiderin in the interstitium increases, leading to irreversible interstitial changes. The severity of parenchymal abnormalities depends on the duration, frequency, and volume of the hemorrhages.

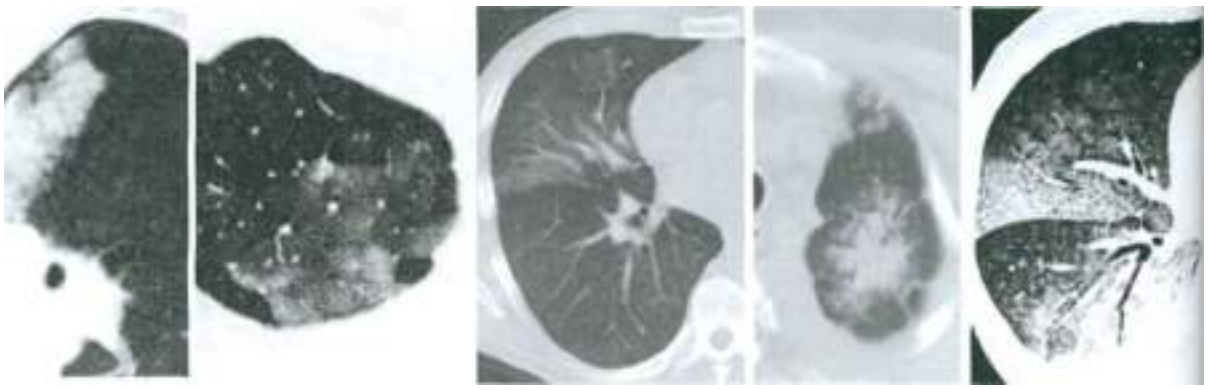

a b c d e

Figure 2.3.2.9.7. Variants of pulmonary hemorrhage. Fresh pulmonary hemorrhage with ill-defined confluent acinar consolidations after trans-pulmonary needle biopsy for central lung cancer (a). Fresh hemorrhage in segments S1+2 of the left lung, presenting as ground-glass opacities corresponding to secondary pulmonary lobules (b). Ground-glass opacities with visible thickened pulmonary vessels; bronchial lumina are not identifiable (c). Intrapulmonary hemorrhage in a patient with Goodpasture's syndrome, presenting as confluent acinar and densely consolidated foci (d). Ground-glass opacities with visible thickened interlobular septa, indicating resorptive processes in hemosiderosis (e).

COPD. The long-term progressive course of chronic obstructive pulmonary disease (COPD) leads to the development of reticular fibrosis of the lung parenchyma (Figs. 2.3.2.9.8–9).

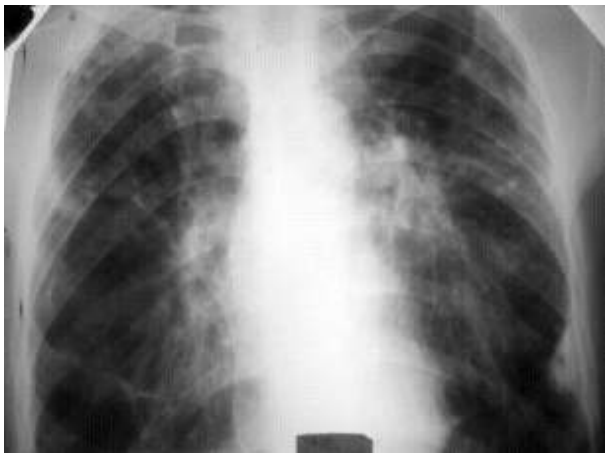

Figure 2.3.2.9.8. COPD with reticular fibrosis of the lung parenchyma.

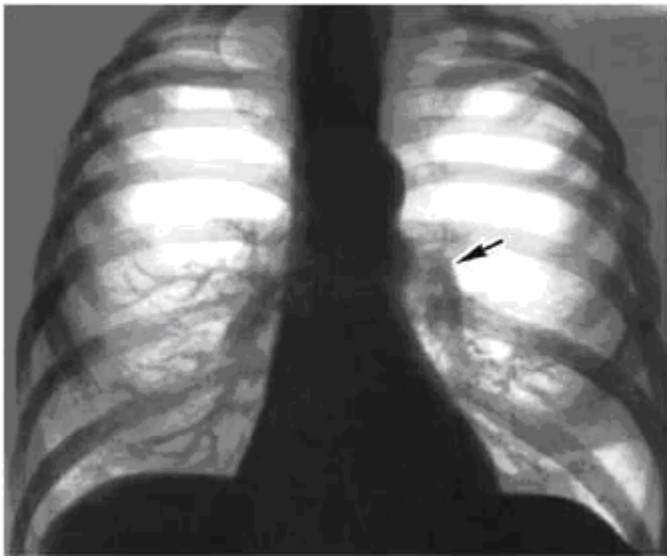

Figure 2.3.2.9.9. Chest radiograph of a patient with pulmonary emphysema and cor pulmonale: the heart is relatively small, the pulmonary artery conus (indicated by the arrow) is prominent, the hila are enlarged due to dilation of major pulmonary arterial branches, and the peripheral vascular pattern is diminished.

Anamnesis and clinical presentation are crucial for diagnosis. Key features include expiratory dyspnea that partially improves after inhaled cholinolytics and β-adrenergic agonists; dry or productive cough; diffuse cyanosis and acrocyanosis; barrel-shaped chest; apical lung hyperinflation; widened intercostal spaces; clubbing (“drumstick” fingers); a hyperresonant percussion note; prolonged expiratory phase on auscultation compared to inspiration; scattered dry wheezes (sibilant and sonorous); and on cardiac auscultation, an accentuated second heart sound over the pulmonary artery. The underlying pathomorphology is a combination of emphysema, reduced cardiac blood filling, and pulmonary hypertension due to peribronchial sclerosis.

Characteristic radiographic findings include coarse reticular remodeling and increased lung markings, predominant involvement of the medial lung zones, bronchial wall thickening, dilation of large and narrowing of small branches of the pulmonary artery, emphysema, low and flattened diaphragmatic domes, relatively small cardiac silhouette, and right ventricular hypertrophy (chronic cor pulmonale). Pulmonary function testing reveals an obstructive pattern of respiratory insufficiency that is irreversible or only minimally reversible after inhaled β-agonists (FEV_1 increase <15%). Diagnosis is supported by bronchoscopy with mucosal biopsy demonstrating focal or diffuse endobronchitis, bronchial lumen narrowing, hypercrinia, and dyscrinia. Sputum analysis shows leukocytosis, numerous desquamated epithelial cells, and absence of M. tuberculosis growth.

Cardiogenic pneumosclerosis may produce a reticular or reticulonodular pattern in the lung fields (Fig. 2.3.2.9.10).

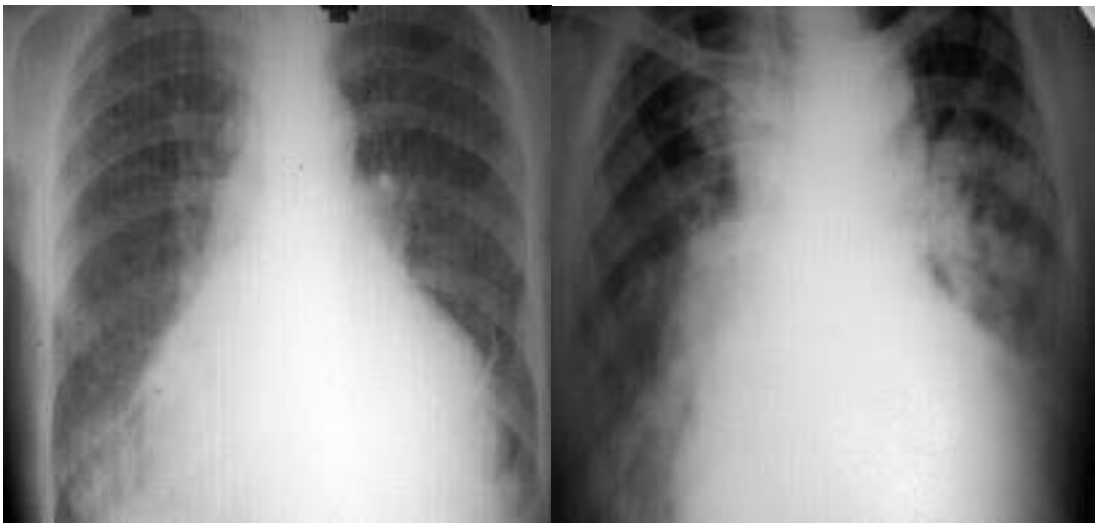

Figure 2.3.2.9.10. Cardiogenic pneumosclerosis with development of a reticular or reticulonodular pattern in the lung fields.

It is most commonly caused by pulmonary hypertension in the small circulation due to decompensated congenital or acquired heart defects: stenosis of the left atrioventricular orifice, rheumatic mitral valve insufficiency, relative mitral insufficiency in dilated cardiomyopathy, post-infarction cardiosclerosis, etc. Its identification—aside from clinical data—is supported by several radiographic signs: uniform involvement of both lungs; a combination of fine reticular deformation of the lung pattern with radial strands extending from the hila and ribbon-like shadows tapering evenly toward the periphery; and changes in the size and shape of the heart (mitral configuration, cardiomegaly, etc.). The cardiac origin of pneumofibrosis is confirmed by anamnesis and by the presence of a loud second heart sound over the pulmonary artery, abnormalities on phonocardiography and ECG, and echocardiographic evidence of valvular disease.

Idiopathic pulmonary hemosiderosis is a condition characterized by recurrent alveolar hemorrhages and a wave-like relapsing course. Diagnostic criteria include: frequent and prolonged hemoptysis, progressive dyspnea, scattered fine moist crackles, sudden appearance of multiple diffusely distributed focal shadows on chest radiography with rapid spontaneous resolution (over 1–3 weeks) followed by development of interstitial fibrosis, detection of siderophages in sputum, hypochromic

anemia, reduced serum iron, identification of siderophages and interstitial fibrosis in lung biopsy specimens, and negative tuberculin tests (Fig. 2.3.2.9.11).

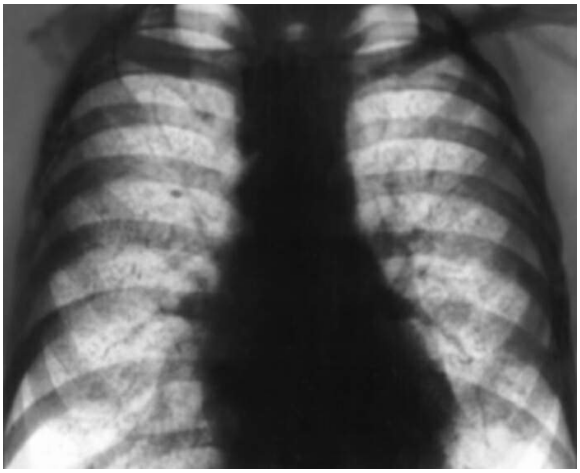
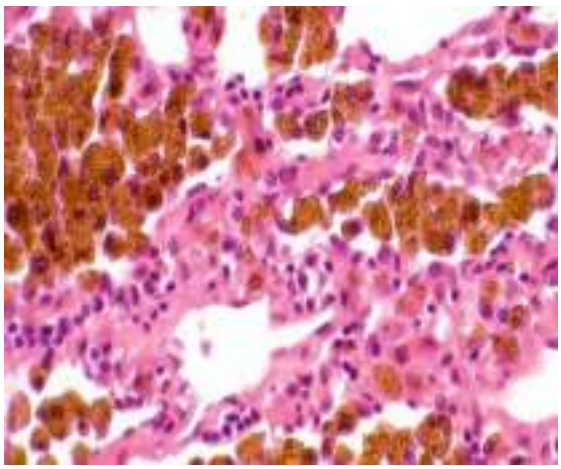

Fig. 2.3.2.9.11. Idiopathic pulmonary hemosiderosis

Fig. 2.3.2.8.44 b. The same patient after three months of treatment. Areas of increased density of the pulmonary parenchyma have disappeared, and thickened, well-defined interlobular septa are visible.

Bronchiectasis. It is often necessary to distinguish disseminated tuberculosis from pathological processes that do not belong to the group of pulmonary disseminations. The most common of these is widespread bronchiectasis. In a routine X-ray examination, multiple bronchiectasis can produce a picture of a combination of interstitial and focal changes that resemble disseminated tuberculosis. The use of CT allows for reliable differentiation between changes in lung tissue and bronchi, assessment of the prevalence of the process, and morphological nature of bronchiectasis.

Bronchiectasis is a local enlargement of the bronchial tree. These changes can be local or widespread and, in some cases, very mild. Currently, they are most commonly observed in patients with cystic fibrosis (mucoviscidosis), mucociliary dysfunction, and immunodeficiency diseases. Reversible bronchiectasis can occur against the background of pneumonia and completely resolve within 4-6 months.

One of the criteria for bronchiectasis is an increase in the internal diameter of the bronchus relative to the diameter of the corresponding artery. Normally, the artery has a slightly larger caliber than the bronchus. However, the ratio of bronchial diameter to arterial diameter

varies (from 0.8 to 1.4), so two additional criteria are used: the absence of bronchial narrowing to the periphery (the bronchus has the same diameter as its parent branch for more than 2 cm) and visualization of the bronchi within 1 cm of the costal pleura or in the mediastinal pleura.
The ratio of bronchial and arterial diameters can be considered a reliable criterion in itself only if it reaches at least 1.5. Values between 1 and 1.5 should be noted in several bronchi or combined with other findings (wall thickening and no narrowing of the lumen to the periphery). It is necessary to carefully evaluate the diameter of the transverse sections of the small bronchi, avoid comparisons near the bifurcation of the bronchi and vessels, and not overestimate the width of the bronchi in areas of local vasoconstriction. On 10 mm thick sections, normal bronchi are visible only in the inner third of the lungs, and on high-resolution CT scans, in the inner 2/3.
There are three morphological types of bronchiectasis: cylindrical (tubular, spindle-shaped), varicose, and cystic. Depending on the relationship of the bronchi to the plane of the section, cylindrical bronchiectasis may have a “seal” configuration in the transverse section or “tram tracks” in the longitudinal sections on CT. The “tram tracks” symptom can often be traced far to the periphery (Fig. 2.3.2.9.1 a, c). The rare varicose form is recognized by noticeable fluctuations in the caliber of the bronchi in the longitudinal section (Fig. 2.3.2.9.1 a). In cystic bronchiectasis, secretions are often retained with the formation of horizontal fluid levels (Fig. 2.3.2.9.1 c, d). Air-filled cystic formations in areas of atelectasis resemble a bunch of grapes.
a) b) c) d)

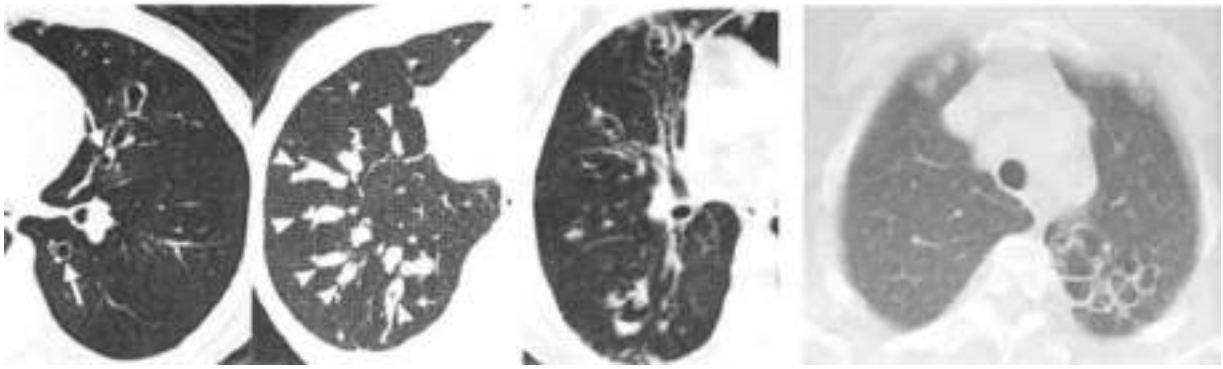

Fig. 2.3.2.9.1. Bronchiectasis. Cylindrical bronchiectasis (a). Diffuse bronchiectasis with mucous plugs in the lower lobe of the right lung. The bronchi are wider than the accompanying arteries (b). Varicose and

cystic bronchiectasis with horizontal fluid levels (c). Cystic bronchiectasis in the upper lobe of the left lung without fluid levels (d).
Enlarged bronchi filled with secretions appear as V- or Y-shaped structures of soft tissue density (Fig. 2.3.2.9.2). Thickening of the bronchial walls indicates a bronchitic component or mucosal edema. Retention cysts are particularly common in bronchiectasis associated with cystic fibrosis and allergic bronchopulmonary aspergillosis.
Bronchioloectasis is only detected when the dilated bronchioles are filled with mucus. CT shows thin branched structures of soft tissue density in the subpleural zone (0.5-1 cm from the pleura) with small bulbous endings – “tree in bud” (Fig. 2.3.2.9.3-4).
Isolated limited enlargement of a mucus-filled bronchus may be an indirect symptom of a small endobronchial tumor.

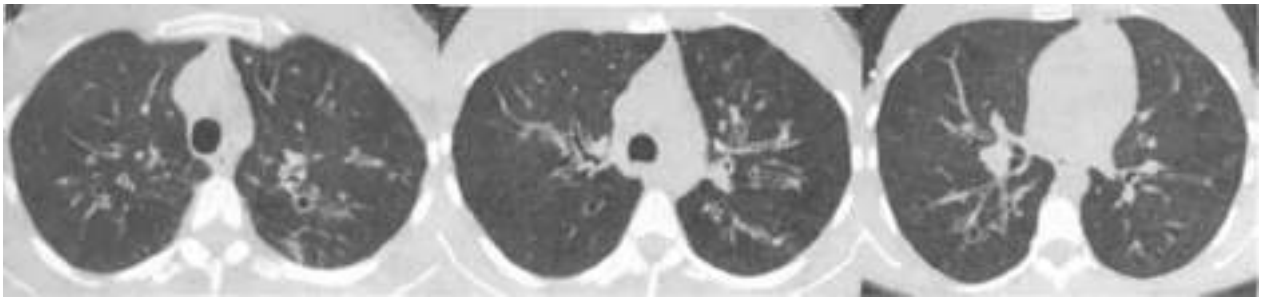

Fig. 2.3.2.9.2. Bronchiectasis. Widespread cylindrical and cystic bronchiectasis (seal symptom) with mucus plugs and typical V- and Y-shaped figures. Thickening of the bronchial walls is noted.

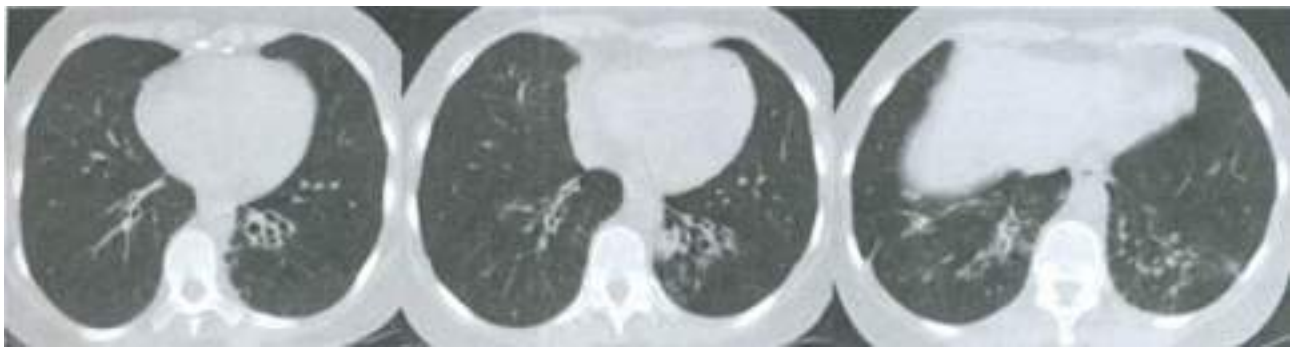

Fig. 2.3.2.9.3. Bronchiectasis of the lower lobes of the lungs. Cylindrical and cystic bronchiectasis with mucus plugs, typical V- and Y-shaped figures, the “tree in bud” symptom is determined in the cortical sections. Thickening of the bronchial walls with areas of consolidation of the surrounding lung tissue is noted.

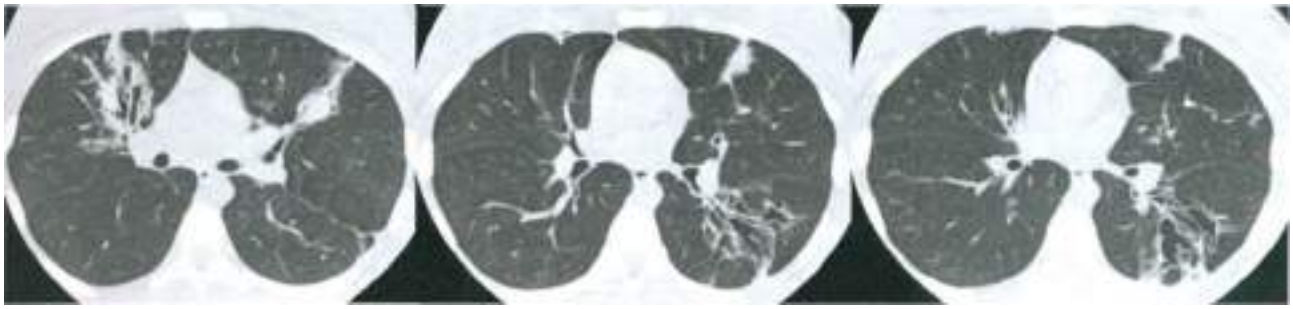

Fig. 2.3.2.9.4. Diffuse varicose bronchiectasis with infiltrated walls and areas of consolidation of the surrounding tissue in a patient with mucociliary dysfunction.

Pulmonary emphysema. Sometimes pathological changes in the lungs of patients with emphysema during routine X-ray examination may resemble disseminated tuberculosis due to multiple areas of pulmonary tissue hypoventilation. CT of the chest allows these diseases to be reliably distinguished (Fig. 2.3.2.9.5-6).

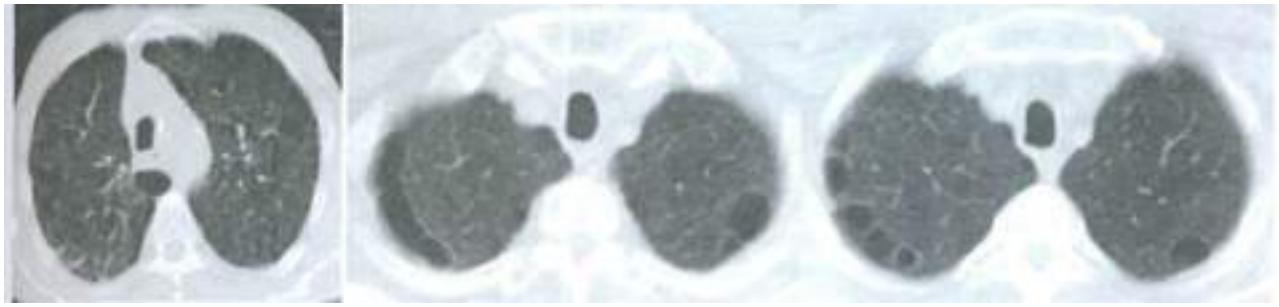

Fig. 2.3.2.9.5. Forms of pulmonary emphysema. Centrilobular emphysema with small limited areas of swelling within the intact periphery of the lobules (often seen in smokers). There is concomitant paraseptal emphysema with subpleural bullae (a). Paraseptal emphysema with multiple subpleural bullae (b).

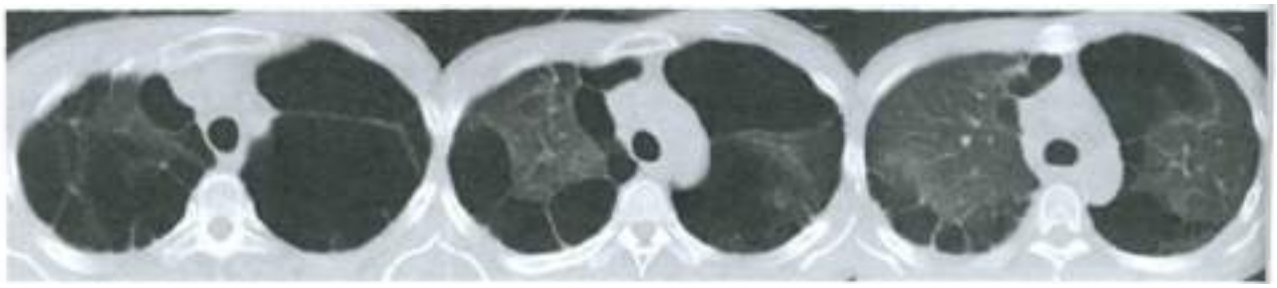

Fig. 2.3.2.9.6. Panlobular form of pulmonary emphysema with destruction of all intralobular alveoli, depleted vascularization, and progressive tissue loss.

Pulmonary hemorrhage. The CT picture varies from small, indistinct acinar consolidations to diffuse “ground glass” consolidations and widespread homogeneous consolidations with the symptom of air

bronchography (Fig. 2.3.2.9.7). Such changes disappear after 2-3 days, but some uneven spotting or linear formations may persist for a longer time.

In chronic recurrent hemorrhages, the amount of hemosiderin in the interstitium increases, and irreversible interstitial changes join. The severity of parenchymal changes depends on the age and sequence of hemorrhage and the amount of blood spilled.

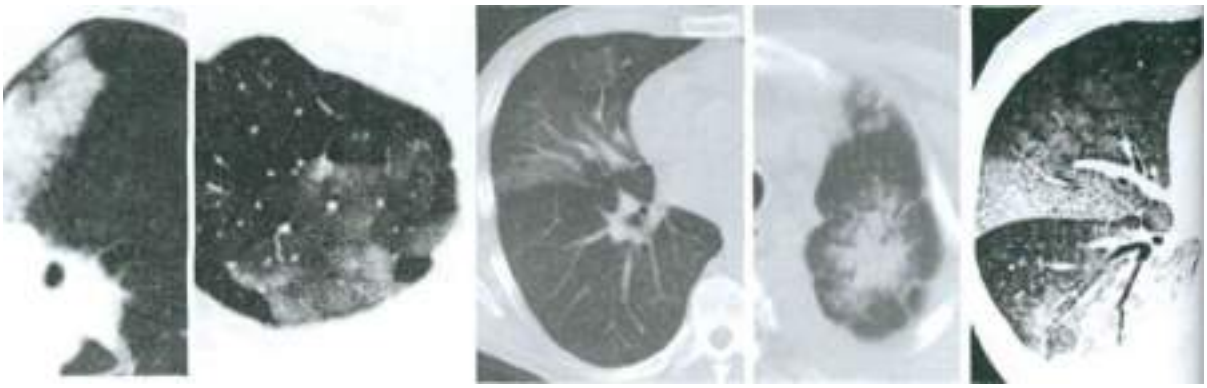

a b c d e

Fig. 2.3.2.9.7. Variants of pulmonary hemorrhages. Fresh pulmonary hemorrhage with indistinct confluent acinar foci of consolidation after transpulmonary needle biopsy for central lung cancer (a). Fresh hemorrhage in S1+2 of the left lung manifests as areas of “ground glass” opacity corresponding to secondary pulmonary lobules (b). “Ground glass” opacity against a background of thickened pulmonary vessels, bronchial lumens are not visible (c). Intrapulmonary hemorrhage in a patient with Goodpasture's syndrome manifests as confluent acinar and densely consolidated foci (d). Frosted glass opacities against a background of thickened interlobular septa, indicating resorptive processes in hemosiderosis (e).

COPD. The long-term progressive course of chronic obstructive pulmonary disease (COPD) leads to the formation of reticular fibrosis of the lung tissue (Fig. 2.3.2.9.8-9).

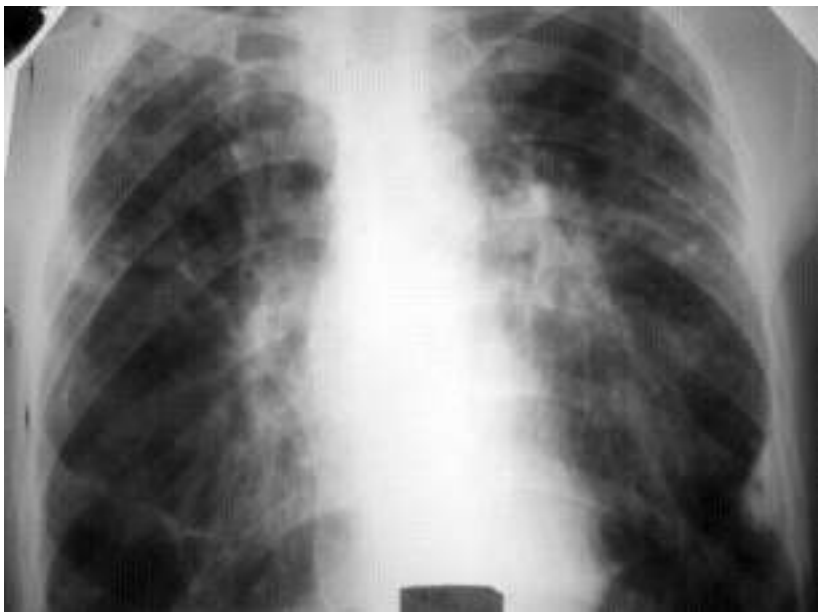

Fig. 2.3.2.9.8. COPD, reticular fibrosis of the lung tissue.

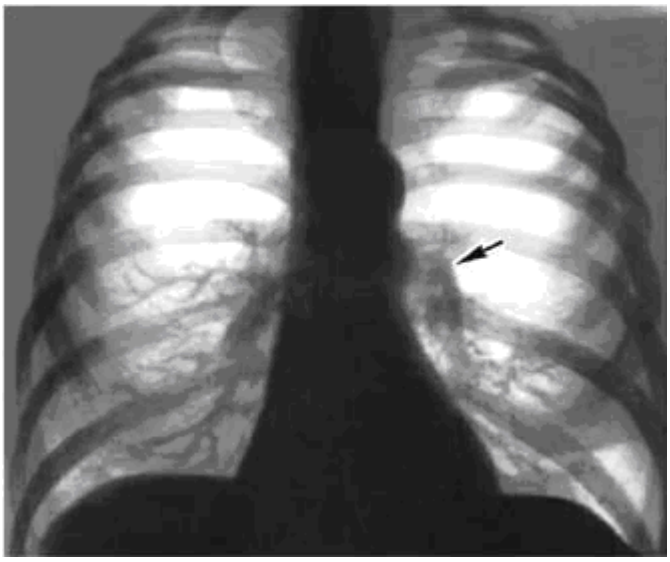

Fig. 2.3.2.9.9. X-ray of the chest cavity of a patient with pulmonary emphysema and CHD: the heart is relatively small, the pulmonary cone arch (indicated by the arrow) is enlarged, the roots are enlarged due to large branches of the pulmonary arteries, and the peripheral vascular pattern of the lungs is depleted.

Anamnestic data and clinical picture are important for diagnosis (expiratory dyspnea, which slightly decreases after inhalation of anticholinergics and β-adrenomimetics, dry or wet cough, diffuse cyanosis and acrocyanosis, barrel chest, bulging of the lung apices, widening of the intercostal spaces, deformation of the distal phalanges of the fingers in the form of “drumsticks,” boxy percussion tone over the

lungs, auscultation of the lungs: prolongation of the exhalation phase compared to the inhalation phase, scattered dry wheezing and buzzing rales, auscultation of the heart: accent of the II tone over the pulmonary artery), the pathomorphological basis of which is a combination of emphysema, low cardiac output, and pulmonary hypertension due to peribronchial sclerosis. A characteristic feature of radiological changes is large-cell restructuring of the structure and intensification of the pulmonary pattern, predominant damage to the medial sections of the lungs, thickening of the bronchial walls, expansion of large and narrowing of small branches of the pulmonary artery, pulmonary emphysema, low position and flattening of the diaphragmatic dome, relatively small size of the cardiac shadow, and right ventricular hypertrophy (chronic pulmonary heart). FEV1 testing reveals obstructive respiratory failure, which is irreversible or weakly reversible (FEV1 increase less than 15%) after the use of inhaled β-adrenomimetics. The diagnosis is confirmed after bronchoscopy with biopsy of the bronchial mucosa, which indicates focal or diffuse endobronchitis, narrowing of the bronchial lumen, hyperkinesis, and dyskinesis. Sputum analysis reveals leukocytosis, a large amount of desquamated epithelium, and no bacterial culture.

Cardiogenic pneumosclerosis can cause the development of a reticular or reticular-focal pattern in the lung fields (Fig. 2.3.2.9.10).

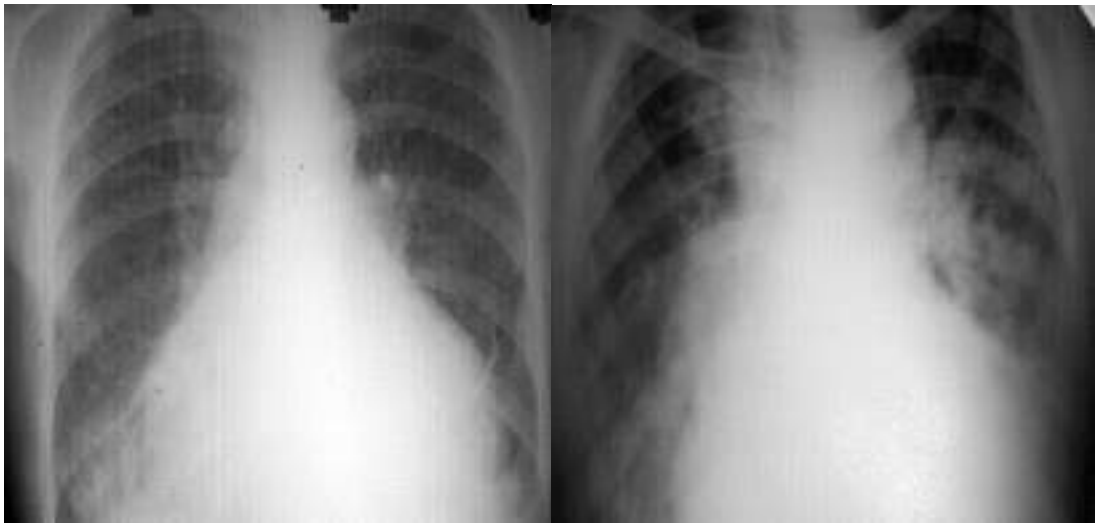

Fig. 2.3.2.9.10. Cardiogenic pneumosclerosis, development of a reticular or reticular-focal pattern in the pulmonary fields.

It is most often caused by hypertension in the pulmonary circulation due to decompensation of congenital or acquired heart defects: stenosis of the left atrioventricular opening, mitral valve insufficiency of rheumatic

origin, relative mitral valve insufficiency in dilated cardiomyopathy; post-infarction cardiosclerosis, etc. In addition to clinical data, a number of radiological symptoms contribute to its identification: uniformity of lung damage, a combination of fine-mesh deformation of the pulmonary pattern with radial strands extending from the roots of the lungs and ribbon-like shadows that narrow uniformly toward the periphery; changes in the size and shape of the heart (mitral configuration, cardiomegaly, etc.). The cardiac origin of pneumofibrosis is confirmed by medical history data, as well as the presence of an accent of the II tone over the pulmonary artery, changes in the phonocardiogram, electrocardiogram, and echocardiography (presence of defects).

Idiopathic pulmonary hemosiderosis is a disease characterized by repeated hemorrhages in the alveoli and a wave-like recurrent course. Diagnostic criteria: frequent and prolonged hemoptysis, progressive dyspnea, scattered moist small-bubble rales, RD OGK: sudden appearance of multiple diffusely located focal shadows with their rapid spontaneous disappearance (within 1-3 weeks) and development of interstitial fibrosis, detection of siderophages in sputum, hypochromic anemia, decreased iron content in the blood, detection of siderophages and interstitial fibrosis in lung tissue biopsies, negative tuberculin tests (Fig. 2.3.2.9.11).

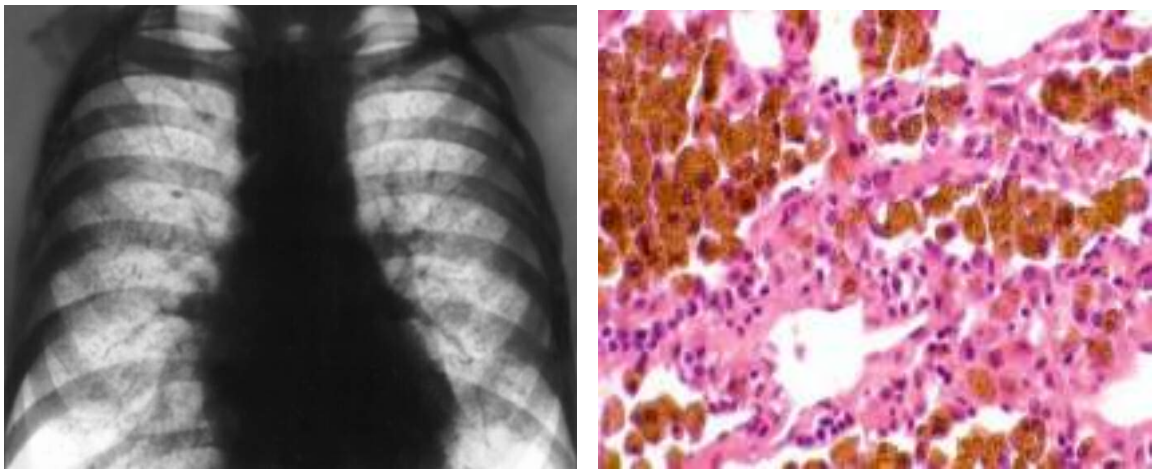

Fig. 2.3.2.9.11. Idiopathic pulmonary hemosiderosis.

2.4 Focal pulmonary tuberculosis

Focal pulmonary tuberculosis is characterized by an asymptomatic course and the presence of small (up to 10 mm in diameter) foci of various origins and ages, predominantly productive in nature, within 1-2 segments in one or both lungs.

The use of CT allows for a detailed assessment of the nature of changes in lung tissue in patients with focal tuberculosis. This is necessary in cases where, during a routine X-ray examination, the presence of foci is questionable or their nature cannot be assessed in detail.

The typical location of foci is the apical and posterior segments of the upper lobe (S1 and S2). Less often, foci are found in the apical segment of the lower lobe (S6). According to CT data, the foci are located deep in the lung tissue, peribronchially, and range in size from 1 to 10 mm. More often, the foci are polymorphic in nature. The most typical is a combination of one or two large foci with a larger number of small and medium ones (Fig. 2.4.1). Large foci usually have a homogeneous structure, and in the center of some of them, the lumen of the bronchus may be visible in cross-section. This picture should not be interpreted as the presence of a cavity of destruction. True cavities in the foci are larger, resulting in the image of the focus being a thin-walled cavity. Such cavities are usually not visible on conventional X-ray tomography and are only detected by high-resolution CT. The contours of the largest foci at this stage of the process are blurred and uneven. The density of the lung tissue in the area of the foci may be slightly increased due to perifocal edema and the presence of multiple small foci.

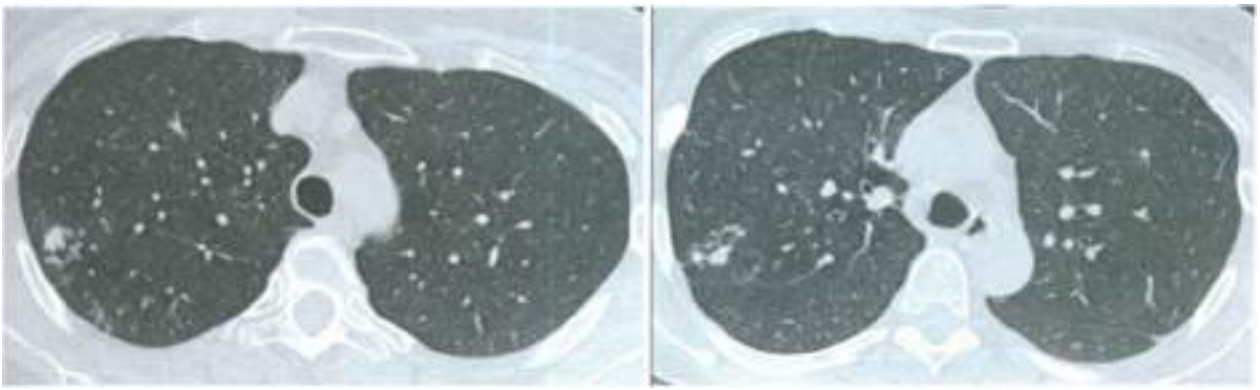

Fig. 2.4.1. Focal tuberculosis. In S2 of the right lung, there are multiple polymorphic foci with blurred contours.

Small foci with a diameter of 1-3 mm are located in the surrounding large foci of lung tissue throughout the segment or part of it. They are localized mainly in the walls of secondary pulmonary lobules and intralobular septa. The development of lymphostasis leads to thickening and densification of these interstitial structures. The walls of the small bronchi in the area of pathological changes are also thickened and visible when using high-resolution CT.

The prolonged course of focal tuberculosis, especially against the background of antibiotic treatment, leads to a significant change in the computed tomography picture (Fig. 2.4.2-4). Along with focal changes in the lung tissue, areas of panlobular and paraseptal emphysema, small emphysematous bullae, as well as linear soft tissue strands directed from the area of pathological changes to the pleura appear.

The volume of the affected segments gradually decreases due to the development of local pneumosclerosis. It is the presence of emphysema in the lung tissue surrounding the foci that allows CT to reliably distinguish early, initial tuberculous changes from long-standing ones.

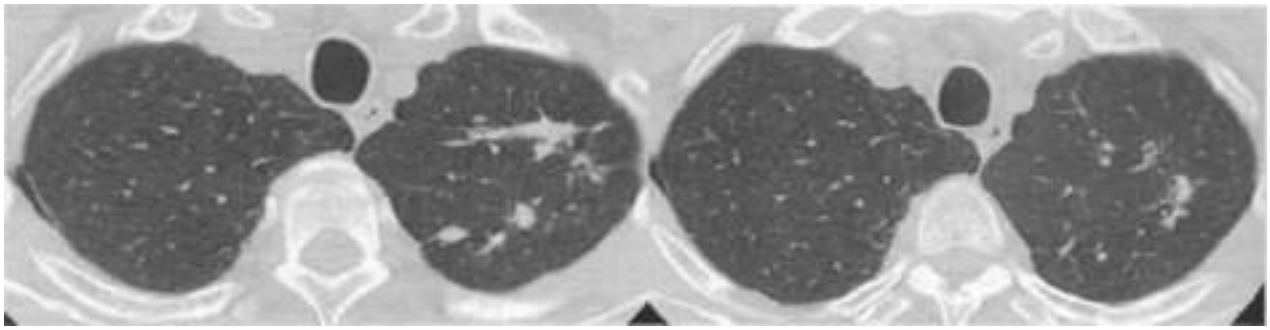

Fig. 2.4.2. Focal tuberculosis. In S1+2 of the left lung, there are multiple polymorphic nodules with uneven, relatively clear contours, with areas of paraseptal emphysema and linear soft tissue strands directed from the area of pathological changes to the pleura.

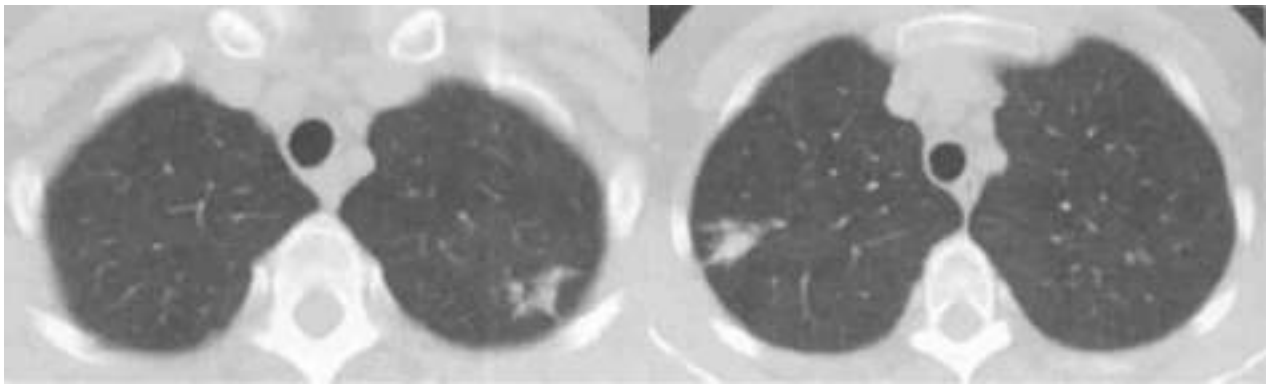

Fig. 2.4.3. Focal tuberculosis of the upper lobes of the lungs. In S1+2 of the left lung, there are polymorphic nodular formations located close to each other against the background of limited fibrosis with linear soft tissue strands directed from the area of pathological changes to the pleura and containing lime inclusions.

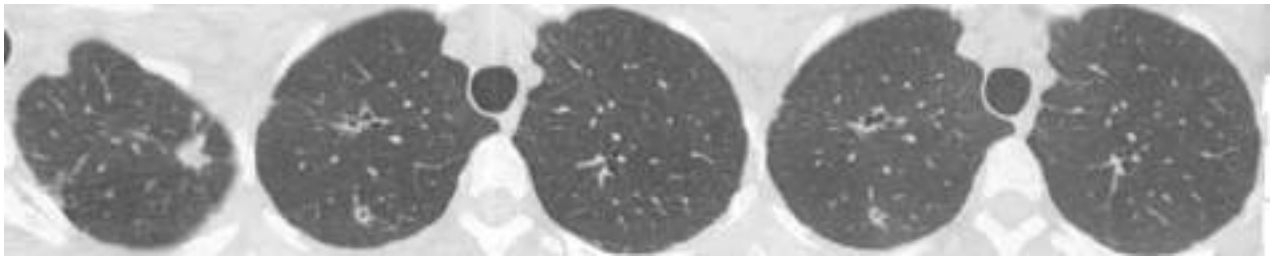

Fig. 2.4.4. Focal tuberculosis of the upper lobes of the lungs, MBT-. S1+2 of the left lung shows confluent focal shadows with blurred contours and linear soft tissue strands directed from the area of pathological changes to the pleura. In S1+2 of the right lung, dilated bronchi with thickened walls (focal bronchiectasis) are visible in the transverse section.

In determining the duration of the tuberculous process, high-resolution CT has significant advantages over conventional X-ray tomography. A decrease in the size of large foci and the disappearance or reduction in the number of small foci during dynamic observation indicates a positive trend in the pathological process (Fig. 2.4.5 a, b).

In most patients, focal tuberculosis results in the formation of small linear scars located deep in the lung tissue. Here, there are also isolated alveolar foci with lime inclusions and local thickening of the costal pleura. Small air cavities caused by emphysema are visible in the lung tissue surrounding the foci. Unlike the initial changes, small interstitial foci in the walls of the lobules are absent at this stage of the disease. These features are clinically important in determining the activity of the tuberculous process (Fig. 2.4.6).

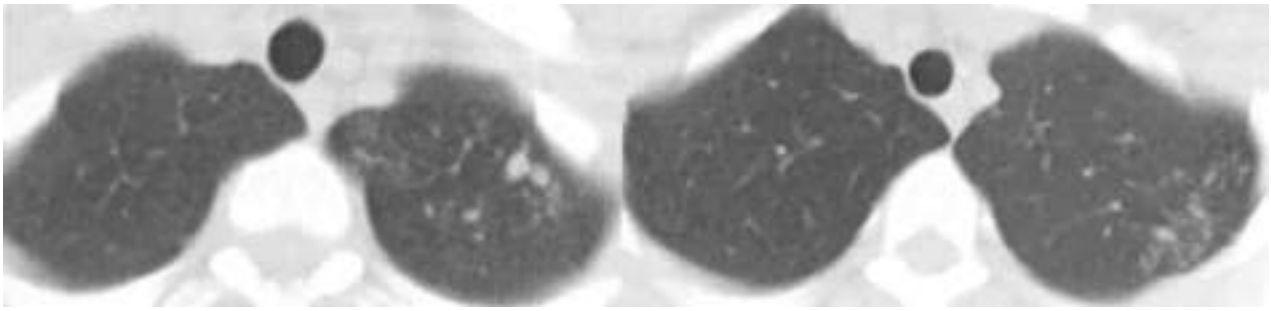

Fig. 2.4.5 a. Focal tuberculosis S1+2 of the left lung, MBT-, before treatment.

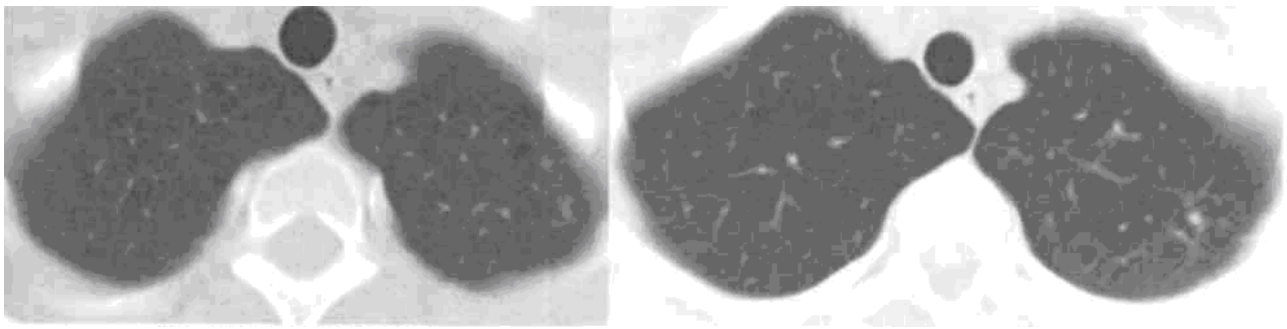

Fig. 2.4.5 b. The same patient after completing the main course of antimycobacterial therapy.

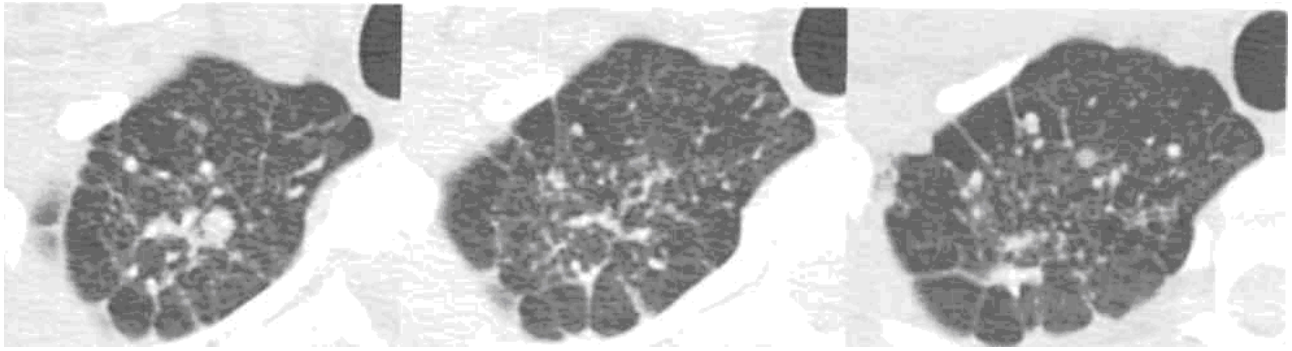

Fig. 2.4.6. Residual changes after cured focal tuberculosis of the upper lobe of the right lung. Multiple foci with calcification against a background of small linear scars and small air cavities caused by emphysema, local thickening of the costal pleura.

With CT angiography, with bolus administration of contrast medium, it can be established that the densitometric indicators of most tuberculous foci do not change (Fig. 2.4.7). In some patients, the contrast medium accumulates in the capsule, creating an edge enhancement effect.

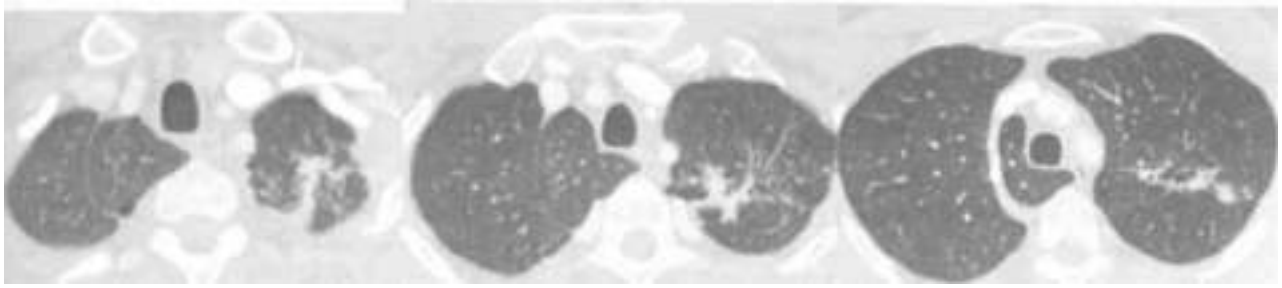

Fig. 2.4.7. Residual changes after cured focal tuberculosis of the upper lobe of the left lung. Multiple polymorphic foci against a background of areas of fibrosis with lime inclusions, local thickening of the costal pleura.

In some cases, after the completion of the main course of antimycobacterial treatment, during dynamic observation, an ambiguous nature of the involution process may be observed, along with resorption, densification, and scarring of the primary changes, new areas of

densification, foci, and, less frequently, tuberculomas appear in the surrounding tissue. Ignorance of these features of the tuberculous process often leads to overdiagnosis of relapses and unjustified repeat courses of treatment. In this case, microbiological diagnostic methods come to the fore.

Differential diagnosis. Focal tuberculosis must first be distinguished from other forms of pulmonary tuberculosis that have a similar radiographic picture.

Infiltrative tuberculosis can manifest itself on radiographic examination mainly as focal changes in the apical regions of the lungs. The presence of perifocal infiltration, especially of an interstitial nature, of the “frosted glass” type, is more accurately determined by high-resolution CT. The presence of perifocal infiltration around the foci allows infiltrative tuberculosis to be reliably distinguished from focal tuberculosis (Fig. 2.4.8).

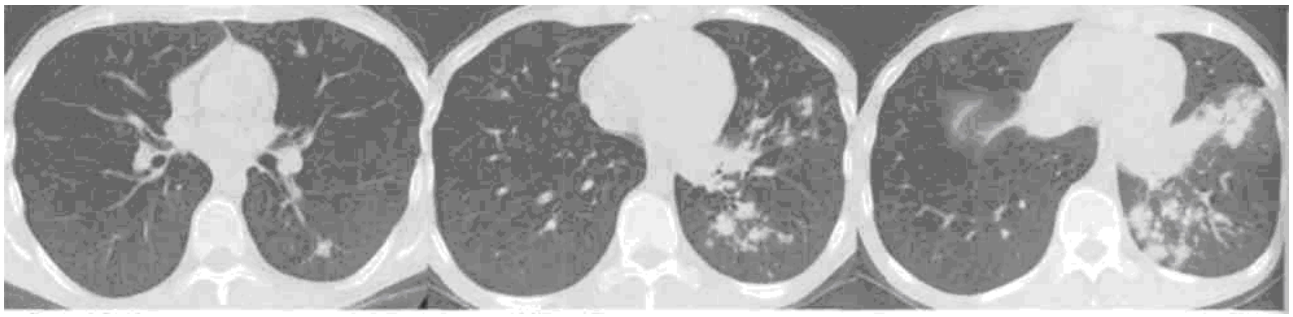

Fig. 2.4.8. Infiltrative pulmonary tuberculosis, MBT+. Polymorphic focal shadows are unevenly distributed in both lungs. In the lower lobe of the left lung, there are groups of foci of varying sizes with pronounced perifocal infiltration.

Tuberculosis of the small bronchi (tuberculous endobronchitis) can lead to the formation of small cysts. They are round, oval, or triangular in shape, with clear, even contours, ranging in size from 5 to 15 mm. On X-ray examination, these changes are very similar to focal tuberculosis. However, axial sections allow for a more accurate determination of the connection of each such formation with a small bronchus (Fig. 2.4.9). The walls of the bronchi are thickened, their lumen is slightly enlarged and ends in a retention cyst. The lumen of the bronchi in cysts is never determined. A common finding is droplet calcifications in the area where the draining bronchus ends.

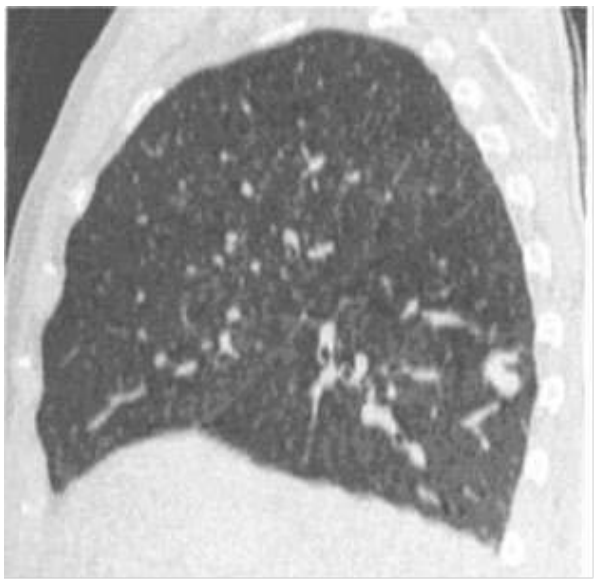

Fig. 2.4.9. Tuberculosis of the small bronchi.

Bronchopneumonia has to be differentiated from focal tuberculosis relatively rarely, usually when pneumonic infiltration is localized in the apical segments of the lungs. Unlike focal tuberculosis, lobular and acinar pneumonic foci have blurred contours and are surrounded by a wide zone of perifocal infiltration. Such changes on axial sections are more reminiscent of infiltrative tuberculosis. However, in pneumonia, there are no small cavities of destruction in the foci, and in the zone of infiltration, there are no interstitial foci characteristic of tuberculosis in the walls of the lobules and in the interlobular pleura. Such foci arise as a result of lymphogenous spread of tuberculosis infection (Fig. 2.4.10-12).

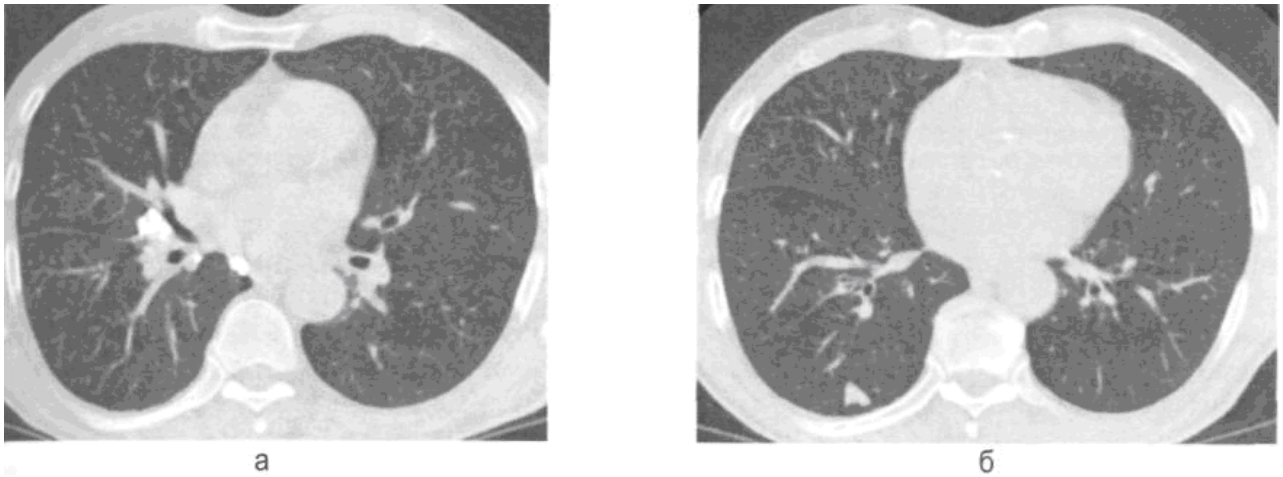

Fig. 2.4.10. Retention cyst S9 of the right lung. Calcified intrathoracic lymph nodes (a). Pathological formation 2.1 x 1.1 cm, triangular in shape (b). On CT reconstruction in the lateral projection, the formation has a typical V-shaped form.

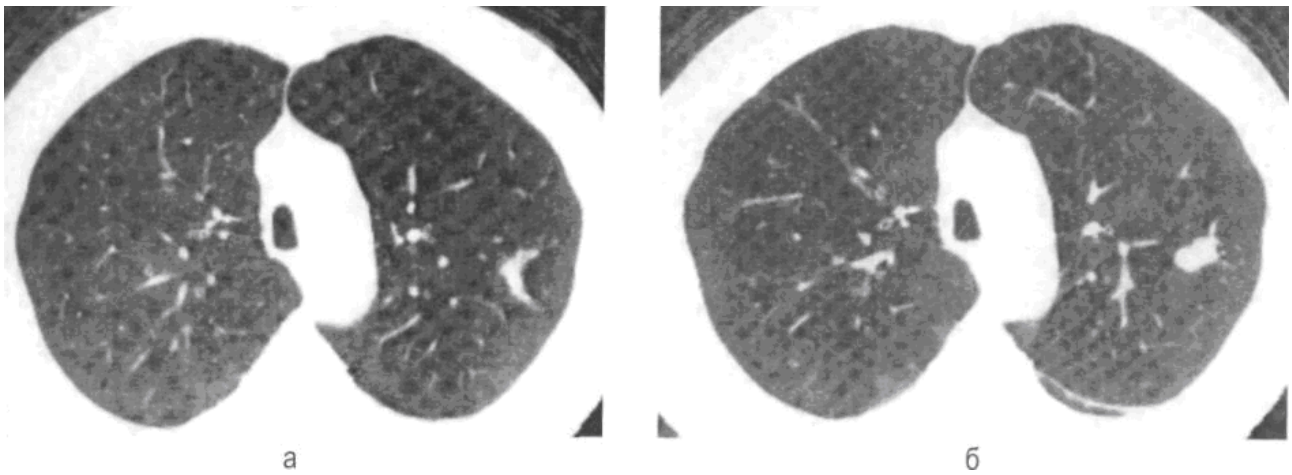

Fig. 2.4.11. Retention cyst of the upper lobe of the left lung. Typical dichotomous branching of dilated small bronchi (a). On one of the sections (b), the cyst has an almost regular oval shape.

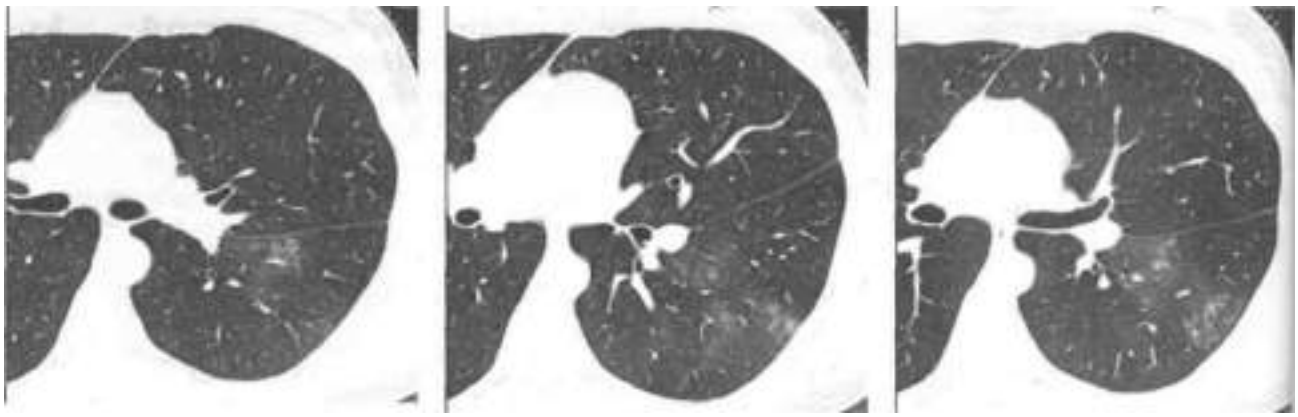

Fig. 2.4.12. Focal pneumonia, high-resolution CT. In S2 of the left lung, there are multiple monomorphic foci with blurred contours and a zone of peripheral infiltration.

Disseminated processes in the lungs in the early stages of their development may resemble focal tuberculosis. In sarcoidosis (Fig. 2.4.13), histiocytosis, and pneumoconiosis, focal changes often occur in the posterior segments of the upper lobes. The use of CT allows one to reliably distinguish between local changes in the apical region in focal tuberculosis and disseminated changes affecting a significant part of both lungs in non-tuberculous diseases. The informative value of CT, and especially high-resolution CT, in resolving this issue is significantly higher than that of conventional X-ray tomography.

Occasionally, pathological changes in the chest organs in patients with suspected focal tuberculosis may be due to rib development abnormalities, bullous emphysema, or arteriovenous malformation (aneurysm) (Fig. 2.4.14-15).

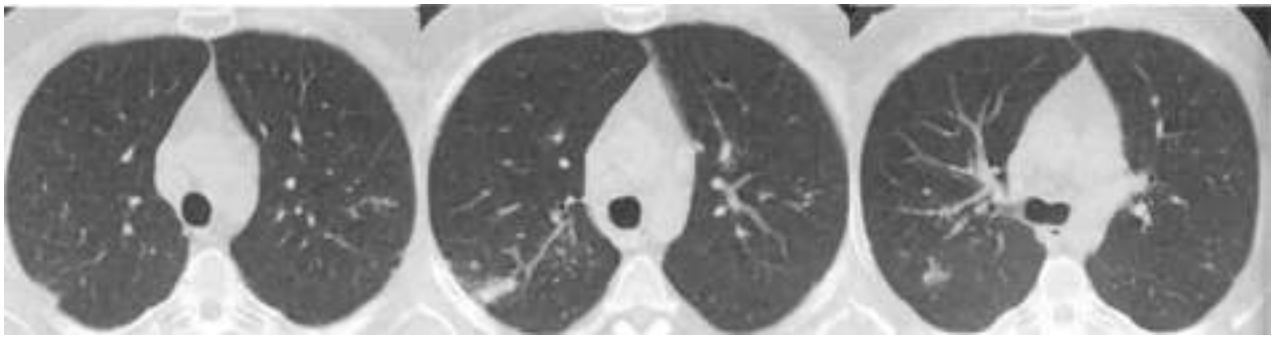

Fig. 2.4.13. Focal changes in the upper lobes of the lungs in sarcoidosis. CT allows the detection of multiple enlarged mediastinal lymph nodes that are not visible on X-ray tomography.

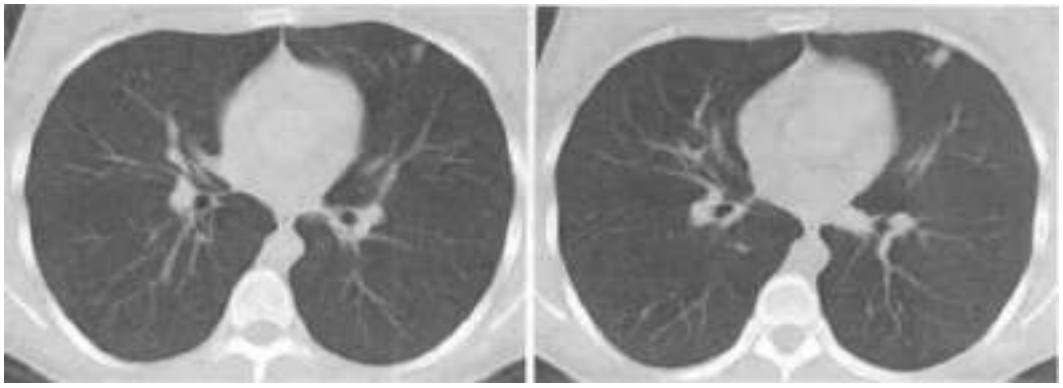

Fig. 2.4.14. Arteriovenous malformation. In $S_{(4)\ of}$the left lung, there is a round focal shadow with a diameter of10 мм , which has a feeding artery and a draining vein.

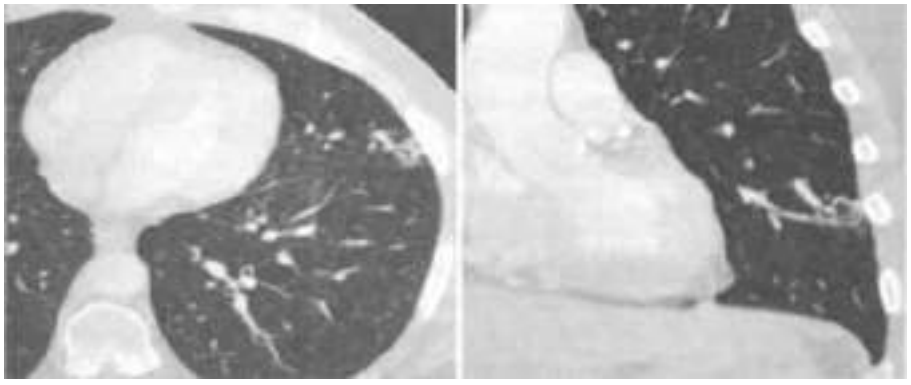

Fig. 2.4.15. Arteriovenous malformation. In $S_5$of the left lung, there is a group of small confluent focal shadows with a feeding artery and a draining vein.

Sometimes focal tuberculosis has to be differentiated from the so-called accessory lobe of the unpaired vein**,** which occurs in approximately 1% of the population. In such cases, the arch of the unpaired vein is displaced laterally and higher than normal. On a conventional X-ray, a large focal shadow is visualised above the projection of the right upper lobe bronchus (more often in the form of a drop), and on a CT scan of the lungs at the level of Th_{II}– an accessory lobe of the unpaired vein,

which is limited by a pleural duplication and an unpaired vein (Fig. 2.4.16).

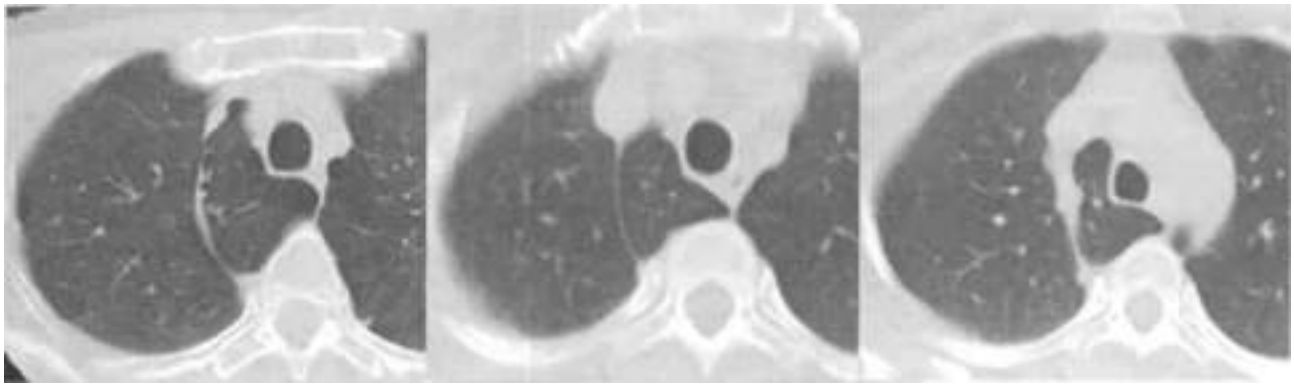

Fig. 2.4.16. CT variants of the accessory lobe of the unpaired vein.

2.5. Differential diagnosis of pulmonary infiltrates. Diagnosis of infiltrative pulmonary tuberculosis

The term "pulmonary infiltrate" (PI) refers to a group of diseases that differ in aetiology, pathogenesis and morphological changes, the main feature of which is the presence of an inflammatory process in the lungs. Infiltrative-pneumonic foci are dominant in the clinical picture of pulmonary pathology. Direct signs of LI:

1) Localised increase in bronchophony. 2) Presence of bronchial breathing over the lung parenchyma. 3) X-ray examination data; the radiological term "infiltrate" implies that the pathologically altered area of the lung (usually in the form of darkening) has blurred contours and smoothly transitions into normal lung tissue. 4) Local accumulation of radioisotope during gallium-67 scanning. 5) Detection of thrombus outlines and infarct pneumonia during angiopulmonography.

The presence of LI in a patient should be suspected when the following symptoms and syndromes are detected: 1) respiratory failure; 2) chronic hypoxia (with prolonged hypoxia, dystrophic changes in the fingers, such as "drumsticks," and nails, such as "watch glass," are detected); 3) bronchopulmonary syndrome (shortness of breath, cough with phlegm, changes in percussion sound and the presence of respiratory noises in the lungs); 4) signs of pulmonary hypertension; 5) right ventricular heart failure, especially chronic; 6) hyperthermia; 7) lymphadenopathy; particular attention should be paid to enlargement of the supra- and subclavian lymph nodes, which may indicate tuberculosis or cancer of the apex.

At the first stage, a diagnostic search plan should be drawn up, which includes diseases in which pulmonary infiltrate is the leading syndrome:

1. Inflammatory lung diseases.
1.1. Infectious inflammatory lung diseases.
1.1.1. Specific.
1. Infiltrative pulmonary tuberculosis.
2. Syphilis (syphiloma) of the lungs.
1.1.2. Non-specific.
1.1.2.1. Pneumonia.
1.1.2.1.1. Community-acquired pneumonia.
1. Typical pneumonia.
2. Atypical pneumonia.
2. Nosocomial (hospital-acquired) pneumonia.
3. Pneumonia in patients with immunodeficiency conditions.
4. Aspiration pneumonia.
1.2.2. Pulmonary suppuration.
1. Lung abscess.
2. Lung gangrene.
3. Infarction pneumonia.
4. Paraneoplastic pneumonia.
1.2. Inflammatory diseases of the lungs of a non-infectious nature.
1.2.1. Pulmonary eosinophilia.
1.2.1.1. Primary (idiopathic, cryptogenic) eosinophilia.
1.2.1.1.1. Eosinophilic bronchial asthma.
1.2.1.1.2. Leffler's pneumonia.
1.2.1.2. Secondary (symptomatic) pulmonary eosinophilia.
1.2.1.2.1. Parasitic infections.
1.2.1.2.2. Fungal infection.
3. Drug-induced disease.
4. Paraneoplastic eosinophilia (carcinomas, haemoblastoses).
5. Pulmonary eosinophilia with systemic manifestations (Leffler's syndrome).
6. Lung damage in rheumatism and other diffuse connective tissue diseases.
1.2.1.3. Dressler's syndrome.

2. Pulmonary infiltrates of a tumour nature. 3 primary localisation in the lungs; intra-bronchial; extra-bronchial; secondary (metastatic).

In inflammatory lung diseases, patients in most cases show a combination of pulmonary infiltrate, bronchopulmonary, hyperthermia, mesenchymal cell proliferation syndromes (increased ESR, changes in white blood cell count, appearance of C-reactive protein, increased fibrinogen content, etc.). In addition, attention should be paid to manifestations of systemic inflammation – arthralgia and arthritis, skin rashes, hepatosplenomegaly, and polylymphadenopathy. At a certain stage of the disease, they are detected simultaneously with pulmonary infiltrates, although it should be remembered that they may alternate. An important feature of inflammatory infiltrates is their regression – complete resorption or scar formation. After establishing the inflammatory genesis of pulmonary infiltrates, it is determined whether they are infectious or non-infectious.

In order to determine the infectious nature of infiltrative processes in the lungs, the following should be taken into account:

1). Epidemiological history. Lung damage during epidemics of influenza and other acute respiratory viral infections, contact with tuberculosis patients or previous tuberculosis infection, simultaneous or prolonged (7-10 days) appearance of patients in organised groups (kindergarten, school, military units, etc.) are highly likely to indicate an infectious process.

2). In addition to direct contact with infected patients, it is also necessary to investigate the possibility of infection from natural reservoirs – construction and earthworks, living near open freshwater reservoirs, occupational activities, and above all – contact with animals. Factors contributing to the suppression of local immunity; pathways and systemic immunological tolerance – poor living conditions, hypothermia, long business trips with frequent time zone changes, prolonged use of glucocorticosteroids, cytostatics, young age of patients, aspiration of vomit.

3). The dynamics of symptom onset. Acute onset, rapid increase in clinical symptoms from the lungs, especially in combination with intoxication, quite convincingly indicate the infectious nature of the pulmonary infiltrate.

4). The presence of other foci of infection and risk factors for its penetration into the lungs – chronic sinusitis, trophic ulcers, infectious endocarditis, thrombophlebitis, injuries with disruption of integrity and contamination of the wound. Next, we will discuss the most common LI using the example of differential diagnosis with pulmonary tuberculosis.

In the group of tuberculous diseases, infiltrates and their variants dominate, while in the group of non-specific diseases, various types of pneumonia, both croupous and focal, of various aetiologies are predominant. Therefore, differential diagnosis between them is of great importance.

In cases of tuberculous infiltration, patients usually report an acute onset of the disease, but it is often possible to identify previously existing general symptoms – weakness, cough, night sweats and unstable temperature – which the patient did not consider particularly significant. It is important to know that tuberculous lobular pneumonia, like lobar pneumonia, almost always develops on the basis of previously existing tuberculous foci. The localisation of the process must be taken into account in controversial cases (Fig. 2.5.1-2).

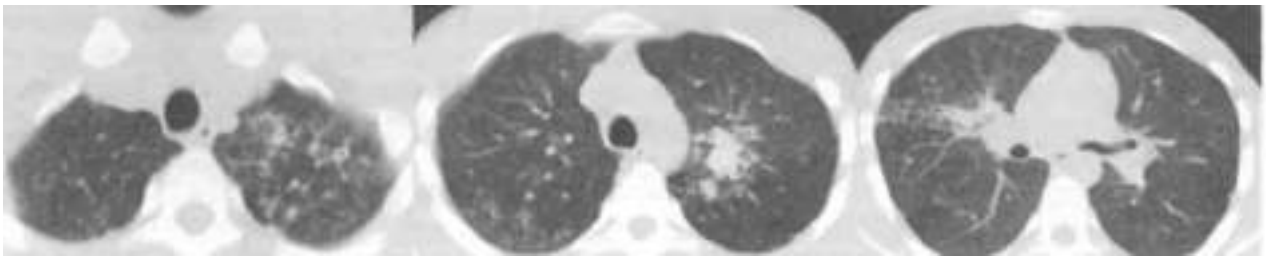

Fig. 2.5.1. Infiltrative pulmonary tuberculosis, MBT+. Multiple polymorphic foci with blurred contours against a background of interstitial changes, mainly in the upper lobes of the lungs.

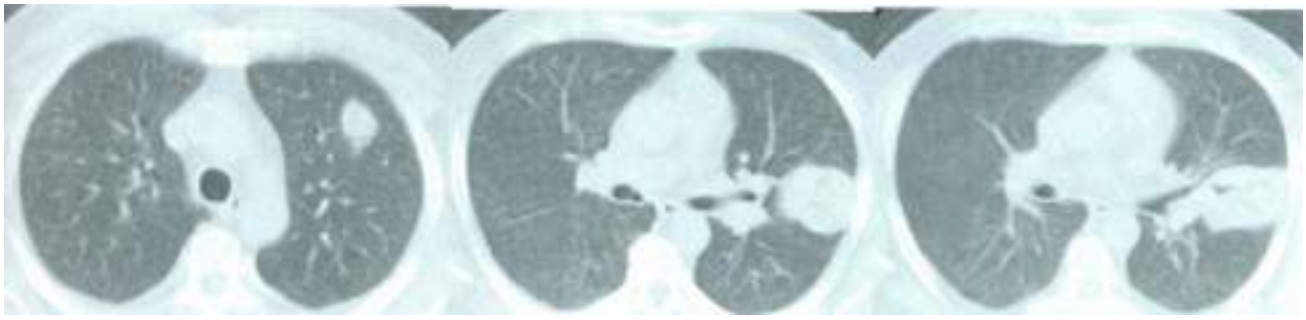

Fig. 2.5.2. Infiltrative tuberculosis of the upper lobe of the left lung (round infiltrate), MBT-, Hist+ in a patient with diabetes mellitus. Infiltrates in S_2 and S_3 without clear contours of heterogeneous structure due to light stripes of deformed bronchial lumens.

Tuberculous infiltrates are usually located under the clavicle in the lateral part, in the area of the posterior apical bronchus, leaving the apices free in more than half of cases. In non-tuberculous diseases, the process is most often observed in the lower lobes, and often originates from the root region. Although acute tuberculous processes can affect a significant part of the lung, their area is in most cases smaller than in non-specific pneumonia. Round, oval foci with a clear peripheral border, and even more so compact foci with sharply defined contours, excluding tumours, are in most cases characteristic of tuberculous infiltrates (Fig. 2.5.3-6).

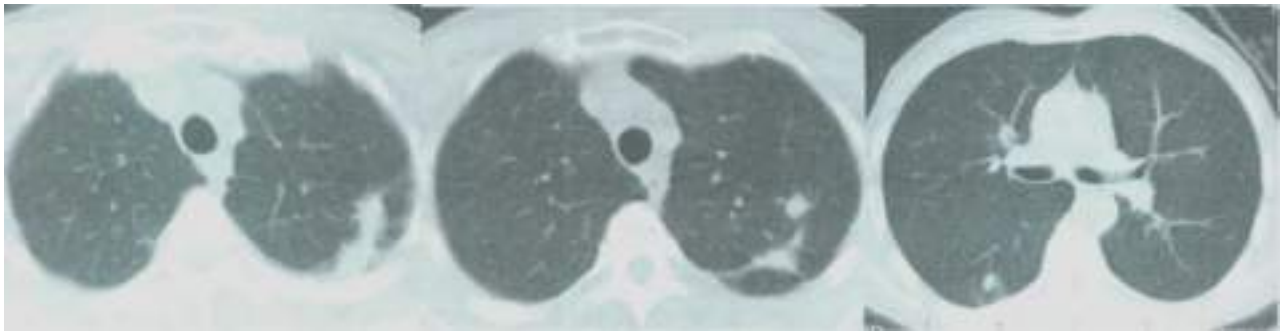

Fig. 2.5.3. Infiltrative tuberculosis S_{1+2} of the left and S_6 of the right lung, MBT-. Bronchopulmonary infiltrates with a characteristic feature – a contour of the interlobar pleura concave towards the densified lung tissue.

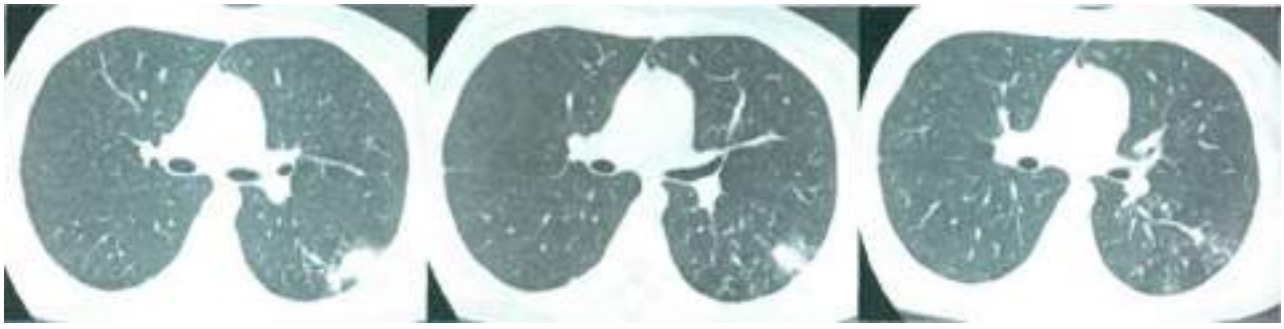

Fig. 2.5.4. Infiltrative tuberculosis $S_{(6)}$ $_{of}$the left lung (bronchopulmonary infiltrate), MBT-. Several large foci merge into a single irregularly shaped infiltrate with blurred contours, with multiple polymorphic foci in the surrounding lung tissue.

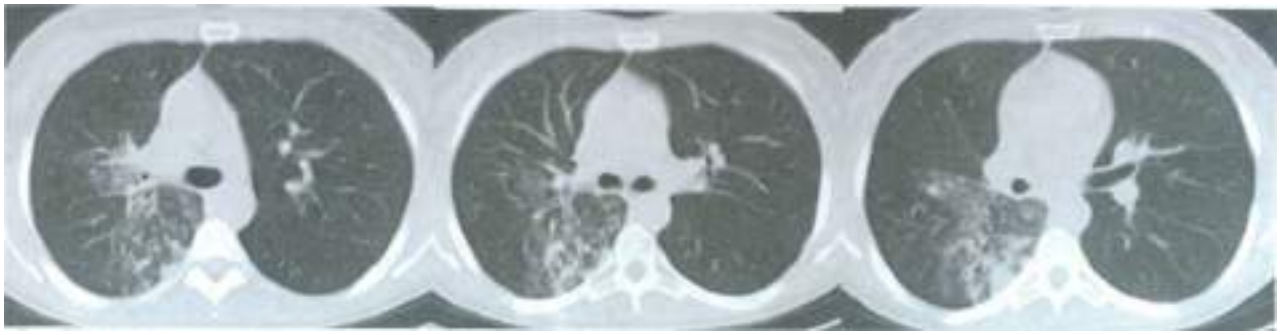

Fig. 2.5.5. Infiltrative tuberculosis of the right lung (cloud-like infiltrate), MBT+. Against the background of heterogeneous infiltration in S_6 of the right lung, thickened walls of subsegmental bronchi and blurred contours of vessels are visible.

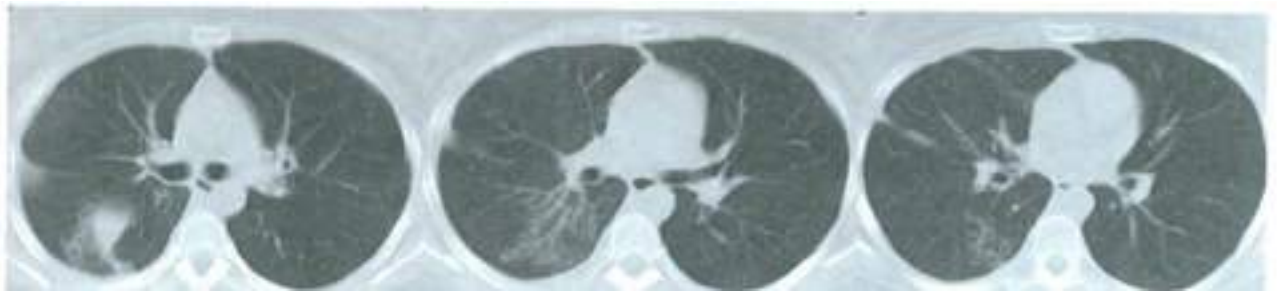

Fig. 2.5.6. Infiltrative tuberculosis of the upper lobe of the right lung (cloud-like infiltrate), MBT+. In S_6 of the right lung, infiltration of the lung tissue is of a non-homogeneous structure, without clear contours. Multiple polymorphic foci in the surrounding lung tissue. The interlobar pleura is thickened and infiltrated.

With tuberculous infiltrates, even with round cloud-like forms, and sometimes with lobitis, auscultatory changes may be completely absent, especially in the early stages of the disease (Fig. 2.5.7-9). No rales are heard, bronchial breathing is weakly expressed; most often it is only weakened. With tuberculous indurating infiltrates, auscultatory phenomena are not sharply expressed, while with nonspecific sclerosis, rales of various calibres are heard over a large area. In children and adolescents with lung damage, so-called mixed breathing can be heard, when inhalation and exhalation belong to different types. Thus, inhalation may be vesicular, and exhalation may be bronchial. This ratio is possible in older children with focal pneumonia, when small foci of inflammation are surrounded by intact lung tissue containing air. A similar ratio can be found in specific pulmonary processes.

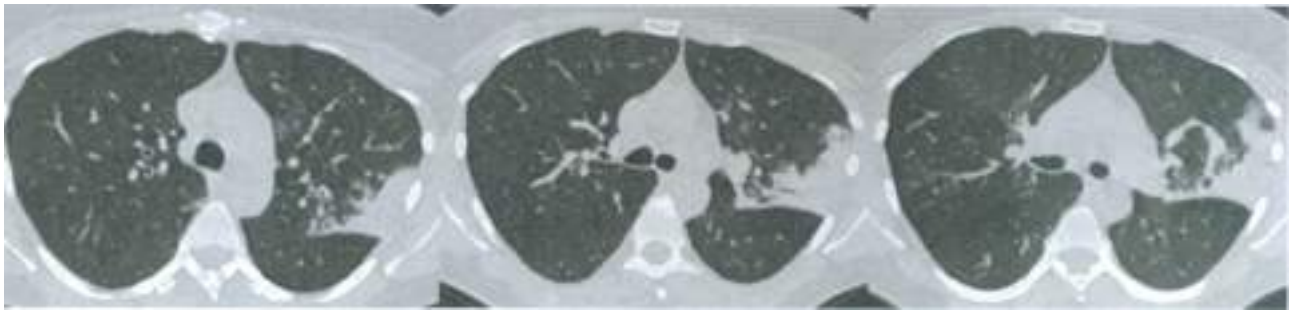

Fig. 2.5.7. Infiltrative tuberculosis of the upper lobes of the lungs (pericarditis), MBT+. The infiltrate in $S_2$of the left lung is triangular in shape, mostly touching the costal and interlobar pleura, the contour of

the interlobar pleura is concave towards the compacted lung tissue, surrounded by multiple polymorphic focal shadows.

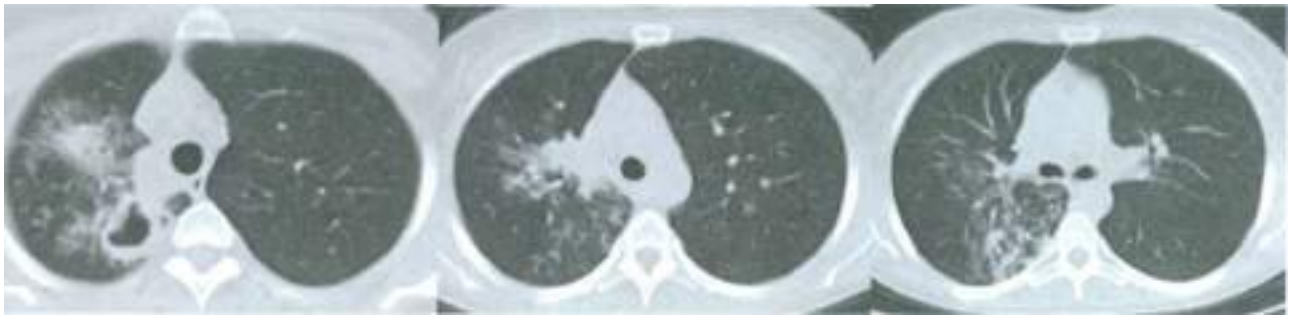

Fig. 2.5.8. Infiltrative tuberculosis of the right lung, MBT+. In S_6 of the right lung, a large cavity of irregular shape with walls of varying thickness and a small amount of fluid is adjacent to the chest wall. Lumina are visible in the area of perifocal infiltration.

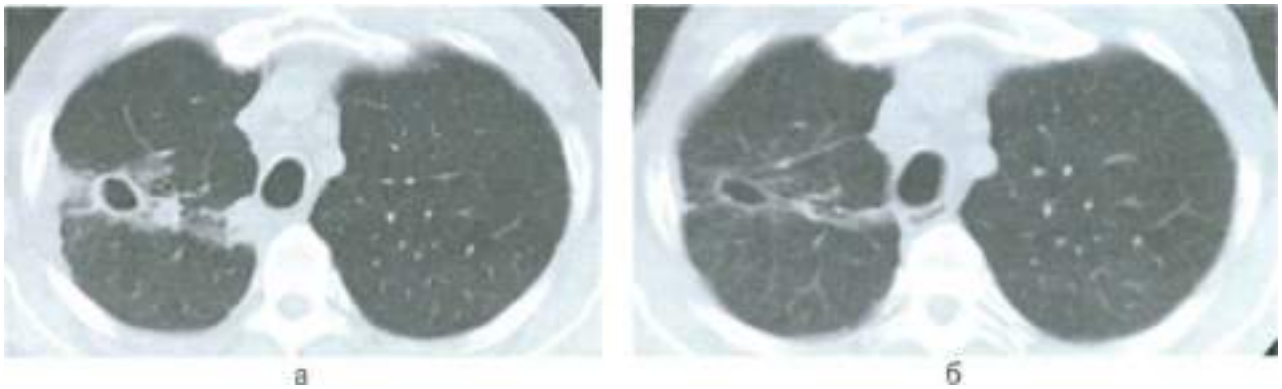

Fig. 2.5.9. Infiltrative tuberculosis $S_{(2)}$ of the right lung, MBT+, before treatment (a). Result after completion of the main course of antimycobacterial therapy. Major final changes – in the area of fibrotic changes, a small slit-like final cavity with thin walls is visible, MBT-.

Cloud-like shadows of irregular shape are most often of non-specific origin. Rounded shadows with more or less clearly defined contours are most often of a tuberculous nature. In fresh infiltrates of a tuberculous nature, there is almost always a drainage pathway leading from the infiltrate to the root. It is considered an integral part of an active infiltrate; in non-specific processes, it is less common and significantly less pronounced. As for fever, leukocytosis, left shift, and accelerated ESR, they are more pronounced in pneumonia. The tuberculin test is positive for tuberculous infiltrates.

In differential diagnosis, Leffler's eosinophilic infiltrate (Fig. 2.5.10-11) can cause certain difficulties.

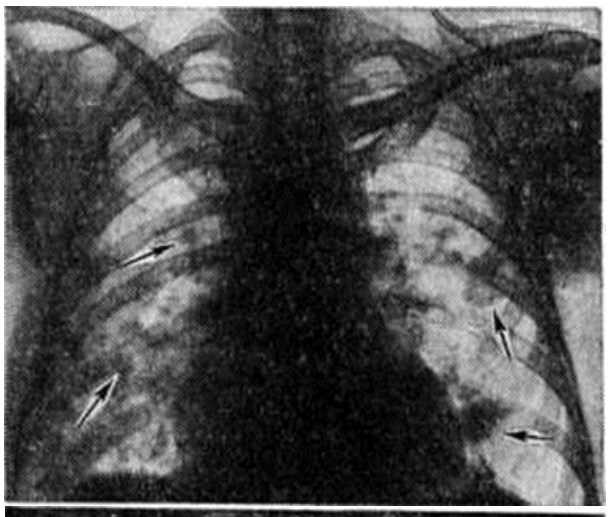

Fig. 2.5.10. Chest X-ray of a patient with Leffler's syndrome: multiple bilateral infiltrates in both lungs (indicated by an arrow).

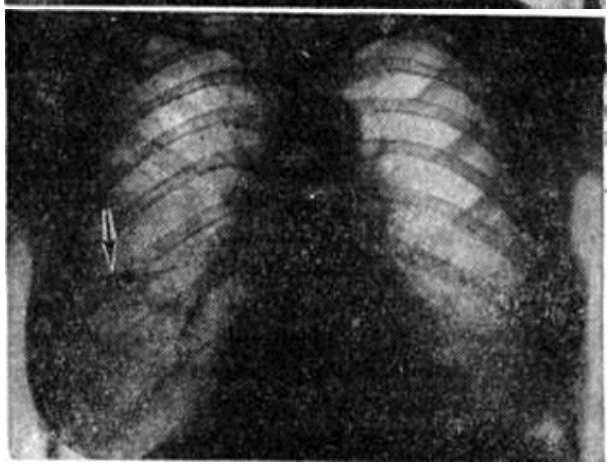

Fig. 2.5.11. Chest X-ray of a patient with Leffler's syndrome: infiltrate in the right lung (indicated by an arrow).

The latter is caused by allergens of animal or plant origin (ascariasis, trichinosis, pollen, fungi, microorganisms). The morphological substrate is focal eosinophilic pneumonia. Patients are bothered by frequent coughing, a feeling of tightness in the chest, and a temperature rise to 38^0C. With tuberculous infiltrate, the patient often feels well and has a slight cough. Percussion may reveal no changes in eosinophilic infiltrates, while auscultation sometimes reveals isolated dry rales and a small number of unstable fine-bubbled wet rales. An X-ray of eosinophilic infiltration shows darkening with blurred edges, mainly homogeneous in nature, of various sizes; in tuberculosis, a round, homogeneous area of darkening in the subclavian zone. Eosinophilic infiltrates are characterised by rapid appearance and equally rapid disappearance (sometimes within 3-4 days), while in tuberculosis, the infiltrate resolves slowly. In the blood and sputum, eosinophilic infiltrates contain many eosinophils (30-40-60% in the blood); eosinophilia is not characteristic of tuberculosis. ESR is within normal limits in cases of transient infiltrates and accelerated in cases of tuberculosis.

In young men and adolescents, it is possible to develop so-called rheumatic pneumonia. Its distinctive features are the localisation of foci similar to tuberculous infiltrates (more often in the upper part of the lung); lability of areas of opacity in the lungs; significant neutrophilic leukocytosis; frequent addition of pleurisy and pericarditis; it is observed mainly in patients with recurrent visceral rheumatism.

Pulmonary infarction is characterised by sudden onset of chest pain, shortness of breath, and haemoptysis, which gives rise to differential diagnosis with both tuberculosis and croupous pneumonia. The cause of thromboembolism of the pulmonary artery branches may be thrombophlebitis of the lower extremities, recent surgery, childbirth, fractures of the tubular bones, etc. Percussion reveals dullness of sound, and auscultation reveals pleural friction noise, moist fine and medium-sized bubbling rales. The radiographic shadow of an infarction may be triangular if the occluded vessel is located in the frontal plane; if it is located in the sagittal plane, the shadow is round or polygonal; if located in the oblique plane, it has an elongated oval shape.

The differential diagnosis of a round tuberculous infiltrate and pulmonary echinococcus causes certain difficulties. Patients may have no complaints until the latter ruptures, with normal temperature, while with a tuberculous infiltrate, the temperature is subfebrile. It is important to note whether the patient has had contact with animals in the case of echinococcus or with tuberculosis patients in the case of a tuberculous infiltrate. In echinococcosis, significant eosinophilia occurs in 50% of patients, with a positive Katsoni test, while in tuberculous infiltrate, the tuberculin test is often positive. The radiological picture of echinococcus of the lung before rupture into the bronchi looks like a homogeneous round or oval shadow with clear contours. After the echinococcal cyst breaks into the bronchus, a cavity with gas and fluid at the bottom is observed. With a round tuberculous infiltrate, the shadow is not always homogeneous, but is connected by a "track" to the lymph node, which does not occur with echinococcus.

A lung abscess (before it ruptures into the bronchus) may show a shadow on the X-ray similar to a round tuberculous infiltrate of Asman (Fig. 2.5.12-13).

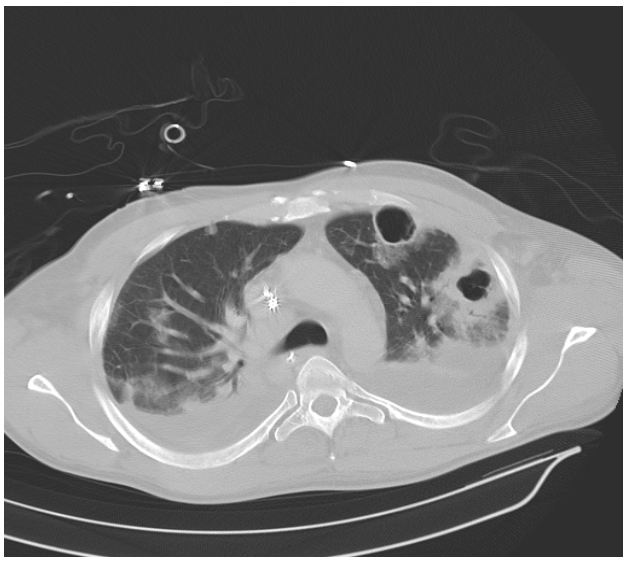

Fig. 2.5.12. Lung abscess (before it breaks into the bronchus).

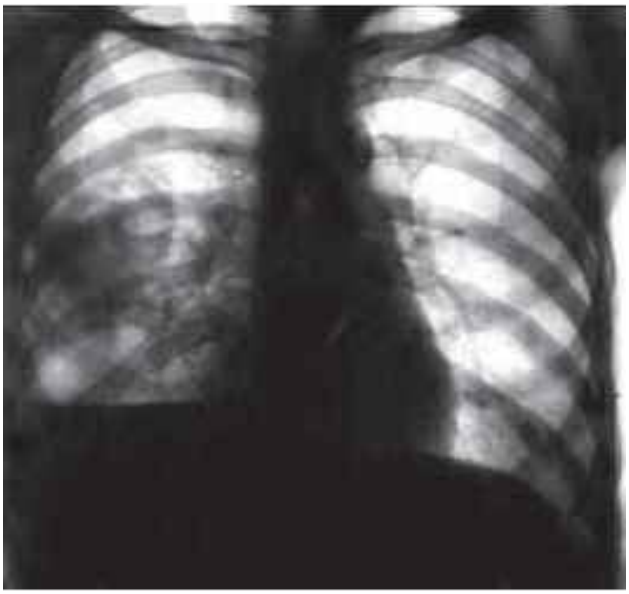

Fig. 2.5.13. Lung abscess (before it breaks into the bronchus).

A peribronchial lymphangitis tract may extend from a lung abscess (as in the case of a tuberculous infiltrate) to the root. Even before the abscess ruptures, the patient experiences a foul odour from the mouth with a small amount of sputum, chest pain, and pain when pressing on the rib or intercostal space in the projection of the abscess. Significant intoxication and chills are characteristic. Significant shortness of breath, hectic fever, profuse sweating. On percussion – limited dullness, on auscultation in the focus area – fine-bubbled moist rales. On the X-ray – a shadow of a pneumonic infiltrate. The tuberculin test is negative, peripheral blood shows hyperleukocytosis, a shift to the left, and an ESR of 50-60 мм /hour. Rupture of the abscess into the bronchi is accompanied by coughing and the discharge of a significant amount of sputum (about 1 L). The patient's condition improves. The sputum

settles into three layers; microscopy reveals many leukocytes and sometimes elastic fibres. An X-ray shows a cavity with fluid on the background of a pneumonic shadow. The presence of focal changes around the cavity is more characteristic of tuberculosis than of an abscess. Multiple cavities are more indicative of tuberculous cavities than abscesses. A common location for abscesses is the VI segment of the lower lobe. The presence of elastic fibres in the absence of tubercle bacilli suggests an abscess.

Pneumonia should be distinguished from infiltrates of various origins. The shadow formed during atelectasis can in some cases stimulate both specific and non-specific infiltrative processes on X-ray. Lung atelectasis is more common in cancer and less common in tuberculosis. Sometimes it develops as a result of compression of the bronchus by enlarged lymph nodes (tuberculosis, lymphogranulomatosis, lymphosarcoma, etc.) – compression atelectasis. Percussion of the lungs reveals an area of dullness, with breathing above it sharply weakened or absent. In atelectasis, the shadow on the X-ray is homogeneous and uniform, resembling frosted glass. After diagnosing a patient with lung atelectasis, it is necessary to determine its origin. First of all, it is necessary to make a differential diagnosis between cancer and tuberculosis. This differential diagnostic process is based on data from bronchoscopy with biopsy, computed tomography, and in some cases magnetic resonance imaging; sputum analysis to detect tuberculosis bacilli and atypical cells. Atelectasis is divided into total (all lungs), lobar, segmental, lobular, and acinar. It can be aseptic, or it can be complicated by pneumonia, fibrotorax, bronchiectasis, abscess, or gangrene.

It is important to differentiate between pneumonia, tuberculosis, and actinomycosis. The latter is rare. The clinical picture of actinomycosis is similar to that of ordinary pneumonia: cough with mucous sputum, fever, pain in the side, dullness of percussion sound, moist rales of varying calibre over the affected area of the lungs. If there is a cavity, amphoric breathing occurs. In differential diagnosis, three signs that are characteristic of actinomycosis and not characteristic of pneumonia or pulmonary tuberculosis are sometimes helpful: extrathoracic localisation in the form of woody infiltrates with fistulas in the lower jaw area,

sometimes bright yellow-brown sputum colouration and typical chest wall lesions (phlegmon, cold abscesses, fistulas with thick pus discharge). Such changes do not occur in tuberculosis. Actinomycosis is characterised by a burning "fiery" pain when pressing on the skin of the chest, which is absent in pneumonia and pulmonary tuberculosis. Microscopy of sputum diagnoses actinomycosis if threads with flask-like formations at the ends are found, which radiate from the centre. Allergic tests for actinolysate are positive, for tuberculin – negative. A chest X-ray in lobar actinomycosis shows an intense, non-homogeneous shadow with small bright spots, as well as small and medium-sized focal shadows. Lung tissue in lobar mycosis looks like an airless, dense mass on section.

A number of rare diseases should also be differentiated from pulmonary infiltrates, including pulmonary cysts, encapsulated pleurisy, etc. In the absence of clinical manifestations, computed tomography, Mantoux test, clinical blood analysis, and acute-phase inflammation indicators will help in the diagnosis.

Leukaemic lymphomas located in the lungs occur in patients with leukaemia, which is confirmed by peripheral blood tests, bone marrow smears, and characteristic biochemical tests.

Lung damage is observed in the late stages of tertiary syphilis – late visceral syphilis. Pulmonary infiltrate is rarely the leading syndrome. In this period, the clinical picture of cardiovascular system damage dominates, and syphiloma of the lungs may be detected accidentally.

The syphilitic nature of pulmonary infiltrates should be suspected in the following cases: 1) relatively young age of the patient; 2) presence of a prolonged, exhausting cough without sputum; 3) prolonged course of respiratory failure syndrome without pronounced manifestations of bronchopulmonary and bronchial obstructive syndromes; 4) negative results of tuberculosis testing. Determination of the syphilitic nature of the disease is based on serological diagnosis.

Dressler's syndrome usually develops 6 weeks after the acute stage of myocardial infarction, but it can happen earlier – on the 2nd or 3rd day, especially with repeated heart attacks. In classic cases, there is a triad of fibrinous pericarditis, pleurisy, and interstitial pneumonitis. But more often, a combination of pericarditis with pleurisy or pneumonitis is

observed. The main clinical symptom is pain in the heart area. Pericardial or pleuropericardial noise is detected. Bronchopulmonary syndrome is absent in most cases. There are also syndromes of fever, mesenchymal cell proliferation, and infiltrative changes in the lower lobes closer to the root of the lungs.

Any infiltrative neoplasm may be potentially neoplastic and always requires exclusion of malignant growth. The presence of the following symptoms in a patient primarily requires the exclusion of lung tumours: 1) lymphadenopathy 2) persistent fever resistant to antibiotics; 3) rapid weight loss in the patient; 4) constant chest pain without clear localisation and irradiation; 5) recurrent pneumonia in the same area of the lungs; 6) discrepancy between the size of the pathological focus and the amount of sputum secreted by the patient; 7) increasing bronchial obstruction resistant to beta-agonists and glucocorticosteroids; 8) Trousseau's thrombophlebitis; 9) aseptic thromboendocarditis; 10) a combination of these signs with haematological changes — anaemia, blastemia. Peripheral lung cancer located in the upper lobe (Penckstorf's cancer) presents a unique clinical picture. Even before its radiological detection, attention should be paid to neurological symptoms (Horner's syndrome): ptosis, enophthalmos, miosis are detected on the side of the tumour, brachial plexitis may occur, and supraclavicular lymph nodes are enlarged. Benign tumours in most cases do not manifest clinically and are detected incidentally during X-ray examination.

Metastatic tumours. Numerous pulmonary infiltrates are detected in both lungs; they are heterogeneous and round in shape. Over time, cancerous lymphangitis develops – the pulmonary pattern intensifies, the roots of the lungs thicken, from which radial shadows emanate. Repeated X-ray examinations reveal "sprinkling" of metastases — pulmonary infiltrates that were previously larger in size, as well as new ones that are smaller in size and intensity. Most often, metastases in the lungs are caused by tumours of the uterus, kidneys, gonads, large intestine, bones, thyroid or mammary glands, as well as lymphogranulomatosis and leukaemia.

Variants of the course of pneumonia depending on the aetiological factor. Pneumococcal pneumonia – caused by pneumococcus. It is characterised by a sharp increase in capillary permeability. There is a

passive release of plasma proteins, including the largest ones – fibrinogen, as well as diapedesis of erythrocytes. Croupous pneumonia is pneumococcal pneumonia that occurs when the body's response to microbial aggression is heightened. In croupous pneumonia, sputum is viscous, sticky, glassy, uniformly brown, and rusty. At first, sputum is scanty, then it becomes abundant, and after the crisis, it becomes purulent. Microscopy: erythrocytes, neutrophils, fibrin threads, alveolar epithelium, blood pigment. Bacterioscopy: separately polarised cells.

Staphylococcal pneumonia – with multifocal and bilateral inflammation, which tends to be localized. Staphylococcal pneumonia can have several chronic forms:

- primary, more often bilateral, has an acute onset with high fever, chills, cough with purulent sputum, shortness of breath and frequent lung abscesses, pleurisy. On the part of the blood, high leukocytosis and toxic granularity of neutrophils are characteristic;
- metastatic staphylococcal pneumonia is staphylococcal destruction of the lungs (due to haematogenous spread) – bilateral damage, severe course, septic condition, multiple foci of abscesses combined with bullae;
- Infiltrative form – severe course;
- bullous form – course is not severe, intoxication is insignificant, extensive cavities on the X-ray;
- abscessing form – severe course, pronounced respiratory failure, significant intoxication, hectic fever; X-ray shows multiple cavities with fluid levels against a background of infiltration;
- pulmonary-pleural form often causes complications (pneumothorax, pyopneumothorax).

Streptococcal pneumonia – acute onset, severe course, pronounced intoxication and fever, X-ray shows pneumonic infiltrates with cavities of decay, purulent pleurisy.

Friedländer pneumonia – pneumonia caused by Klebsiella. The course is severe, typical, the lobe is damaged, the lesion is confluent with multiple areas of decay, infiltrate-like necrosis of the lung tissue, abscess formation. It is localised in the upper lobe, intoxication is pronounced. Sputum is viscous with the smell of burnt meat, sticky, brick

red in places. Microscopy: numerous elastic fibres. Bacterioscopy: many small Gram-negative rods.

Pneumonia caused by Hemophilus influenzae – typical clinical picture, but the epiglottis and small bronchi are always damaged, with clinical signs of laryngobronchitis. Pneumonia caused by Pseudomonas aeruginosa is severe, with a tendency to disseminate and abscess, often complicated by pyopneumothorax. It is observed in weakened patients after heart and lung surgery, in individuals who have taken antibiotics for a long time and irrationally.

Community-acquired pneumonia is caused by numerous aetiological agents – mycoplasma, Haemophilus influenzae, Legionella, but the most common among them is pneumococcus (80-90%). Criteria for severity of pneumonia: respiratory rate greater than 30 breaths per minute, severe respiratory failure requiring mechanical ventilation, radiographic evidence of bilateral involvement of multiple lobes, possible shock (systolic blood pressure less than90 мм mmHg and diastolic blood pressure less than60 мм mmHg), the need for vasopressors lasts more than 4 hours, urine output is less than 20 ml/hour, indicating renal failure. Such patients should be treated in intensive care units. Severe community-acquired pneumonia is caused by Streptococcus pneumoniae, Mycoplasma pneumoniae, respiratory viruses H. influenzae, tuberculosis mycobacteria, and fungi.

Atypical pneumonia is characterised by bronchopulmonary damage and the presence of other systemic organ damage with atypical pathogens. Pathogenic strains that cause active pneumonia include Mycoplasma pneumoniae, Legionella, Chlamydia pneumoniae, Chlamydia psittaci, Coxiella burnetii, and fungi. A distinctive feature of the pathogenesis of "atypical" pneumonia is the intracellular location of the pathogen.

Pneumonia caused by Legionella. Contributing factors for the development of Legionnaires' disease pneumonia: smoking, advanced age, chronic bronchopulmonary diseases, corticosteroid therapy, organ transplantation, neutropenia, AIDS. A distinctive feature of the pathogenesis of legionellosis is an incubation period of 9-10 days. After phagocytosis by alveolar macrophages, the microbes do not die, but damage the macrophages, followed by phagocytosis by other cells and

multiplication in them. Cellular and humoral immune mechanisms are unable to destroy Legionella, and glucocorticoids slow down the elimination of microbes from the lungs. Legionellosis pneumonia occurs as lobar, sometimes as total, subtotal with severe intoxication, infectious-toxic shock, respiratory failure, interstitial pulmonary oedema, kidney and liver damage. The characteristic features of these types of pneumonia are those of a "viral" disease: dry cough, lethargy, diarrhoea, lymphopenia without pronounced neutropenia, a sharp increase in ESR (60-80 mm/hour), and hyponatraemia.

Mycoplasma pneumonia. Children aged 5 to 14 years and young adults are often affected. The clinical manifestation of the infection is tracheobronchitis, and pneumonia occurs in 3-10% of cases and is often accompanied by pleural effusion, respiratory failure, lung consolidation, abscesses, and bronchiectasis.

Nosocomial pneumonia (hospital-acquired). Factors contributing to the severe course of pneumonia include advanced age of patients, the presence of chronic concomitant lung diseases and severe somatic pathology with functional insufficiency of organs and systems, immunodeficiency states, previous cytostatic and glucocorticoid therapy. About half of all cases of nosocomial pneumonia occur in intensive care units, especially in postoperative wards. Pathogenesis of nosocomial pneumonia: aspiration of flora from the upper respiratory tract, especially due to intubation and decreased gastrointestinal motility and gastric emptying.

Pneumocystis pneumonia is often found in AIDS patients (80%) and is the cause of death in every fourth patient.

Viral pneumonia. The role of viruses in the development of pneumonia has not been sufficiently clarified. Some cases of pneumonia develop under conditions of direct viral exposure to the capillaries and alveolar tissue. Some cases of pneumonia, in which the virus acts as a "conductor" causing panbronchitis and activating the microbial flora, occur due to a decrease in the effectiveness of antimicrobial defence. True viral pneumonia develops acutely, with severe intoxication: toxicosis, hyperthermia, headache, pain in the eyeballs and muscles, and meningeal symptoms. From the first day, haemorrhagic bronchitis

develops as a manifestation of vasculitis, and as it progresses, haemorrhagic pneumonia develops.

Adenovirus infection begins with pharyngoconjunctivitis, especially in children with significant mucous discharge from the nose, moderate intoxication, and subfebrile temperature. The appearance of fever, pronounced intoxication, increasing catarrhal symptoms, and sometimes intestinal dyspepsia after 2-3 weeks indicates the development of pneumonia.

Parainfluenza virus. The entire respiratory system is damaged, manifested by pronounced rhinitis, laryngitis, and tracheitis. Clinical picture of focal pneumonia. The area of infiltration is small. On the X-ray, there is a cloud-like darkening.

Syncytial respiratory viral infection. It begins with subfebrile temperature, rhinitis, pharyngitis. Bronchitis, bronchiolitis with non-productive cough, expiratory dyspnoea, dry rales, tympanitis may develop. The appearance of fever, localised or scattered fine-bubbled rales and crepitus against this background indicates the activation of bacterial flora, most often Haemophilus influenzae, which leads to the development of pneumonia.

Secondary pneumonia can occur against a background of atelectasis, aspiration, hypostasis, wounds and injuries (primary and secondary), and pulmonary infarction.

In many cases, pneumonia in elderly and senile patients does not have a pronounced onset, there is no clear beginning, chills, chest pain, cough, general symptoms prevail: weakness, apathy, anorexia, impaired consciousness, etc. There is no cyanosis of the skin of the face or lips, rapid shallow breathing, reduced percussion sound, increased voice tremor, and often no bronchial breathing. X-ray examination often does not reveal homogeneous opacity, but widespread patchy opacity is often noted.

2.6. Caseous pneumonia

Caseous pneumonia is an acute specific pneumonia characterised by rapidly increasing caseous-necrotic changes and a severe course, which often progresses rapidly and leads to a fatal outcome. It is characterised by: severe condition of the patient, pronounced symptoms of intoxication, profuse catarrhal manifestations in the lungs, leukocytosis,

a sharp shift to the left in the leukocyte formula, lymphopenia, massive mycobacterial excretion. Caseous pneumonia occurs in the form of lobar and lobular forms.

The CT picture of lobar caseous pneumonia differs little from that of lobitis. However, the extremely severe clinical course allows this most unfavourable type of infiltrate to be diagnosed (Fig. 2.6.1). In cases where caseous pneumonia is lobular, multiple lamellar focal and focal shadows are detected in both lungs, which tend to merge. Numerous areas of irregularly shaped destruction are detected (Fig. 2.6.2 a).

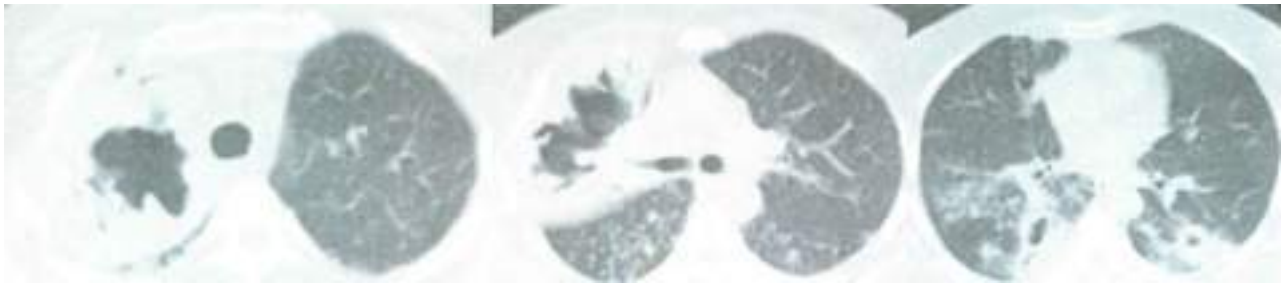

Fig. 2.6.1. Caseous pneumonia, MBT+ (lobar form). The upper lobe of the right lung is infiltrated, with a large cavity of decay with uneven wide walls without a fluid level, the base of which is adjacent to the costal and interlobar pleura. In the infiltration zone, spaces of deformed bronchi and bronchiectasis are visualised. In the lower lobes of the lungs, there are multiple polymorphic focal and infiltrative shadows with cavities of decay.

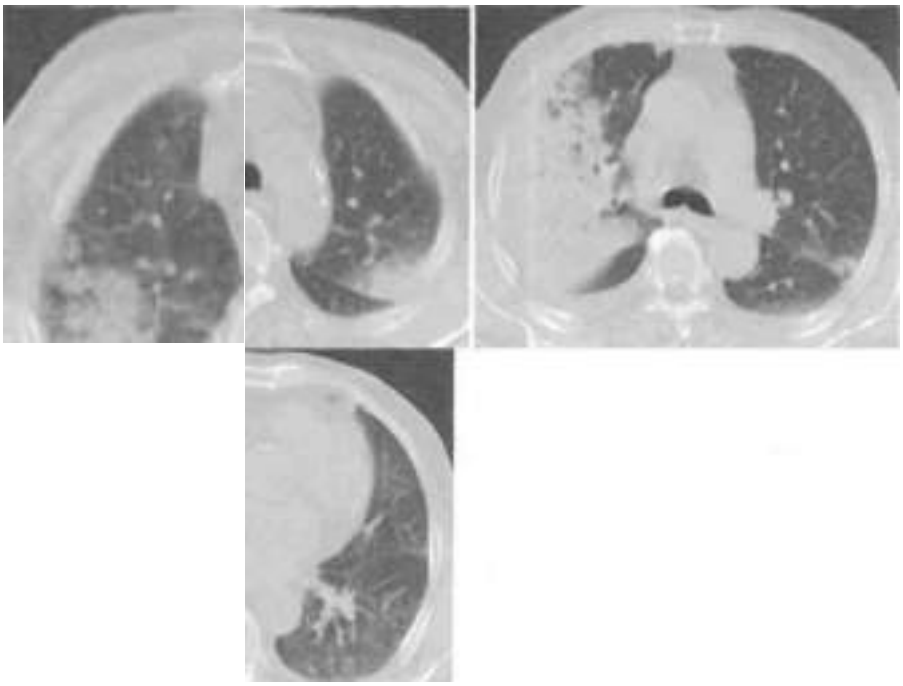

Fig. 2.6.2 a. Caseous pneumonia, MBT+ (globular form). In both lungs, multiple focal and focal shadows are determined, which tend to merge, numerous small destructions of lung tissue.

As caseous pneumonia progresses, giant cavities sometimes form. More often, multiple medium-sized cavities of decay are found. The rapid appearance of new focal and infiltrative shadows is characteristic, both on the side of the primary lesion and in the other lung. Unlike other types of tuberculous inflammation, caseous degeneration of the lung is not accompanied by the development of fibrosis.

The mortality rate for caseous pneumonia reaches 80%. Early diagnosis and urgent, vigorous anti-mycobacterial therapy in a specialised hospital give the patient a chance of survival.

In cases of successful treatment, caseous pneumonia can gradually progress to pulmonary cirrhosis (Fig. 2.6.2 b). An unfavourable outcome may be fibrocavernous pulmonary tuberculosis.

The decisive role in the early diagnosis of caseous pneumonia belongs, first of all, to sputum examination, as well as X-ray examination. Massive mycobacterial excretion is determined in 100% of cases, therefore, differential diagnosis is usually not performed.

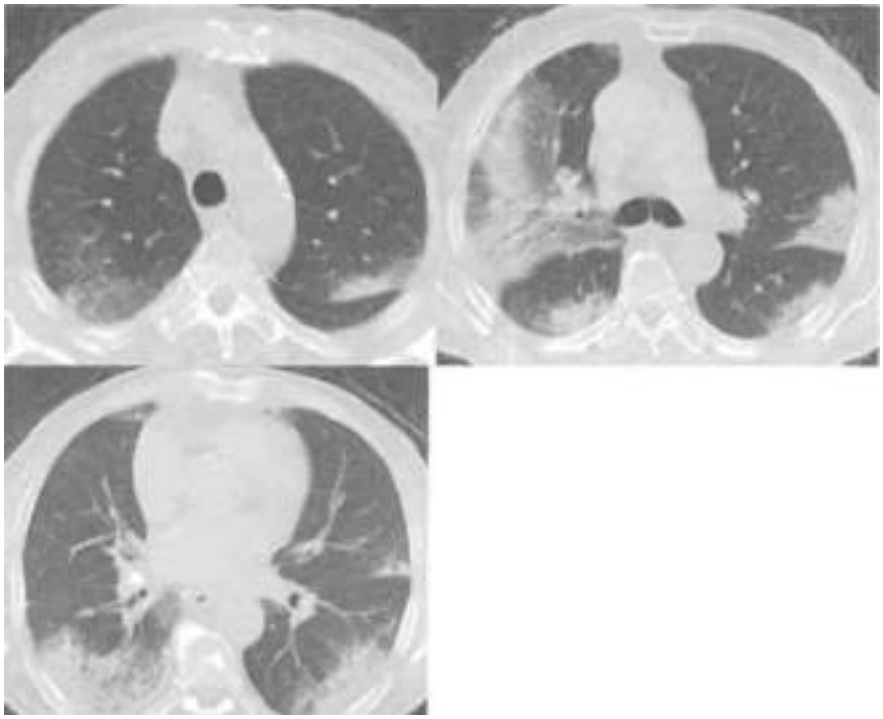

Fig. 2.6.2 b. The same patient after 12 months of treatment. Significant consolidation and cirrhotic focal infiltrative changes in the lungs are evident.

2.7. Pulmonary tuberculoma

Pulmonary tuberculoma is a formation of various origins, usually encapsulated with a predominance of caseosis, with a diameter of more than10 мм and an asymptomatic clinical picture.

In the vast majority of cases, tuberculoma forms during chemotherapy (80%) or spontaneously from infiltrative tuberculosis, caseous pneumonia, focal tuberculosis (conglomeration of foci), destructive tuberculosis (bronchial obliteration and cavern filling with caseous material).

Occasionally, a tuberculoma may form from the pulmonary component of the primary complex. Most often, tuberculomas occur in young people aged 20-40 years.

There are several types of tuberculoma: infiltrative-pneumonic type (a rounded focus of desquamative-necrotic pneumonia in the stage of incomplete restriction and capsule formation), caseous (encapsulated caseous of homogeneous, conglomerate or layered structure), filled or blocked cavity ("pseudotuberculoma").

Most often, tuberculomas are solitary (75-85%), but they can also be multiple. Depending on their size, tuberculomas are divided into: small – up to2 см in diameter (approximately 20%); medium – 2-4 см s (approximately 63%); large – more than4 см s (approximately 17%).

CT scans provide a more accurate assessment of the contours and structure of rounded formations than X-rays and conventional tomograms, revealing calcifications and small foci in the surrounding lung tissue.

Tuberculomas are depicted on CT as rounded or irregularly shaped pathological formations, located in most patients in the upper lobes of the lungs. They are usually localised in the cortical sections of the lung, but do not come into contact with the visceral pleura. The contours of tuberculomas are clear, uneven, and wavy. In the lung tissue surrounding the pathological formation, small foci, areas of emphysema, and isolated strands to the pleura may be visible. The walls of the bronchi are slightly thickened. In other parts of the lungs, foci, calcifications, fibrotic changes, apical or costal pleural thickening are often detected (Fig. 2.7.1-5).

A recently formed tuberculoma is usually homogeneous and round in shape. An "older" tuberculoma has a heterogeneous structure, sometimes layered.

Reactivation of the inflammatory process leads to a change in symptoms. Multiple small foci appear in the lung tissue surrounding the tuberculoma, located in the interlobular septa, and the contours of the formation become less distinct. A characteristic feature of the activation of the process is the presence of a cavity of destruction in the tuberculoma. Usually, the cavity is located eccentrically, in the area of the mouth of the draining bronchus, has an irregular shape and does not contain fluid (Fig. 2.7.6-7).

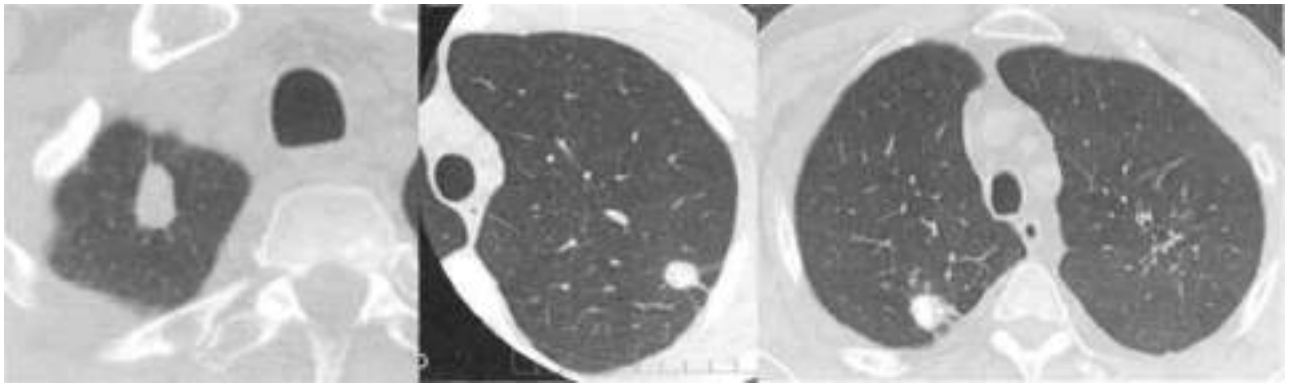

Fig. 2.7.1. Variant of tuberculoma – caseous. Tuberculoma $S_1$of the right lung, Hist+. Oval-shaped focal shadow, relatively homogeneous with thin cortico-pleural strands (a). Tuberculoma $S_{(2)\ of}$the left lung, Hist+. A round focal shadow with clear contours, inhomogeneous due to calcification in the centre, with thin cortico-pleural strands (b). Tuberculoma $S_{(2)\ of}$the right lung, MBT-. A round focal shadow with clear contours, inhomogeneous due to calcification, with thick cortico-pleural strands (c).

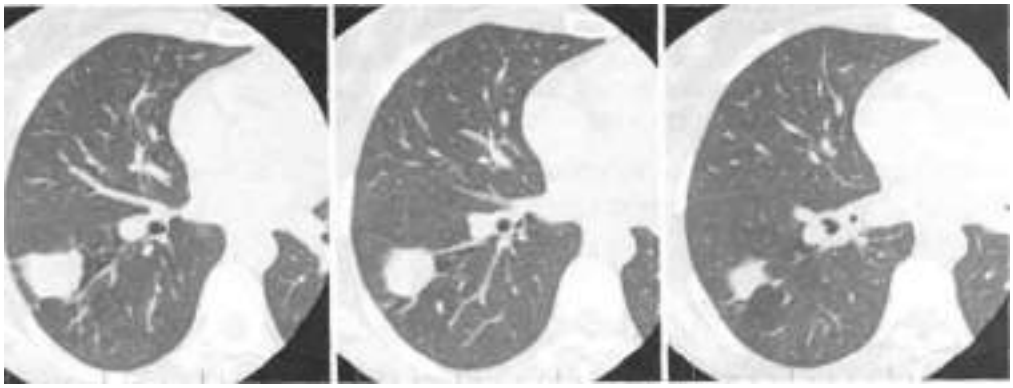

Fig. 2.7.2. Tuberculoma $S_{(6)}$ of the right lung, MBT-, Hist+ (infiltrative-pneumonic type). A focal shadow measuring 3.2×2.1 cm, homogeneous

with clear uneven contours and cortico-pleural strands, localised in the cortical sections of the lungs. There are isolated polymorphic foci in the surrounding tissue.

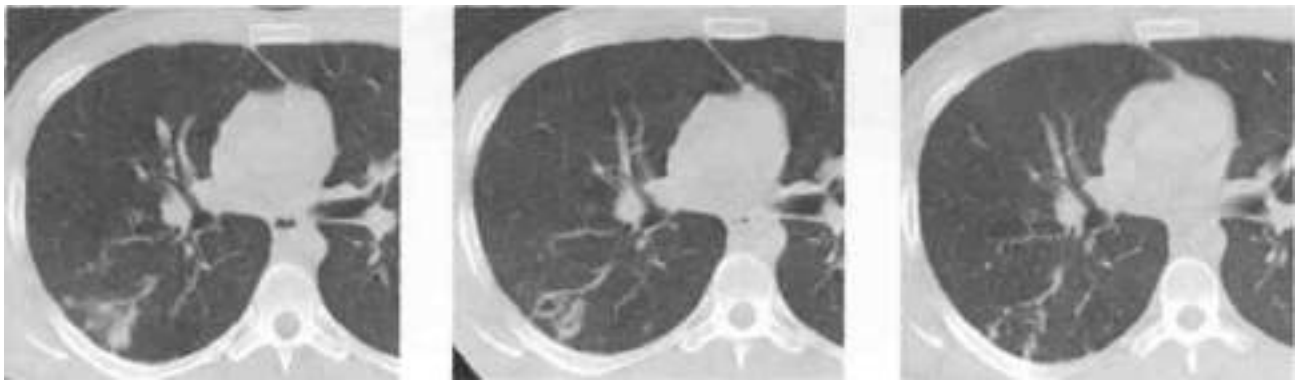

a **b** **c**

Fig. 2.7.3. Tuberculoma $S_{(6)}$ $_{of}$the right lung, MBT+ ("pseudotuberculoma" – filled cavity). Focal shadows with blurred contours are grouped in a V-shape (a). After five months of treatment, tuberculous destruction with the formation of cystic bronchiectasis is noted (b). After eight months of treatment, multiple small polymorphic focal shadows with areas of fibrosis are determined at the site of the tubercle.

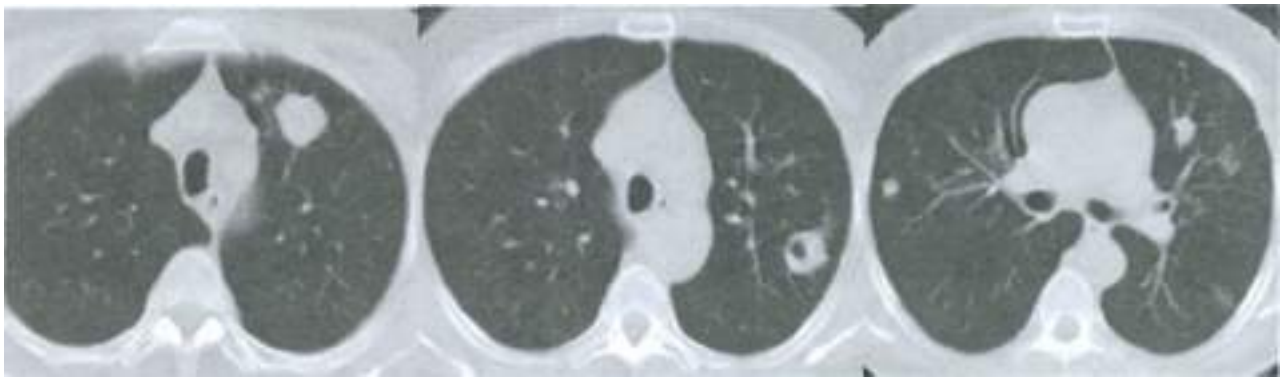

Fig. 2.7.4. Multiple pulmonary tuberculomas, MBT+. Focal shadows ranging from 1.1 to2,4 см in diameter with uneven contours and separate strands to the pleura. The tuberculoma in $S_2$of the left lung has a cavity of decay, located eccentrically in the area of the mouth of the draining bronchus, and does not contain fluid. There are multiple small polymorphic foci in the surrounding lung tissue.

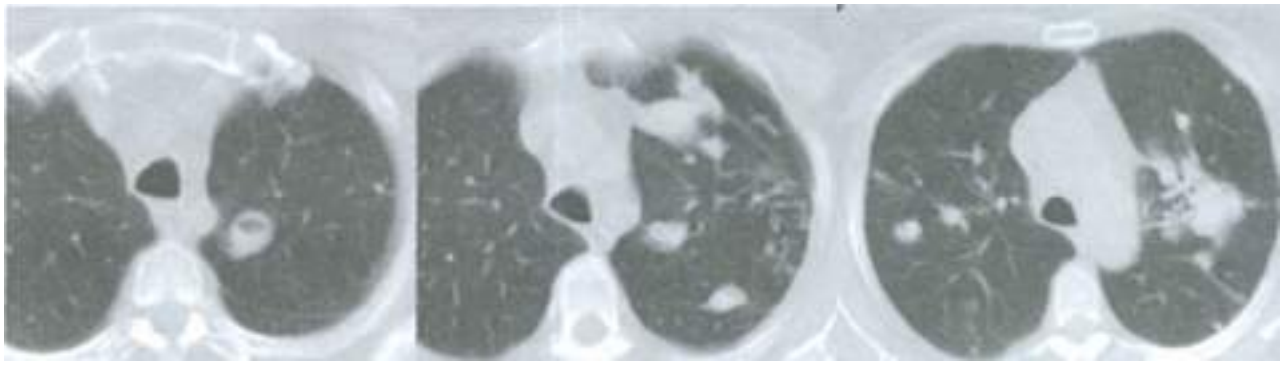

Fig. 2.7.5. Multiple pulmonary tuberculomas, MBT+, in a patient with diabetes mellitus. Focal shadows ranging from 1.1 to 3,8 cm in diameter with blurred, uneven contours and strands to the pleura; some have cavities of decay, which are eccentrically located, and areas of calcification. Multiple small polymorphic foci in the surrounding lung tissue.

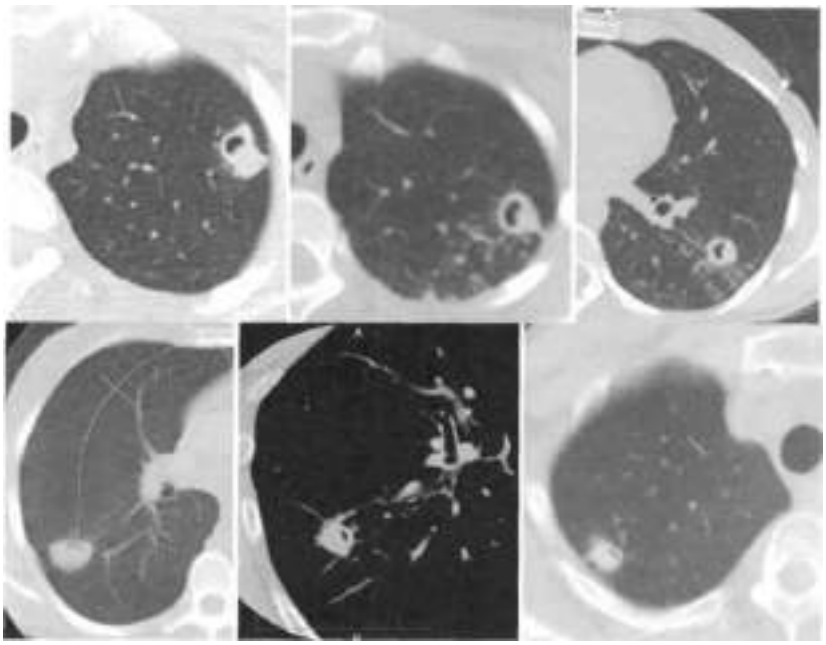

Fig. 2.7.6. Variants of cavities of decay in tuberculomas. The cavities are eccentrically located in the area of the mouth of the draining bronchus, have an irregular crescent shape and do not contain fluid.

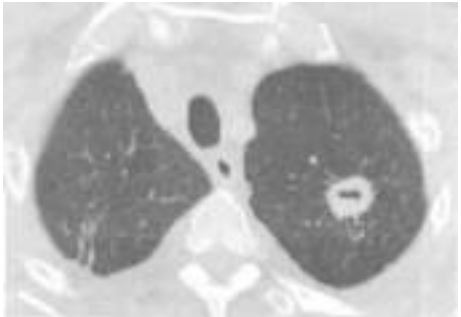

Fig. 2.7.7. Tuberculoma $S_{(1+2)\ of}$the left lung, MBT+. The cavity of decay is located in the centre, has an irregular shape and contains no fluid.

The main distinguishing feature of tuberculomas is the presence of focal, layered or diffuse calcifications, in the detection of which CT has significant advantages over conventional X-ray examination. Calcifications in tuberculomas have high density (over +200 HU) and clear contours. They are particularly evident on thin sections using targeted reconstruction.

An important differential diagnostic feature of tubercles is their characteristic reaction to bolus injection of contrast medium. With dynamic scanning, during a series of tomographic sections at the same level followed by the construction of a graph of contrast medium accumulation, it can be established that the densitometric indicators of most tubercles do not change. In some patients, the contrast agent accumulates in the capsule, creating an edge enhancement effect (Fig. 2.7.8).

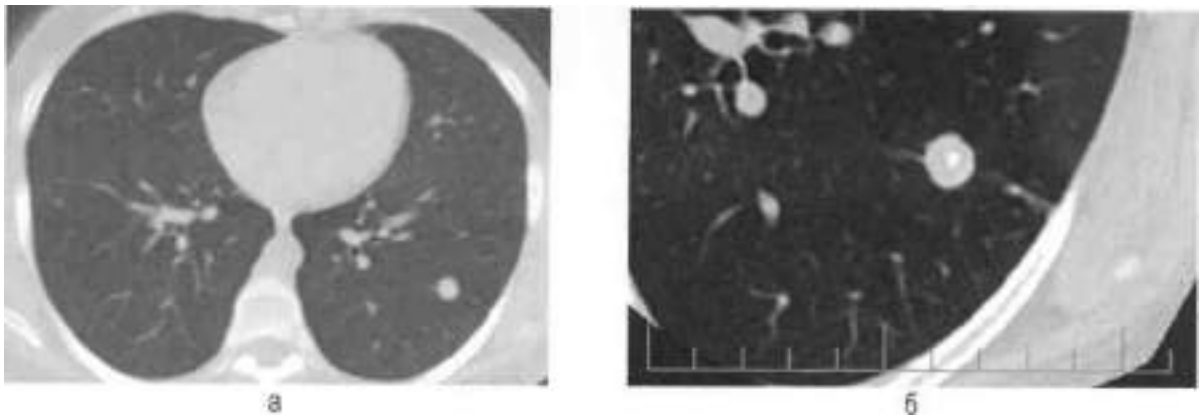

Fig. 2.7.8. Tuberculoma $S_{(6)\ of}$the left lung. The focal shadow is1,2 см in diameter and has clear, even contours. The surrounding tissue is unchanged (a). With bolus administration, the contrast agent accumulates in the capsule and creates a rim enhancement effect (targeted reconstruction of the left lung, high-resolution CT) (b).

The presence of calcifications and a typical reaction to the administration of contrast medium, and in some patients the presence of multiple polymorphic foci in the surrounding tissue, allows tuberculomas to be distinguished from other round formations in the lungs (Fig. 2.7.9-12). Without the use of enhancement techniques and in the absence of calcifications, it is not possible to make a definitive conclusion about the presence of tuberculomas. It should be noted that the shape, size, nature of the contours and the presence of foci in the surrounding lung

tissue of the formation are not pathognomonic signs for tuberculomas and may be observed in other diseases. In these cases, the diagnosis is established on the basis of a retrospective study of the archive of X-rays and fluorograms or by transbronchial or transthoracic needle biopsy.

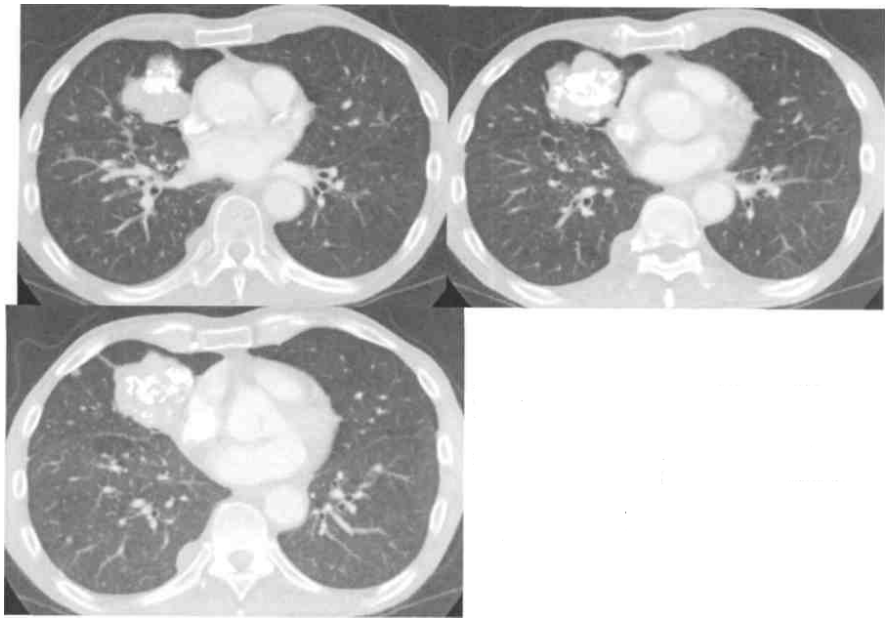

Fig. 2.7.9. Layered tuberculoma $S_5$of the right lung, MBT-. A focal shadow measuring 5.4×5.8×6.0 cm with clear uneven contours and a heterogeneous structure. With bolus administration, the contrast agent does not accumulate in the capsule and tissue.

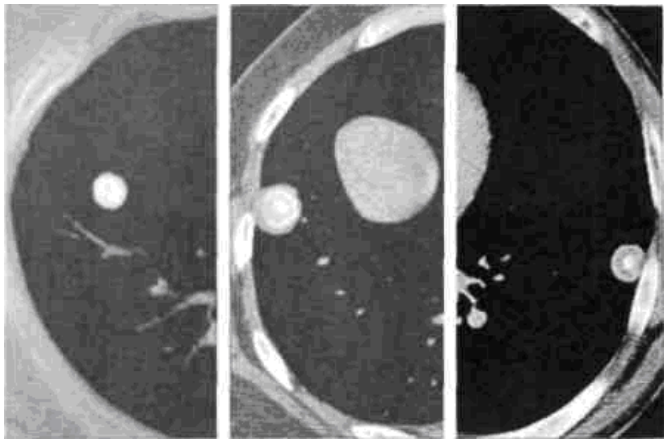

Fig. 2.7.10. Variants of layered tuberculomas.

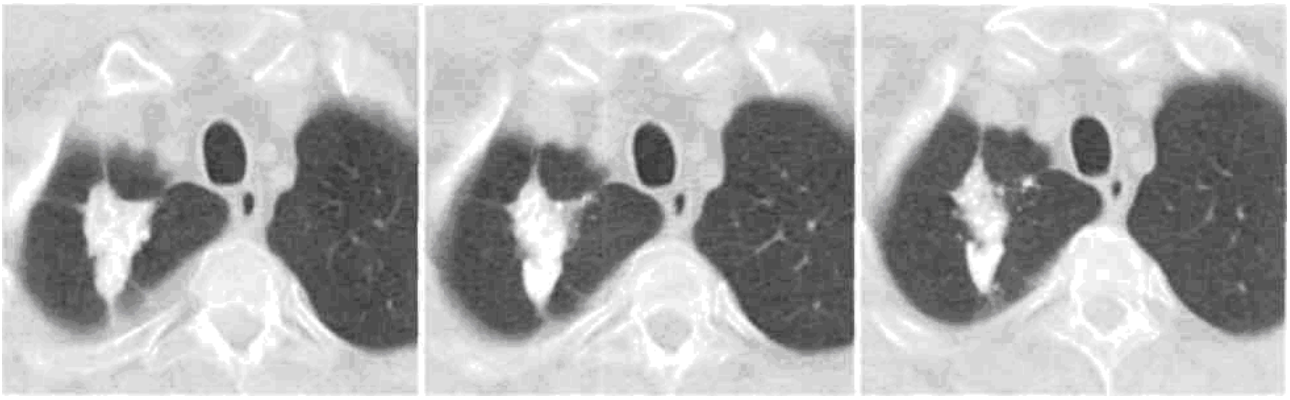

Fig. 2.7.11. Residual changes after spontaneously healed tuberculosis $S_{(1)}$ ofthe right lung with an outlet into the tubercle (layered). A focal shadow measuring 2.5×4.0×4.4 cm with clear uneven contours and a heterogeneous structure. Linear soft tissue strands extend from the area of pathological changes to the pleura, local thickening of the costal pleura.

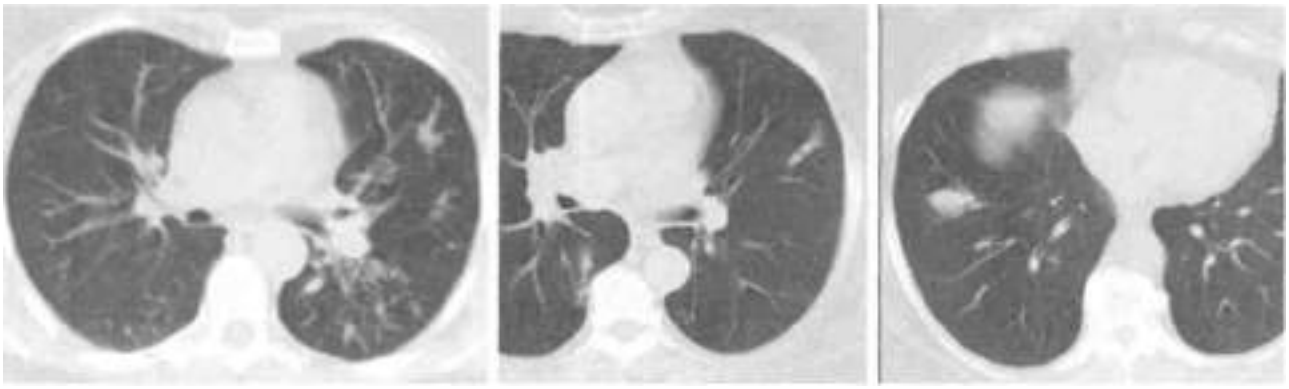

Fig. 2.7.12. Variants of retention cysts in patients with tuberculosis. In $S_{(3)}$ ofthe left lung, the focal shadow has a typical V-shaped form (a). In $S_4$of the left lung, there is a pathological formation of an elongated shape and heterogeneous structure, connected to a small bronchus (b). In $S_6$of the right lung, there is a pathological formation of a rounded shape with clear contours, connected to a small bronchus (c).

Differential diagnosis. Among round formations up to2 см , tuberculomas account for up to 35%. These circumstances indicate the high practical significance of this form of tuberculosis in differential diagnosis, primarily with peripheral lung cancer.

The differential diagnosis of tuberculoma is often difficult due to its radiological similarity to various spherical formations in the lungs, which account for up to 84%. Most often these are malignant (peripheral

cancer, solitary metastasis) and benign tumours, parasitic and non-parasitic filled cysts, eosinophilic infiltrate, inflammatory granulomas, arteriovenous aneurysm, aspergilloma and others.

Usually, no MBT is found in the sputum of patients with tuberculoma. Only when the tuberculoma disintegrates is mycobacterial excretion noted (in approximately 10-30% of patients, usually negligible).

The diagnosis is made based on the results of a comprehensive examination, including transbronchial and transaxial biopsy and exploratory thoracotomy.

Tuberculosis of the small bronchi (tuberculous endobronchitis) can lead to the formation of small retention cysts. They are round, oval, triangular, flask-shaped or irregular (in the form of a two- or three-leaf clover), with clear, even contours, ranging in size from 5 to15 мм. On X-ray examination, these changes are very similar to focal tuberculosis. However, axial sections allow for a more accurate determination of the connection between each such formation and the small bronchus (Fig. 2.7.13). The walls of the bronchi are thickened, their lumen is slightly enlarged and ends in a retention cyst. The lumen of the bronchi in cysts is never determined. However, a common finding is droplet calcification in the area of the end of the draining bronchus.

Peripheral cancer and solitary metastasis may resemble a single tubercle. The use of CT allows for an exceptionally clear, vivid image of a cancerous tumour, which is similar to a macroscopic specimen. This is especially important when localising formations in areas of the lungs that are difficult to examine using conventional tomography.

Peripheral cancer is depicted on cross-sections as a round or irregularly shaped pathological formation with blurred, bumpy contours. The blurring and radiance of the contours is associated with the development of lymphangitis in the adjacent lung tissue. Adenocarcinomas are characterized by long, thick, sparse rays extending from the tumor node to the pleura and lung root. Squamous cell carcinoma is characterized by shorter rays, up to 5-7 мм , and more frequent rays.

An additional symptom is the absence of foci in the surrounding lung tissue in most patients with peripheral cancer. In patients with poorly differentiated cancer, radiation may be absent altogether, and the contours of the pathological formation appear smooth and relatively

clear. These forms of tumour are the most difficult to diagnose differentially. Early enlargement of the lymph nodes of the lung root and mediastinum, as well as rapid tumour growth, are of some significance. However, the final diagnosis is established by histological examination.

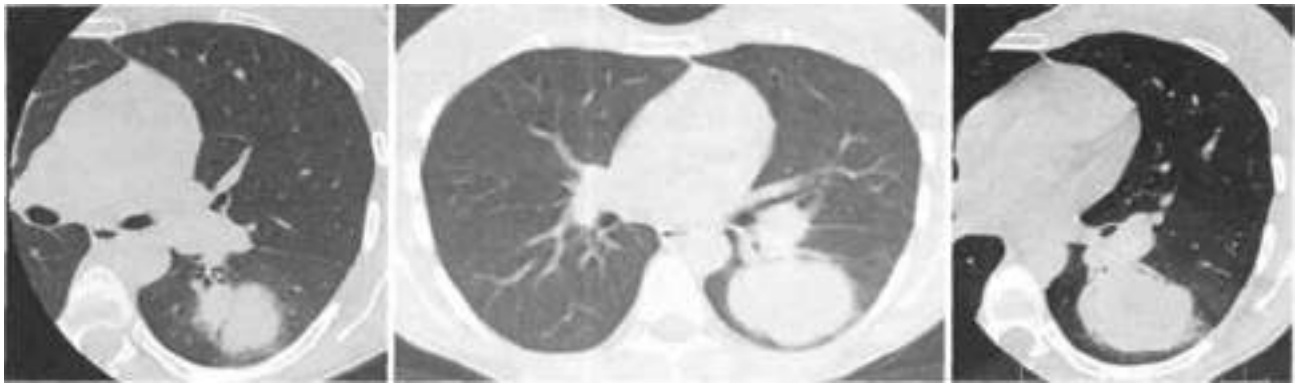

Fig. 2.7.13. Small cell lung cancer with metastases in the intrathoracic and bronchopulmonary lymph nodes, Hist+. A large multi-nodular focal shadow in $S_{(6)\ of}$the left lung, measuring 4.0×5.7×5.8 cm, has relatively uneven, blurred contours.

Calcifications in *cancerous tumours and solitary metastases* are rare, occurring in 5-7% of patients. Calcifications are usually observed in glandular cancers, both primary and metastatic, as well as in metastases of osteogenic sarcomas. Calcifications in adenocarcinomas can be droplet-like or amorphous. Droplet calcifications appear as small eccentrically located foci. Amorphous calcifications are separate areas of increased density (+100... +160 HU) that have an irregular or rounded shape and blurred contours. Such calcifications have no differential diagnostic significance, as they can also be found in tuberculomas.
During dynamic scanning after bolus administration of a contrast agent, the density of malignant tumours increases 1.5-2 times within 2-5 minutes from the start of administration. This is the most important differential diagnostic feature, since the contrast agent does not accumulate in tuberculomas.
Solitary metastases in the lungs pose a particular problem. Solitary metastases are rare (about 5% of all solitary nodes in the lungs). The likelihood of metastatic origin of nodes in the lungs increases with their number. Metastases are most often found in the outer third of the lungs (90%) and near the pleura. They predominate in the lower lobes (66%).

Up to 40% of metastases are accompanied by a feeding vessel symptom (Fig. 3.7.14). It should be noted that in the presence of a single round formation in a patient with a known extra-thoracic tumour, the probability of solitary metastasis does not exceed 40-50%. More than 60% of solitary round formations that have arisen in the lungs in patients with a known tumour are bronchogenic cancer, and only 24% are metastases. In the presence of tumours of the head, neck, lungs, mammary gland, stomach, and prostate gland, the probability of bronchogenic cancer is even higher, especially in smokers. Conversely, in patients with sarcomas and melanomas, solitary formations in the lungs are more often found to be metastases.

In addition to bronchogenic cancer, solitary rounded formations detected by CT may also be benign in nature. These include granulomas, including tuberculomas, local pneumosclerosis, enlarged intrapulmonary lymph nodes, and some others. Like metastases, most of these formations are round in shape and have clear contours. The use of spiral CT allows round formations in the lungs to be differentiated depending on the presence of calcifications and the degree of contrast agent accumulation in them after bolus intravenous administration.

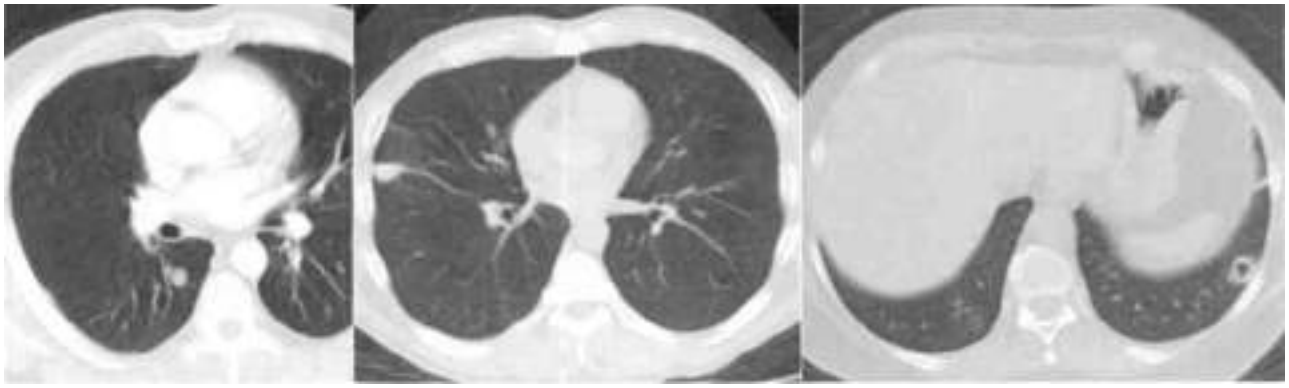

Fig. 2.7.14. Variants of cancer metastases, Hist+. In $S_{(6)\ of}$the right lung, colon cancer metastases measuring1,1 см with clear contours (a). In $S_6$of the right lung, metastases of left kidney cancer (b). In $S_{(9)\ of}$the left lung, uterine cancer metastases have a cavity of decay (c).

Central benign lung *tumours* are usually *adenomas* in histological nature. On CT, they appear as round pathological formations with clear, even or wavy contours in the absence of changes in the surrounding lung tissue (Fig. 2.7.15). Calcifications in adenomas are extremely rare.

During dynamic scanning, adenomas accumulate contrast material more slowly and to a much lesser extent than malignant tumours. This is due to the less pronounced vascular network in such formations. However, a uniform increase in densitometric indicators by 30-50% allows adenomas and other benign tumours to be reliably distinguished from tubercles.

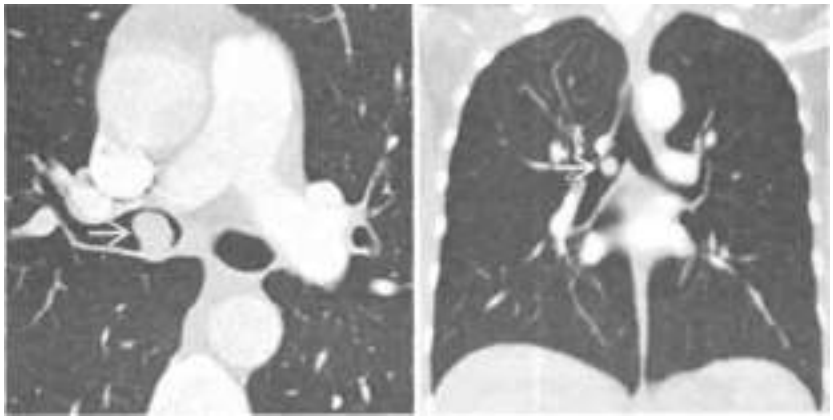

Fig. 2.7.15. Endobronchial tumour (carcinoid) of the right main bronchus.

Peripheral benign tumours are most often *hamartomas* in histological nature. They are dysembryogenic formations.

Hamartomas account for more than 5% of all solitary pulmonary nodules and in the vast majority of cases (over 95%) are found in people over 40 years of age.

Nodules in hamartomas are usually smaller than4 см and are more often lobular than rounded. They can grow slowly.

Approximately 90% of these formations occur in the peripheral parts of the lungs, within 2 cm of the pleura.

The characteristic clear, not quite even contours of the formations can be detected by conventional X-ray tomography. The structure of the tumour should be assessed by CT. On axial sections, benign tumours usually have a homogeneous structure and soft tissue density, on average +20...+40 HU. To differentiate such formations from peripheral cancer, solitary metastasis, tuberculoma, and arteriovenous aneurysm, it is necessary to use dynamic CT techniques. Benign tumours accumulate contrast material, but their density increases slightly, by no more than 20 HU.

In approximately $^{1}/_{3}$ of cases, droplet or central calcification in the form of corn kernels (rorcorn) is detected. Cases of fatty inclusions, which are considered pathognomonic, are determined with the same frequency (Fig. 2.7.16).

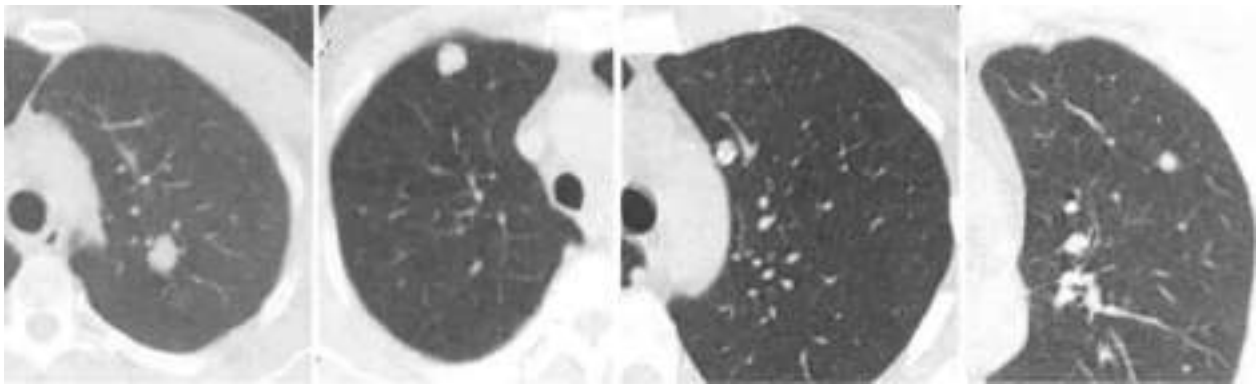

a b c d

Fig. 2.7.16. CT variants of gamartoma. In S_2 of the left lung, there is a homogeneous focal shadow (1,4 см) in diameter, with uneven contours, Hist+ (a). In $S_3$of the right lung, there is a focal shadow1,3 см) in diameter of irregular shape, Hist+ (b). In $S_3$of the left lung, there is a focal shadow 1.1 cm in diameter, including popcorn-type calcification (c). In $S_3$of the left lung, there is a focal shadow 0.8 cm in diameter, including popcorn-type calcification (d).

Fat in the pulmonary nodes usually indicates hamartoma, but may also be observed in liposarcoma metastases (Fig. 2.7.17-18). Determining the presence of intrapulmonary fat requires density measurement on thin sections (1-2 мм) to eliminate the influence of the partial volume effect.

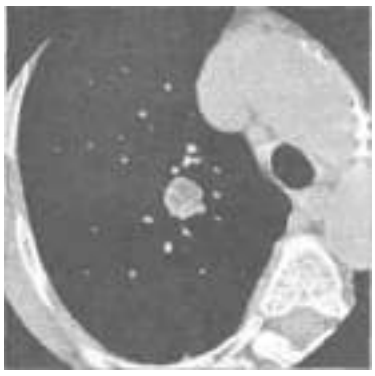

Fig. 2.7.17. Haematoma $S_{(2)}$ of the right lung. Focal shadow 1,8см in diameter, rounded in shape.

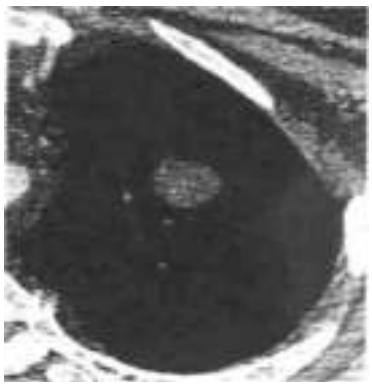

Fig. 2.7.18. Metastasis in $S_{(3)}$ $_{of}$the left lung with liposarcoma. The focal shadow has a clear contour and includes adipose tissue.

Carcinoid belongs to the group of neuroendocrine tumours and may be accompanied by ectopic production of hormones, such as ACTH. Pulmonary parenchyma is a rare location for carcinoids (only 10% of intrathoracic tumours of this type). Peripheral carcinoids tend to metastasise (50% of cases).

An intrapulmonary carcinoid appears as a well-defined node (Fig. 2.7.19). Isolated bronchial dilatation filled with mucus may be the only indirect sign of a carcinoid occluding the bronchial lumen. Cavities in these lesions are rare. Up to 30% of carcinoids contain calcifications. Most of them intensify significantly after intravenous contrast. Depending on the histological subtype, they may grow slowly.

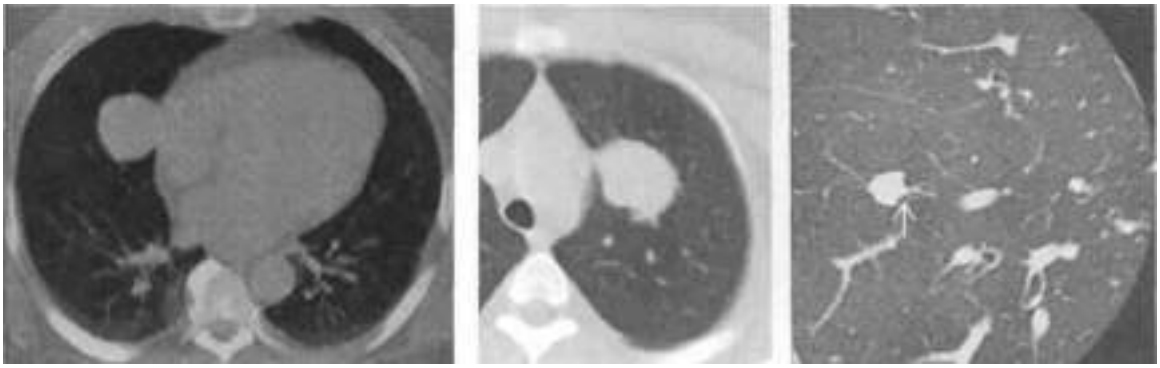

a **b** **c**

Fig. 2.7.19. Variants of intrapulmonary carcinoid. The focal shadow in $S_{(5)}$ of the right lung has clearly defined contours (a). In $S_{(3)}$ of the left lung, the focal shadow is 3.7 cm in diameter, has uneven contours and punctate calcification in the centre, and the surrounding lung tissue is unchanged (b). The carcinoid thickening is located within the lobe and is connected to the bronchus (c).

Bronchogenic cysts filled with fluid are thin-walled, single-chambered cystic formations, which are homoplastic dysembryomas in origin, with walls similar in structure to those of the bronchi and trachea. They are round in shape, have smooth, clear contours and a thin, smooth capsule

that is clearly visible on cross-sections. Densitometric analysis allows them to be reliably distinguished from soft tissue formations and tubercles.

Arteriovenous aneurysms (AVA) (vascular malformations) more often congenital than acquired (post-traumatic), are characterised by pathological shunting of blood between the pulmonary arteries and veins, less often between the bronchial and pulmonary arteries or between the bronchial arteries and pulmonary veins.

Between 40% and 60% of patients with AVA suffer from Rendu-Osler disease with telangiectasia of the skin or mucous membranes, as well as AVA in other organs (e.g., the liver).

AVA appear as rounded focal and focal shadows ranging in diameter from a few millimetres to several centimetres and usually have a feeding artery and a draining vein (the "slingshot" symptom) (Fig. 2.7.20). The use of spiral CT allows for exceptionally clear three-dimensional reconstructions of AVMs. When using surface volume reconstruction, the topography of the altered vessels is clearly visible without the additional administration of contrast medium (Fig. 2.7.21).

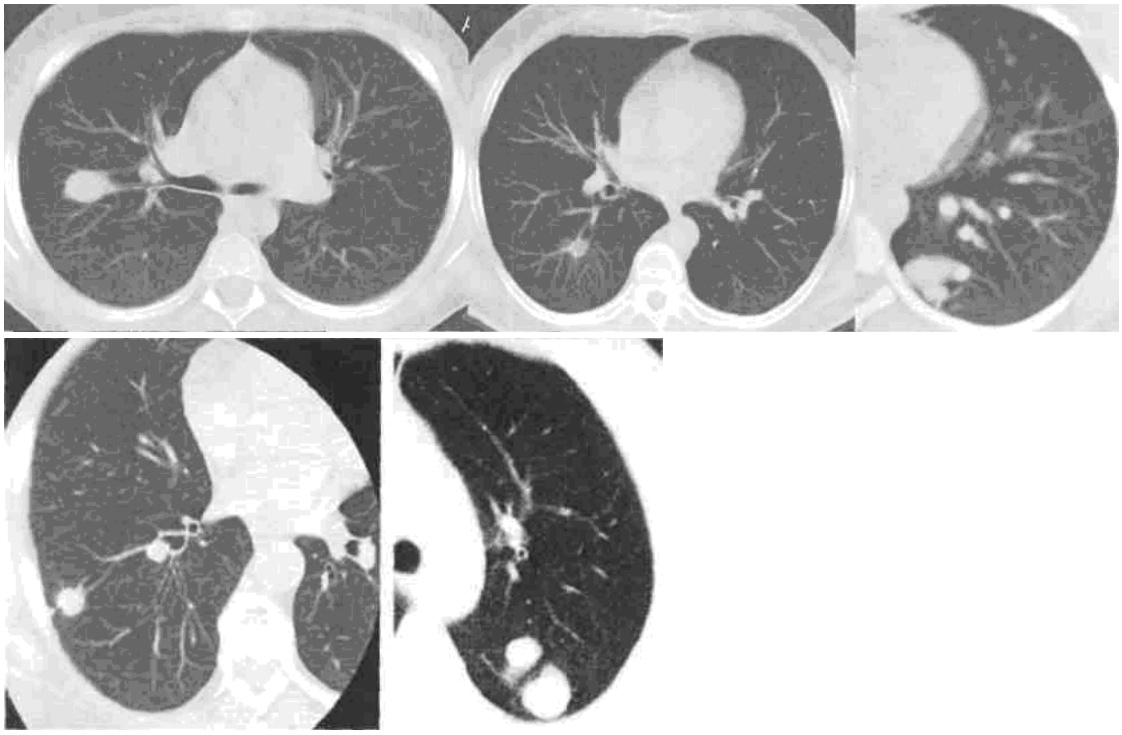

Fig. 2.7.20. Variants of pulmonary arteriovenous malformations. Round focal shadows have a feeding artery and a draining vein.

In complex AVMs, multiple feeding arteries and draining veins are detected. Most pulmonary AVMs (60-70%) are solitary and located in the central parts of the lungs. Calcifications are rarely found in them.
Intense contrast enhancement synchronous with arterial contrast is pathognomonic for AVMs. Only in rare cases is there no enhancement due to thrombosis.

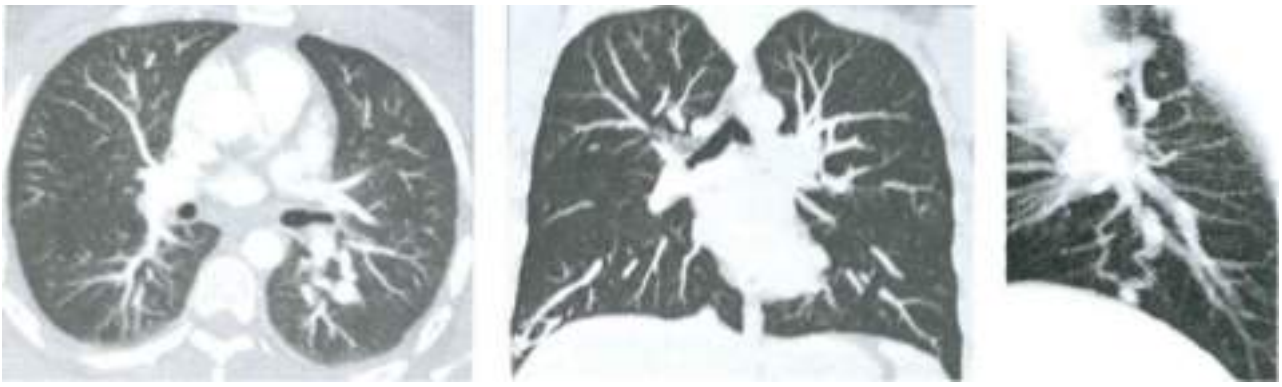

Fig. 2.7.21. Arteriovenous malformation in S_6 of the left, S_9 of the right (b) and S_8 of the left lung (c). CT angiography. Intense contrast enhancement synchronous with arterial contrast enhancement.

Sarcoidosis of the lungs can occasionally take the form of a solitary neoplasm (Fig. 3.7.22). Diagnosis is aided by the detection of enlarged mediastinal and bronchopulmonary lymph nodes, as well as nodules located mainly along the central bronchovascular bundles, and in the subpleural areas, uneven or nodular thickening of the septa, uneven contours of the interstitial layers.

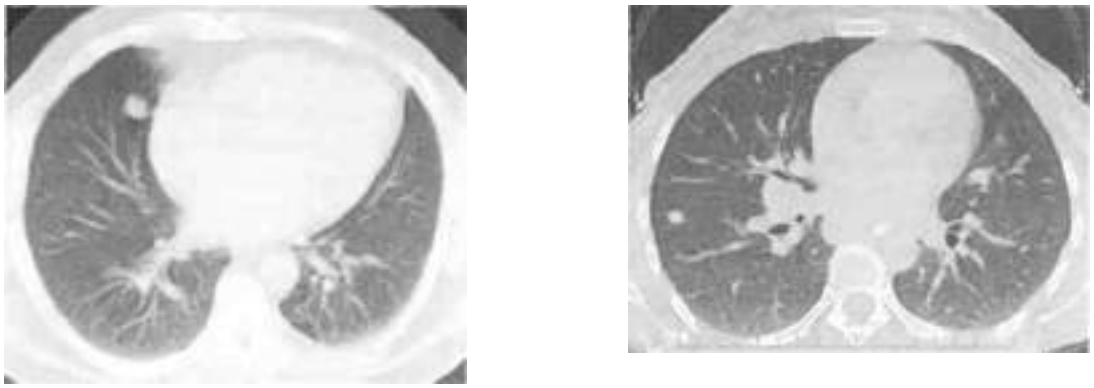

Fig. 2.7.22. Variants of sarcoidosis of the lungs and intrathoracic lymph nodes, Hist+. Homogeneous focal shadow in S_5 of the right lung with clear contours, small nodules located along the bronchovascular bundles (a). In S_6 of the right lung, there is a small focal shadow, with

small nodules located along the bronchovascular bundles and enlarged hilar lymph nodes (b).

2.8. Fibrocavernous tuberculosis

Fibrocavernous tuberculosis of the lungs is characterised by the presence of a fibrous cavity, the development of fibrous changes in the surrounding lung tissue, foci of bronchogenic contamination of varying ages in the same and/or opposite lung, constant or periodic mycobacterial excretion, chronic wave-like, usually progressive course.

As a rule, the bronchi draining the cavity are affected, and other morphological changes occur in the lungs: pneumosclerosis, emphysema, bronchiectasis. Fibrous-cavernous tuberculosis develops with infiltrative or disseminated forms in the case of a progressive course of the disease. The prevalence of changes in the lungs may vary, the process can be unilateral or bilateral with the presence of one or multiple cavities.

CT data allow for a detailed assessment of the entire spectrum of pathological changes in fibro-cavernous tuberculosis. In the lung tissue, mainly in the apical and posterior segments of the upper lobes, single or multiple cavities with thick walls are found. The diameter of such cavities can vary from 1 to 7-8 см. The detection of small and, conversely, giant cavities can be difficult with conventional X-ray examination, especially in the presence of pronounced pleural layers in the apical pleura. The outer contours of the cavities are uneven due to a sharp thickening of the interlobular and intralobular septa, areas of emphysema and linear scars. Bronchiectasis is visible in areas of lung tissue consolidation caused by fibrosis. Multiple polymorphic foci are located peribronchially and in the walls of the lobules. The costal, interlobar, and mediastinal pleura are thickened and sharply consolidated. The volume of the upper lobes is reduced.

Multiple polymorphic foci are found in the basal segments, resulting from bronchogenic contamination. Cavities and small infiltrates may also be located here. Usually, the basal segments of the lungs are distended due to the development of emphysema. The roots of the lungs are displaced upward and outward from the mediastinum, and the pulmonary arteries may be significantly dilated as a result of the development of arterial hypertension (Fig. 2.8.1-10).

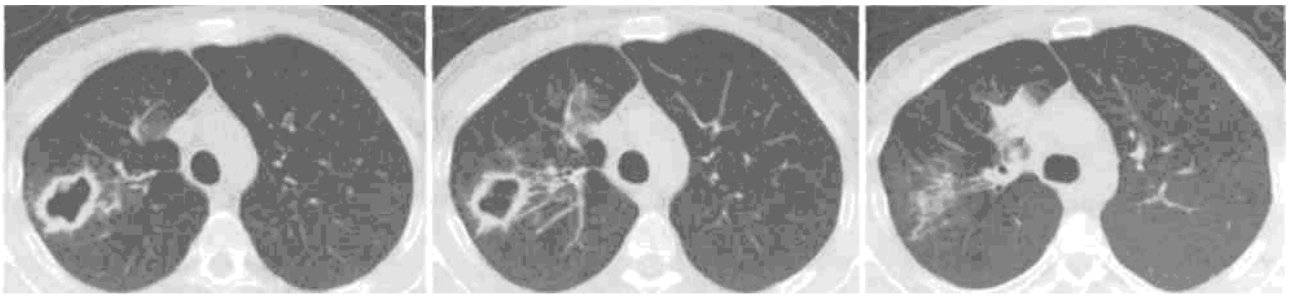

Fig. 2.8.1. Fibrocavernous pulmonary tuberculosis, MBT+. In $S_2$of the right lung, there is an irregularly shaped cavity with uneven, wide walls and no fluid level. Fibrotic changes and multiple polymorphic foci of bronchogenic contamination of varying ages in the surrounding lung tissue.

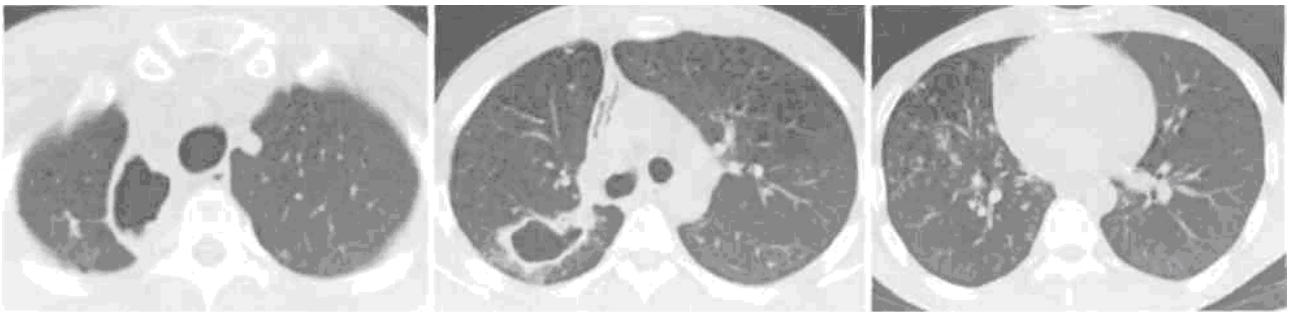

Fig. 2.8.2. Fibrocavernous tuberculosis of the lungs, MBT+. In $S_{1.6}$ of the right lung, there is an irregularly shaped cavity of decay with uneven wide walls without fluid level. S_4 of the right lung shows cirrhotic changes with light stripes of dilated and deformed bronchi.

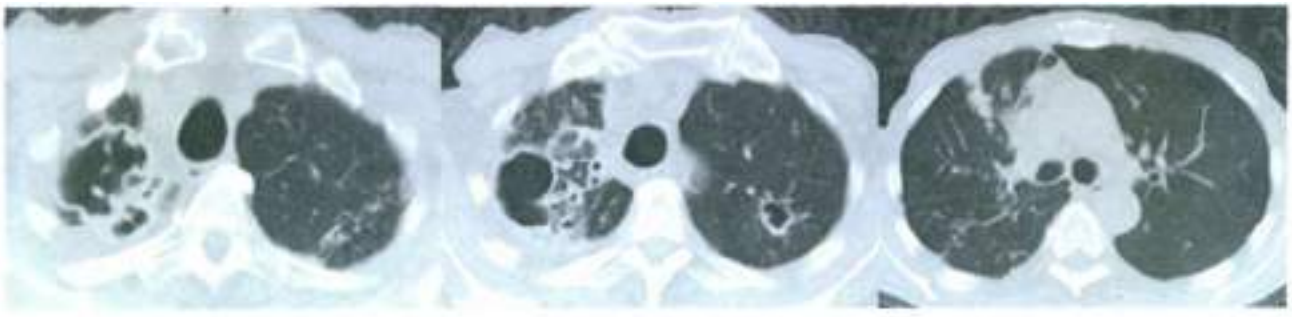

Fig. 2.8.3. Fibrocavernous tuberculosis of the lungs, MBT+. In the upper lobes of the lungs, there are irregularly shaped cavities with uneven, wide walls and no fluid level, pronounced fibrotic changes in the upper lobe of the right lung with multiple bronchiectasis, and multiple polymorphic foci of bronchogenic contamination in both lungs.

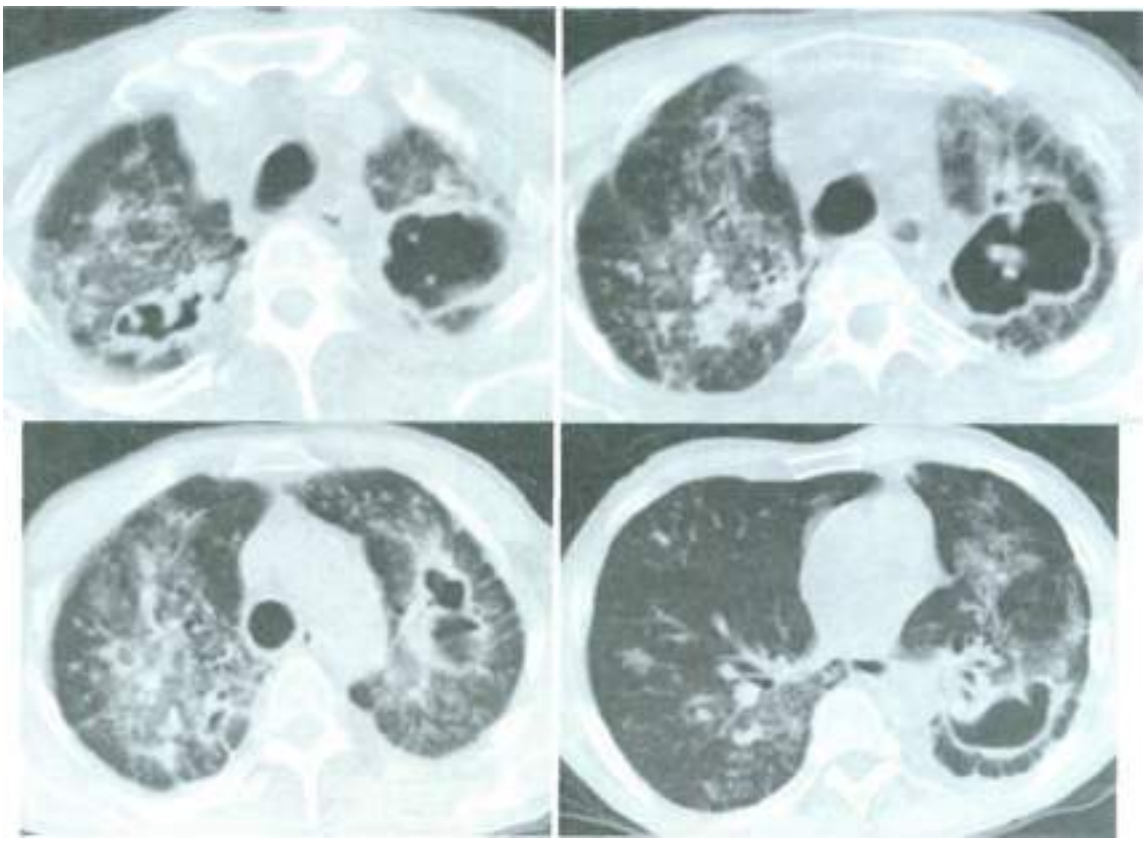

Fig. 2.8.4 a. Fibrocavernous pulmonary tuberculosis, MBT+ (before treatment). In the upper lobes and $S_6$of the left lung, there are irregularly shaped cavities with uneven wide walls without fluid level, pronounced fibrous changes in the upper lobes, multiple polymorphic foci of bronchogenic contamination in both lungs.

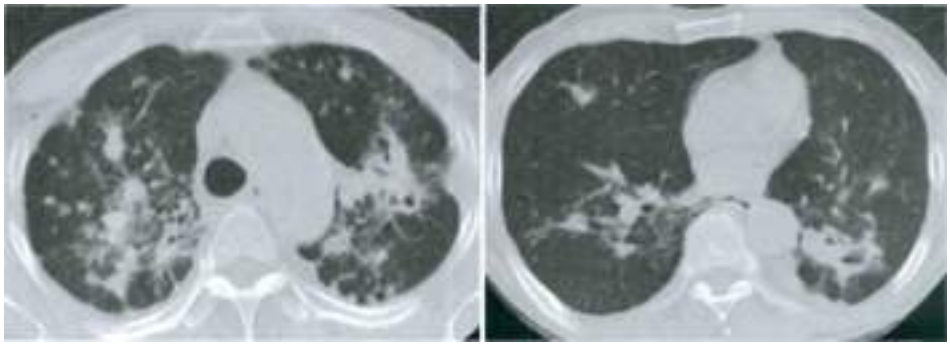

Fig. 2.8.4 b. The same patient. After five months of treatment, positive dynamics were observed in the form of scarring of the cavities in the upper lobes of the lungs, and the cavity in $S_6$of the left lung significantly decreased in volume. Pronounced cirrhotic and fibrotic changes in the upper lobes of the lungs. The costal pleura is unevenly thickened. In the

basal sections, there are multiple polymorphic foci of bronchogenic contamination and pronounced emphysematous changes.

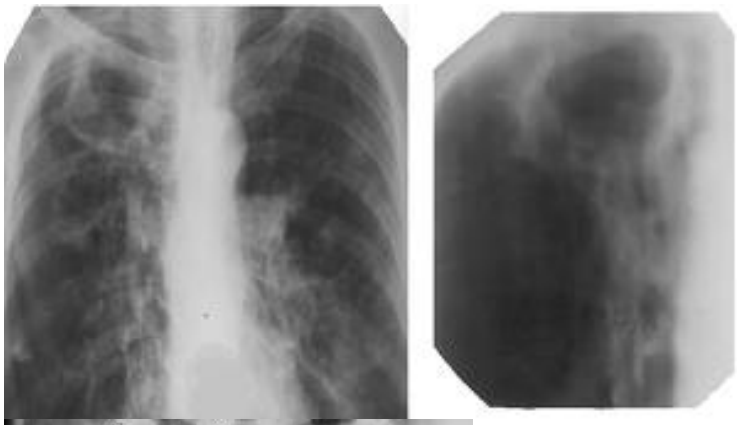

Fig. 2.8.5. Fibrocavernous pulmonary tuberculosis.

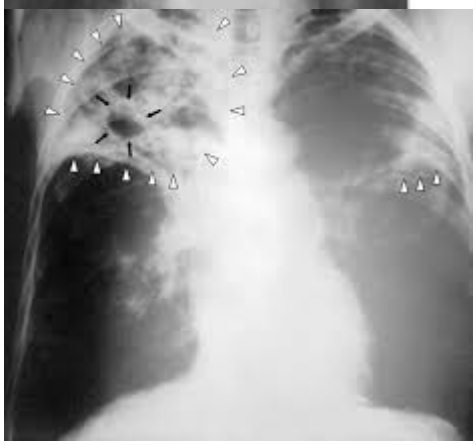

Fig. 2.8.6. Fibrocavernous pulmonary tuberculosis.

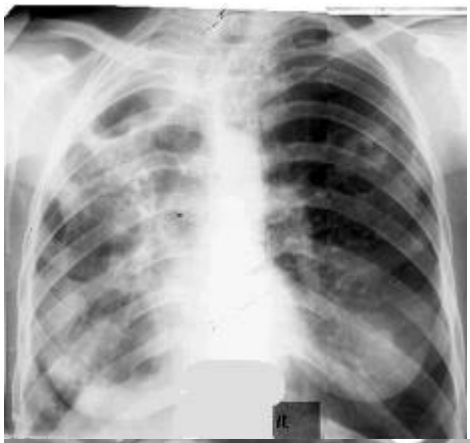

Fig. 2.8.7. Fibrocavernous tuberculosis of the lungs.

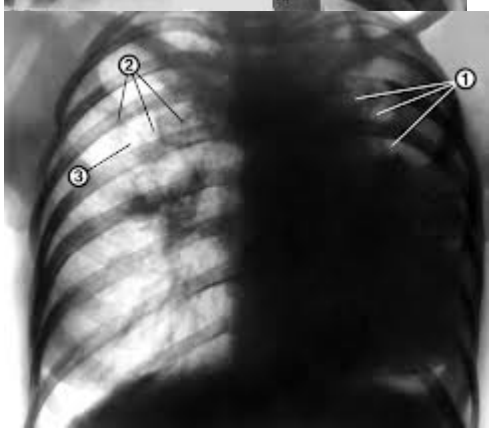

Fig. 2.8.8. Fibrocavernous tuberculosis of the lungs.

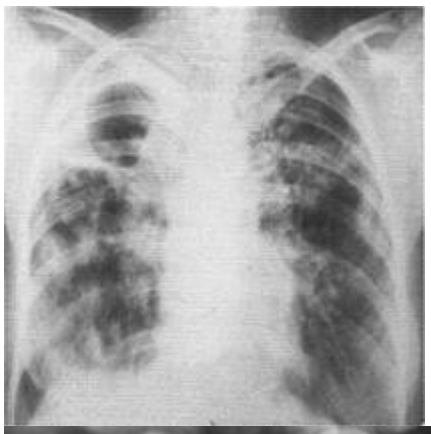

Fig. 2.8.9. Fibrocavernous tuberculosis of the lungs.

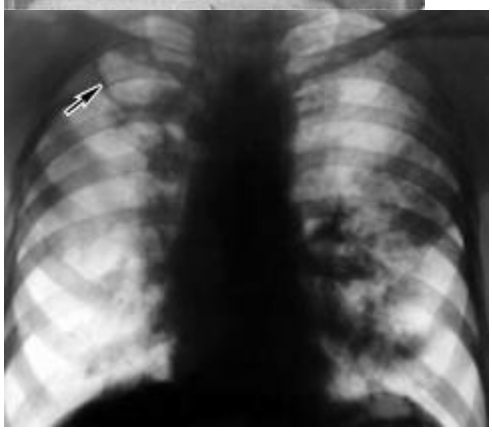

Fig. 2.8.10. Fibrocavernous tuberculosis of the lungs.

2.9. Cirrhotic pulmonary tuberculosis

Cirrhotic pulmonary tuberculosis is characterised by extensive scar tissue growth, among which active tuberculosis foci remain, causing periodic exacerbations and possible meagre mycobacterial excretion.

Cirrhotic pulmonary tuberculosis occurs as a result of the involution of fibro-cavernous, chronic disseminated, massive infiltrative pulmonary tuberculosis, pleural lesions, tuberculosis of the intrathoracic lymph nodes, complicated by bronchopulmonary lesions.

Cirrhotic tuberculosis can be segmental or lobar, limited or widespread, unilateral or bilateral, and is characterised by the development of bronchiectasis and pulmonary emphysema.

Cirrhotic changes, in which a fibrous cavity with bronchogenic contamination and repeated prolonged mycobacterial excretion is detected, should be classified as fibro-cavernous tuberculosis. Cirrhotic tuberculosis must be distinguished from pulmonary cirrhosis, which is a post-tuberculosis change without signs of activity. Pulmonary cirrhosis is classified as a residual change after clinical recovery.

The CT semiotics of cirrhotic tuberculosis is determined primarily by the initial form of the inflammatory process. In patients who have undergone

disseminated and fibro-cavernous tuberculosis, bilateral cirrhosis develops with damage to a significant part of the upper lobes of both lungs. In this case, the lung tissue is unevenly compacted, with large areas of "frosted glass" and local alveolar changes. Against the background of these changes, multiple, often small foci with clear contours are visible. Some of them may be calcified (Fig. 2.9.1-4). Unlike active disseminated tuberculosis, diffuse post-tuberculosis cirrhosis is associated with widespread bronchiectasis and emphysema. These changes may not be visible on conventional X-rays, but can be reliably detected by CT.

With the development of cirrhosis against the background of infiltrative, focal, and primary tuberculosis, local, more often unilateral, partial and segmental changes predominate (Fig. 2.9.5-11). The volume of the affected part of the lung is significantly reduced, and the adjacent sections are distended. Bronchiectasis, emphysematous cavities, and multiple, partially calcified foci are visible in the area of consolidation.

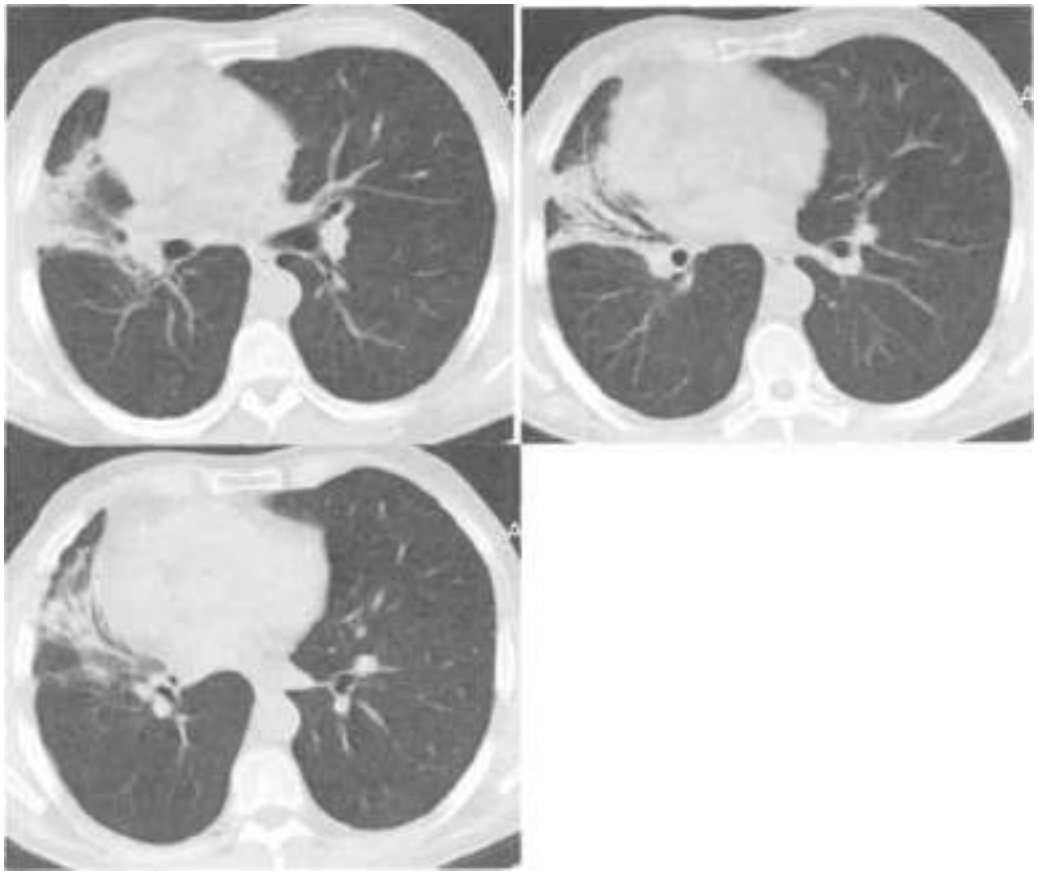

Fig. 2.9.1. Cirrhotic tuberculosis of the middle lobe, MBT+. The volume of the affected lobe is significantly reduced, there are areas of "ground

glass" and zones of heterogeneous thickening with fractional bronchiectasis, the mediastinum is shifted to the right.
If cirrhosis has developed against a background of obstructive atelectasis, the lumen of the partial or segmental bronchus is narrowed, and focal calcifications are visible peribronchially around it. Such changes most often occur in the middle lobe of the right lung. CT has significant advantages over X-ray examination and bronchoscopy in assessing such changes. The combination of bronchostenosis, peribronchial calcifications, and bronchiectasis in the airless lobe is typical for tuberculous cirrhosis.

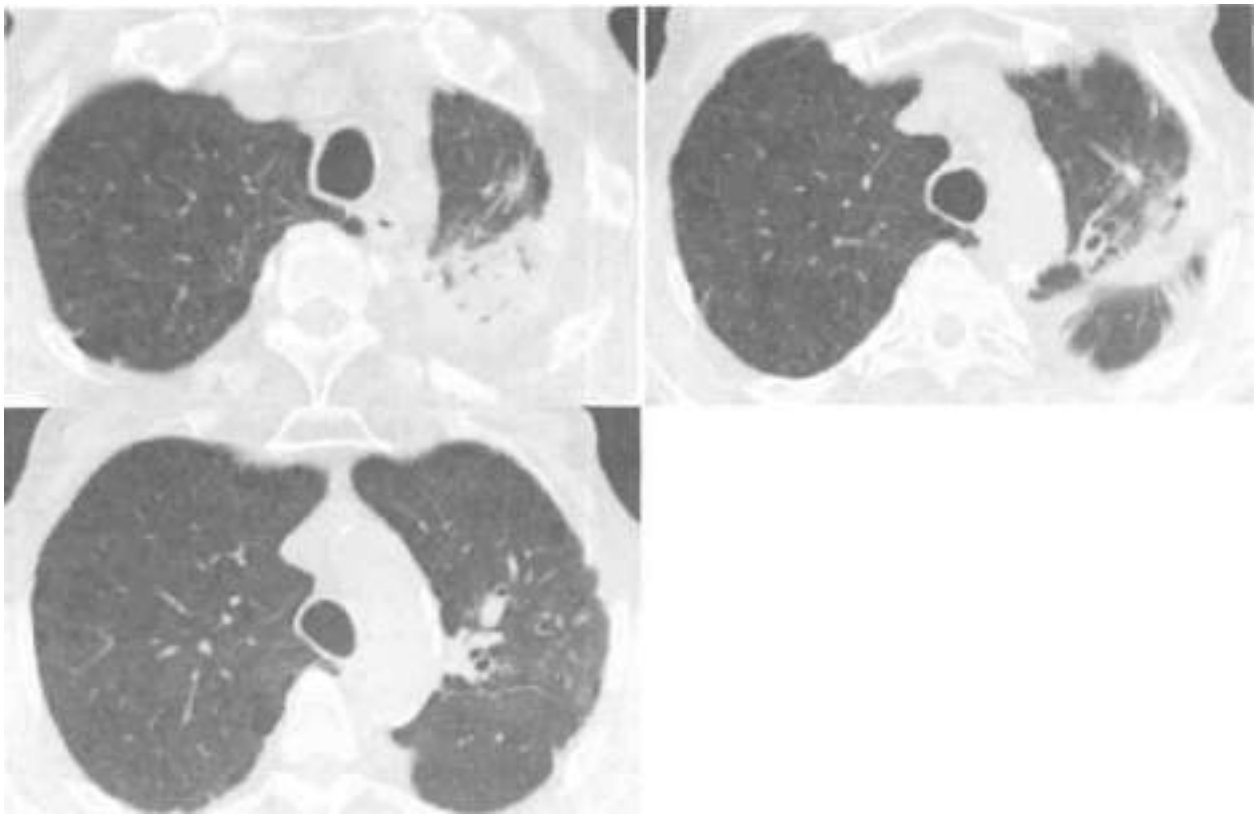

Fig. 2.9.2 Cirrhotic tuberculosis of the upper lobe of the left lung, MBT+. The volume of the lobe is significantly reduced, fractional bronchiectasis and multiple foci are visible in the area of heterogeneous thickening, the costal pleura is thickened with uneven contours, and the mediastinum is shifted to the left.

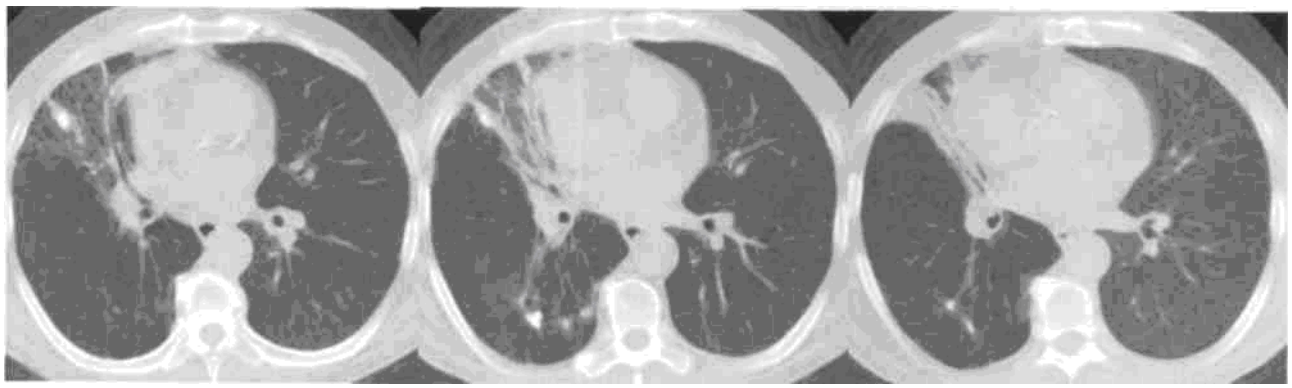

Fig. 2.9.3. Cirrhotic tuberculosis of the middle and lower lobes of the right lung, MBT+. The volume of the affected lobe is significantly reduced, with areas of "ground glass" opacity and zones of heterogeneous thickening with fractional bronchiectasis. There are isolated calcifications of various sizes and shapes, the mediastinum is shifted to the right.

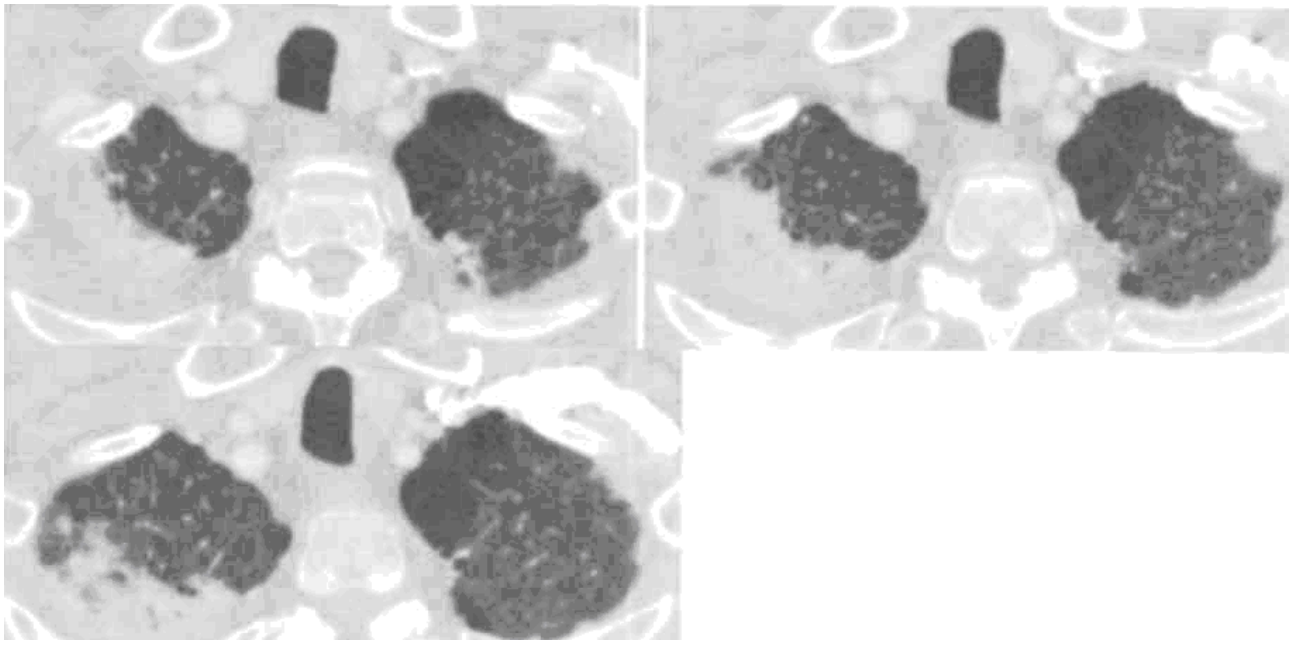

Fig. 2.9.4. Cirrhotic tuberculosis of the upper lobes of the lungs, MBT+. The volume of the lobe is significantly reduced, fractional bronchiectasis and numerous foci of calcification are visible in the area of heterogeneous thickening, the costal pleura is thickened and has uneven contours, and there is pronounced paraseptal emphysema with subpleural bullae.

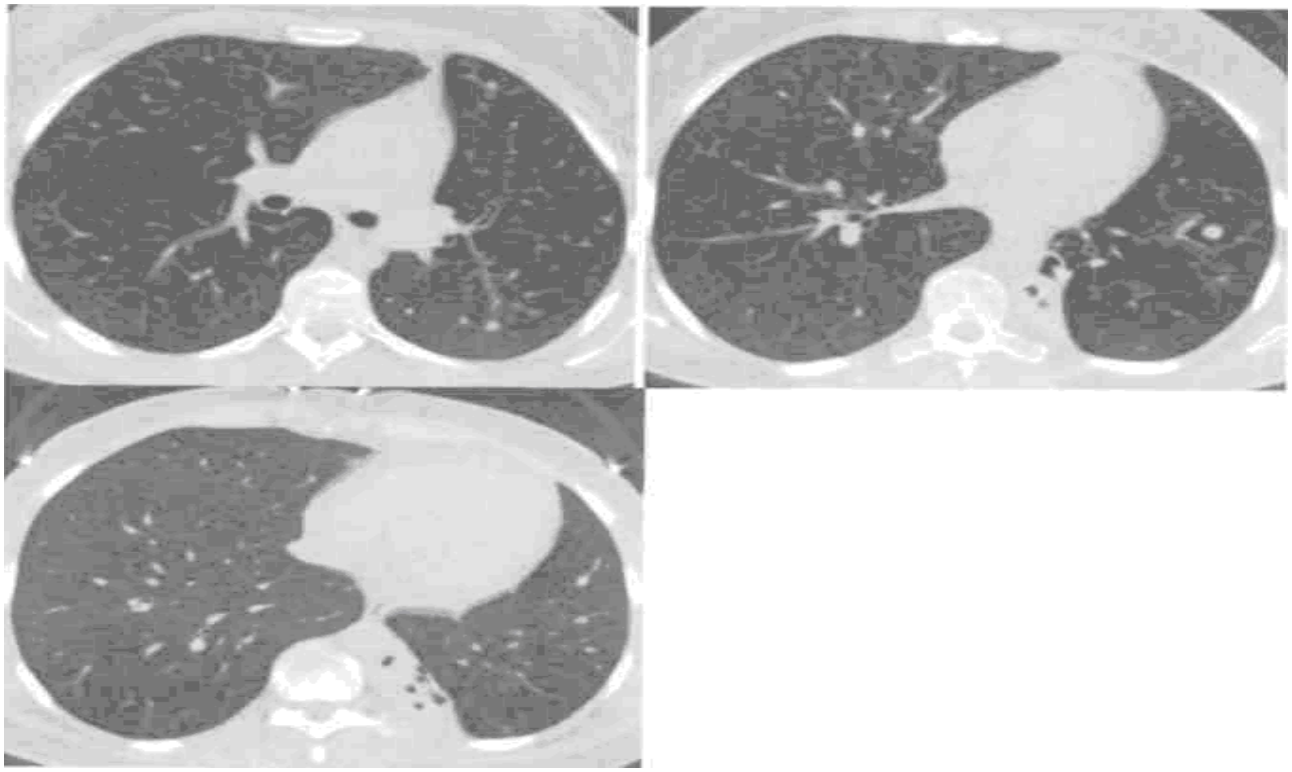

Fig. 2.9.5. Condition after treatment of tuberculosis with transition to cirrhosis S_{10} of the left lung. Against the background of the cirrhotic segment, light stripes of dilated and deformed bronchi are visible. Multiple dense foci in both lungs.

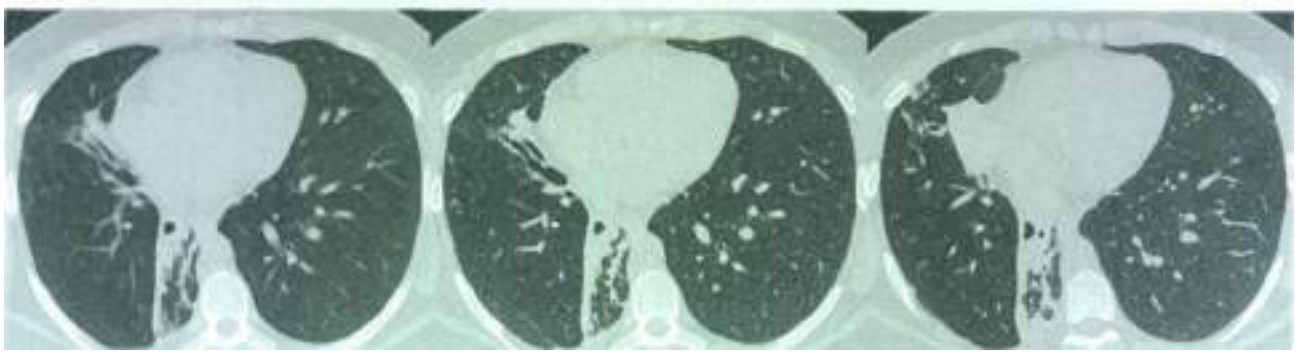

Fig. 2.9.6. Condition after cured tuberculosis with transition to cirrhosis of the middle and lower lobes of the right lung. Against the background of cirrhotic changes in sharply reduced segments, light stripes of dilated and deformed bronchi (bronchiectasis) are determined, the lumens of the segmental bronchi are narrowed, multiple dense foci.

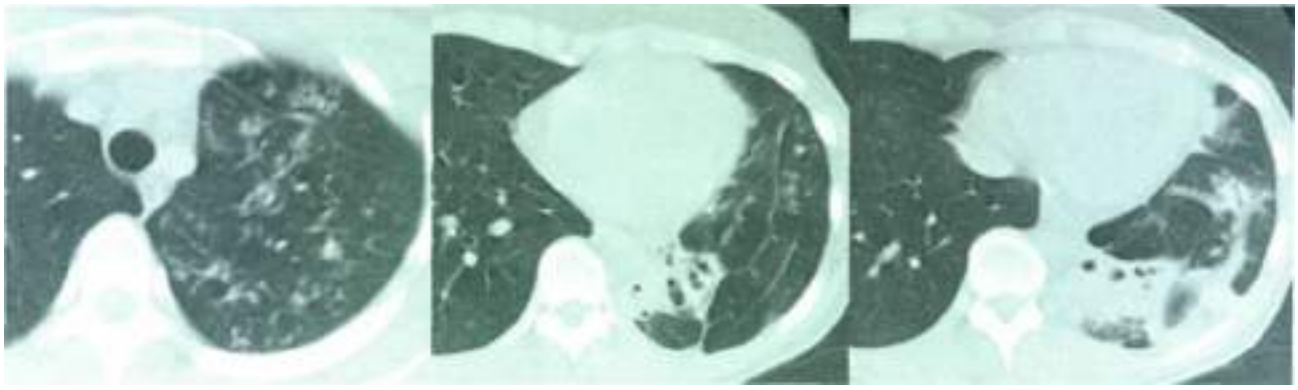

Fig. **2.9.7.** Condition after cured tuberculosis with transition to fibrotic-focal changes in the upper lobe and cirrhosis of the lower lobe of the left lung. In the upper lobe of the left lung, there are multiple polymorphic foci against a background of areas of pneumofibrosis. In the cirrhotic changes $S_{8,9,10}$ of the left lung, sac-like bronchiectasis is determined. The volume of the left lung is significantly reduced, with emphysema in the basal sections.

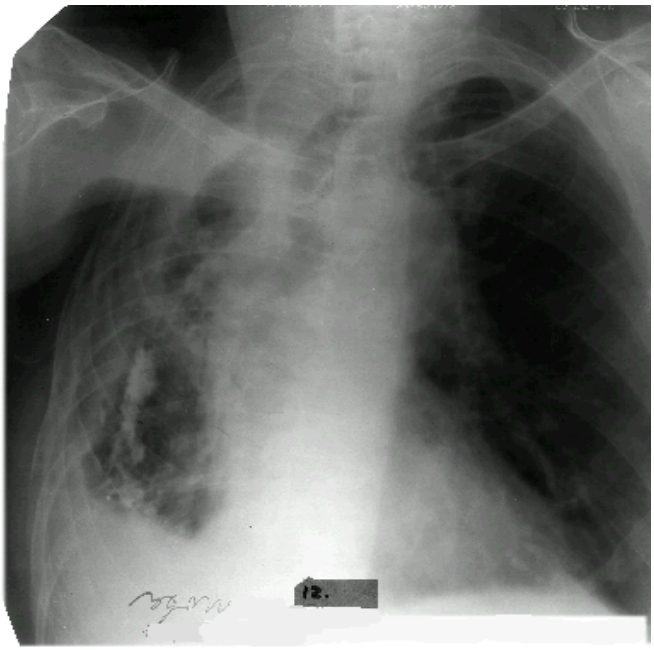

Fig. 2.9.8. Cirrhotic pulmonary tuberculosis.

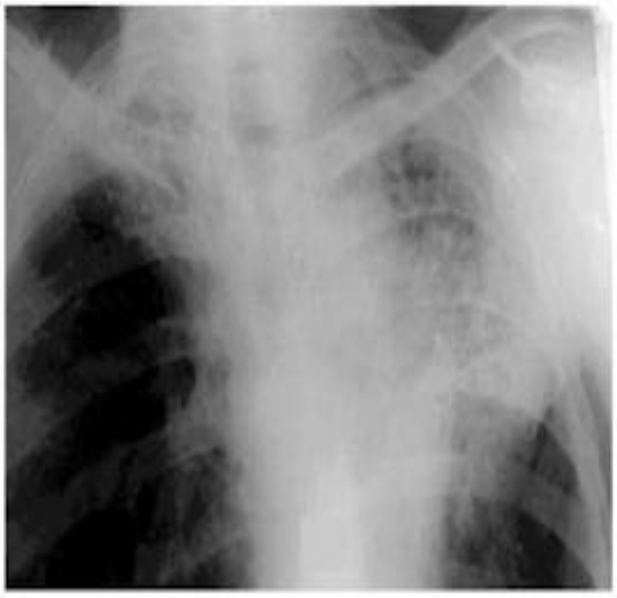

Fig. 2.9.9. Cirrhotic pulmonary tuberculosis.

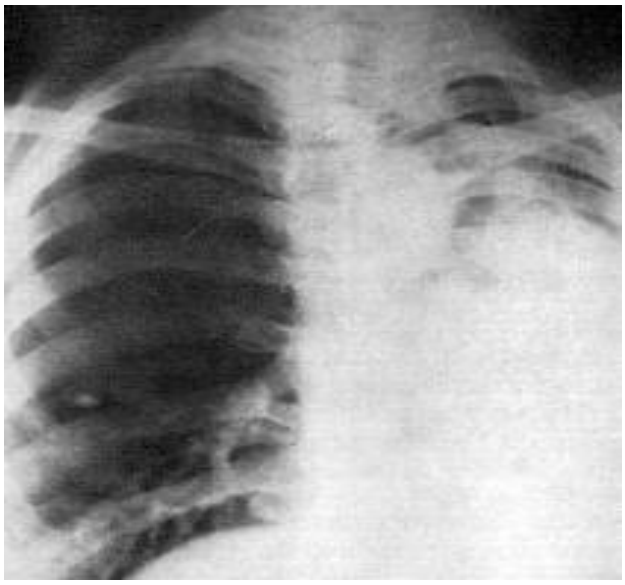

Fig. 2.9.10. Cirrhotic pulmonary tuberculosis.

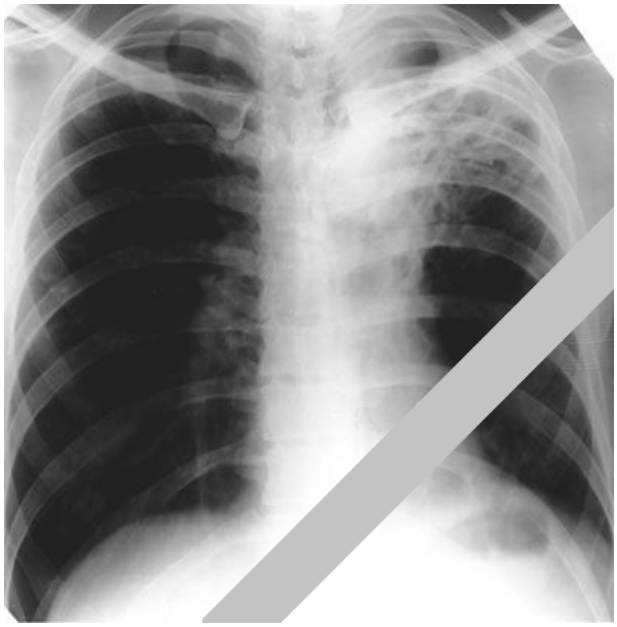

Fig. 2.9.11. Cirrhotic pulmonary tuberculosis.

2.10. Tuberculosis of the trachea and bronchi

Tuberculosis of the bronchi and trachea occurs as a complication of other forms of primary and secondary tuberculosis of the lungs and intrathoracic lymph nodes. Only occasionally are these lesions isolated.

There are three main forms of tuberculosis of the bronchi and trachea: infiltrative, ulcerative and fistulous (lymphobronchial, bronchopleural fistulas). Complications include stenosis of varying degrees, granulations and broncholiths. Under the influence of treatment, clinical cure may occur – without residual changes or with residual changes in the form of scars, fibrous thickening, stenosis, etc. (Fig. 2.10.1).

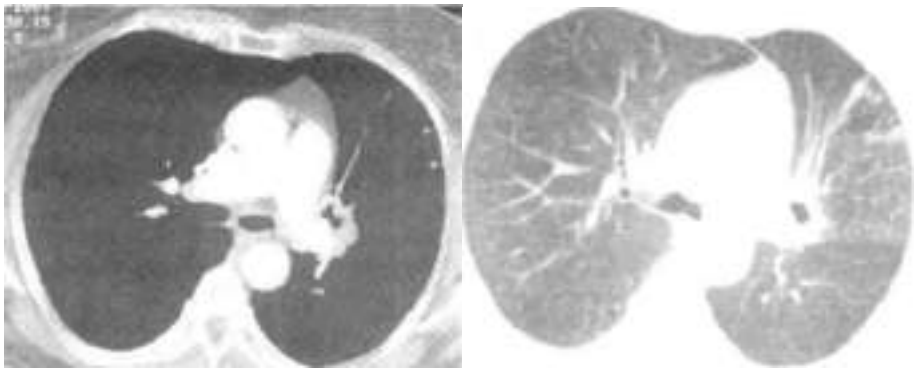

Fig. 2.10.1. Tuberculosis of the bronchus of the upper lobe of the left lung. CT angiography. In the bronchopulmonary node at the root of the left lung, there is a cavity of decay connected to the upper lobe bronchus by a fistulous tract. Bronchogenic contamination in the lung tissue.

Tuberculosis of the small bronchi or tuberculous endobronchitis occurs in any form of specific process in the lungs, in particular in tuberculous foci and infiltrates, in the draining cavities of the bronchi, and is not an independent form of the inflammatory process. In some patients, bronchogenic or lymphobronchogenic spread of infection leads to tuberculous inflammation of the bronchi outside the area of the main pathological process. The subsequent stenosis of the segmental or subsegmental bronchus is accompanied by the expansion of the distal parts of the bronchial tree. As a result, retention cysts filled with bronchial secretions are formed (Fig. 2.10.2-3).

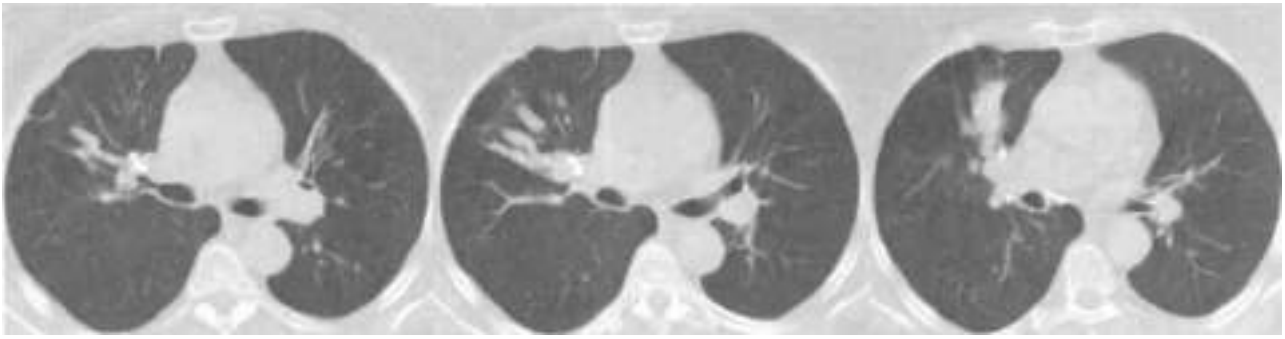

Fig. 2.10.2. Retention cysts in the middle lobe in a patient with tuberculosis, MBT+. Calcification (broncholiths) in the middle lobe bronchus area, bronchial lumen in cysts is not visible.

Tuberculosis of the trachea and large bronchi is usually associated with damage to the adjacent lymph nodes. Typical localization of changes is the middle lobe bronchus and main bronchi, especially the left one. An inflammatory infiltrate forms around the affected bronchus – a conglomerate formed by caseous-altered lymph nodes that have merged. The lumen of the bronchus narrows until it is completely obstructed. When a fistula forms in the corresponding lobe of the lung, bronchogenic dissemination may occur.

The use of CT allows you to identify and study in detail the narrowed area, its location, length, as well as the condition of the peribronchial tissues and lungs. If there are typical foci in the lung tissue, diagnosis is greatly simplified. However, in the absence of changes in the lungs or in the formation of atelectasis, it is not possible to distinguish a conglomerate of enlarged lymph nodes from central cancer and carcinoid tumours. The diagnosis is based on bronchoscopy data, biopsy, and the results of sputum or bronchial lavage fluid tests.

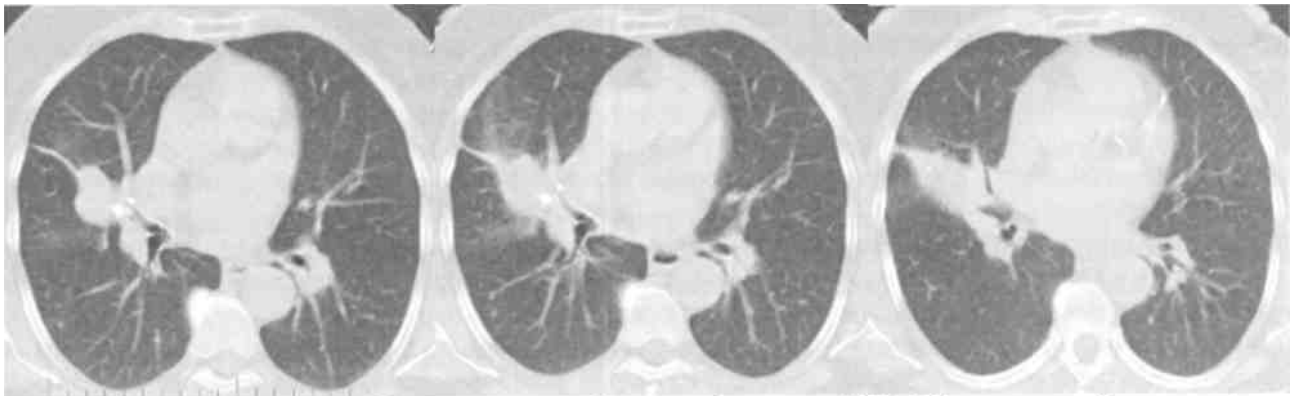

Fig. 2.10.3. Retention cyst in $S_4$of the right lung in a patient with tuberculosis, MBT+. Calcification (broncholiths) in the area of the end of the draining bronchus, the cyst has a typical V-shaped form, the lumen of the bronchi in the cyst is not visible.

Broncholiths are calcified fragments of caseous masses that have fallen into the lumen of the bronchus in the lymph nodes.

2.11. Miliary tuberculosis

Miliary tuberculosis is a haematogenous, almost always generalised form of tuberculosis, characterised by a uniform dense rash of small, millet-like tuberculous nodules in the lungs. It is predominantly generalised with the formation of foci in the lungs, liver, spleen, intestines, and meninges. Less commonly, miliary tuberculosis occurs as a lesion of the lungs only.

Based on the clinical course, the following *variants* are distinguished *typhoid*, characterised by fever and severe intoxication; *pulmonary,* in which the clinical picture is dominated by symptoms of respiratory failure against a background of intoxication; *meningeal* (meningitis and meningoencephalitis) as a manifestation of generalised tuberculosis.

In CT examination, acute small-focal and miliary disseminations are characterized by the presence of a large number of monomorphic foci in both lungs, located throughout both lungs from the apices to the diaphragm and from the chest wall to the mediastinum (Fig. 2.11.1-8).

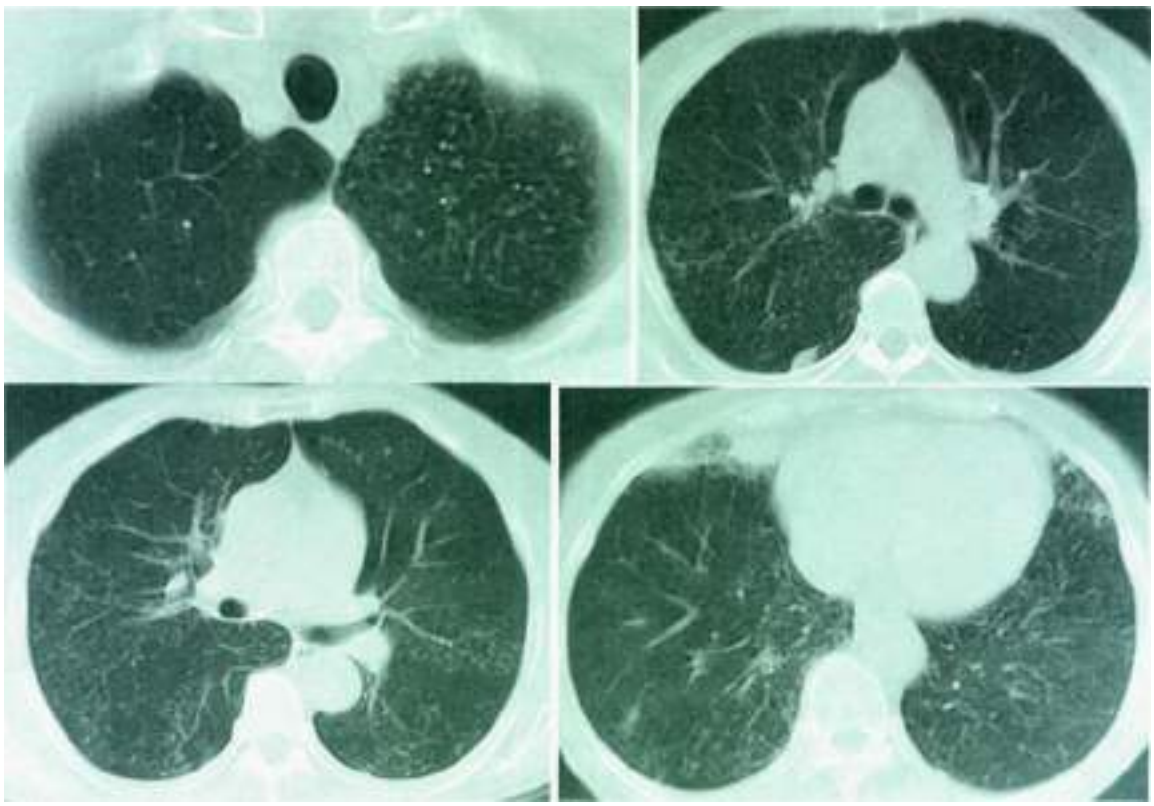

Fig. 2.11.1. Acute haematogenous disseminated pulmonary tuberculosis, HIST+. Multiple monomorphic small foci are located chaotically in both lungs without connection to the interstitial structures.

The foci have a regular rounded or oval shape, relatively clear contours, and a homogeneous structure. There are no cavities of destruction or pulmonary emphysema. Most of the foci are located randomly in the lung tissue, and it is usually impossible to establish their relationship with the anatomical elements of the lung lobules. Focal changes are combined with a moderately pronounced reaction of interstitial structures in the form of diffuse thickening of the interlobular septa. In some of them, small foci are determined. Some of the foci are located in the cortical and interlobar pleura.

The differential diagnosis of miliary tuberculosis can be quite difficult. The most common ones in the practice of phthisiatric institutions are: atypical and viral pneumonia, cancer metastases, sarcoidosis, disseminated fungal lesions, pneumoconiosis.

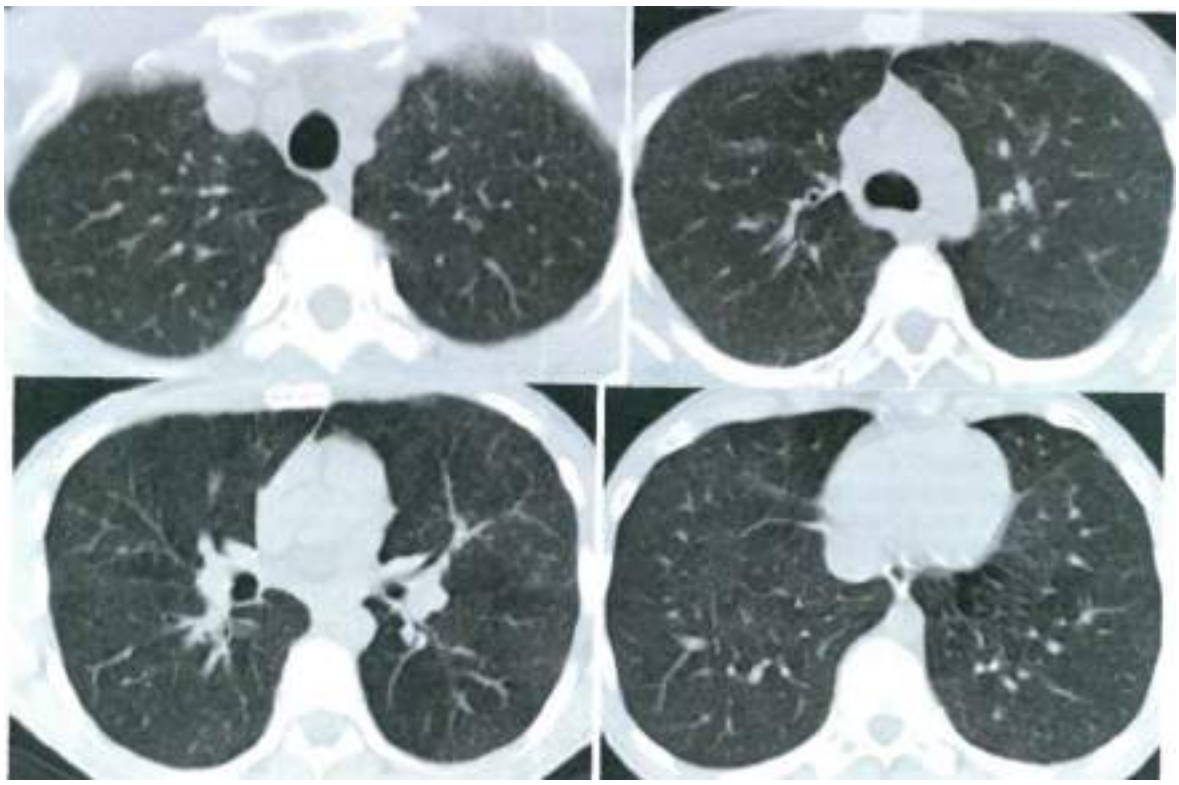

Fig. 2.11.2. Acute haematogenous disseminated pulmonary tuberculosis, HIST+. Multiple monomorphic small foci are randomly located in both lungs, combined with a moderately pronounced reaction of interstitial structures in the form of diffuse thickening of the interlobular septa of the "frosted glass" type.

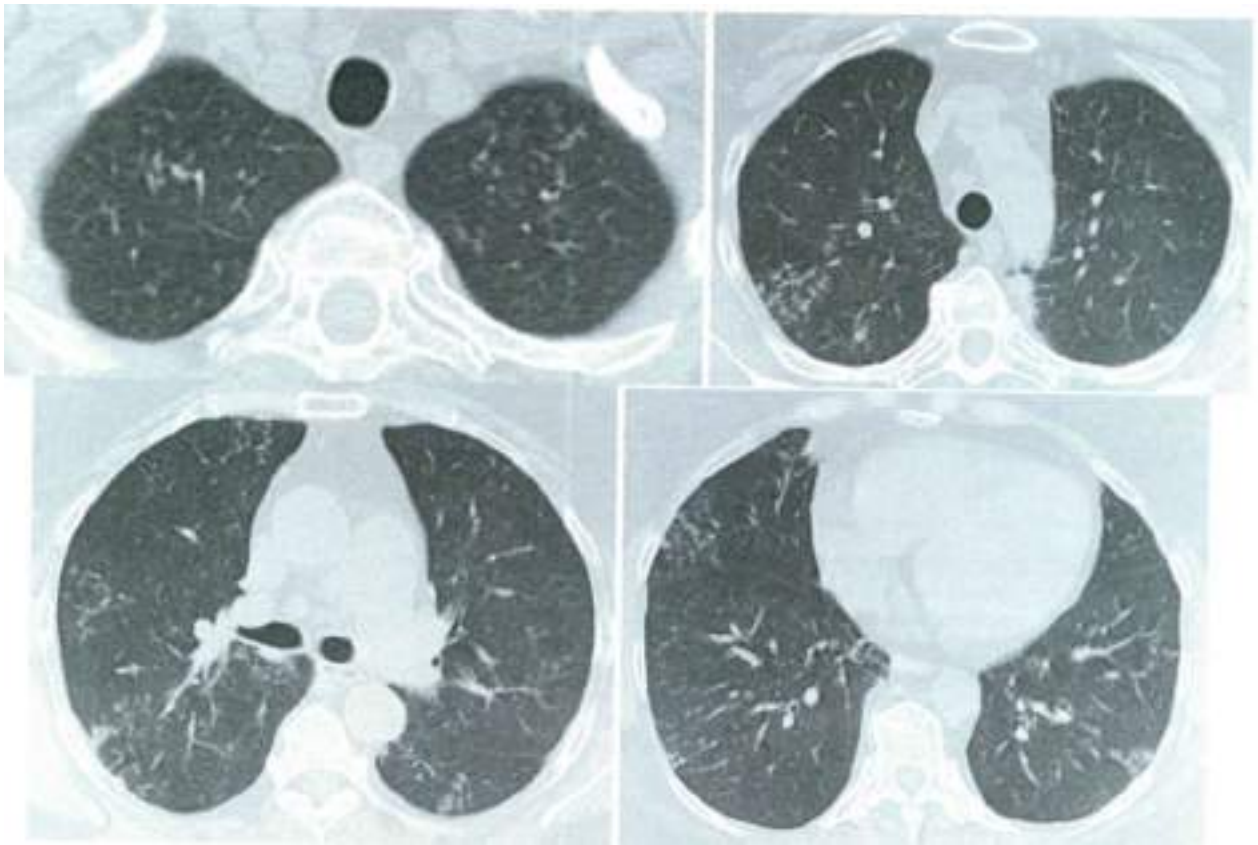

Fig. 2.11.3. Acute haematogenous disseminated pulmonary tuberculosis, HIST+. Multiple small foci are randomly distributed in both lungs, combined with a moderately pronounced reaction of interstitial structures in the form of diffuse thickening of interlobular septa of the "frosted glass" type.

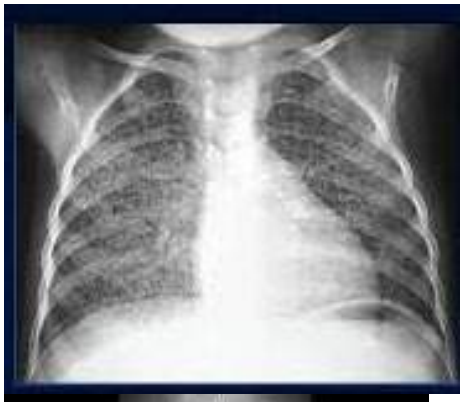

Fig. 2.11.4. Miliary tuberculosis.

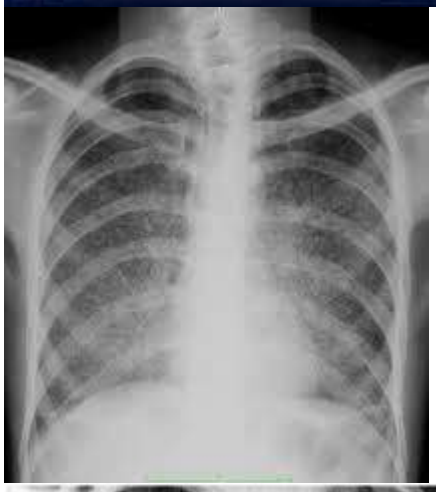

Fig. 2.11.5. Miliary tuberculosis.

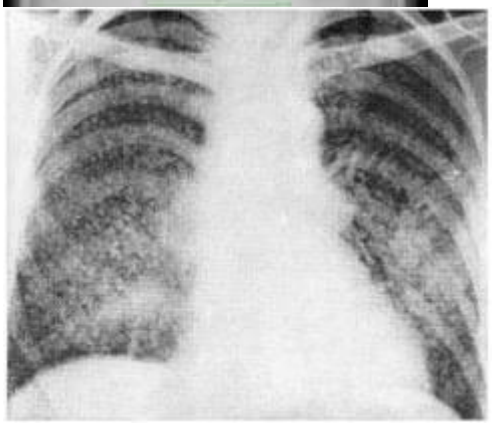

Fig. 2.11.6. Miliary tuberculosis.

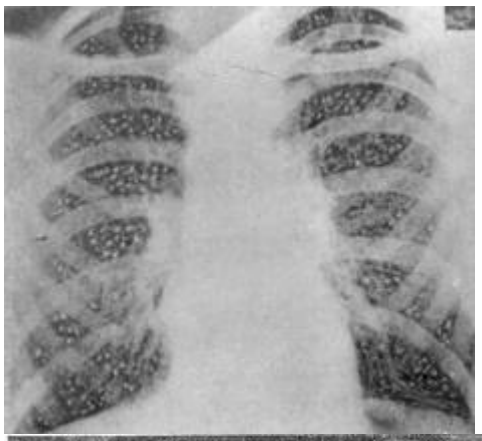

Fig. 2.11.7. Miliary tuberculosis.

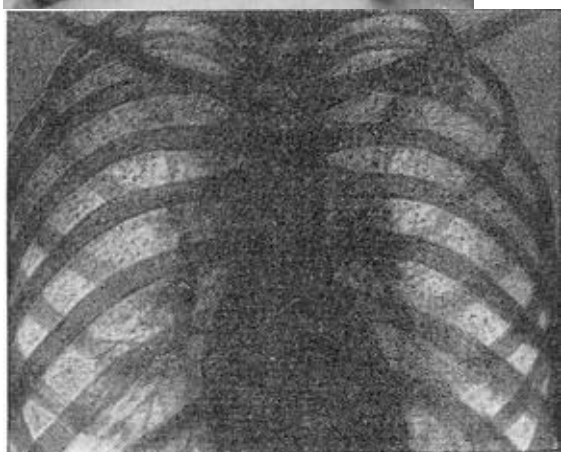

Fig. 2.11.8. Miliary tuberculosis.

2.12. Differential diagnosis of Pleural Effusion

Pleurisy is an inflammation of the pleural layers with the formation of fibrin on their surface or the accumulation of various types of exudate in the pleural cavity. As a rule, pleurisy (P) is not an independent disease, but complicates the course of pathological processes in the lungs, chest, diaphragm, mediastinal organs and subdiaphragmatic space, or is one of the manifestations of systemic diseases. Recently, there has been a significant increase in the prevalence of parapneumonic and tuberculous pleurisy, which requires improvement in the methods of diagnosis and treatment of these complications.

Pleural effusion is one of the most common pathological syndromes in internal medicine, occurring in 5-10% of therapeutic patients. About 40% of pneumonia cases are accompanied by more or less severe pleurisy. At the same time, depending on the aetiology of pneumonia, its incidence varies from 10% to 70-95%.

Metastatic pleurisy is a complication of lung cancer, breast cancer, as well as lymphomas and leukaemias. Thus, in lung cancer, it occurs in

24-50% of cases, in breast cancer – up to 48%, in lymphomas – up to 26%, and in ovarian cancer – up to 10% of patients. Systemic lupus erythematosus occurs with pleural involvement in 50% of patients.

Classification of pleurisy. According to aetiology, the following types are distinguished:

Infectious:

- tuberculous (20-50%);
- bacterial;
- pneumococcal (parallel to pneumonia, parapneumonic (developing together with pneumonia) and metapneumonic (after pneumonia) pleurisy may develop);
- staphylococcal (mainly causes empyema of the pleura);
- mycoplasma;
- caused by Friedlander's bacillus;
- caused by Pseudomonas aeruginosa, Escherichia coli;
- fungal;
- aspergillosis;
- candidomycosis;
- blastomycosis;
- parasitic.

Aseptic:

- carcinomatous (40%);
- metastatic (lung cancer accompanied by pleurisy in 43%, breast cancer in 23%, lymphoma in 8%);
- mesothelioma – primary tumour of the pleura. Occurs with a frequency of 2:1000. Most often affects men aged 20-40 who have had contact with asbestos. Characterised by the appearance of haemorrhagic exudate, with an average prognosis of 1-2 years after diagnosis.
- Enzymatic – acute pancreatitis;
- allergic;
- post-infarction allergic (Dresler's syndrome). It manifests itself in three Ps: pleurisy, pericarditis, pneumonitis. The fourth P is shoulder pain.
- pulmonary artery embolism;
- systemic vasculitis;

- Wegener's granulomatosis;
- nodular periarteritis;
- systemic connective tissue diseases;
- rheumatoid arthritis;
- post-traumatic;
- electrical shock;
- Becket's sarcoidosis;
- uremic;
- radiation therapy.

By the nature of the exudate:

- fibrinous;
- serous-fibrinous;
- serous;
- purulent;
- putrid;
- haemorrhagic;
- eosinophilic;
- cholesterolic;
- chylous.

By course:

- acute;
- subacute;
- chronic.

By prevalence

- diffuse;
- encapsulated;
- apical;
- paracostal;
- osseo-diaphragmatic;
- basal;
- paramediastinal;
- intercostal.

From a clinical point of view, depending on the type of effusion, it is advisable to distinguish between dry, exudative and purulent pleurisy. Most often, pleurisy complicates the course of pneumonia, tuberculosis,

malignant tumours and systemic connective tissue diseases. In 20% of cases, it is not possible to establish the cause of pleurisy.

There are four syndromes in the clinical course:

- dry pleurisy syndrome;
- exudative pleurisy syndrome;
- empyema pleura syndrome;
- underlying disease syndrome.

Clinical features of fibrinous pleurisy. Complaints of pain when breathing, coughing, or leaning to the opposite side. Prolonged low-grade fever, especially in the evening, sweating. Objectively: breathing is shallow, rapid, the patient's position is forced (the patient lies on the affected side to reduce pain). On physical examination, along with the symptoms of the underlying disease, localised or widespread pleural friction noise is heard.

In exudative pleurisy, the pain may weaken, but the patient experiences a feeling of heaviness in one or both halves of the chest, progressive shortness of breath, dry or slightly productive cough (reflexive). The patient assumes a forced position. On examination, cyanosis, acrocyanosis, and swollen neck veins are found. On examination of the chest: bulging of the intercostal spaces, the affected half lags behind during breathing. On palpation, limited excursion, no vocal tremor. Percussion reveals dullness of the pulmonary sound. Auscultation reveals no breath sounds (if the amount of fluid is small, breath sounds may be present; if there is pus, breath sounds may become harsh or bronchial. In the horizontal position, vesicular breathing will be weakened).

Plan for examining a patient with effusion in the pleural cavity.

1. Clinical examination (complaints, medical history, physical data).
1. Chest X-ray, tomography, bronchoscopy, bronchography, computed tomography/
2. Thoracocentesis (pleural puncture).
3. Examination of pleural fluid: appearance, protein content, LDH, glucose, amyloid levels, etc.
4. Cytological examination of pleural effusion.
5. Invasive examination methods: thoracoscopy, pleural biopsy, lung scan, angiography.

Pleural puncture is of great importance in the diagnosis of pleurisy.
Thoracocentesis is performed in the 7th intercostal space along the posterior axillary or scapular line at the upper edge below the underlying rib. The fluid obtained is examined to determine its colour and consistency. It is necessary to determine whether it is transudate or exudate: it is necessary to determine the amount of protein, perform a Rivolta test, and examine the LDH content. Transudate: protein content less than 32 g/l, LDH level less than 1.3 mmol/l, Rivolta test negative. Exudate: protein greater than 36 g/l, LDH level 1.75 mmol/l, Rivalta test positive. To clearly determine transudate or exudate, it is necessary to determine the coefficients – the level of protein in the effusion / the level of protein in the blood serum, the level of total LDH in the effusion / the level of LDH in the serum. If these coefficients are less than 0.5 and 0.6, respectively, then it is transudate. Transudate mainly occurs in three conditions: circulatory failure, liver cirrhosis, and nephrotic syndrome. If the ratios are greater than 0.5 and 0.6, it is exudate, and further investigations should be directed towards determining the cause of pleurisy.
The basis for diagnosing pleurisy is chest X-ray imaging: classic signs of exudative pleurisy are homogeneous opacification of lung tissue with an inclined upper fluid level (Fig. 2.12.1-16). Classic signs appear in cases of diffuse pleurisy, if the amount of fluid exceeds 1 l. If there is less than a litre of fluid, it accumulates in the sinuses and smoothes the lower lateral sinus. It can be difficult to make a diagnosis if there is total opacification of one or both halves of the chest (total acute pneumonia and lung atelectasis are direct contraindications to thoracocentesis). If it is fluid, there is a contralateral displacement of the mediastinal organs. In hydropneumothorax, the fluid level is horizontal. In interstitial pleurisy, the fluid level appears as a biconvex lens.

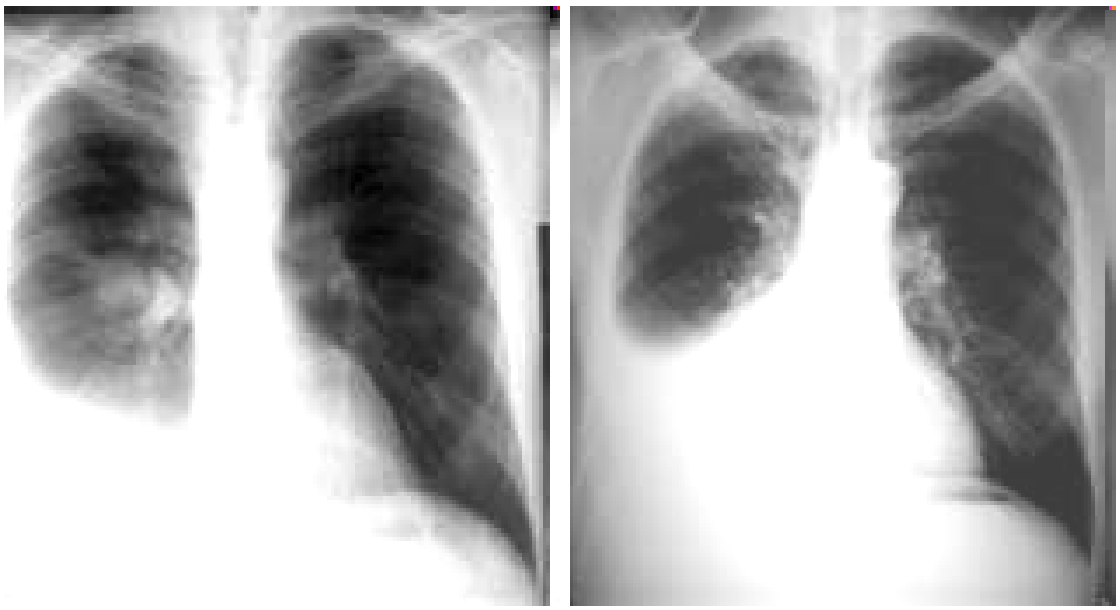

Fig. 2.12.1. Right-sided exudative pleurisy of tuberculous aetiology.

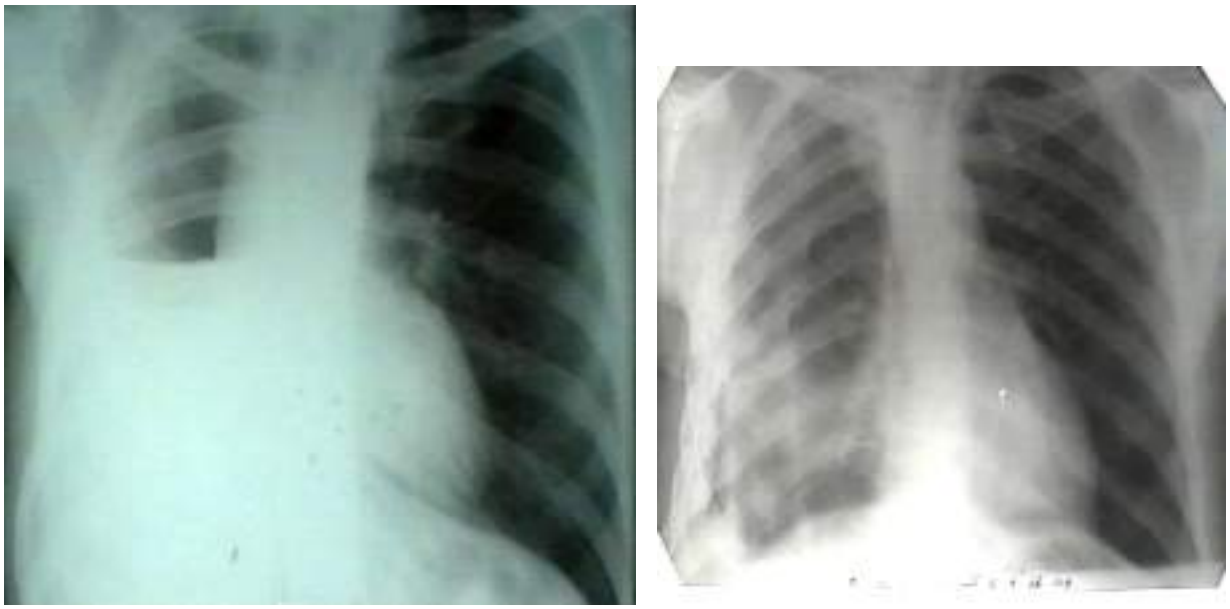

Fig. 2.12.2. Right-sided exudative pleurisy.

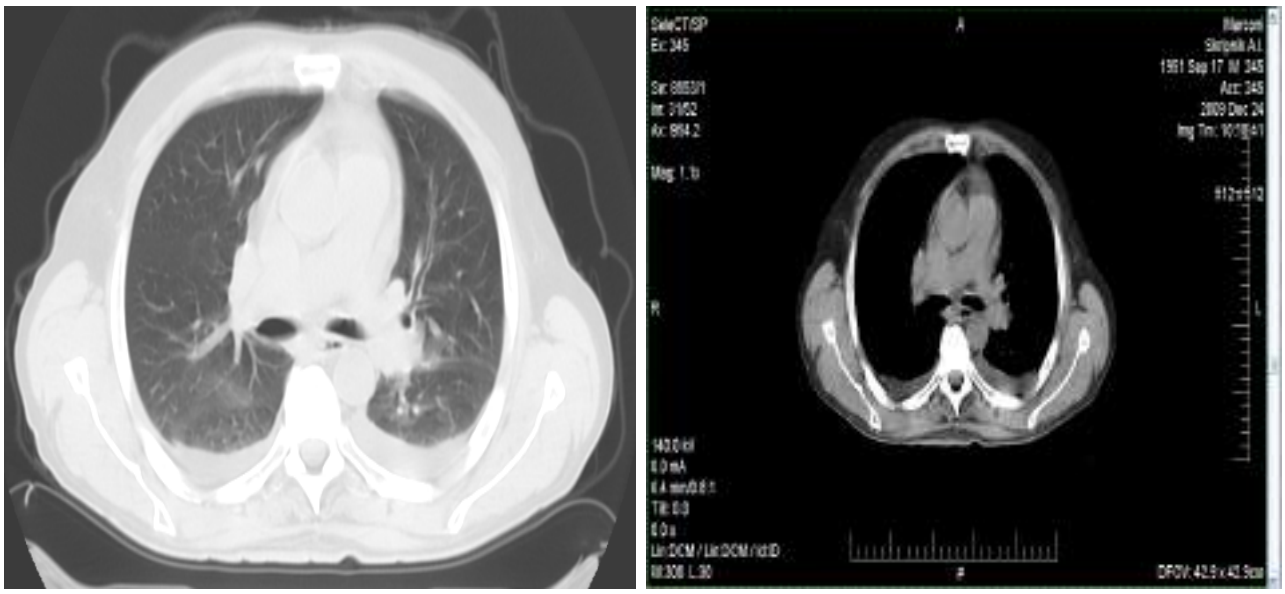

Fig. 2.12.3. Effusion into the pleural cavity.

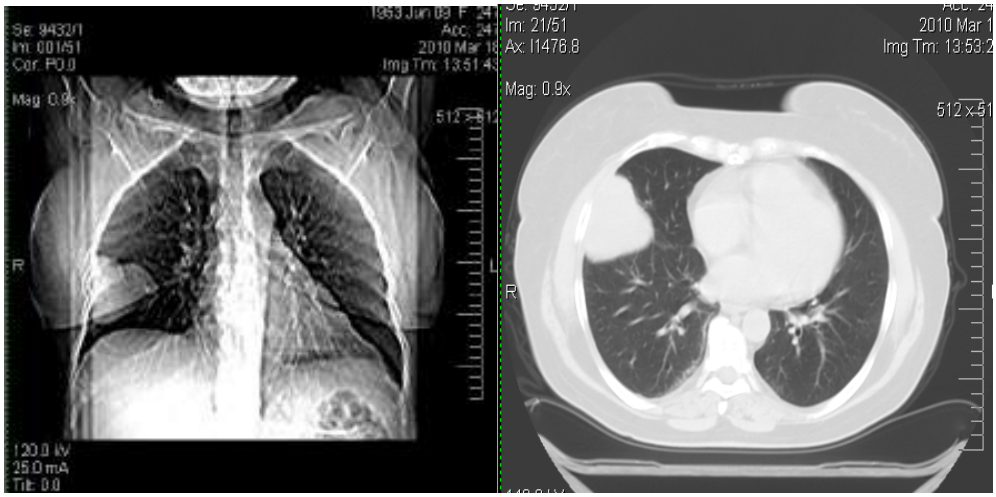

Fig. 2.12.4. Encapsulated effusion.

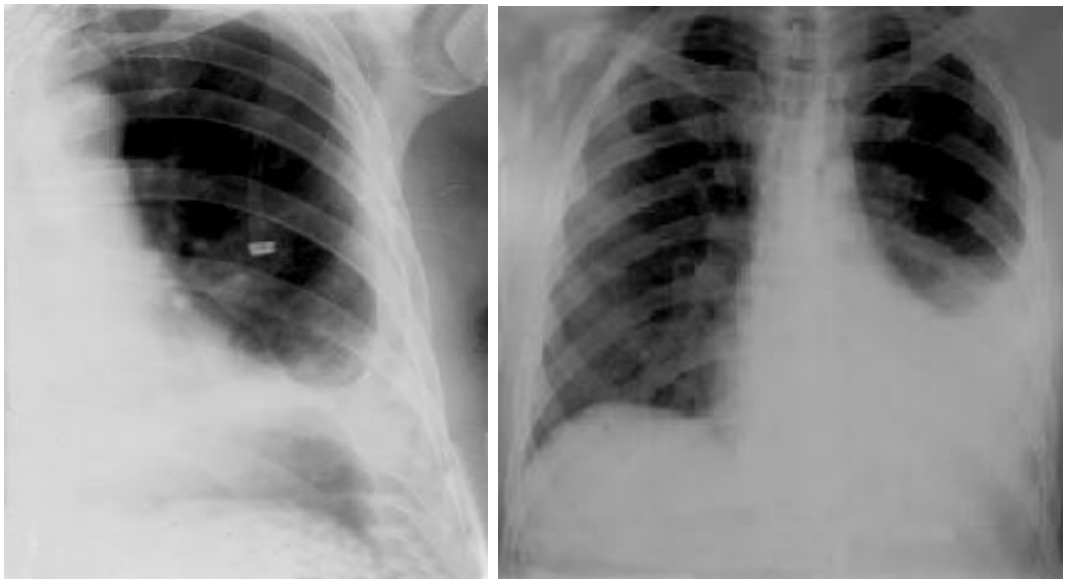

Fig. 2.12.5. Left-sided pleurisy.

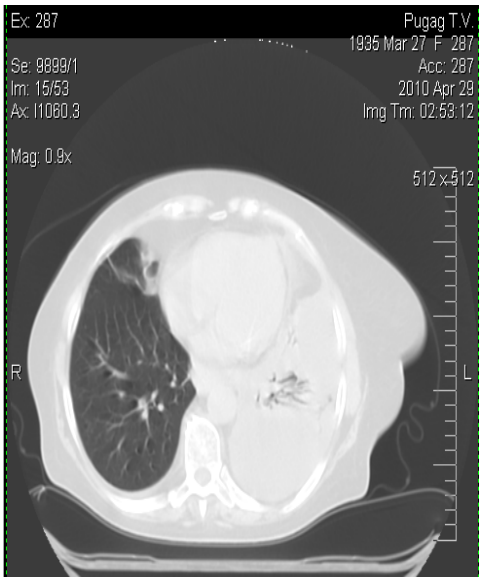

Fig. 2.12.6. Computed tomography of left-sided pleurisy.

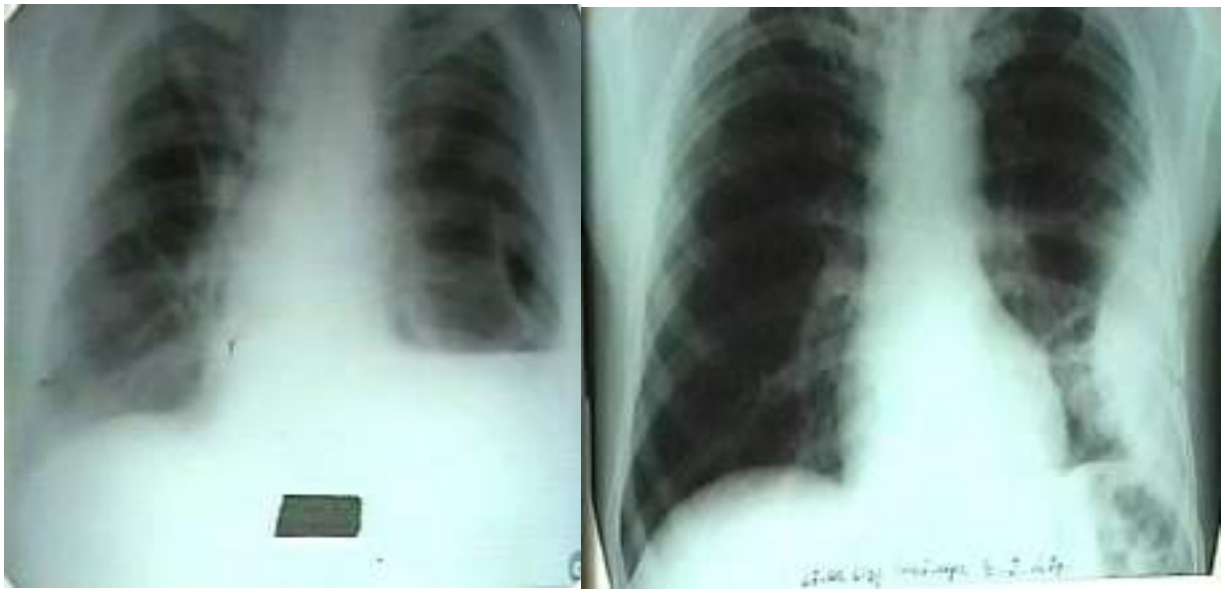

Fig. 2.12.7. Pleural effusion.

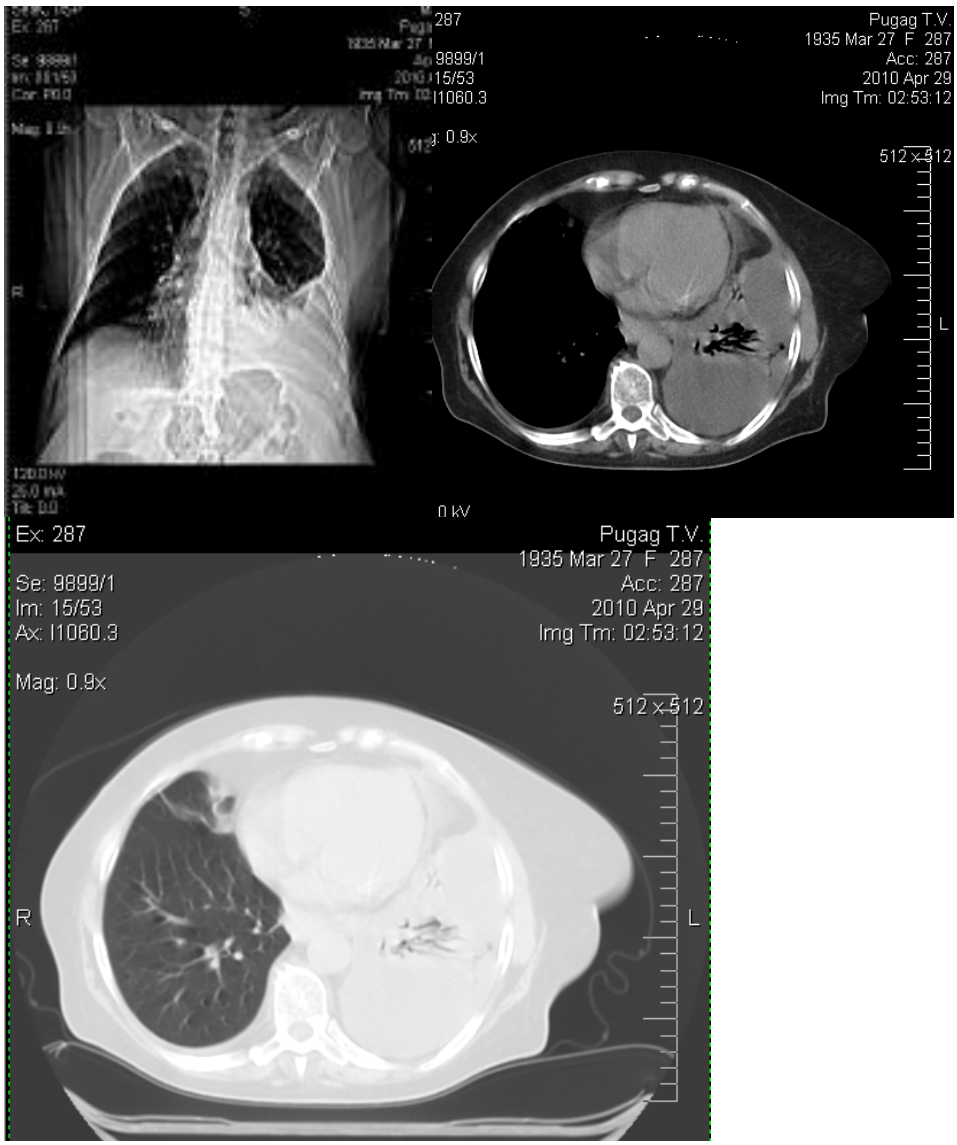

Fig. 2.12.8. Pleural effusion.

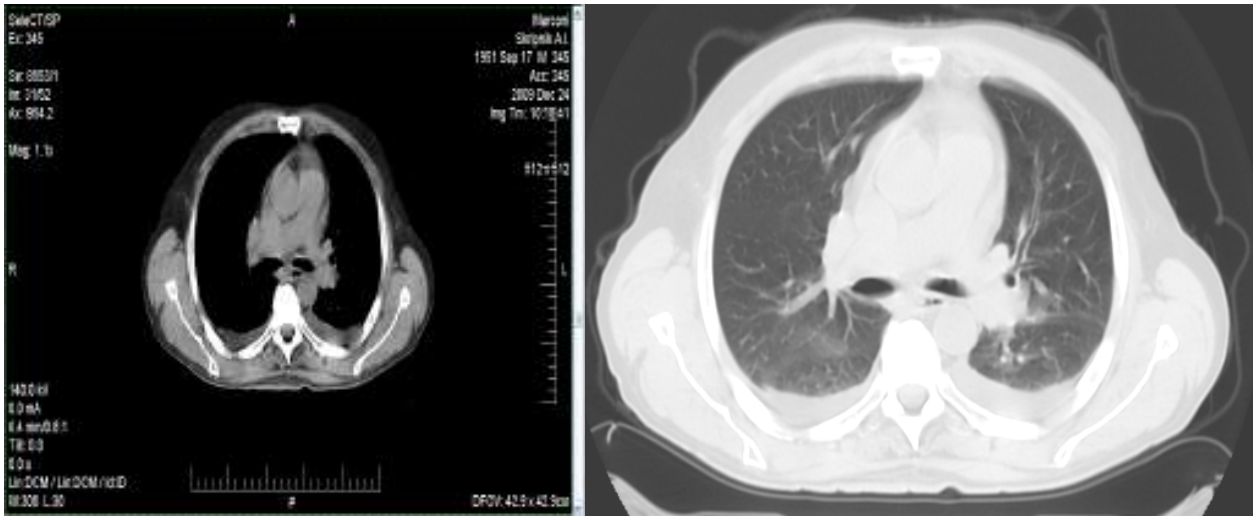

Fig. 2.12.9. Pleural effusion.

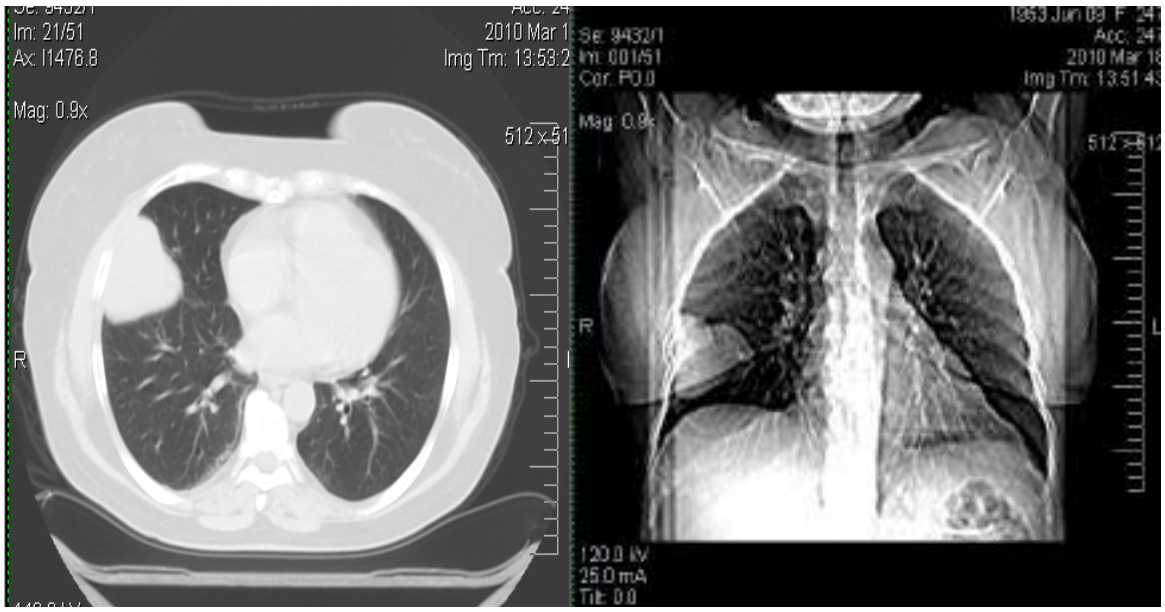

Fig. 2.12.10. Pleural effusion.

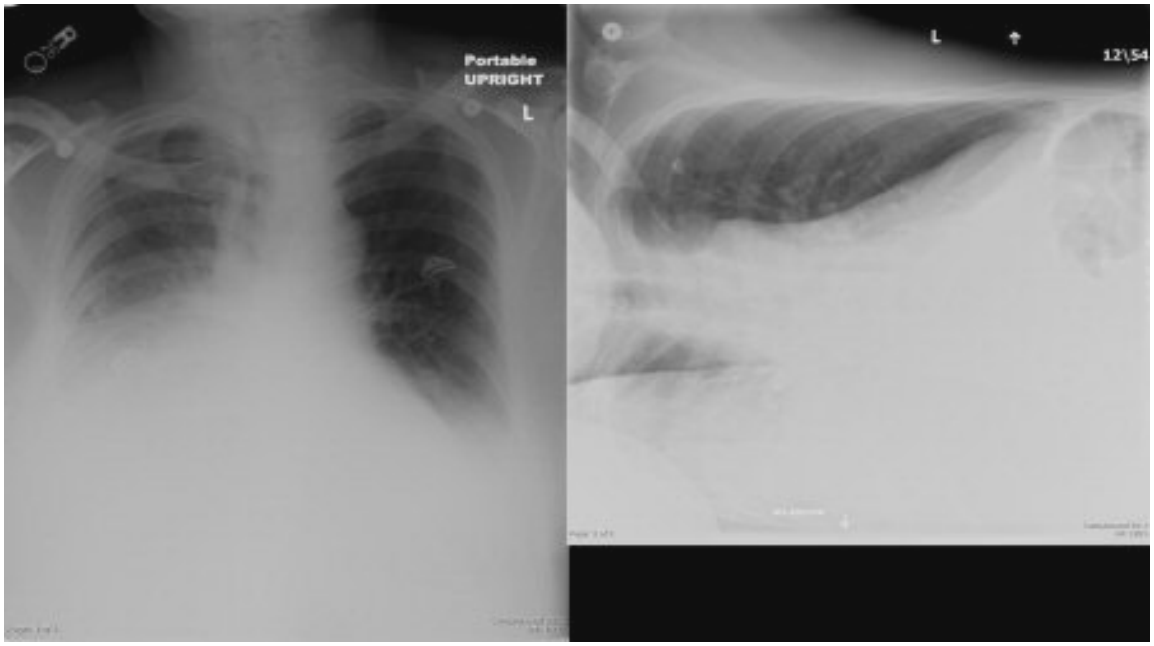

Fig. 2.12.11. Exudative pleurisy.

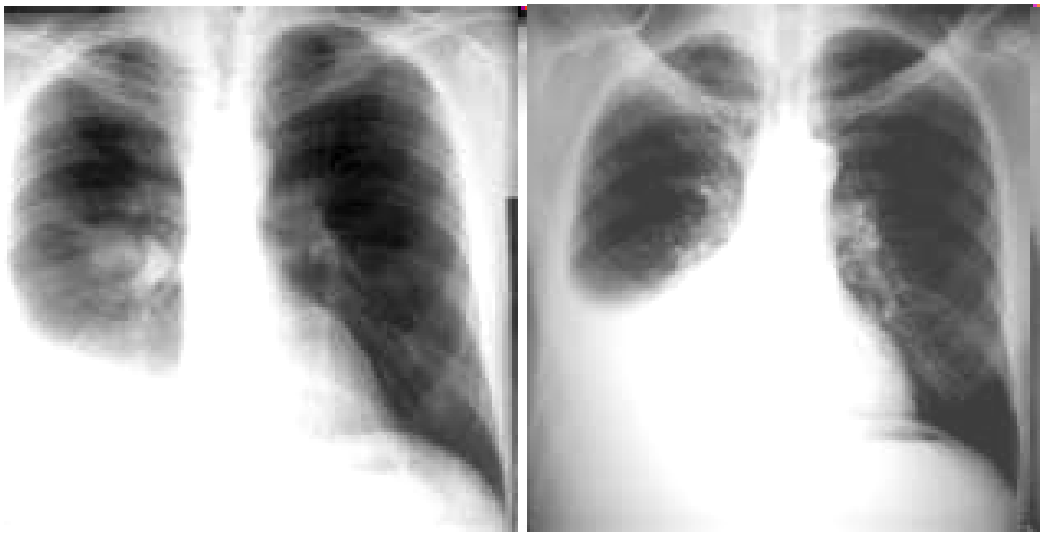

Fig. 2.12.12. Tuberculous right-sided exudative pleurisy (free).

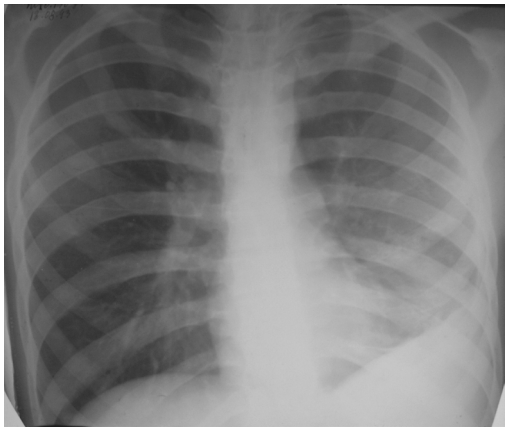

Fig. 2.12.13. Tuberculous left-sided exudative pleurisy (encapsulated).

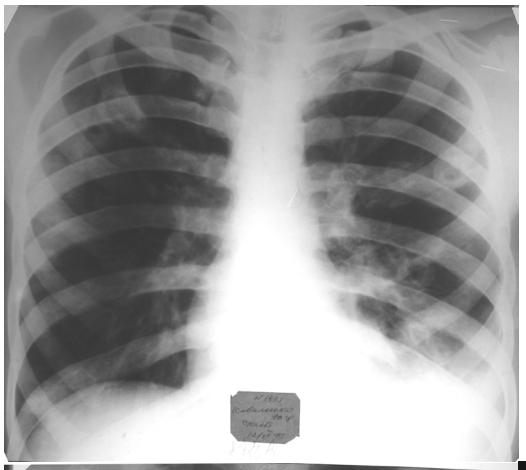

Fig. 2.12.14. Infiltrative TB of the lungs in the decay phase, MBT+, complicated by left-sided exudative pleurisy.

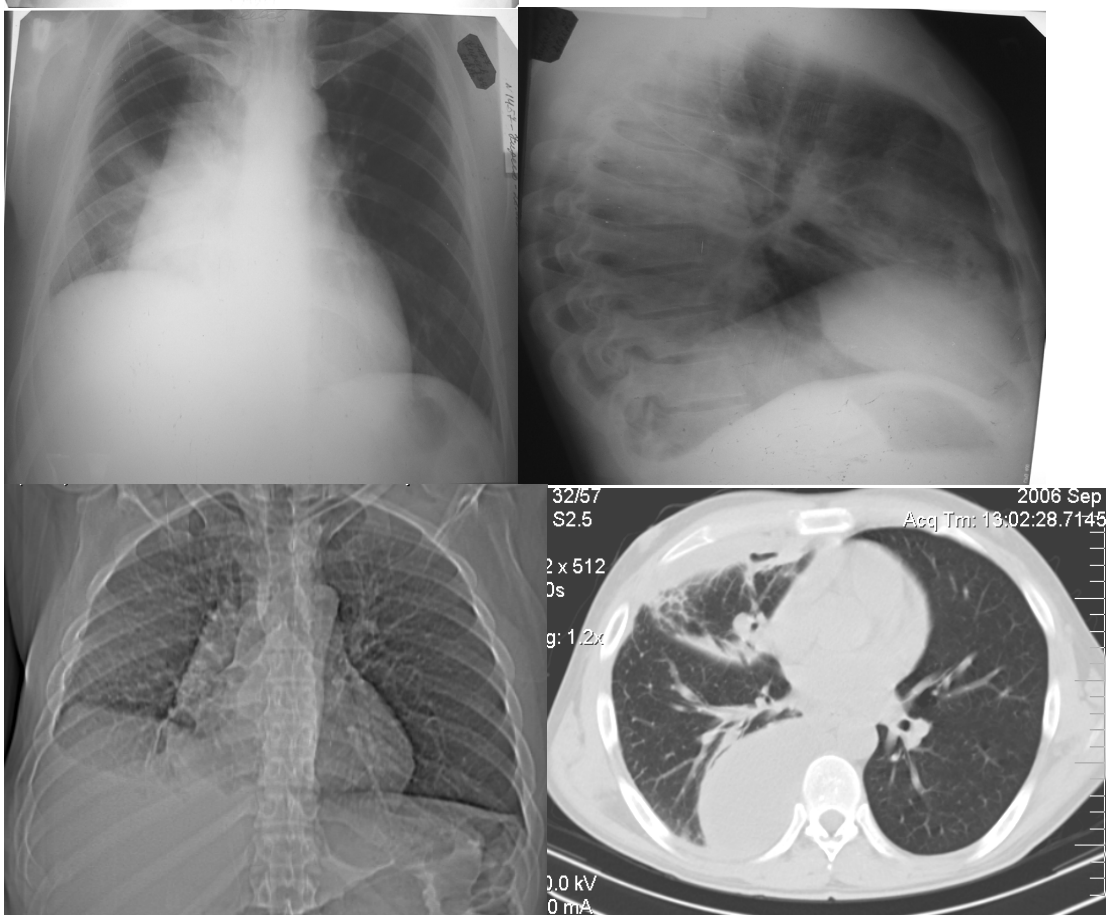

Fig. 2.12.15. Abscess of the middle lobe, complicated by mediastinal, encapsulated pleurisy.

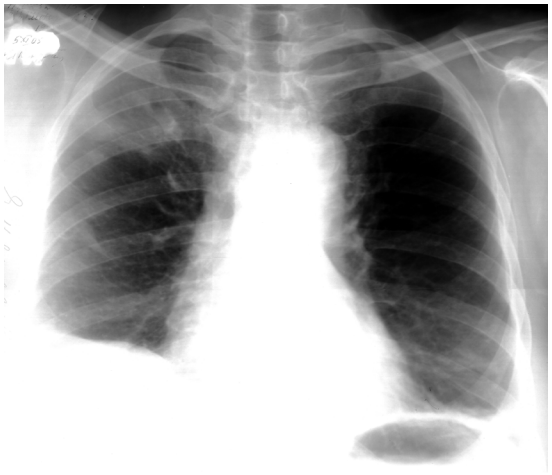

Fig. 2.12.16. Metastatic pneumonia complicated by right-sided exudative pleurisy.

The clinical picture of empyema pleura is characterised by hectic fever, pronounced signs of intoxication, and changes in auscultatory data (Fig. 2.12.17-20).

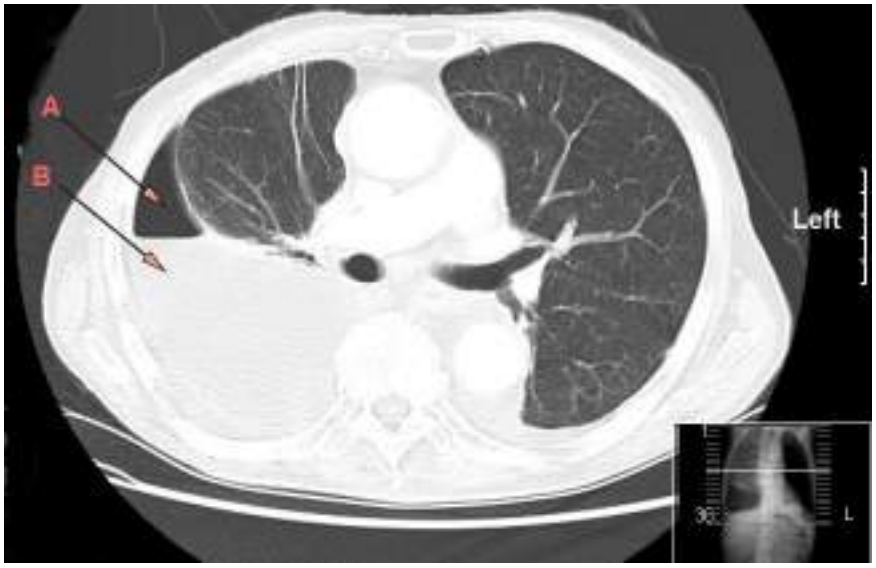

Fig. 2.12.17. Pleural empyema.

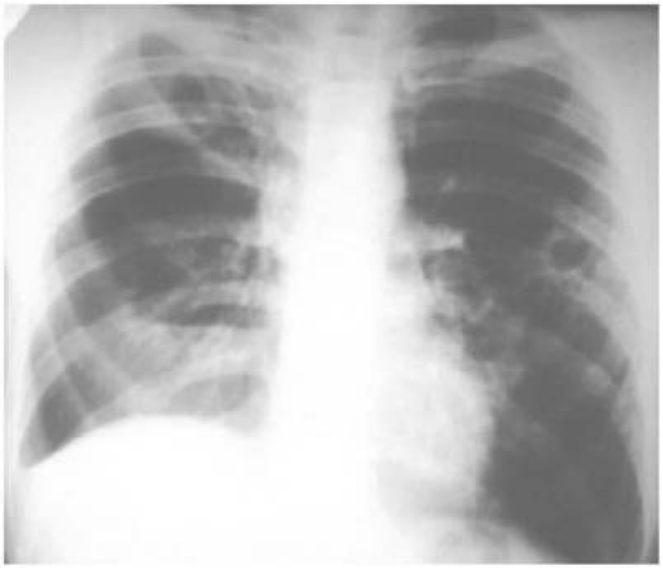

Fig. 2.12.18. Pleurisy empyema.

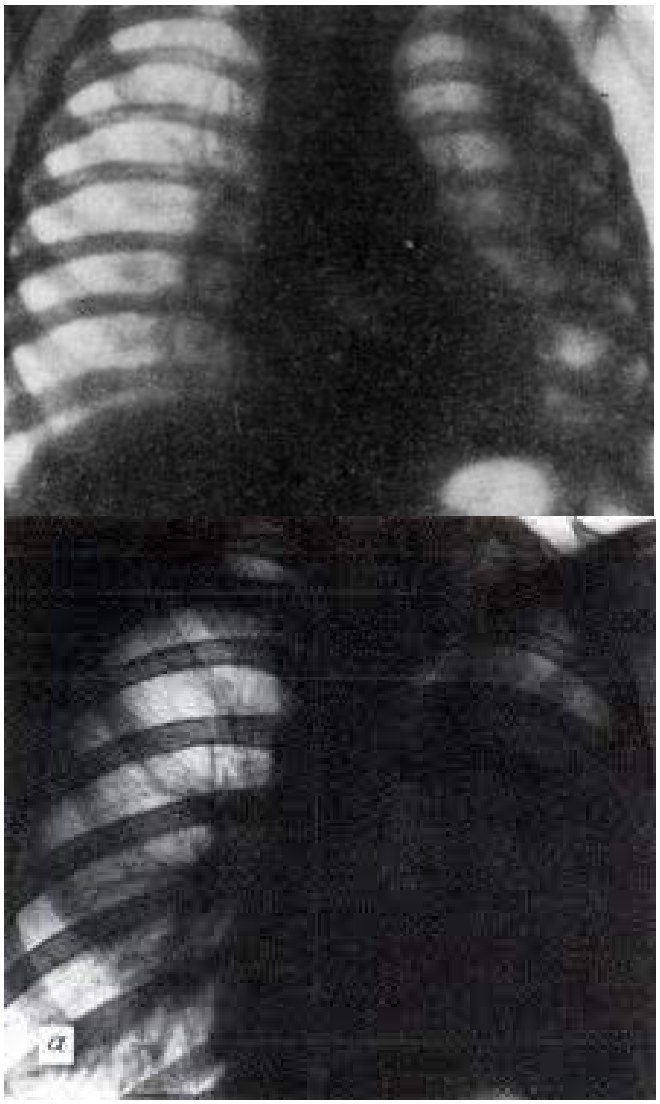

Fig. 2.12.19. Empyema of the pleura.

Fig. 2.12.20. Pleural empyema.

Algorithm for differential diagnosis of pleural effusion syndrome. Differential diagnosis of inflammatory, neoplastic, and congestive pleural

effusion. The first stage of differential search in this direction is presented in Table 2.12.1. At this stage, the most difficult and responsible task is to exclude (or confirm) the neoplastic nature of pleural effusion. In most cases of neoplasms, there is a gradual development of effusion and the presence of known risk factors for neoplasms. Radiological methods allow the detection of additional pathological shadows and the determination of indications for bronchological examination. Pleural fluid is often haemorrhagic in nature and contains tumour markers. The detection of tumour cells is an absolute diagnostic criterion and signifies the successful completion of the diagnostic search. In the absence of tumour cells in the pleural fluid and in the presence of a suspected neoplastic process, thoracoscopy with biopsy is performed, which in most cases allows diagnostically significant material to be obtained.

Table 2.12.1.

The main differences between inflammatory, tumour and congestive pleural effusions

Examination methods	**Inflammation**	**Tumours**	**Congestion**
Clinical	Epidemiological signs. Acute onset. Intoxication.	Risk factors. Gradual onset.	Diseases leading to congestion. Gradual onset. Risk factors for TIA.
Radiation.	Visualisation of effusion. Detection of additional shadows (lungs, mediastinum)		
Examination of pleural contents.	Exudate. Antigens, antibodies. Neutrophils. Lymphocytes. Eosinophils. Bacteria, fungi, protozoa.	Haemorrhagic exudate. Tumour markers. Tumour cells.	Transudate. Lymphocytes. Erythrocytes (in TEAL).
Thoracoscopy	Visualisation of pleural layers. Selection of biopsy site.		

Pleural biopsy	Inflammation. Fibrosis.	Tumour.	

Differential diagnosis of inflammatory pleurisy. Inflammatory pleurisy can be divided into six groups (Table 2.12.2):

Table 2.12.2.

Classification of inflammatory pleurisy

1) Infectious.	Bacterial, fungal, viral, etc.
2) Parasitic.	Amoebiasis, echinococcosis, paragonimiasis, etc.
3) Fermentogenic.	Pancreatogenic.
4) Allergic and autoimmune	Exogenous allergic alveolitis, drug allergy, Dressler's syndrome.
5) For rheumatic diseases.	Systemic lupus erythematosus, rheumatoid arthritis, rheumatism, etc.
6) Traumatic.	Traumatic, radiation therapy, burns, etc.

Among infectious pleurisy, it is most often necessary to conduct a differential diagnosis between tuberculous, pneumonic, and fungal lesions of the pleura.

Tuberculous pleurisy rarely occurs as the sole manifestation of tuberculosis (Fig. 2.12.21). It is more often combined with disseminated, focal, infiltrative pulmonary tuberculosis, bronchadenitis, or primary tuberculosis complex. Tuberculous pleurisy may be the first manifestation of primary tuberculosis. In 3% of cases, tuberculous pleurisy is an incidental finding. A.G. Khomenko distinguishes three main variants of tuberculous pleurisy: allergic, perifocal, and tuberculous pleurisy.

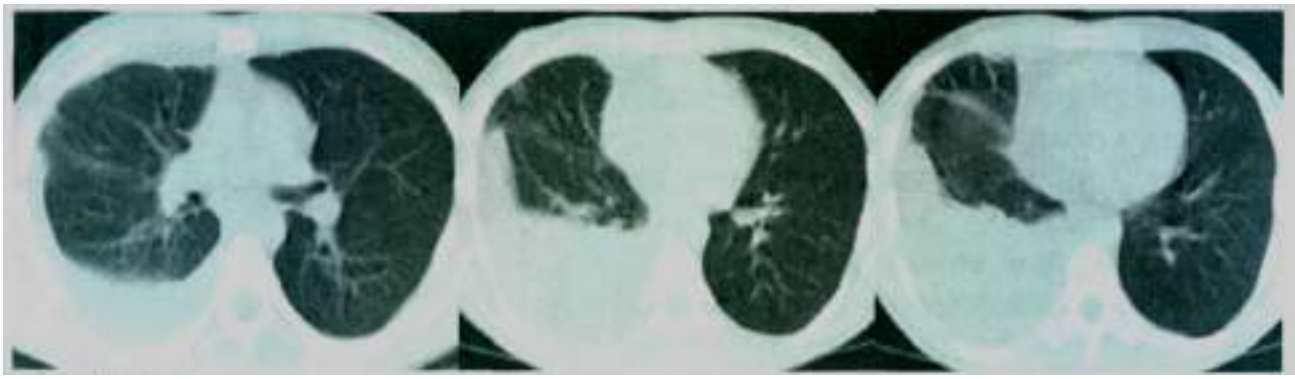

Fig. 2.12.21. Tuberculous exudative pleurisy. In the right pleural cavity, there is free effusion, the thickness of which increases from the apices to the diaphragm, and the pleural layers are thickened.

Allergic pleurisy is characterised by an acute onset with pain and fever, with rapid (within a month) positive dynamics of the process. Allergic pleurisy occurs in patients with primary tuberculosis in cases of recent infection or chronic primary tuberculosis infection. These patients are characterised by a hyperergic tuberculin reaction, and eosinophilia is often observed. The exudate is more often lymphocytic, sometimes eosinophils are found. Mycobacteria are usually not found in the exudate. Exudative pleurisy in these patients is often accompanied by other manifestations of primary tuberculosis: flikten, nodular erythema, polyarthritis.

Perifocal pleurisy occurs as a result of the involvement of the pleural layers in the inflammatory process in patients with pulmonary forms of tuberculosis. The course of such pleurisy is prolonged. The disease may be recurrent. Chest X-ray examination in such patients reveals one of the forms of tuberculous lung damage (focal, infiltrative, or cavernous). In most cases, the exudate is serous, lymphocytic, and mycobacteria are usually not detected.

Table 2.12.3.

Epidemiological analysis of infectious pleurisy

Tuberculosis	**Pneumonia**	**Mycoses**
Tuberculous pleurisy Allergic pleurisy Perifocal pleurisy Tuberculosis of the	Dependence of clinical presentation on the pathogen.	Clinical signs of immunodeficiency. Chest fistulas (actinomycosis).

pleura.		
Radiographically - TB archive.	No TB archive.	Lymphadenopathy. Focal lung damage.
Antigens, antibodies, mycobacteria in exudate.	Bacteriological verification 40-70%. Serodiagnostics - antigens and antibodies.	In exudate: lymphocytes, eosinophils, flora, antibodies.
Pleural biopsy. Caseous necrosis. MBT, L-forms.		Fungi in pleural biopsies.
Biological test - infection of animals with exudate, biopsy.		

Pleural tuberculosis may be the only manifestation of the disease, but it may also be combined with other localisations of tuberculous lesions. The morphological substrate of pleural tuberculosis is granulomatous tuberculous inflammation with elements of caseous necrosis. At the same time, there is a pronounced exudative reaction, which causes the accumulation of effusion. Depending on the size of the foci and the prevalence of the lesion, the exudate can be either serous or purulent with a predominance of neutrophils. Tuberculosis mycobacteria are often found in the exudate. A special place among pleurisy of a tuberculous nature is occupied by pleural empyema, which develops when the natural mechanisms of exudate resorption are blocked (Fig. 2.12.22 a, b).

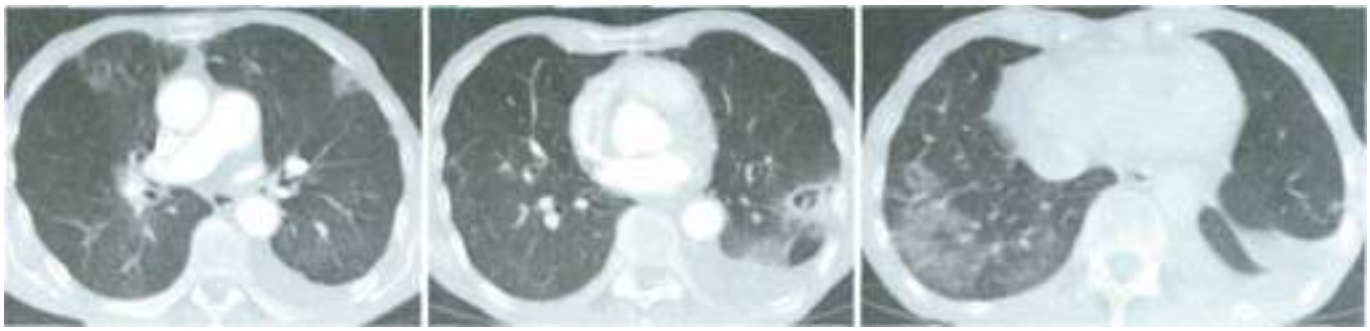

Fig. 2.12.22. a. Infiltrative pulmonary tuberculosis in the decay phase, MBT+, complicated by left-sided exudative pleurisy. After bolus administration of a contrast agent, the density of pleural effusion does not increase.

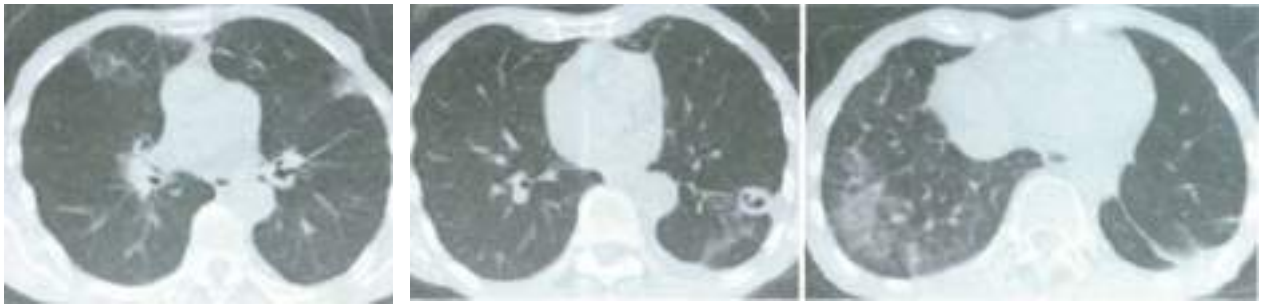

Fig. 2.12.22 b. The same patient after two months of treatment. Infiltrative changes in the lungs and the cavity of decay have decreased, left-sided pleural effusion is in the stage of organisation – thickening of the pleura and formation of pleural adhesions.

In all variants of tuberculous pleurisy, it is very important to detect mycobacteria, their antigens or antibodies to them in the exudate, to detect extrapleural forms of tuberculosis, and to obtain specific results of pleural biopsy.

Almost 40% of pneumonia cases are accompanied by pleurisy of varying severity. Parapneumonic effusion is defined as effusion that has developed in connection with a pulmonary infection, such as pneumonia or lung abscess. Depending on the aetiology of pneumonia, the incidence of pleurisy varies from 10% (Klebsiella pneumoniae) to 70-95% (Streptococcus pneumoniae, Staphylococcus aureus). Between 10 and 15% of parapneumonic effusions progress, become infected and require the insertion of a chest tube.

In lower lobe pneumonia, pleural effusion may not be diagnosed without additional ultrasound. The detection of a pneumonic focus in the lung parenchyma is diagnostically significant. Bacteriological detection of the pathogen is possible in pleural fluid. Most often, positive results of culture studies are obtained with anaerobic flora (up to 70%) and rarely with pneumococcal infection (4%). For the aetiological diagnosis of pleurisy, it is important to detect microorganism antigens and antibodies to them in the exudate, as well as a rapid response to adequate antibiotic therapy.

Fungal pleurisy occurs mainly in individuals with signs of immunodeficiency. The risk group includes individuals who take immunosuppressants and corticosteroids for a long time (after internal organ transplantation), as well as patients with chronic diseases that contribute to a decrease in antifungal immunity (diabetes mellitus, HIV infection, etc.). The course of the disease has much in common with tuberculosis. Usually, mycotic pleurisy is combined with fungal damage to the lung parenchyma. The detection of fungi in repeated culture studies of pleural fluid is of decisive importance in diagnosis. In the presence of fistulas (actinomycosis), culture testing of their contents allows the diagnosis to be verified. Serodiagnostics is of auxiliary importance. The frequency of parasitic lesions of the pleura is determined by the epidemiological characteristics of parasitic diseases. The main differential diagnostic features of these diseases are as follows.

Amoebic pleurisy usually occurs when an amoebic liver abscess breaks through the diaphragm. This is accompanied by sharp pain in the right hypochondrium and shortness of breath. Pleural effusion looks like "chocolate syrup" and contains particles of liver parenchyma and neutrophils. Amoebas are detected in only 10% of cases. Serodiagnostics usually helps to clarify the aetiological diagnosis.

Echinococcal lesions of the pleura occur when an echinococcal cyst of the lung, liver, or spleen ruptures into the pleural cavity. Less commonly, the cyst develops primarily in the pleural cavity. When the cyst ruptures into the pleural cavity, acute pain and shortness of breath occur. Often, the rupture of a suppurated cyst leads to the formation of empyema. The presence of a subpleurally located echinococcal cyst often leads to the formation of a bronchopleural fistula. The detection of parasite scolexes and echinococcal cyst membranes in the exudate and pleural biopsy, as well as positive serodiagnostic results, are of diagnostic significance.

Exudative pleurisy is a typical manifestation of paragonimiasis. In 40% of patients with paragonimiasis, dry migratory recurrent pleurisy is diagnosed. In one third of patients with paragonimiasis, exudative pleurisy is combined with focal and infiltrative lung damage. These types of pleurisy are characterised by a prolonged course with the formation of massive pleural adhesions. The exudate is predominantly eosinophilic.

Diagnosis is based on the detection of parasite eggs in pleural fluid and sputum and on increased antibody titres to parasite antigens.

Table 2.12.4. Signs of parasitic pleurisy

Amoebiasis	Echinococcosis	Paragonimiasis
Amoebic liver abscess	Rupture of a cyst into the pleural cavity	Dry, migrating
Rupture through the diaphragm	Empyema of the pleura	Recurrent pleurisy
Severe pain, shortness of breath	Fistula formation	Focal changes in the lungs
Pleural contents – "chocolate syrup"	Detection of scolexes with hooks	Eosinophilia
Neutrophils	Positive serological tests	Positive serological tests
Hepatocyte particles		Detection of eggs

Exudative pleurisy is a common manifestation of systemic connective tissue diseases. Systemic lupus erythematosus (SLE) occurs in up to 50% of cases with pleural involvement. Pleural effusion in such patients is often bilateral, with serous, lymphocytic exudate. The detection of clinical and laboratory signs of SLE, especially antinuclear antibodies and LE cells, allows the nature of pleurisy to be established. A distinctive feature of lupus pleurisy is the high effectiveness of corticosteroid therapy. Exudative pleurisy in rheumatoid arthritis tends to be chronic and recurrent. The exudate is serous, lymphocytic, with low glucose content and high rheumatoid factor titres. The effectiveness of corticosteroids is inconsistent. The detection of other manifestations of rheumatoid polyarthritis is important in the diagnosis. Exudative pleurisy in rheumatism has a minimal number of specific signs. The diagnosis is based on the detection of typical clinical features of rheumatism and requires the exclusion of other possible causes of pleurisy. Specific granulomas are rarely found in histological examination of pleural biopsies.

Thus, the differential diagnosis of pleural effusions should be carried out consistently, taking into account clinical, laboratory and instrumental

data in order to find absolute diagnostic criteria for the disease. A very important element of diagnosis is the detection and identification of extrapleural signs of the disease that is the cause of pleural effusion. Despite the wealth of additional information provided by the examination of pleural fluid and pleural biopsies, it is not always possible to obtain absolute diagnostic signs. In the absence of absolute diagnostic criteria for the nosological classification of pleurisy (microflora, specific granulomas or tumour cells), the diagnosis is established based on a combination of indirect signs, including an assessment of the effectiveness of the prescribed therapy.

List of References

1. Асмолов О. К. Атлас клініко-рентгенологічної діагностики легеневого туберкульозу: навчальний посібник / О. К. Асмолов, О.В. Павлова. Одеса: Друк, 2009. 96 с.
2. Centers for Disease Control and Prevention. Clinical and laboratory diagnosis for tuberculosis. Available from: https://www.cdc.gov/tb/hcp/testing-diagnosis/index.html.
3. European Centre for Disease Prevention and Control. European Union standards for tuberculosis care – 2017 update. Stockholm: ECDC; 2017. Available from: https://www.ecdc.europa.eu/en/publications-data/european-union-standards-tuberculosis-care-2017-update.
4. Feshchenko YuI, Melnyk VP, Ilnytskyi IH, editors. Pulmonology and phthisiology. National textbook in two volumes. Kyiv–Lviv: Atlas; 2015. Available from: https://catalog.lounb.org.ua/bib/392350
5. Hatabu H, et al. Chest imaging 2021. *J Clin Med*. 2021;10(1):1–5. Available from: https://pmc.ncbi.nlm.nih.gov/articles/PMC7769704/.
6. Kelly B. The chest radiograph. *Breathe (Sheff)*. 2012;8(1):74-81. Available from: https://pmc.ncbi.nlm.nih.gov/articles/PMC3632825/.
7. Ministry of Health of Ukraine. Standards of medical care: Tuberculosis. Order No. 102, 19 Jan 2023. Available from: https://phc.org.ua/sites/default/files/users/user90/MOZ_nakaz_19.01.2023_102_standarty_dodatky.pdf.
8. Nel M, van Rensburg A, Kritzinger F, et al. Chest imaging for pulmonary tuberculosis: an update. *Eur Respir Rev*. 2022;31(164):210228. Available from: https://europepmc.org/article/pmc/pmc8878790.
9. Petrenko VI, Todoriko LD, Shevchenko OS, et al. Фтизіатрія: підручник. Kyiv: Medytsyna; 2018. 472 p.
10. Public Health Center of Ukraine. National recommendations for prevention and preventive treatment of tuberculosis. 2023. Available from: https://phc.org.ua/sites/default/files/users/user90/PHC_A4_naz_recomendationTB_1023_online.pdf.
11. Radiopaedia.org. Primary pulmonary tuberculosis. Available from: https://radiopaedia.org/articles/primary-pulmonary-tuberculosis.
12. Radiopaedia.org. Pulmonary manifestations of tuberculosis. Available from: https://radiopaedia.org/articles/tuberculosis-pulmonary-manifestations-1.

13. Radiopaedia.org. Radiopaedia reference articles and case library. Available from: https://radiopaedia.org.
14. Specialty imaging. HRCT of the lung anatomic basis, imaging features, differential diagnosis / [edited by] Jud W. Gurney. – 1st ed. – 2010. – 552 p.
15. Verschakelen J.A., De Wever W. Tomography of the Lung. Series: Medical Radiology // World Scientific Publishing Co.-2007. – 196 p.
16. World Health Organization. Rapid diagnostics for tuberculosis detection. 3rd ed. Geneva: WHO; 2023. Available from: https://www.who.int/publications/i/item/9789240089488.
17. World Health Organization. WHO consolidated guidelines on tuberculosis. Module 3: diagnosis. Geneva: WHO; 2021. Available from: https://www.who.int/publications/i/item/9789240107984.

Application 1

Тест-scheme: "X-RAY DIAGNOSTICS of tuberculosis"

Review of the Chest Film

1. The shadow character:

1. Nides type
2. Infiltrative type
3. Ring shaped
4. Linear type shadowes

2. Size:

1. to 3 мм
2. 4-10 мм
3. 11-15 мм
4. 16-30 мм
5. 31-59 мм
6. 60 мм & more

3. Location:

Lobar and segmental lung structure

a) right lung;

1. upper field
2. middle field
3. lower field

b) left lung;

1. upper field
2. middle field
3. lower field

4. Number of shadows:

a) a single;
b) a group;
c) dissemination

5. Form of shadow:

a) rounded,
b) triangular,
d) polycyclic,
e) polyangular ,
f) irregular

6. Outlines of a shadow:

a) unclear outlines;
b) sharp;

7. Shadow's intensity:

a) low (feeble);
b) medium ;

c) high

9.Changing around or in other lung parts:

1.No changes

2. Bronchogenic nides dissemination

3. Presence Нонн's nides /i

4. Pleural changes (thikining)

5. Emphysema

6. Lung picture (increased/scarced) in both linear&/or reticular (fiber net-work).

7. Infiltrative path or fibrous traces to the root (connection with lung root)

8. Structure of shadow:

a) homogenous,

b) inhomogeneous

CONCLUSION:

1.Tuberculosis inrathoracic lymph nodes.

2. Primary TB complex.

3. Infiltrative lung tuberculosis

4. Lung tuberculoma.

5. Lung fibrousis-cavernous tuberculosis.

6. Disseminative lung tuberculosis
(miliary tuberculosis).

7. Focal (nides) lung tuberculosis .

8. Lung cirrhotic tuberculosis.

9. Tuberculosis pleurisy.